COMPATIBILITY AND STRUCTURAL INTERACTION IN PASSENGER VEHICLE COLLISIONS

A THESIS SUBMITTED IN FULFILMENT OF THE REQUIREMENTS FOR THE DEGREE OF DOCTOR OF PHILOSOPHY

Gareth E Thomas

B.Eng.

School of Aerospace, Mechanical and Manufacturing Engineering

Faculty of Engineering

RMIT University

December, 2005

COMPATIBILITY AND STRUCTURAL INTERACTION IN PASSENGER VEHICLE COLLISIONS

A THESIS SUBMITTED IN FULFILMENT OF THE REQUIREMENTS FOR THE DEGREE OF DOCTOR OF PHILOSOPHY

Gareth E Thomas

B.Eng.

School of Aerospace, Mechanical and Manufacturing Engineering

Faculty of Engineering

RMIT University

December, 2005

Declaration

I certify that except where due acknowledgement has been made, the work is that of the author alone; the work has not been submitted previously, in whole or in part, to qualify for any other academic award; the content of this thesis is the result of work which has been carried out since the official commencement date of the approved research program; and, any editorial work, paid or unpaid, carried out by a third party is acknowledged.

Gareth E Thomas

December, 2005.

Abstract

This research contributes to the existing body of knowledge relating to crash compatibility (the minimisation of injury risk faced by all participants involved in a collision in traffic). The research focuses on the topic of structural interaction in collisions involving passenger vehicles, a phenomenon describing the efficiency of energy dissipation within existing deformation-zones of a passenger vehicle during a collision. A new definition for structural interaction was developed and several metrics to evaluate structural interaction and compatibility in car-to-car collisions were proposed, based on the commonly known Equivalent Energy Speed (EES) metric. The new EES metrics describe equivalent closing velocities for a given collision based on the energy dissipated within the front-ends (EESFF) and the entire structure (EESVV) of both vehicles involved in a head-on collision. These metrics form the basis of the new knowledge generated by this research.

Additionally, a new method was developed to measure the amount of energy dissipated through structural deformation in a collision, based on accelerometer readings. This method was applied to several experimental and simulation-based car-to-car collisions and the validity of the method was proven. Based on the energy dissipation which occurred in the car-to-car collisions analysed, the degree of compatibility reached and the level of structural interaction which occurred in each collision was evaluated by applying the newly developed EESFF and EESVV metrics.

Three factors influence the crash compatibility of passenger cars; geometry, stiffness and mass.

It was concluded, based on a review of existing literature, that controlling mass and stiffness was limited by goal conflicts and feasibility issues. Requirements for vehicles to carry out different functions (such as commuting to work and towing and transporting goods) also ensures the continued demand for vehicles of different

mass. Controlling stiffness is not considered to be feasible as, in order for passenger cars to exhibit stiffness compatibility, varying degrees of self protection would result (assuming all vehicles provide a similar amount of available deformation travel). Given the high relevance of single vehicle collisions in the real-world accident scene, concluded in an analysis of German accident data, it is not considered appropriate that vehicles reduce their self protection levels with the sole aim of improving partner protection and compatibility.

Two measures were concluded to offer the greatest feasibility to improve the compatibility-potential of passenger cars:

- **ensuring adequate passenger compartment strength** (particularly relevant for smaller vehicles)
- **controlling vehicle geometry** to improve structural interaction.

The core of this research relates to **structural interaction** in collisions involving passenger cars. Structural interaction relates to the efficiency of the dissipation of kinetic energy through structural deformation.

In the first stage of this research, the statistical significance of compatibility-relevant collision configurations was identified. This was achieved through extracting and manipulating German accident data from the Volkswagen-GIDAS (German In-Depth Accident Study) database. It was concluded, based on the analysis, that car-to-truck and car-to-car, head-on collisions were the most statistically relevant collision configurations with respect to passenger-car compatibility. The majority of this research focused on car-to-car, head-on collisions.

The phenomenon of structural interaction was further clarified through the development of new theory with the aim of objectively describing structural interaction. A definition for structural interaction was developed based on a comparison of structural deformation in fixed barrier and car-to-car head-on collisions. A method of predicting maximal structural interaction for a car-to-car, head-on collision, by statically combining the force-displacement characteristics exhibited by each vehicle in a fixed barrier collision, was developed.

With respect to the injury risk faced by the vehicle occupant, two implications of structural interaction were identified:

- **Compartment intrusion** (maximising structural interaction increases energy dissipation in the vehicle front-end thereby reducing the risk of intrusions)

- **Compartment accelerations** (Structural interaction influences interaction forces and thereby compartment accelerations)

Whilst increasing structural interaction reduces the risk of compartment deformation and global intrusions, it does lead to an increase in compartment accelerations. The influence of structural interaction on acceleration induced injury was investigated based on MADYMO occupant simulations. It was concluded that increasing structural interaction for all collision velocities is the most appropriate design goal.

Two **metrics** were also developed to reflect both the degree of compatibility and the collision severity for car-to-car head-on collisions. An energy equivalent closing speed for a vehicle-vehicle collision (EESVV) was proposed to convey the severity of a given car-to-car head-on collision. Another closing speed metric was also developed to reflect the degree of compatibility exhibited by two vehicles in a given collision (EESFF) based on the energy dissipated in both vehicle front-ends.

Several fixed barrier crash tests have been proposed in different configurations and with different assessment criteria. All assessments aim to evaluate the geometrical characteristics of the front-ends of passenger vehicles. A set of factors required from a compatibility assessment focused on assessing vehicle geometry were identified. The proposed compatibility assessment procedures were evaluated based on their ability to predict the potential for structural interaction offered by passenger vehicles.

A method to measure energy dissipation occurring through structural deformation was developed, based on accelerometers located at the base of the A and B pillars combined with the vehicle masses. The method was applied to several experimental car-to-car, head-on collisions and the EESVV and EESFF values calculated. For all of the collisions analysed, the EESVV was less than 5% lower than the actual closing

speed of the collision. This confirmed the accuracy of the measurement of energy dissipation based on accelerometers. For two of the four car-to-car head-on crashes analysed, the EESFF was calculated as well, conveying the degree of compatibility exhibited by the vehicles involved in the collision.

To further investigate structural interaction, several car-to-car head-on collision simulations were carried out. The accelerometer-based method of measuring energy dissipation through structural deformation was also applied in numerical crash test simulations. An error of 1.4% to 2% was observed between the total energy dissipation calculated based on accelerometers and the total change in internal energy of the vehicle structure, acquired from the simulations. This further confirmed the accuracy of the method to calculate energy dissipation through structural deformation based on accelerometers.

For these collision simulations, the EESFF value reflected the isolated influence of structural interaction, as the vehicles were identical. The degree of structural interaction which occurred in the standard crash configuration was significantly lower than the predicted maximum. This was reflected by an actual EESFF value of 99.9km/h for the standard car-to-car collisions compared to a theoretical maximum of 107.1km/h, predicted based on a fixed rigid barrier collision.

The influence of the vertical **geometric overlap** of the front-end structures on the resulting degree of structural interaction was investigated in a simulation matrix. Results showed that an increasing vertical misalignment of front-structures lead to a decrease in structural interaction. A reduction in the EESFF from 99.9km/h to 97.3km/h was observed for an increase in the degree of vertical misalignment from 0mm and 100mm.

Several **constructive measures** were investigated with the aim of improving the degree of structural interaction in the original collision configuration. The strength of the compartment had the most significant influence. Changes in cross member stiffness and wheel-house strength brought about little change. In addition, several simulations were carried out with a planar rigid panel of no mass located in the front-end of one of the vehicles. The panels were able to translate freely, parallel to the initial ve-

locity vector of both vehicles. For each of the panels investigated (100mm, 250mm, 1000mm vertical width) the EESFF increased to approximately equal the maximum theoretical EESFF value. This confirmed the potential for improvement in structural interaction in the standard car-to-car collision. It also confirmed the accuracy of the prediction of maximum possible structural interaction for a car-to-car, head-on collision at 50% overlap, based on structural performance in a fixed rigid barrier collision.

Acknowledgements

This Ph.D. thesis is the culmination of several years of research carried out within the Volkswagen AG Accident Analysis Department in Wolfsburg, Germany. I would like to thank all members of the Accident Research Team for their personal and professional support.

I sincerely thank Professor Sylvester Abanteriba for the organization of the international program at RMIT University, enabling such mutually beneficial international partnerships between industry and RMIT University worldwide.

Many thanks are owed in particular to Dr. Thomas Schwarz for the industry-based supervision of this Ph.D. His enthusiasm, motivation and support were deciding throughout all phases of the research.

I would also like to sincerely thank Dr. Robert Zobel for his guidance and support as head of the Volkswagen Accident Analysis Department and for his much valued advice and ideas.

Many thanks are also owed to Dr. Mirko Junge, for his valued feedback during the preparation of the written thesis and Holger Becker for his advice on the analysis of accident statistics.

Finally, I would like to thank Dr. Monir Takla of RMIT University, Melbourne, Australia for the senior level supervision of this thesis.

Nomenclature

a	Acceleration vector
D_V	Energy dissipated through deformation of the structure of a given vehicle
D_b	Energy dissipated through deformation of the structure of a given vehicle in a barrier test
D_{VV}	Energy dissipated through deformation of the structure of both vehicles involved in a head - on collision
D_F	Energy dissipated through deformation of the front - end of a given vehicle
D_{FF}	Energy dissipated through deformation of both vehicle's front - ends in a head - on collision
E_k	Kinetic Energy
EES	Equivalent Energy Speed
EESV	Equivalent Energy Speed considering the deformation of the entire structure a given vehicle
EESF	Equivalent Energy Speed considering the deformation of the front - end of a given vehicle
EESVV	Equivalent Energy Speed considering the deformation of the entire structure of both vehicles in a head - on collision
EESFF	Equivalent Energy Speed considering the deformation of the front - ends of two vehicles involved in a head - on collision

F_{peak}	Maximum front – end deformation force exhibited by a vehicle
M	Momentum
v	Velocity
v_b	Initial velocity of a vehicle in a fixed barrier collision
v_r	Resultant velocity of both vehicles after a head – on collision
v_c	Closing velocity of two vehicles involved in a collision
Δv	Absolute change in velocity of a vehicle during a collision
s	Linear deformation/crush of the vehicle structure
s_b	Linear deformation/crush of the vehicle structure in a fixed barrier collision
s_{crit}	The degree of deformation of both front - ends in a head - on collision after which the compartment of one vehicle is under threat of being overloaded

List of Acronyms

AAM	Alliance of Automobile Manufacturers (USA)
ACEA	Association des Constructeurs Européens d' Automobiles (EUR)
AHOF	Average Height of Force
AIS	Abbreviated Injury Scale
EES	Equivalent Energy Speed
ESP	Electronic Stabilisation Program
EUCAR	European Council for Automotive R&D
EURO NCAP	European New Car Assessment Program
FMVSS 208	Federal Motor Vehicle Safety Standard 208 (USA)
FWDB	Full-Width Deformable Barrier
FWRB	Full-Width Rigid Barrier
HIC	Head Injury Criterion
VC	Viscous Criterion
IHRA	International Harmonised Research Activities
IRTAD	International Road Traffic and Accident Database
LTV	Light Trucks and Vans
MAIS	Maximum AIS Injury sustained by a given traffic accident victim
MDB	Moving Deformable Barrier
NHTSA	National Highway Traffic Safety Administration (USA)
PDB	Progressive Deformable Barrier
PEAS	Primary Energy Absorbing Structures
SUV	Sports Utility Vehicle
TRL	Transport Research Laboratory (U.K.)
VDI	Vehicle Deformation Index
VW-GIDAS	Volkswagen – German In-Depth Accident Study

Contents

1 Aims and background of the research

1.1 Introduction

Between 1990 and 1998, the number of fatalities occurring in traffic accidents within the European Union member states decreased steadily, despite an increase in new vehicle registrations and the total number of kilometres driven [1] [2]. This can be largely attributed to an improvement in the safety levels of passenger vehicles. Despite this considerable improvement, the number of accidents remains very high and the socio-economic implications of traffic accidents are profound[1]. Demands placed on the automobile manufacturer by customers and governments, with respect to vehicle safety, have increased greatly in response.

Traditionally, vehicle safety has been considered in terms of primary safety (accident avoidance) and secondary safety (mitigation of injuries in the event of a collision) [4]. However, a third type of safety technology has emerged which does not entirely fit into either of these categories and relates to the reduction of the collision severity. Emergency braking to reduce the severity of a collision through braking immediately before a collision is one such system. Modern safety research revolves around the three main categories of **accident avoidance, reduction of collision severity** and **mitigation of injuries** after the collision occurs [5].

In the last decades, safety assessments and regulations have focussed mainly on the mitigation of injury in the case of a collision, in particular on the degree of protection offered by passenger vehicles to their own occupants [6] [7] [8]. The level of protection offered to the occupants of passenger vehicles in the case of a collision has improved significantly in response [9]. This has taken place through both optimising the deformation characteristics of the vehicle structure and through advancements in restraint-system effectiveness.

[1] 5842 persons were killed in traffic accidents (died within 30 days of the accident) on German roads in 2004 of which 3238 were passenger car occupants. 440126 persons were seriously injured (requiring hospitalisation longer than 24 hours) on German Roads in 2004 of which 259605 were passenger car occupants [3].

Aims and background of the research

With recent advancements in electronics, technologies focussed on accident avoidance have become increasingly effective and broadly implemented [2]. The Electronic Stabilization Program (ESP) has been claimed to be one of the most influential safety mechanisms since the introduction of the 3-point safety-belt [10] [11] [12]. A Volkswagen study based on existing accident data concluded that ESP could have prevented up to 80% of all accidents in which skidding occurred before the impact [12].

Despite the high potential of accident avoidance measures and technologies to reduce the accident severity, the mitigation of injuries in unavoidable collisions is still an issue of high relevance in today's traffic environment. The attrition rate (rate at which vehicles leave the field) also needs to be considered. Even if highly efficient measures to avoid and or reduce the severity of accidents were introduced into the vehicle today, it would be many years before such measures would achieve 100% market penetration.

Currently, standardised crash testing procedures evaluate the protection offered to the occupants in case of a collision (injury mitigation). Various acceleration, force and velocity readings taken from different regions of anthropometric devices (crash test dummies), developed to be standardised representations of the human population, are the main focus of the assessment in most tests [7] [13] [14]. Such tests ensure that a high level of protection is provided to the occupants of the given vehicle for the given crash test configuration. However, real-world accident data indicates that occupants of some vehicles face a higher risk than others in car-to-car collisions. This can be largely attributed to differences in vehicle mass, stiffness and geometry, resulting in incompatibility between vehicles involved in collisions. In general terms, compatibility can be described as reducing the risk of injury or death faced by all participants involved in traffic accidents [15].

The incompatibilities between vehicles involved in collisions are often categorised in terms of differences in **mass**, **stiffness**[2] and **geometry** [16] [17] [18] [19]. In order to improve crash compatibility, future evaluations relating to injury mitigation in collisions will need to evaluate the protection offered to the passengers of the other car involved in the collision as well (partner protection). Improving the protection of the passengers of other cars involved in collisions with the car being designed could compromise the safety of the passengers of the car itself, unless extreme care is taken. It is generally accepted that any measures taken to improve the compatibility potential of passenger vehicles should not compromise the current levels of protection provided by passenger vehicles to their own occupants [20] [21] [22]. This leads to several goal conflicts when considering an improvement in both the self- and partner protection levels provided by passenger vehicles.

Research groups around the world are focussing on controlling front-end geometry as a first step to improve the crash compatibility potential offered by passenger cars [16] [20]. Increasing geometrical compatibility appears to be the most feasible way to achieve a simultaneous improvement in self- and partner protection. As vehicle geometry can not be objectively described, the consequences of geometry on the outcome of collisions involving two passenger cars is subjectively referred to using the term; **"structural interaction".** Three compatibility assessment procedures are currently being considered for implementation around the world, each focusing on evaluating and controlling vehicle geometry to improve structural interaction [23] [24] [25] [26] [27]. Neither an objective definition nor a quantitative understanding of the phenomenon of structural interaction is currently available.

The main goal of this research is to develop an objective definition for structural interaction and to measure and evaluate the level of structural interaction in both experimental and simulation-based car-to-car head-on collisions. The aims of the research are listed more specifically overleaf.

- **To evaluate the statistical significance of compatibility-relevant collision configurations based on real-world accident data**

[2] In discussions of vehicle safety, the term stiffness is used to describe the magnitude of the resistance forces exhibited by the vehicle whilst undergoing deformation. This convention is adopted throughout this thesis.

- **To objectively define the phenomenon of structural interaction within the greater context of existing crash compatibility theory**

- **To identify the key requirements of a compatibility assessment procedure focussed on improving the structural interaction potential offered by passenger cars**

- **To develop a method to measure and evaluate structural interaction in experimental and FEM-based car-to-car, head-on collisions**

- **To investigate constructive measures in vehicle design, aimed at improving the structural interaction potential of passenger cars, based on FEM numerical simulations.**

The research focuses on the compatibility issue in Europe, with statistical analyses carried out based on German accident data and with the car-to-car collision configuration forming the main focus for the development of methods to measure and evaluate structural interaction. However, the methods to measure and evaluate structural interaction presented in this thesis can be transferred to other collision configurations, including car-to-SUV (Sports Utility Vehicle) and car-to-LTV (Light Trucks and Vans), which dominate accident statistics in North America.

1.2 Thesis structure

This thesis can be divided into a literature review and three distinct sections, Figure 1.

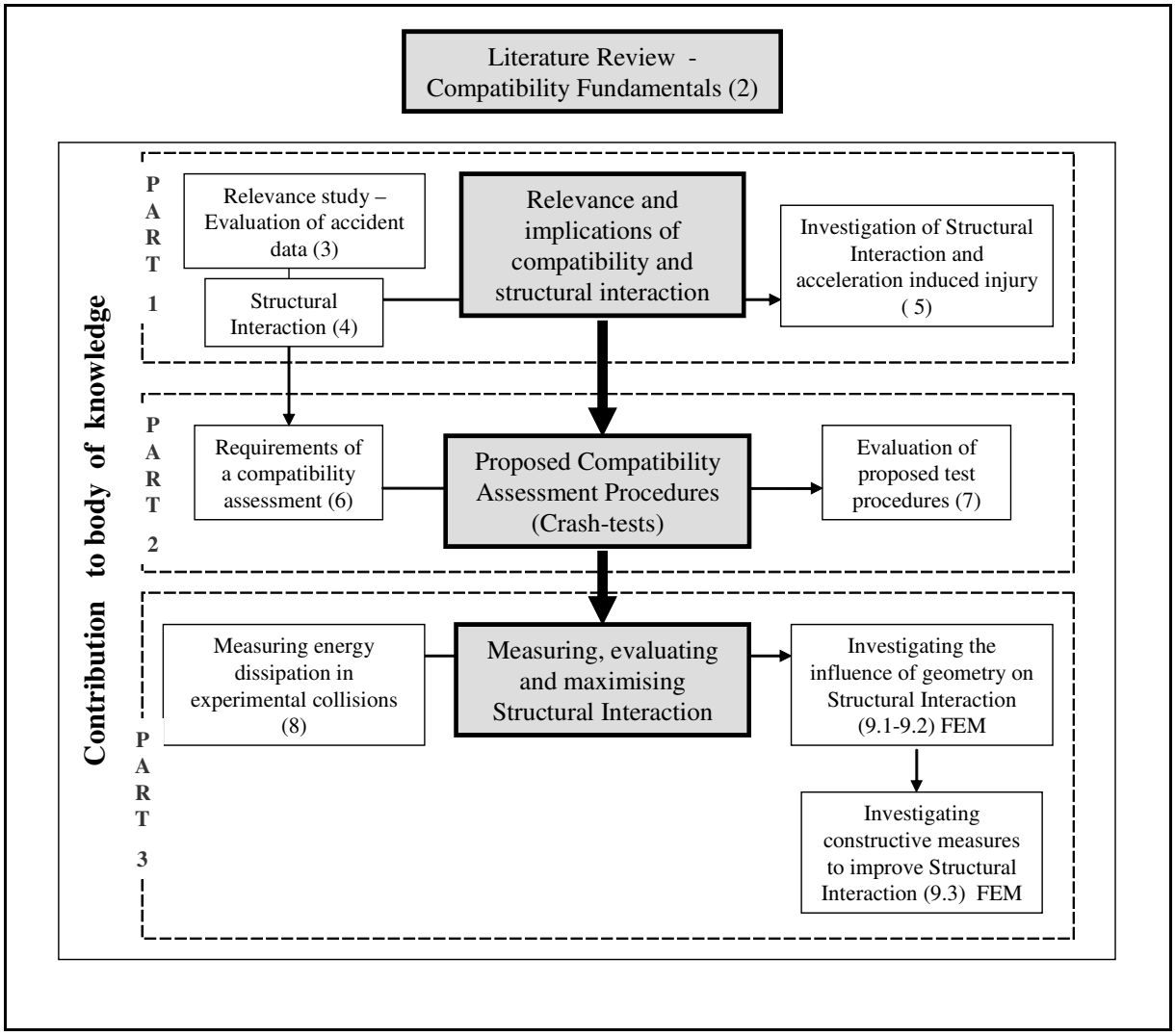

Figure 1 Thesis Structure

Literature Review

In chapter 2, the current body of knowledge relating to crash compatibility is summarised and expanded upon. Existing studies of accident data, carried out to determine the relevance of compatibility in real-world collisions, are summarised in the beginning of the chapter. Following this, the influence of geometry, front-end stiffness and mass in car-to-car and car-to-truck collisions is discussed based on physical princi-

ples and mathematical formulae, building upon the current body of knowledge. Finally, the most feasible measures to improve the compatibility potential of passenger cars are identified and discussed.

Part 1 Relevance and implications of crash compatibility and structural interaction

In chapter 3, the real-world relevance of crash compatibility is investigated in an analysis of accident data. Accident statistics were extracted from the Volkswagen-GIDAS (German In-Depth Accident Study) database and manipulated by adding dataset restrictions to the initial (complete) dataset in a hierarchical approach.

In chapter 4, a definition for structural interaction is developed, based on the sparse amount of published literature relating to the phenomenon of structural interaction, documented in chapter 2. Several new metrics are also developed based on the conventional Equivalent Energy Speed metric (EES). These metrics are central to the new theory presented in this thesis and form the basis of the evaluation of structural interaction in later chapters.

The influence of structural interaction on acceleration-induced injury is investigated in car-to-car head-on collision simulations in chapter 5, based on occupant simulations.

Part 2 Proposed compatibility assessment procedures (Crash tests)

The second section of the thesis relates to compatibility assessment procedures (crash tests). Based on the observations made in chapters 1 to 5, the general requirements of a compatibility assessment procedure, focused on improving structural interaction, are identified in chapter 6.

In chapter 7, three currently proposed compatibility test procedures are critically evaluated. The requirements of a compatibility assessment procedure, identified in chapter 6, form the basis of this evaluation.

Part 3 Measuring, evaluating and maximising Structural Interaction

A method is developed in 8.1 to measure the degree of energy dissipation occurring through structural deformation in a crash test, based on accelerometers. This method is applied to several experimental crash tests in sections 8.2 and 8.3. In section 8.4, an initial evaluation of structural interaction is carried out for a number of car-to-car, head-on collisions.

In Chapter 9, the method to measure energy dissipation, developed in chapter 8, is applied and validated in FEM numerical crash test simulations. The influence of the vertical overlap of front-end structures on the resulting level of structural interaction is investigated. To complete the research, several constructive measures aimed at improving the structural interaction potential of passenger cars are investigated. The new EES metrics developed in chapter 4 form the basis of this evaluation.

2 Literature Review: Crash compatibility fundamentals

In this chapter, the fundamental considerations relating to crash compatibility are introduced, based on and building upon published literature. Published studies of accident data are reviewed and the influence of geometry, front-end stiffness and mass on compatibility in car-to-car and car-to-truck collisions is interpreted and discussed. In conclusion, the most feasible measures to improve crash compatibility are identified.

2.1 Background –Assessing vehicle safety

Today's safety assessments demand a high level of self protection from passenger cars. The self protection level of a passenger vehicle is commonly measured in relation to the occupants. Whilst self-protection is the focus of most safety assessments, the level of protection offered by a vehicle to pedestrians has also recently entered the domain of vehicle safety legislation.

To maximise occupant protection in collisions, both **compartment accelerations** and **intrusions** into the passenger compartment need to be minimised [28] [29] [30]. The injuries sustained by occupants involved in collisions can be caused by intrusions (leading to direct contact with the vehicle interior), high compartment accelerations or a combination of both.

Simultaneously minimising intrusions and compartment accelerations can be considered as a trade-off in vehicle design. To decrease compartment accelerations, lower interaction forces are required. When lower interaction forces are present, however, a greater degree of front-end deformation is required to dissipate a given amount of kinetic energy. Therefore, when interaction forces are reduced, the risk of compartment deformation increases.

In standardised consumer crash testing procedures such as EURO NCAP [8] as well as regulatory tests such as FMVSS 208 [7] and ECE-R94 [6], injury risk is estimated using numerous criteria. These criteria are based on the response of instrumented crash test dummies, developed to be representative of the bio-mechanical characteristics of human beings. The Head Injury Criterion (HIC) and Chest Acceleration, for example, are two criteria which reflect the risk of acceleration induced injury [31]. One study found that EURO NCAP's star rating of the potential for injury mitigation in collisions correlated well with the risk of serious injury or death faced by vehicle occupants in real world collisions [9][3].

Compartment accelerations are one cause of occupant injury. In frontal impacts, a modern restraint system offers a high level of protection to the occupant, filtering accelerations and preventing contact with the vehicle interior. However, with increasing collision severity, the risk of serious injury or death increases correspondingly, up to a point where restraint systems are not able to provide adequate protection. The risk of injury depends not only on the peak compartment accelerations but the shape of the acceleration-time characteristic and the time-frame over which high accelerations occur [32]. This relationship between crash severity and injury risk shows that there are upper limits for the mitigation of injury in collisions, which are also influenced by the tolerances of the human body to withstand accelerations. These limits are different for each occupant depending on their age, gender and other physiological factors[4].In any case, above certain collision severities, accident avoidance or a reduction in the crash severity itself are the only feasible strategies to protect the vehicle occupant.

[3] In EURO NCAP testing, vehicles are rated based on a star system, receiving 1 to 5 stars. The study concluded that the occupants of vehicles receiving 1 or 2 stars faced a higher risk of death or serious injury than occupants of vehicles receiving 4 or 5 stars. However, the report also mentions that the EURO NCAP star rating should not be viewed as a tool to definitively predict real-world safety performance.

[4] Zobel [33] Showed the risk faced by occupants in collisions to be strongly dependent on both occupant height and gender. The "aging population" phenomenon, occurring in the developed world, will result in a dramatic increase in the number of older drivers during the next decades [34]. This problem has been recognized by the US National Highway Traffic Safety Administration (NHTSA) and the implications for passenger vehicle safety discussed (See also [35] and [36]).

The functionality of the restraint system is only relevant as long as the passenger compartment remains intact and sufficient **survival space** is made available to the occupant. If a high amount of compartment deformation occurs, severe injuries could be sustained, even if a modern restraint system is deployed. Intrusions could lead to direct contact between the occupant and the hard (and intruding) components of the inside of the occupant compartment, even at low compartment acceleration levels. Compartment integrity ensures the occupant has adequate survival space and is therefore a fundamental requirement for occupant protection (see also [29] [30] [37]).

During collisions involving two vehicles, the risk of injury needs to be minimised for the occupants of both vehicles. This can be considered the goal of the concept of crash compatibility. The causes of incompatibility between passenger cars are commonly divided into three influence factors; **geometry, front-end stiffness and mass** [2] [17] [38] [39] [40]. Extensive research has been carried out to determine the influence of these factors on compatibility in real-world and experimental collisions [41] [42] [43] [44] [45]. A great deal of theory also exists describing the influence of each of these factors in the car-to-car head-on collision configuration based on physical principles and mathematical formulae ([15] [18] [29] [33] [46] [47] [48] [49]). This chapter summarises the field of research of crash compatibility, drawing on the existing body of knowledge. Furthermore, the goal conflicts and feasibility issues faced when controlling geometry, front-end stiffness and mass, to improve the potential for crash compatibility offered by passenger cars, are discussed.

2.2 Summary of existing accident data

The influence of geometry, front-end stiffness and mass can be investigated based on real-world accident data. Aggressivity ratings for passenger vehicles involved in collisions with other passenger vehicles were calculated by the National Highway Traffic Safety Administration (NHTSA) in the USA [25]. Aggressivity was measured based on the injury risk faced by the occupants of the struck vehicle in collisions involving two passenger vehicles. A correlation between vehicle aggressivity and mass was identified, indicating that heavier cars are more aggressive. However, the correlation between mass and vehicle aggressivity is only conclusive if vehicle geometry,

front-end stiffness and mass act as independent influence factors, which is not the case. These factors exhibit a degree of interdependency.

Studies have shown a relationship between mass and front-end stiffness, with heavier vehicles stiffer than lighter vehicles ([39] [50] [51]) based on accident statistics and physical principles. In other publications, a correlation between mass and geometry has been determined as well. In a Japanese publication, based on the fixed barrier crash testing of 22 vehicles, a correlation was observed between the height of vehicle structures (longitudinal height and engine top height) and vehicle mass [44]. Due to the inter-dependency between mass, geometry and stiffness, it cannot be concluded that aggressivity is linked only to vehicle mass. If the degree of stiffness compatibility and geometrical compatibility between all vehicles were to be improved, the influence of mass on aggressivity may be less significant than the correlation between mass and aggressivity suggests.

Other studies by NHTSA reveal that geometry has a significant influence on vehicle aggressivity as, within certain mass classes, a range of aggressivity values were calculated. This was concluded to be related to geometrical differences between passenger vehicles within the same mass classes. Sport Utility Vehicles (SUVs) and Pick-Ups were identified as being much more aggressive than passenger cars of the same mass [44] [45]. Geometry is concluded to be a significant factor influencing vehicle aggressivity in many other publications, for both head-on and front-to-side collisions [52] [53] [54] [55] [56] [57] [58].

The influence of geometry, however, is related to the collision severity. Some publications have claimed that poor geometrical compatibility may even lead to an improvement in occupant protection at lower collision severities [41] [42]. A reduction in the degree of geometrical compatibility leads to lower interaction forces and reduced passenger compartment accelerations, as front structures are activated to a lesser degree. Most researchers agree that reducing geometrical compatibility to improve occupant protection in collisions of low severity is an inappropriate goal, as reduced geometrical compatibility leads to an increased risk of compartment intrusions in collisions of high severity. The lower interaction forces and compartment accelerations resulting from poor geometrical compatibility may also delay the deployment of re-

straint systems, which are often triggered based on the acceleration-time characteristic of the passenger compartment during a collision (i.e. compartment accelerations are used to quantify the collision severity which acts as the basis for restraint system deployment) [59]. A delayed deployment of the restraint system may also reduce the effectiveness of the restraint system and, correspondingly, the level of protection offered to vehicle occupants.

Based on accident data, determining the isolated influence of geometry, front-end stiffness and mass in collisions involving two passenger vehicles is complex, given the interdependency between these variables. Whilst analyses of accident statistics can document the magnitude of the compatibility problem, the potential for improvement in compatibility through changes in front-end stiffness and geometry is difficult to quantify. In the following section, the theoretical influence of geometry, front-end stiffness and mass is discussed based on physical principles.

2.3 Compatibility theory

In this section, the theoretical influence of geometry, front-end stiffness and mass in car-to-car head-on collisions is discussed. An understanding of the theoretical influence of these three influence parameters is essential to determine the potential benefit and feasibility of controlling geometry, front-end stiffness and mass, to improve crash compatibility.

2.3.1 Geometry

Unlike mass and stiffness, vehicle geometry is difficult to objectively define. Geometry can be interpreted as the shape or the external form of a vehicle. With respect to compatibility, it is more appropriate to consider geometry in terms of the location and distribution of support forces offered to another vehicle, within the geometrical form of a vehicle (often referred to as the distribution of stiffness). This can be determined in fixed barrier crash tests, through a measurement of wall forces or barrier deformation [23] [60] [61].The cross beam, longitudinals and engine/transmission are structures often described as being highly relevant in vehicle collisions. Theoretically, if the force distribution of two vehicles is similar, higher interaction forces in a collision in-

volving these two vehicles would result and a higher degree of energy could be dissipated through structural deformation, within a given amount of deformation travel [17].

The front-end structure of a passenger vehicle can be considered to consist of multiple “load paths”, which connect the foremost surface of the front-end of the vehicle to the passenger compartment. In a frontal collision, load paths are designed to deform in preference to the passenger compartment, to dissipate kinetic energy within the crumple-zone (deformation-zone) of the front-end. If two vehicles exhibit poor geometrical compatibility in a head-on collision, not all of the load paths within the front-end of a passenger vehicle are forced to deform. A lack of geometrical compatibility therefore leads to a lower dissipation of kinetic energy through deformation of the front-end. In the most extreme cases (e.g. car-to-truck underrun accidents) a lack of geometrical compatibility can be dangerous for the occupants of passenger vehicles, even at low closing velocities. The first contact may occur between the windshield of the passenger vehicle and the truck-trailer, with the front-end of the passenger vehicle remaining largely undeformed. An example of poor geometrical compatibility is shown in Figure 2, below.

Figure 2 A truck underrun accident - An example of poor geometrical compatibility [62]

The front-end of the van shown in the picture underrode the truck trailer. If the two vehicles involved in this collision were to exhibit better geometrical compatibility, a higher degree of energy could have been dissipated through deformation of the front-end of the van. In this case, assuming conventional front-end design, a higher collision velocity could have been tolerated before significant intrusions into the compartment of the van would have occurred.

Vehicle front-end geometry is not evaluated in current regulatory and consumer crash testing. However, a first step toward improving geometrical compatibility was taken by the Alliance of Automobile Manufacturers (AAM) in the USA. A self-commitment was signed by all member manufacturers which specifies the height of primary energy absorbing structures (PEAS) [63].

2.3.2 Front-end stiffness

Front-end stiffness is a commonly used term to describe the magnitude of the forces resisting structural deformation, exhibited by the front-end of a given passenger vehicle. For each vehicle, a force versus displacement characteristic (where displacement refers to the degree of crush of the front-end) can be calculated for a given frontal collision. This characteristic also reflects the amount of deformation energy theoretically available within the front-end, before significant deformation of the compartment occurs[5]. In frontal crash tests against a fixed barrier, most of the initial kinetic energy of the vehicle is dissipated through plastic deformation of the front-end. The rest can be accounted for based on vehicle rebound and rotation and plastic compartment deformation. The front-end force-displacement characteristics of passenger vehicles are therefore optimised in response to the velocity of fixed barrier crash tests, in order to best manage the dissipation of the vehicle's kinetic energy and maximise the protection provided to the occupant [15] [64].

[5] In a collision involving a passenger vehicle, even at low collision velocities, a small degree of compartment deformation may occur, as discussed in the analysis of accident data in the previous section. Throughout this thesis, significant compartment intrusions are defined as those which can be associated with an increase in injury risk faced by the occupants.

In current fixed barrier crash tests, passenger vehicles are tested at the same initial velocity, which has implications for their structural characteristics [7]. It does ensure, however, a similar minimum level of self protection is offered by all vehicles[6].
There is a difference between the amount of available deformation travel within the front-end and the actual undeformed length of the front-end. Rigid, non-deformable components are located within the front-end of conventional passenger cars. After a given degree of front-end deformation, there is no more potential for deformation within the front-end itself and deformation of the compartment occurs. The available deformation length (the maximum degree of crush of the front-end of the vehicle which can occur before compartment deformation begins) is relatively constant for most vehicles, irrespective of vehicle mass [29].

The energy dissipated through deformation of the vehicle in a **fixed barrier** collision ($D_{barrier}$ or D_b) is given as product of the average deformation force ($\overline{F}$) and the total deformation travel (s_b):

$$D_b = \int F ds_b$$

therefore

$$D_b = \overline{F} s_b \tag{1}$$

Assuming the entire initial kinetic energy (E_{kin}) of a vehicle of mass (m) is dissipated through front-end deformation in a collision with a fixed barrier at a velocity (v_b):

$$E_{kin} = D_b$$

$$\overline{F} = \frac{1}{2 s_b} m v_b^2 \tag{2}$$

[6] Several publications have shown that, in collisions against a fixed barrier with a deformable element such as EURO NCAP and ECE R94, the energy absorbed by the deformable element is relatively constant for all vehicles. This has resulted in the common observation that the current tests are more severe for heavier vehicles than for lighter ones. See [65] for a detailed discussion relating to the influence of deformable elements on the self protection level of passenger vehicles.

Assuming all vehicles provide the same available front-end deformation travel (s_b)[7] :

$$\overline{F} \text{ is proportional to } mv_b^2$$

This explains the reason behind the differences in stiffness of vehicles of different mass, observed in published accident data (see section 2.2).

In summary, with respect to the velocity of crash testing procedures:

- **If all vehicles are tested at the same velocity and assuming all vehicles provide the same amount of available deformation travel, the average deformation force increases proportionally with vehicle mass.** *This infers a non-preventable stiffness incompatibility between vehicles of different masses.*

- **For a given vehicle, the average deformation force is proportional to the square of the crash test velocity.** *A small increase in the fixed barrier test velocity would demand a disproportionate increase in front-end stiffness[8].*

Stiffness compatibility

The simplest example of stiffness compatibility in head-on collisions is when two vehicles exhibit an identical force-displacement characteristic in a frontal collision against a fixed barrier. In this case, assuming perfect geometrical compatibility and assuming compartment integrity is maintained in the fixed barrier collision, complete deformation of both front-ends would occur in preference to deformation of either of the vehicle compartments [66]. As indicated by equation (2), this could only occur if vehicles of different mass were tested at different velocities. This means, however, that vehicles of different mass would offer differing degrees of self protection (again assuming the length of available deformation travel is constant for all vehicle) which is considered unacceptable.

[7] An increase in the amount of available deformation travel is not considered appropriate given other customer demands such as parking, turning-circle, handling etc. In addition, an increase in vehicle length infers an increase in mass as well, which also has implications for CO_2 emissions, an important environmental consideration.

[8] See also Seiffert [15] for a discussion of the implications of an increase in the fixed barrier crash test velocity on the potential for compatibility offered by passenger vehicles.

When considering the heavier of the two vehicles involved in a head-on collision, lower average front-end deformation forces are required to protect the lighter opponent. However, this represents a reduction in self protection for the heavier vehicle. A goal conflict exists in the design of the force-displacement characteristics of the front-end of the heavier vehicle, to fulfil competing demands for self- and partner protection. Several force-deflection characteristics were suggested by Appel [46] [48] to overcome this goal conflict, each with varying degrees of feasibility. Among others, rectangular characteristics (constant force) and characteristics involving an extension of the length of the vehicle front-end were discussed. Neither of these measures has proven to be feasible for implementation into modern motor vehicles.

Zobel [19] proposed the Bulkhead Concept, which considers the energy dissipation potential within the front-ends of two vehicles involved in a head-on collision. The Bulkhead Concept has become widely accepted as the most feasible way to approach the stiffness compatibility issue, for head-on collisions involving two passenger cars [29]. The Bulkhead Concept mathematically proves that:

Irrespective to the mass ratio of both vehicles involved in a head-on collision, enough deformation energy is available in both vehicle front-ends for a head-on collision at a closing velocity up to double the standard fixed barrier crash test velocity [49].

It can also be proven that, as the mass ratio of two passenger vehicles involved in a head-on collision deviates from 1, a slightly higher amount of deformation energy is available in the front-ends of both vehicles than the energy that would be required at a closing velocity equal to double the design speed [29].

An important prerequisite for the realisation of the Bulkhead Concept is that the maximum compartment force (resisting deformation) of the compartments of each vehicle exceeds the front-end deformation forces of the other vehicle. This is illustrated in Figure 3.

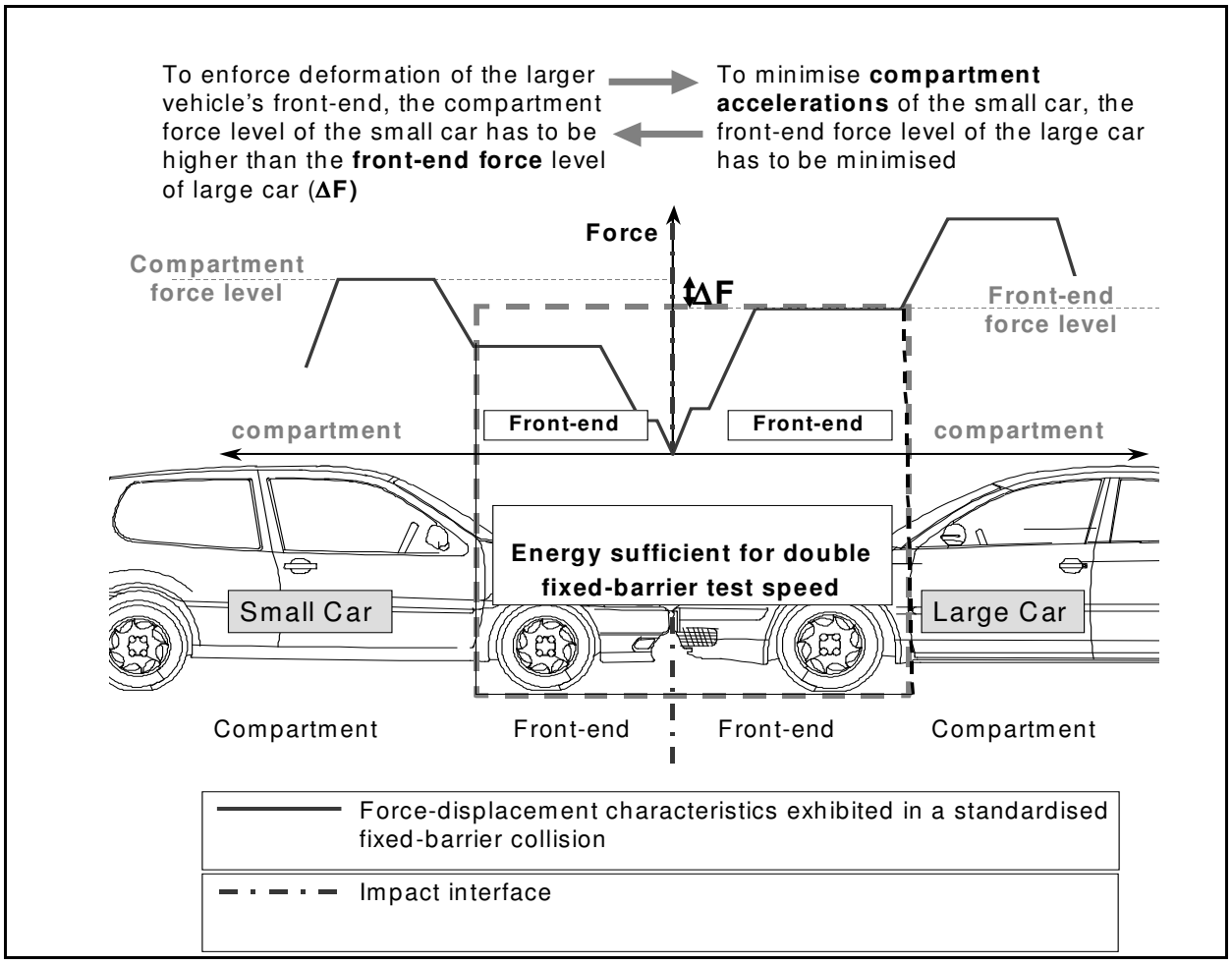

Figure 3 A prerequisite for the Bulkhead Concept: The critical relationship between the front-end deformation force of the heavier vehicle and the compartment resistance force of the lighter vehicle (based on [29])

The fact that all modern vehicles are tested at the same fixed barrier crash test velocity does not necessarily ensure that the force (resisting deformation) of the compartment of each vehicle exceeds the deformation forces of the front-end of the other vehicle involved in the collision, in the head-on configuration. In experimental car-to-car crash tests, the compartment of the small vehicle can undergo a large amount of deformation whilst the front-end of the heavier vehicle remains largely undeformed [21] [29] [42]. High compartment strength is a fundamental requirement for the smaller vehicle to achieve compatibility in head-on collisions at high closing speeds.

2.3.3 Mass

The momentum of a car involved in a collision is directly proportional to its mass. Due to the fact that the change in momentum of two bodies involved in a plastic collision is equal, the lighter body experiences a higher change in velocity during the collision.

Considering the law of the conservation of momentum, the sum of the momentum (M) of each vehicle before the collision is equal to the combined momentum of both vehicles after the collision. Therefore, for a vehicle of mass (m_i) and initial velocity (v_i) and another vehicle of mass (m_j) and initial velocity (v_j) travelling at the same resulting velocity (v_r) after a fully plastic collision, the momentum (M) before and after the crash is given as:

$$M = mv$$

$$M_{before} = M_{after}$$

$$m_i v_i + m_j v_j = (m_i + m_j)(v_r)$$

$$v_r = \frac{v_i + \frac{m_j}{m_i} v_j}{1 + \frac{m_j}{m_i}} \tag{3}$$

** Note: The formulae shown above are based on a simplified one-dimensional analysis, assuming the impact of both vehicles is centroidal. Rotational effects present in eccentric collisions are therefore not considered.*

The change in velocity of vehicle i (Δv_i) is given as the difference between the initial velocity (v_i) and the resulting velocity (v_r) :

$$\Delta v_i = v_r - v_i \tag{4}$$

Substituting equation (3) into equation (4), the change in velocity of vehicle i can be described in terms of the mass ratio (m_i/m_j) of the vehicles and the initial velocity of each vehicle (v_i and v_j):

$$\Delta v_i = \frac{v_i + \frac{m_j}{m_i} v_j}{1 + \frac{m_j}{m_i}} - v_i = \frac{v_j - v_i}{1 + \frac{m_i}{m_j}} \tag{5}$$

which can also be re-written in terms of the closing velocity (v_C) where

$$v_c = v_j - v_i$$

therefore

$$\Delta v_i = \frac{v_c}{\left(1 + \frac{m_i}{m_j}\right)} = v_c \cdot \frac{m_j}{m_j + m_i} \tag{6}$$

Equation (6) shows that the only direct influence of mass in a car-to-car collision is to determine the change in velocity of both cars[9]. This is related to the mass ratio of the vehicles and not the absolute mass of each vehicle.

Based on equation (6), the change in velocity of vehicle i, for a mass ratio (m_i/m_j) smaller than 1, equal to 1 and greater than 1, ranges between the following limits:

[9] The interdependency between mass and stiffness and mass and geometry observed in the summary of existing literature (3.1) doesn't relate to the theoretical influence of mass in car-to-car, head-on collisions. It can be viewed as a result of customer demands placed on the vehicle manufacturing process restricting the dimension of a vehicles, in particular the length of the front-end.

$$\frac{m_i}{m_j} > 1, \qquad 0 < \Delta v_i < \frac{1}{2} v_c$$

$$\frac{m_i}{m_j} = 1, \qquad \Delta v_i = \frac{1}{2} v_c$$

$$\frac{m_i}{m_j} < 1, \qquad \frac{1}{2} v_c < \Delta v_i < v_c$$

Whilst the change in velocity is one consideration in car-to-car collisions, compartment accelerations have to be considered as well. For a mass ratio (m_i/m_j) smaller than 1, vehicle i undergoes a higher change in velocity than vehicle j. As the collision duration is equal for both vehicles, the acceleration of vehicle i exceeds the acceleration of vehicle j.

Zobel calculated the compartment accelerations experienced by the lighter vehicle involved in a head-on collision, to determine an upper mass ratio limit for the Bulkhead Concept [19]. Based on equation (2), describing the average deformation force of a vehicle in a fixed barrier collision and assuming $m_i > m_j$:

The average acceleration of the lighter vehicle vehicle $\bar{a}_j$, involved in a head-on collision, is dependent on the mass ratio of the vehicles (m_i/m_j), the available deformation travel of the large vehicle (s_i) as well as the fixed barrier test-velocity (v_b):

$$\bar{F} = \frac{1}{2 s_b} m v_b^2$$

therefore

$$\bar{a}_j = \frac{1}{2 s_i} \frac{m_i}{m_j} v_b^2 \qquad (7)$$

2.3.4 The implications of mass with respect to the Bulkhead Concept

As described in the beginning of this chapter, the potential for providing adequate protection to occupants involved in collisions decreases as the crash severity and compartment accelerations increase. The Bulkhead Concept proves that the total change in kinetic energy of both vehicles can be dissipated within the front-ends of both vehicles, up to a closing velocity equal to twice the fixed barrier crash test velocity (v_B). This relationship is valid irrespective of mass and assumes that the resistance-to-deformation force of the compartment of each vehicle exceeds the front-end deformation forces of the other vehicle involved in a collision in the head-on configuration (see Figure 3). This doesn't ensure, however, that the corresponding compartment accelerations can be tolerated by the occupants.
For a collision involving two vehicles with a high mass ratio, the occupants of the lighter vehicle experience much higher acceleration loadings and the mass ratio is one limitation on the feasibility of the Bulkhead Concept.

Based on equation (7), for $m_i / m_j = 1.6,\ v_b = 56 km/h\ and\ s_i = 0.6m$, the average compartment acceleration of the lighter vehicle is equal to 32g. For more realistic non-constant force-displacement characteristics, the peak deformation forces would be higher than the average value [33].

A mass ratio of 1:1.6 was therefore proposed as an upper limit for the Bulkhead Concept, when considering the resulting accelerations of the compartment of the lighter vehicle. Around 85% of injured occupants were determined to be involved in collisions in which the mass ratio of the involved vehicles was less than 1:1.6. This was valid for all AIS injury values (i.e. MAIS0+, MAIS2+, MAIS3+, MAIS4+ and MAIS5+)[10]. The study was based on accident data extracted from the VW-GIDAS Accident Database[11].

[10] The AIS (Abbreviated Injury Scale) is used to describe the degree of physical impairment associated with a particular injury. MAIS refers to the maximum AIS number of all AIS injuries sustained by a particular person [67].

[11] For a detailed description of the VW-GIDAS database, consult [68].

2.4 Structural Interaction

Compatibility discussions have traditionally related to the influence of geometry, front-end stiffness and mass in collisions involving two passenger cars. Whilst mass and stiffness can be objectively described (in real number terms), it is more difficult to describe vehicle geometry in an objective manner. To investigate the implications of geometry in car-to-car collisions, the interaction of vehicle structures "Structural Interaction" can be studied. Vehicle geometry can be considered as a parameter which influences the degree of structural interaction that occurs in a given collision.

The influence of car front geometry in real-world collisions has been subjectively discussed for many years. The behaviour of vehicle structures in crash-testing procedures is not always identical to the behaviour in real-world collisions when the object impacted is another vehicle [69]. A vertical misalignment of structures during a collision is often characterised as over-and underriding. The term "fork-effect", a horizontal mismatch of structures resulting in low resistance forces and low energy dissipation through deformation, is also commonly applied [70]. Both of these phenomena influence the degree of structural interaction occurring in a collision. **Structural interaction** has become a commonly used term in safety research circles and many groups have identified good structural interaction as one of the most important requirements for compatibility in car-to-car collisions [17] [20] [60] [71] [72]. **Unlike geometry, mass and stiffness, structural interaction cannot be considered as a parameter which influences crash compatibility, but rather a measure of the degree of compatibility exhibited by two vehicles (or a vehicle and another object such as a tree, guard-rail, etc) in a given collision.**

Several authors have described structural interaction with varying levels of abstraction. In [72] a statement is made that *"only by guaranteeing structural interaction, can structures of different opposing vehicles be used up efficiently".* In [71], structural interaction is described as the amount of energy dissipated in a crash involving two vehicles, compared to that theoretically available, based on the energy dissipation in a fixed barrier collision. Building on this in [61], maximal structural interaction is described as occurring when structural components of the front-end deform at the same force-level as in a fixed barrier crash test. A general statement about structural interaction is made in [23]; *" In order to take advantage of all the potential for energy ab-*

sorption, structures must interact correctly". Two measures to improve the structural interaction potential of passenger cars were proposed in [73]; a homogeneous distribution of load paths and strong connections between load paths.

Optimising the interaction of structures, however, depends on the crash severity. In the final report of the EUCAR-Compatibility Project (a compatibility project funded by the European Union involving numerous experimental car-to-car and car-to-fixed wall crash tests) the following statement was made: *"At low speeds there were indications that it was beneficial to reduce the amount of interaction since this produced lower forces on the occupants. At high severity it was seen as important to maximise the interaction since this ensured higher levels of energy absorption by the structure and a reduction in compartment intrusions"* [42]. This confirms the statement made in section 2.2, that poor geometrical compatibility could lead to a reduction in occupant injury risk in collisions of low severity.

Whilst several researchers have begun to describe the phenomenon of structural interaction, an objective definition was not found in published literature. In chapter 4, a definition for structural interaction is developed and several metrics to evaluate structural interaction presented.

2.4.1 EES –Equivalent Energy Speed

In section 4.4, several new metrics are developed to evaluate the degree of compatibility of a given collision, based on the concept of EES [74].

In a collision with a deformable body, the structure of a passenger vehicle is not necessarily loaded to the same degree as the change in velocity would suggest. Energy could also be dissipated through deformation of the other object, in preference to deformation of the structure of the vehicle in question. In extreme cases, the vehicle in focus may undergo relatively little deformation, whilst the other object is destroyed. The EES (Equivalent Energy Speed) is a commonly used measure to describe the degree of structural loading in a collision. The result is an equivalent velocity which is based on the energy dissipated through deformation of the vehicle structure (D).

$$D = \frac{1}{2} \cdot m \cdot EES^2$$
$$EES = \sqrt{\frac{2D}{m}} \quad (8)$$

The EES metric considers the entire quantity of energy dissipated within a vehicle in a given collision. To enable this metric to be distinguished from new metrics to be introduced in section 4.4, the EES will be referred to as the EESV through this thesis, where V refers to the particular vehicle being considered.

2.5 Car-to-truck collisions

In this section, the formulae describing the influence of geometry, stiffness and mass in car-to-car collisions are applied for the case the case of car-to-truck collisions. See [61] for a more detailed discussion of this topic.

As the mass ratio of the vehicles involved in car-to-truck collisions is much higher than in car-to-car collisions, the implications of geometry, front-end stiffness and mass have to be re-interpreted. **Given the significant differences in the ground clearance of both vehicles, ensuring geometrical compatibility to enable good structural interaction is the most important requirement in car-to-truck collisions.**

In order to improve structural interaction in car-to-truck collisions, underrun protection systems, fitted to the truck, are essential. Rear underrun protection is obligatory by law in the USA and in Europe and must provide protection from the trailer extending down to a ground clearance of 550mm (EUROPE) and 560mm (USA) [75] [76]. A ground clearance of at least 400mm is required for rear truck underrun protection to enable trucks to drive onto sea-bound ferries [77]. If no underrun protection is present, even crashes of low severity could pose a high risk for the occupants of a passenger car.

In car-to-truck accidents, the mass ratio is high (e.g. a collision involving a truck of mass 40 tonnes and a heavy car of mass 2 tonnes, yields a mass ratio of 20:1). For this mass ratio, the change in velocity of each vehicle can be calculated based on equation (6).

$$\Delta v_{car} = \frac{v_c}{\left(1+\frac{2}{40}\right)} = \frac{20}{21} v_c$$

$$\Delta v_{truck} = \frac{v_c}{\left(1+\frac{40}{2}\right)} = \frac{1}{21} v_c$$

The change in velocity of the car is almost equal to the closing velocity of the collision. The change in velocity of the truck is negligible and self protection is not relevant for the truck in this collision configuration. To improve compatibility between trucks and cars, the partner protection provided by the truck in combination with the self protection offered by the car is of relevance. Two types of underrun protection are conceivable, rigid or deformable. Deformable underrun protection offers a higher degree of partner protection, as the change in kinetic energy of the car can be accounted for through deformation of both the car front-end as well as the underrun protection itself. A prerequisite for all truck underrun protection is that adequate force is provided by the underrun protection to deform the front-end of the vehicle.

Based on the deformation energy available in the front-end of the car in a fixed barrier collision, a maximum closing velocity for a car-to-truck collision can be calculated. At this closing velocity, the entire deformation energy available in the front-end of the car is dissipated through deformation and intrusions no greater than those occurring in a frontal crash test are expected to occur.

Based on the assumption that the change in kinetic energy of the car is equal to the closing velocity (v_c), i.e. assuming an infinite mass ratio, the required deformation energy (D_{req}), can be described as [61]:

$$D_{req} = \frac{1}{2} m_{car} v_c^{\,2}$$

For perfectly rigid underrun protection, the change in kinetic energy of the car can be dissipated through deformation of the car structure only. Assuming that the available deformation energy in the front-end of the vehicle ($D_{available}$) is equal to the initial kinetic energy of the vehicle in a fixed barrier collision at a velocity equal to v_b:

$$D_{available} = \frac{1}{2} m_{car} {v_b}^2$$

Theoretically, compartment integrity can be maintained as long as the deformation energy available in the front-end exceeds the required deformation energy (assuming perfect structural interaction and complete activation of the vehicle front-end):

$$D_{req} < D_{available}$$

$$\frac{1}{2} m_{car} {v_c}^2 < \frac{1}{2} m_{car} {v_b}^2$$

$$v_c < v_b$$

Therefore, for the case of rigid underrun protection, maintaining compartment integrity is feasible up to a closing velocity equal to the fixed barrier crash test velocity (v_b). If the underrun protection was deformable and provided the same amount of energy as the car, compartment integrity could be maintained up to a higher closing velocity:

If the underrun protection itself offered an amount of deformation energy equal to that offered by the passenger car:

$$D_{req} < D_{available}$$

$$\frac{1}{2} m_{car} {v_c}^2 < 2\left(\frac{1}{2} m_{car} {v_b}^2\right)$$

$$v_c < \sqrt{2} v_b$$

In this case, however, the change in velocity of the car would be much higher than in the current fixed barrier crash tests. The change in kinetic energy of the occupants would therefore be greater as well. This would pose a further challenge for restraint system design and my lead to an increase in restraint system aggressivity.

Deformable underrun protection must, in all cases, provide a reaction force which exceeds the deformation forces within the front-end of the striking car to ensure all of the deformation energy available in the front-end of the striking car is dissipated.

2.6 Feasible measures to improve compatibility

Whilst the influence of geometry, front-end stiffness and mass in car-to-car, head-on collisions has been documented in this chapter, the feasibility of controlling each of these factors needs to be considered as well. Controlling vehicle geometry appears to be the most feasible step to improve the crash compatibility potential of passenger cars.

Controlling vehicle mass to improve compatibility within the fleet is only effective if the average mass ratio associated with car-to-car collisions is reduced (see section 2.3.3). This demands a convergence of vehicle mass within the vehicle fleet, which infers either an increase in mass for light vehicles or a decrease in mass for heavier vehicles would be required. However, the mass of a vehicle is a consequence of customer demand for different vehicle properties and applications, for fuel economy requirements, for towing or transporting goods as well as vehicle performance and handling and environmental considerations. Placing either an upper or lower restriction on vehicle mass is not considered feasible, as this would contradict customer demand[12].

Controlling vehicle front-end stiffness to improve compatibility offers low feasibility as well. An inherent dependency between mass and stiffness has to be accepted to ensure an equal level of self protection is provided by all vehicles (assuming the amount of available deformation travel is constant for all vehicles). This results in stiffness incompatibility between vehicles of different mass. **Controlling front-end stiffness (based on the mean deformation force) to improve compatibility**

[12] Appel et al [78] and Jewkes et al [79] confirm that a reduction in injury risk would only occur if the average mass ratio of vehicles involved in collisions were to be reduced.

doesn't offer a high level of feasibility, as it would result in a loss in self protection for heavier vehicles.

Note: The statement above (in bold) is based on the analysis carried out in 2.3.2 where front-end stiffness was represented by a term describing the average force level ($\overline{F}$) for the entire deformation travel of the vehicle front-end. The shape of the force-displacement characteristic of the vehicle front-end could be varied for a given $\overline{F}$ value, potentially improving the stiffness compatibility of a collision involving two vehicles. This is beyond the scope of the research presented in this thesis. This topic is covered further in recommendations for further research, 10.2.

Based on the discussion in this chapter, two measures have been identified which offer the greatest potential to improve the crash compatibility potential of passenger vehicles:

- Controlling vehicle geometry (to improve the potential for good structural interaction)
- Ensuring adequate compartment strength

Controlling vehicle geometry to improve structural interaction

Geometry is not considered in current regulatory and consumer-based self protection assessment procedures. Geometry can, within limits, be manipulated independent of vehicle mass. Therefore the goal conflicts and feasibility issues related to controlling mass and stiffness can be overcome. Through controlling geometry with the aim of improving structural interaction, an improvement in both self- and partner protection can be achieved, without reducing the level of self protection offered by passenger vehicles.

As all vehicles translate in the horizontal plane, improving geometrical compatibility in the horizontal direction is complex, as an infinite number of collision configurations could occur. In the vertical direction, the ground clearance of many structures is rela-

tively fixed[13]. The convergence of structures to within certain vertical limits could significantly improve the level of geometrical compatibility within the vehicle fleet. Collisions involving cars and trucks as well as single vehicle collisions involving roadside infrastructure are additional considerations. The ground clearance of car longitudinal members, truck underrun protection systems and roadside infrastructure are shown in Figure 4. This summarises the considerations when determining the geometrical heights of front structures of passenger vehicles, to maximise geometrical compatibility and structural interaction in real-world collisions.

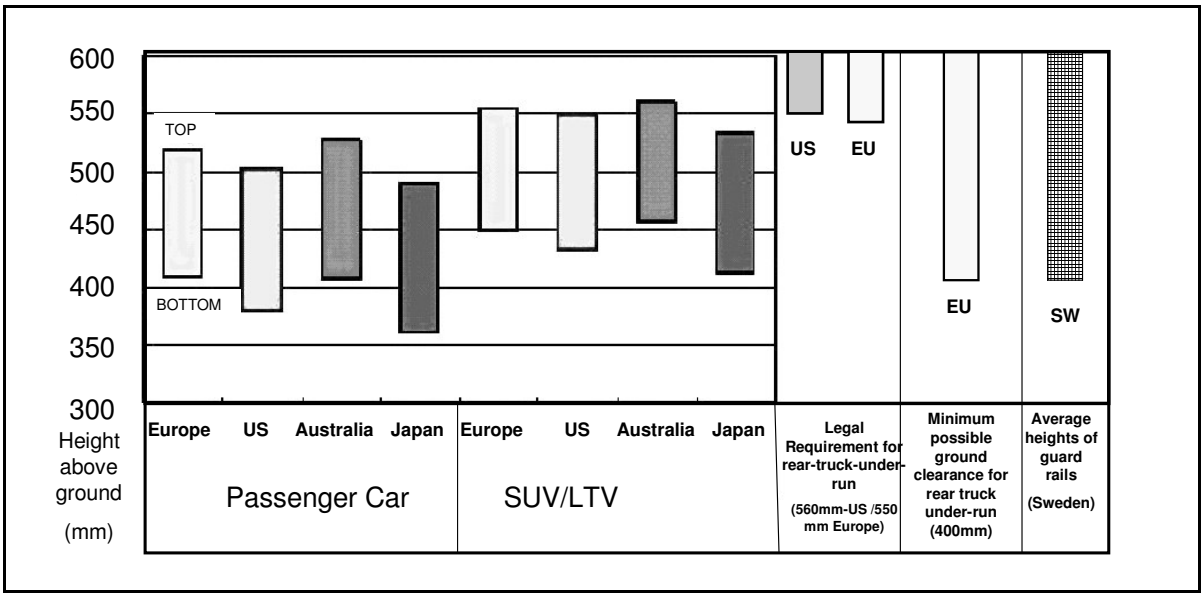

Figure 4 Ground clearance of average top and bottom edges of longitudinal members from fleets around the world, the current legal requirement for the height of rear underrun protection, the minimum allowable ground clearance for rear truck underrun protection and the average heights of guard-rails [20] [75] [76] [81]

Figure 4 shows the differences in longitudinal height for passenger cars, Sport Utility Vehicles (SUVs) and Light Trucks and Vans (LTVs) for fleets around the world. The difference between the average top and bottom height of longitudinal members of SUVs/LTVs and passenger cars is significant. This can be considered to be a reason for the difference in aggressivity observed in the USA for passenger vehicles and SUVs/LTVs of similar mass, as discussed in section 2.2.

[13] The height of vehicle structures is influenced mainly by manufacturing tolerances, suspension travel as well as the dynamic state of the vehicle directly before impact (e.g. the dipping of the front-end of a passenger-car due to braking can lead to a vertical displacement of the tip of the front-end of up to 100mm [80]).

Figure 4 also indicates that lowering rear truck underrun protection to 400mm is essential to achieve greater compatibility with passenger cars[14].

Maximising compartment stability

Ensuring adequate compartment strength for all vehicles would reduce the risk of global compartment intrusion in all collisions. Survival space is a very fundamental requirement of passenger car occupants in collision situations. The Bulkhead Concept (2.3.2 and 2.3.4) also indicates the importance of compartment stability for crash compatibility in head-on collisions, particularly for the smaller of the two vehicles. Increasing compartment stiffness represents an increase in self protection without a corresponding increase in aggressivity.

[14] During a meeting involving European Truck and Trailer manufacturers and passenger car manufacturers, it was concluded that the rear underrun protection for trailers could be lowered to a ground clearance of 400mm. A further extension of truck underrun protection toward ground level was considered unfeasible, due to approach angle requirements (e.g. when boarding truck ferries).

3 Compatibility and real-world accidents

In this chapter, results of an analysis of German accident data are presented. The analysis was carried out through extraction and manipulation of data from a dataset owned by Volkswagen AG[15], which is considered to be representative of the accident environment in Germany. This builds upon the summary of existing accident data included in section 2.2. The goal of this analysis was to provide a transparent evaluation of the relevance of compatibility in real-world accidents.

The ultimate goal of measures to improve automotive safety is to achieve a reduction in the number and severity of injuries sustained by vehicle occupants involved in traffic accidents. The statistical relevance of various compatibility-related collision configurations is estimated, based on the injuries sustained by the occupants of the passenger vehicles involved in collisions. The results are summarised and the collision configurations which are relevant for compatibility are ranked based on their statistical significance and a subjective estimation of the potential for injury reduction within each configuration.

3.1 Description of the statistical sample and analysis method

A hierarchical approach, beginning with few restrictions on the statistical sample, was applied, Figure 5. This enables an overview of the statistical relevance of each accident configuration in the context of the complete traffic accident environment. The analysis considers both the total number of occupants involved in collisions (MAIS0+) in which at least one person was injured and the total number of seriously injured occupants (MAIS 3+). Frontal and side impacts are fundamentally different with re-

[15] The analysis of real-world accidents carried out in this section is based on data from the VW-GIDAS (German-In-Depth-Accident-Study) database [68]. The database contains accident data collected by the Hanover Medical University and the Technical University of Dresden. The initial dataset contains all vehicle occupants involved in a collision in which at least one person sustained an MAIS1+ injury in an accident occurring after and including 1991, irrespective of the build year of the vehicle. Total number of known involved occupants in sample: 23840. Total number of MAIS3+ injured occupants in sample: 901.

spect to the deployment and effectiveness of restraint systems as well as the stiffness and geometry of side and front-structures. Side impacts and front impacts are considered separately in this analysis.

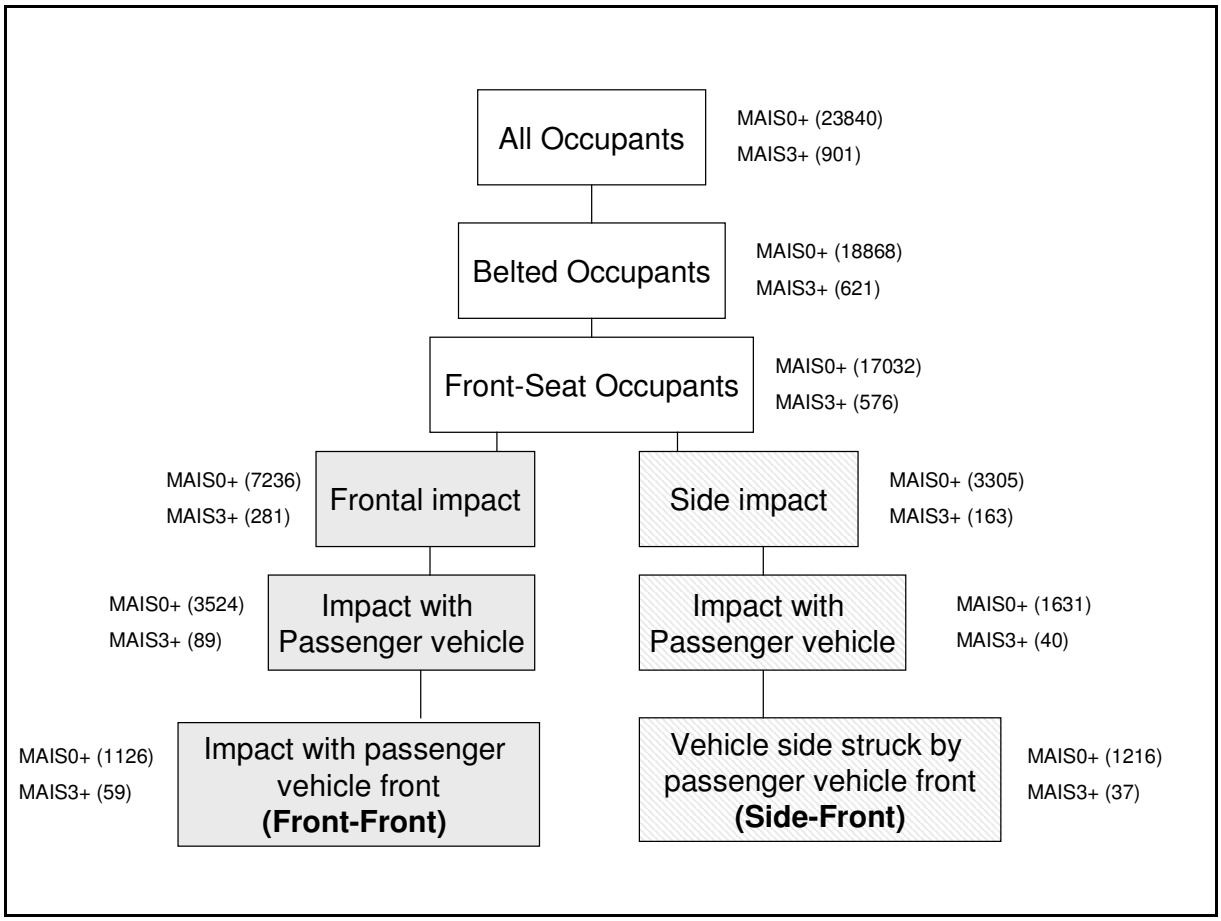

Figure 5 Overview - Hierarchical Analysis of Accident Statistics

In the first stage of the analysis, all occupants involved in accidents of all configurations (MAIS0+), irrespective of the struck region of the vehicle in focus and the other vehicle/object involved in the collision, are considered. The influence of the dataset restrictions, considering only belted occupants and considering only front-seat occupants, are shown in Figure 6.

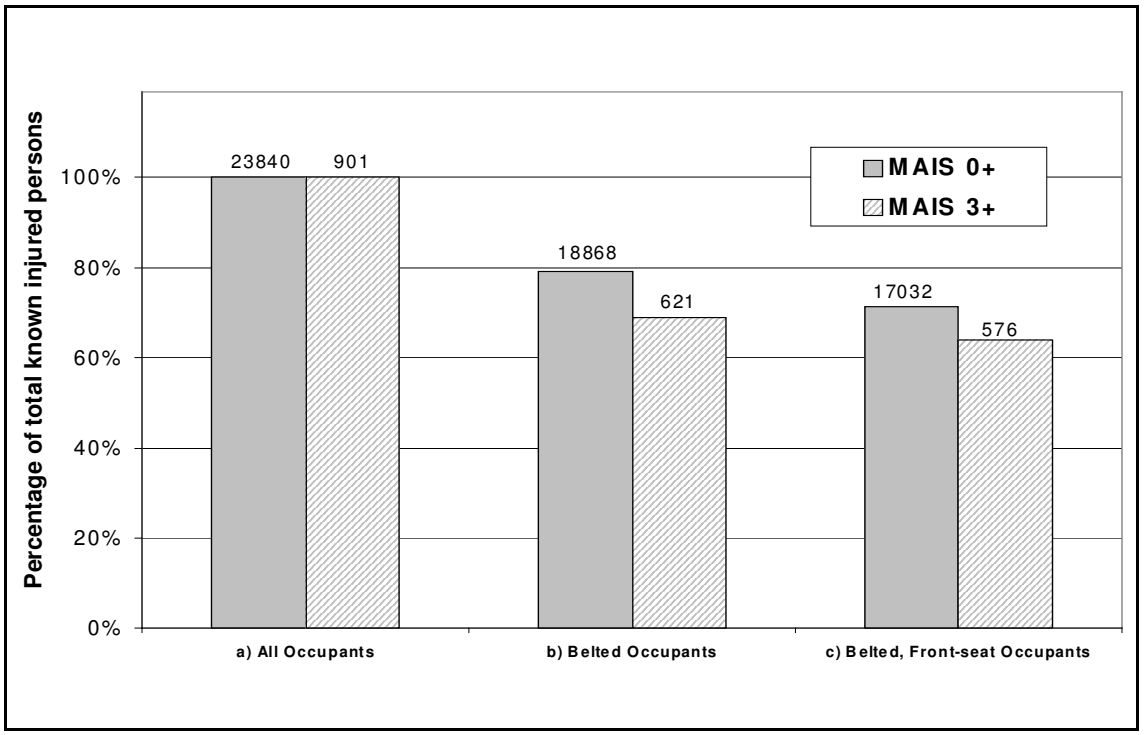

Figure 6 The influence of initial sample set restrictions on occupant injury numbers for all impact configurations

The initial data set restriction (a-to-b) contains the sample considering only belted occupants, reducing the number of known seriously injured (MAIS 3+) occupants to 69% and the total known number of occupants (MAIS 0+) to 79% of the initial number in the sample, Figure 6. The disproportionate decrease in the number of seriously injured (MAIS3+) occupants compared to all occupants (MAIS0+) reflects the lower risk faced by belted occupants of passenger vehicles. Injury risk will be referred to throughout this chapter as the risk of serious injury (MAIS3+) faced by an occupant involved in a collision in which at least one occupant was injured[16], i.e.:

$$\text{Risk of sustaining a serious injury} = \frac{n(MAIS3+)}{n(MAIS0+)}$$

This yields, for all occupants and belted occupants respectively, based on Figure 6:

[16] Risk in this calculation does not represent an exposure-based risk, because not all accidents which occur are considered in the sample analysed. A true exposure figure is therefore lacking as only accidents in which at least one person involved in the accident was injured are considered. The actual risk of serious injury, if all accidents were considered, including those where no persons were injured, would be lower.

$$\text{Risk of sustaining a serious injury (all occupants)} = \frac{n(MAIS3+)}{n(MAIS0+)} = \frac{901}{23840} = 3.78\%$$

$$\text{Risk of sustaining a serious injury (belted occupants)} = \frac{n(MAIS3+)}{n(MAIS0+)} = \frac{621}{18868} = 3.29\%$$

$$\text{Risk of sustaining a serious injury (unbelted occupants)} = \frac{n(MAIS3+)}{n(MAIS0+)} = \frac{901-621}{23840-18868} = 5.63\%$$

Belt usage is mandatory in Europe and belt users are in an overwhelming majority[17]. Unbelted passengers also face twice the risk of serious injury as belted occupants (5.63% compared to 3.29%). In addition, any changes to the vehicle structure are not expected to have a significant influence on injury-risk for non-belted occupants. For these reasons, only belted occupants are considered in the following analyses.

The next restriction on the sample (columns b-to-c, Figure 6) reduces the sample to consider only belted front-seat occupants. The total number of occupants in the sample (MAIS0+) falls to 71% and the number of seriously injured occupants (MAIS3+) falls to 64% of the number present in the original sample. Relatively few rear occupants are injured in vehicle collisions, probably due to low rear-seat occupancy rates and the greater amount of survival space offered to rear-seat occupants in frontal collisions. Given the low number of injured rear occupants, rear occupants are also removed from the sample for further analyses. For the occupants remaining in the dataset, front and side impacts are analysed separately in the following pages.

[17] Based on the International Road Traffic and Accident Database (IRTAD), the belt-usage rate on German roads varied between 90 and 97%. Small differences were observed for highways, country roads and city roads, respectively [82]. The actual belt usage rate in the VW GIDAS database is 91.9% within city limits and 90.9% outside city limits.

3.2 Frontal impacts for belted front-seat passenger vehicle occupants

A large proportion of both MAIS0+ and MAIS3+ belted front-seat occupants are involved in frontal impacts, Figure 7 Columns c-to-d.

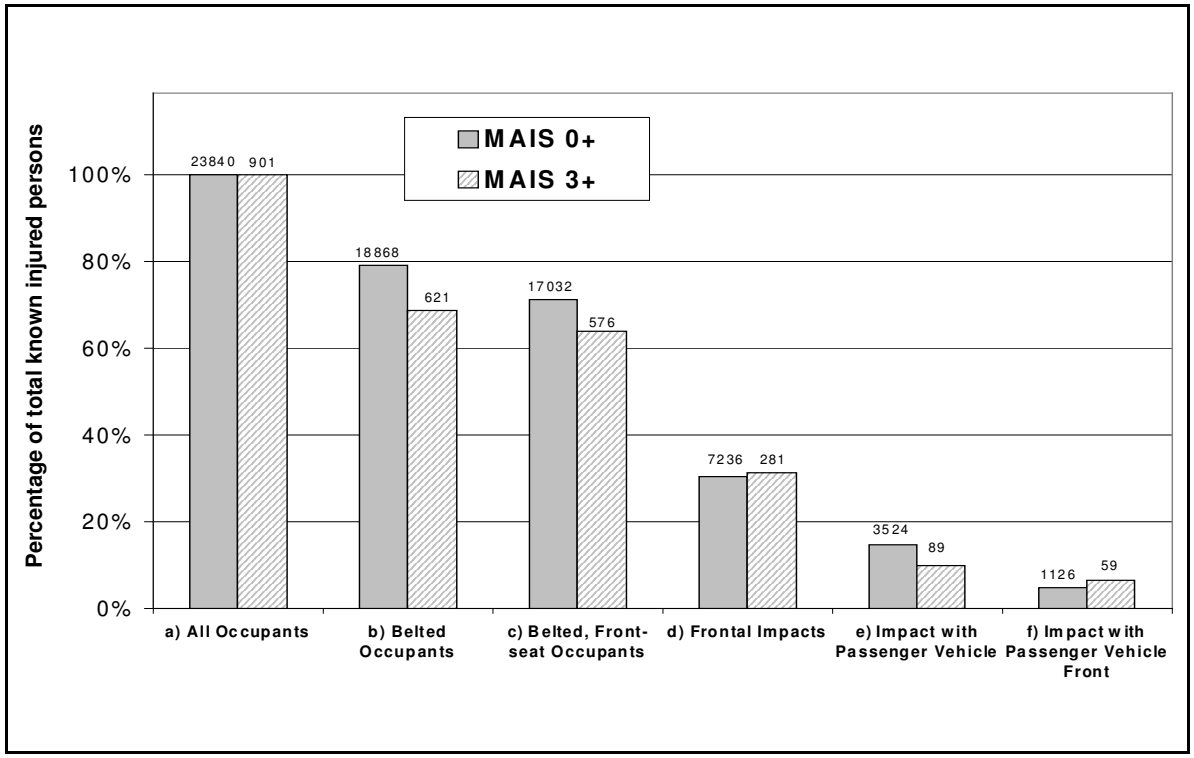

Figure 7 Statistical relevance of frontal impacts for all belted front-seat occupants

To further investigate frontal collisions, the distribution of impact objects for belted front-seat passenger vehicle occupants involved in frontal collisions is shown in Figure 8 and Figure 9.

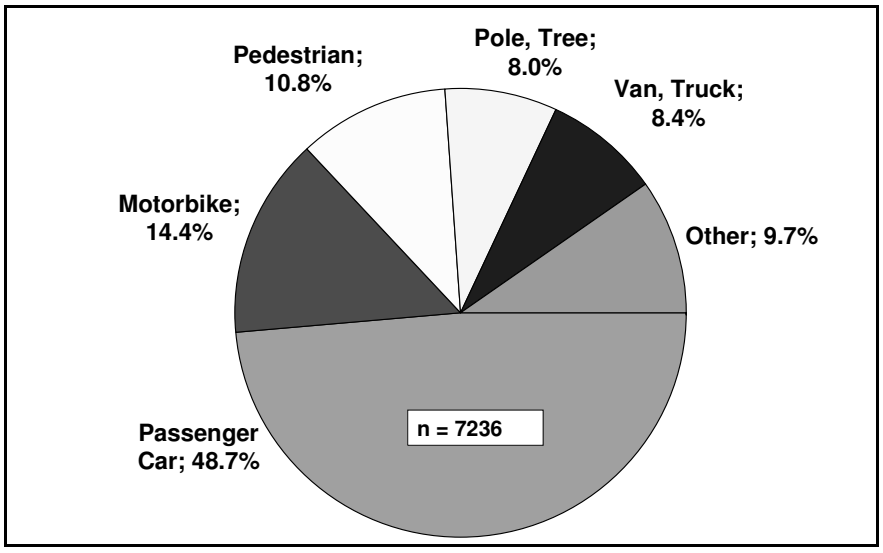

Figure 8 Distribution of all (MAIS 0+) belted front-seat occupants involved in frontal collisions with respect to the impact object

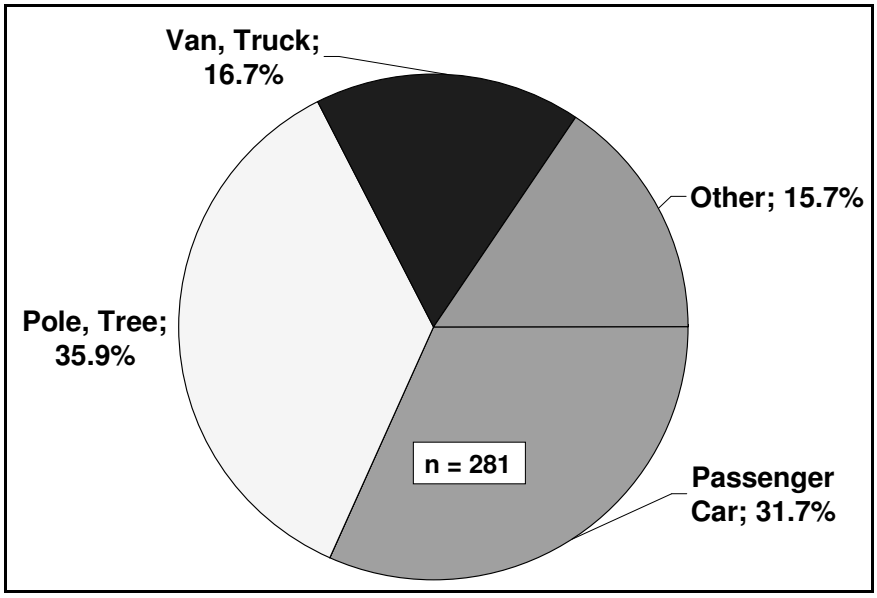

Figure 9 Distribution of all seriously injured (MAIS 3+) belted front-seat occupants involved in frontal collisions with respect to the impact object

Figure 8 and Figure 9 show that the distribution of impact objects varies greatly when considering all (MAIS0+) occupants and all seriously injured (MAIS3+) occupants, respectively. This indicates that the risk of sustaining a serious injury faced by all injured belted front-seat passenger-car occupants varies depending on the impact object. The injury risk faced by the occupants for the different collision configurations is summarised in Figure 10, below.

Accident Configuration	All involved occupants (MAIS0+)	Seriously injured occupants (MAIS3+)	Risk of a MAIS3+ injury
Car front - Car	3524	89	2.5%
Car front - Pole/Tree	579	101	17.4%
Car front - Truck	608	47	7.7%

Figure 10 The risk of serious injury based on the impact object for belted front-seat occupants involved in frontal collisions

The total number of occupants involved in collisions with a pole/tree is relatively low (579, Figure 10) yet the risk of serious (MAIS3+) injury in this collision configuration is very high (17.4%, Figure 10). Conversely, the number of belted front-seat occupants involved in collisions with passengers cars is much higher (3524, Figure 10) whereas the risk of serious injury is much lower (2.5%, Figure 10). A similar number of belted front-seat occupants are involved in collisions with trucks as with poles and trees (608, Figure 10). The relative risk of sustaining a serious injury faced by these occupants is 7.7%.

The results of this section show that collisions with other vehicles and, to a lesser degree, collisions with trucks are also statistically significant, considering the total number of MAIS3+ injuries sustained. Both of these collision configurations are important with respect to compatibility. Collisions with poles/trees, whilst less frequent, pose a very high risk and are therefore of high statistical relevance as well. This underlines the importance of self protection in today's accident environment, confirming the statement made in chapter 2 that the current level of self protection offered by passenger vehicles should not be compromised to improve crash compatibility.

Intrusion in car-to-car head-on collisions

The last step in the hierarchical analysis restricts the sample to include only head-on impacts involving passenger vehicles. This reduces the number of MAIS0+ occupants from 3524 to 1126 and the number of occupants sustaining an MAIS 3+ injury

from 89 to 59, Figure 7. For this collision configuration, the influence of intrusion on occupant injury risk is summarised in Figure 11[18].

	All involved occupants (MAIS0+)	Seriously injured occupants (MAIS3+)	Risk of a MAIS3+ injury
Significant Intrusion	177	38	21.5%
Insignificant Intrusion	949	21	2.2%

Figure 11 Influence of significant compartment intrusion on occupant injury risk for all belted front-seat occupants involved in a head-on collision with another vehicle

Figure 11 indicates that compartment intrusion occurs in relatively few head-on collisions involving passenger cars (177 from 1126 cases, Figure 11). When significant compartment intrusions occur in head-on collisions involving two passenger cars, the risk of serious (MAIS3+) injuries is very high **(**21.5%, Figure 11), around ten times greater than cases where no significant intrusions occur (2.2%, Figure 11)[19]. **The high risk of injury associated with intrusion in car-to-car head-on-collisions indicates that survival space is a fundamental safety requirement for vehicle-occupants involved in frontal collisions.**

3.3 Side impacts for belted front-seat passenger vehicle occupants

The same hierarchical approach used for the analysis of frontal collisions was applied to investigate the statistical relevance of the side impact configuration in real-world collisions. Figure 12 shows the influence of dataset restrictions on the number of MAIS 0+ and MAIS 3+, belted front-seat occupants involved in side impacts.

[18] As a small degree of intrusion into the passenger compartment can occur with no real associated injury risk, the level of intrusion into the passenger compartment is separated into “significant” and “non-significant” intrusion, based on a Vehicle Deformation Index (VDI). Significant intrusion is categorised as all cases where VDI6>=4 (See Appendix 1 for an illustration of the VDI). Above this threshold, compartment intrusion is assumed to be a significant causation of occupant injury.

[19] Collisions in which intrusion occurs may represent crashes of higher severity. Part of the increase in risk faced by the occupants when intrusion occurs could also be due to the fact that higher compartment acceleration levels are associated with these collisions. Schwarz/Busch/Zobel showed, however, that occupants were quite resilient to acceleration based injuries and that compartment integrity is the most fundamental consideration when maximising occupant protection [30].

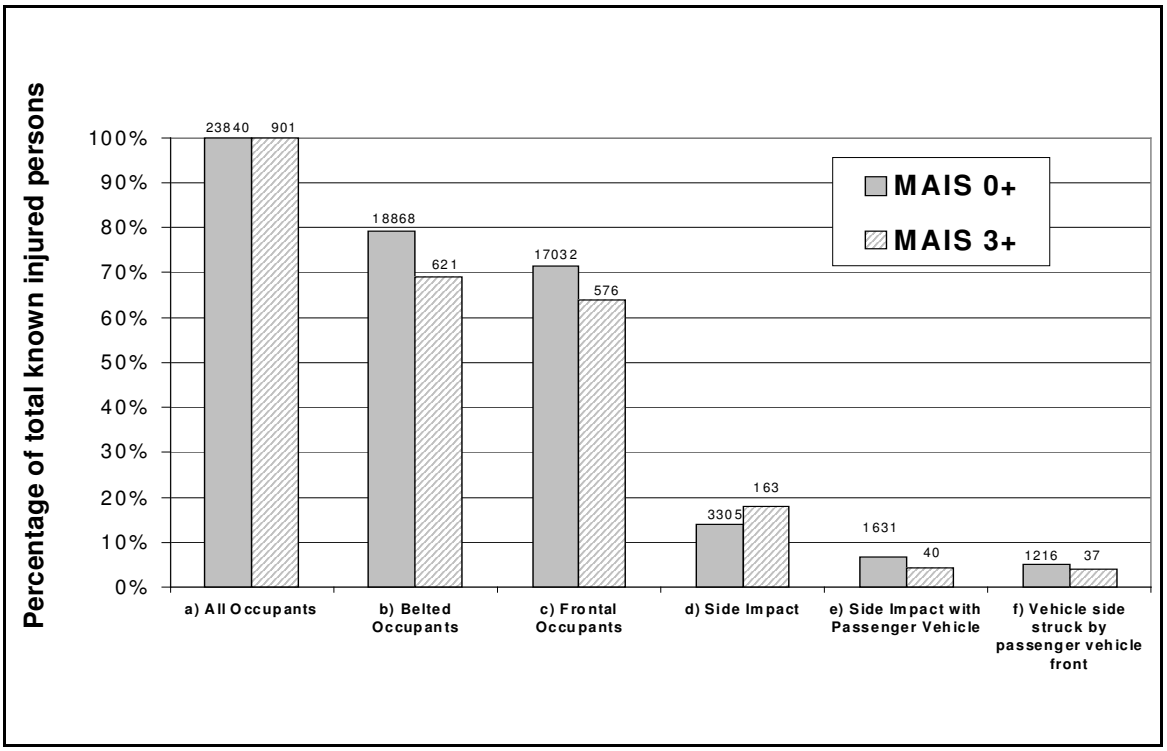

Figure 12 Statistical relevance of side impacts for all belted front-seat occupants

The side impact configuration is of lower statistical relevance than the frontal impact configuration. For all belted front-seat occupants, the number of MAIS 0+ and MAIS 3+ injured occupants is significantly lower (3305, 163, Figure 12, Column d) in the side impact configuration than in the frontal impact configuration (7236, 281, Figure 7, Column d).

Restricting the sample to consider only side impacts with other vehicles, for all belted front-seat occupants (Figure 12, Columns d to e) results in a large reduction in injury numbers. The total number of occupants (MAIS0+) decreases by half (from 3305 to 1631) and the total number of seriously injured occupants (MAIS3+) by a factor of 4 (from 163 to 40).

To deepen the analysis, the statistical significance of side impacts for belted front-seat occupants, based on the impact object, is shown in Figure 13 and Figure 14 for all occupants (MAIS0+) and all seriously injured occupants (MAIS3+), respectively.

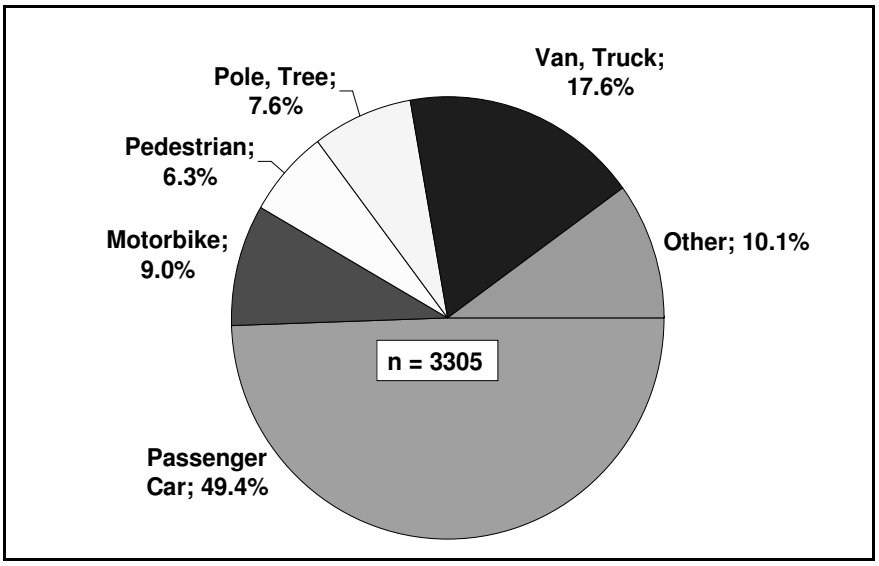

Figure 13 Distribution of all belted front-seat occupants (MAIS0+) involved in side impact collisions with respect to the impact object

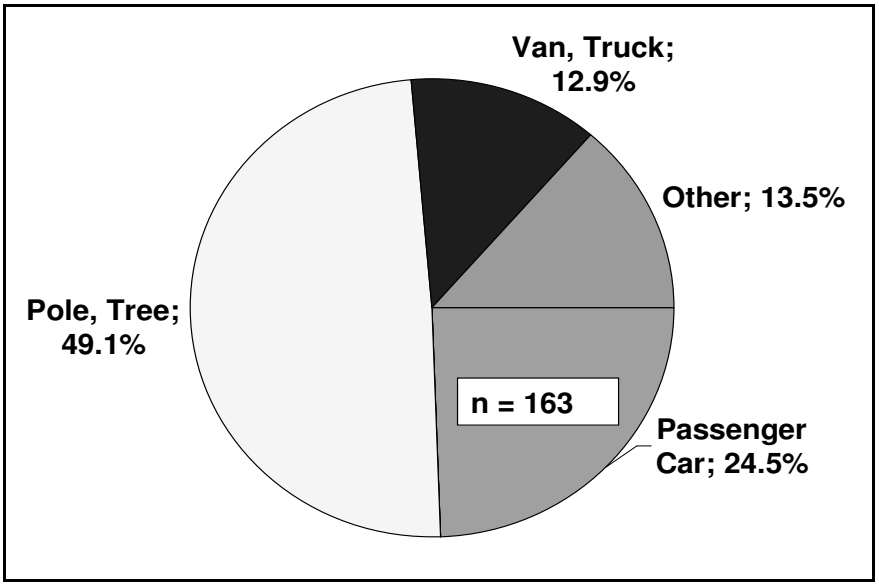

Figure 14 Distribution of all seriously injured (MAIS 3+) belted front-seat occupants involved in side impact collisions with respect to the impact object

As for the frontal impact configuration, the risk of serious injury faced by all injured occupants varies greatly depending on the impact object for the side impact configuration as well. Figure 13 and Figure 14 are summarised in Figure 15 for further discussion.

Accident Configuration	All involved occupants (MAIS0+)	Seriously injured occupants (MAIS3+)	Risk of a MAIS3+ injury
Car side - Car	1631	40	2.5%
Car side - Pole/Tree	251	80	31.9%
Car side - Truck	582	21	3.6%

Figure 15 The risk of serious injury based on the impact object for belted front-seat occupants involved in frontal collisions

The total number of occupants (MAIS 0+) involved in side impacts with a pole/tree is relatively low (251, Figure 13) compared with frontal impacts (579, Figure 10). As observed in the frontal impact configuration, the risk of injury associated with poles/trees is extremely high (31.9%). The risk is much higher than for side impacts involving trucks (3.6%) and side impacts involving other cars (2.5%). **In the side impact collision configuration, poles/trees are the most statistically relevant impact objects.**

Intrusion in side impacts with passenger cars

The accident sample was further restricted to consider only belted front-seat passenger car occupants seated in a vehicle which was struck in the side by another passenger car. The influence of intrusion in this collision configuration is shown in Figure 16 for all occupants (MAIS0+) and all seriously injured occupants (MAIS3+), respectively.

	All involved occupants (MAIS0+)	Seriously injured occupants (MAIS3+)	Risk of a MAIS3+ injury
Significant Intrusion	74	18	24.3%
Insignificant Intrusion	1142	19	1.7%

Figure 16 Influence of significant compartment intrusion on occupant injury risk for all belted front-seat occupants involved in a side impact with another vehicle[20]

[20] As for front impacts, a limit was defined for significant and insignificant intrusions, respectively. This was equal to VDI6>=2. See Appendix 1 for an illustration.

Figure 16 indicates that a very high risk of serious injury (24.3%) is associated with intrusion when the vehicle in focus is struck in the side by the front-end of another passenger vehicle. The risk of serious injury, when insignificant intrusions occur, is very low in comparison (1.7%, Figure 16). Survival space is a fundamental requirement for occupant protection in the side impact configuration as well. The risk values shown in Figure 16 can also be considered to be conservative, as accidents were not categorised based on which side of the vehicle was struck. The injury risk would be significantly lower for collisions in which the opposite side of the vehicle to which the occupant was sitting, was struck.

3.4 Limitations of the analysis of Accident Data

A statistical analysis of accident data is retrospective and has associated limitations. In this investigation, a large time range (1991 to 2002) is considered, to achieve statistically significant results. The resulting sample contains vehicles of different ages. The improvement in occupant protection offered by new vehicles sold today can therefore only be quantified in several years, when the fleet evolves to include more vehicles offering a degree of occupant protection reached by vehicles sold today. This is the main limitation of analyses of accident data and is taken into account in the following summary.

The other limitation is that significant differences have been observed in the automotive fleets around the world. The distribution of vehicle mass, geometrical characteristics as well as the distribution of collision configurations varies between world-regions. The fleet-mix can be considered to be similar in most European countries [65].The conclusions of this analysis are therefore representative of the European accident environment, as far as fleet-mix is concerned.

3.5 Summary: Statistically relevant collision configurations for compatibility

The frontal impact configuration was shown be of much higher statistical relevance than the side impact configuration. The potential for energy dissipation, before the threshold of the compartment is reached, is much higher in frontal collisions given the crumple zones present in the front-end of the vehicle (see Figure 3). In side impacts, a much lower amount of crash energy can be dissipated through deformation before the survival space of the occupant is placed under threat. Furthermore, accident avoidance systems such as ESP (Electronic Stabilisation Program) are also expected to greatly reduce the number of skidding accidents and prevent a large number of side impacts with fixed objects such as poles and trees. As poles and trees dominate side impact statistics and pose a very high risk to vehicle occupants, accident avoidance in side impacts appears to be the most feasible safety strategy. As mentioned in the previous chapter, a Volkswagen study determined that 80% of all skidding accidents could have been avoided through ESP [12].

Given the high relevance of single vehicle collisions in the frontal impact configuration (primarily against poles/trees) the current self protection levels of passenger vehicles clearly need to be maintained. Measures to improve compatibility must not compromise the current self protection level of passenger cars.

It is also important that any measures taken to improve compatibility consider both front-to-front and front-to-side impacts. Although front-to-front impacts are of higher relevance and are the main focus of the research presented in this thesis, before measures to improve front-to-front compatibility are implemented, the influence on front-to-side collisions should be investigated[21]. Front-to-rear collisions are an additional consideration.

With respect to frontal impacts, the statistical analysis showed that impacts with vans/trucks and impacts with cars were of high statistical relevance with respect to all occupants (MAIS0+) and all seriously injured occupants (MAIS3+) contained in the sample. An improvement in compatibility in these configurations would significantly

[21] For more detailed investigations of front-to-side compatibility, consult [83] and [40].

improve the protection offered to these occupants. When considering belted front-seat occupants involved in frontal collisions, these two configurations constitute 57.1% of all occupants (MAIS0+; 48.7% car front-to-car, 8.4% car front-to-truck) and 48.4% of seriously injured occupants (MAIS3+; 31.7% car front-to-car, 16.7% car front-to-truck) involved in accidents on German roads.

These conclusions are considered to be applicable for all western European countries as German accident data is considered provide a good representation of the accident environment across western Europe countries[22]. The conclusions may be different for other world regions, in particular North America, where the fleet composition is significantly different to Western Europe.

[22] It should be noted that fleet composition and accident statistics do vary across western European countries. The compatibility target population was estimated to be larger in the U.K. than in Germany with the accident environment in the U.K. comprising less single vehicle and more multi-vehicle collisions than in Germany [69].

4 Structural Interaction

In section 2.4, the sparse amount of published literature relating to the definition of structural interaction was summarised. The aim of this chapter is to add to the existing body of knowledge relating to structural interaction through the development of new theory. A definition for structural interaction is developed and presented (4.1). In section 4.2, the implications of structural interaction for the vehicle occupant are discussed. In section 4.3, theoretical curves representing maximal structural interaction in car-to-car, head-on collisions are derived and discussed. In section 4.4, several new metrics to evaluate the degree of structural interaction occurring in a frontal collision are presented.

This chapter contains the majority of the new scientific theory generated during this research. The contents of this chapter form the basis of the evaluation of structural interaction carried out and presented throughout the remainder of this thesis.

4.1 A definition for structural interaction

A first step that can be taken toward understanding structural interaction is to compare frontal fixed barrier crash tests and car-to-car head-on collisions.

In a collision with a fixed barrier, the interaction interface remains planar throughout the crash as the wall is also planar and, with respect to the magnitude of the front-end forces of the car, infinitely stiff. Each load path in the vehicle front-end is activated and deformed to the same degree, even if the distribution of forces within the front-end, measured at the wall, is not homogenous. Figure 17 is an illustration of a EURO NCAP crash test involving a Rover 75 and reflects the planar nature of the loading of the front-end of the vehicle.

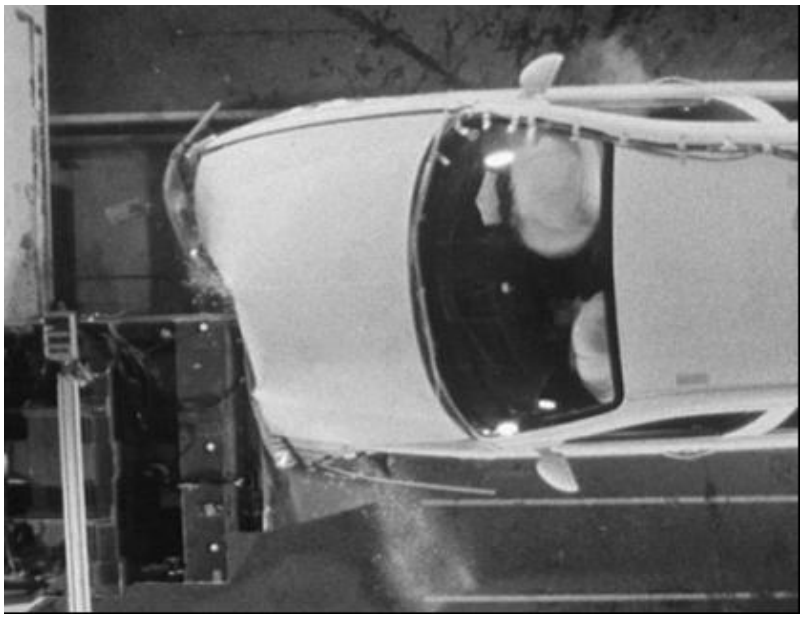

Figure 17 **Rover 75 – EURO NCAP Crash Test – 64km/h. Overlap ratio 40%.**

Post-crash photographs confirm the planar nature of the interaction, **Figure 18**. The dissipation of energy through deformation of the front-end of the vehicle can be assumed to be maximal for a fixed barrier collision. In Figure 17, a deformable element can be seen, located in front of the wall. The element is reasonably soft, so that bottoming out occurs early in the collision. The majority of the interaction in this collision occurs between the vehicle front-end and the wall.

Figure 18 **Post-crash deformation (Rover 75) – EURO NCAP Crash Test – 64km/h. Overlap ratio 40%**

The fixed barrier acts as the ideal impact object, providing infinite support forces to deform each of the load paths within the vehicle front-end. In fixed barrier collisions, structural interaction can be considered to be perfect, as only one of the bodies deforms.

When a passenger car collides frontally with an impact object other than a planar, rigid fixed barrier, the deformation of the front-end is fundamentally different. If the object is deformable, the structures interact together to dissipate the crash energy. In car-to-car collisions, for example, structural interaction is a relevant consideration. In such collisions, uneven deformation of the front-end of both vehicles occurs, resulting in a non-planar interface between the two bodies. The non-planar nature of the collision interface is shown for a car-to-car head-on collision involving a Rover 75, Figure 19.

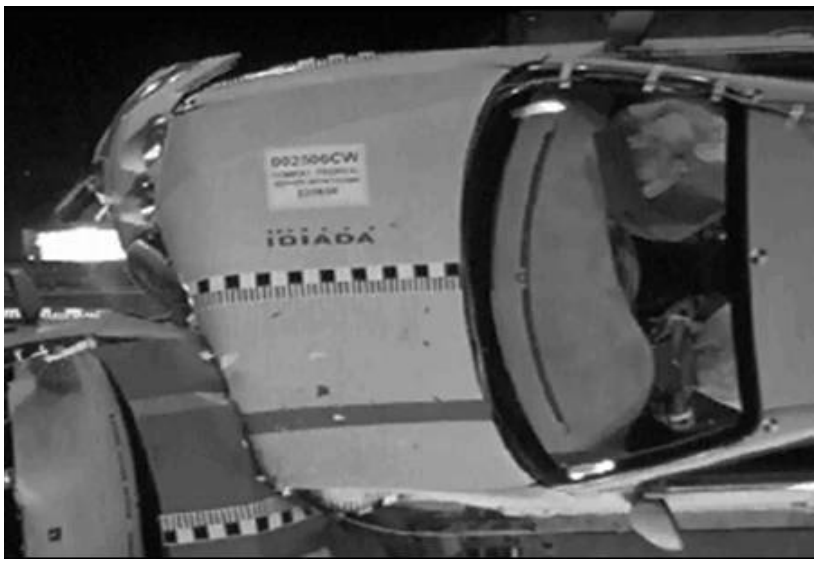

Figure 19 Overhead view - Car-to-car head-on collision – Rover 75 (right) versus small passenger vehicle (left). Closing velocity 112km/h. Overlap ratio 50% of the width of the smaller vehicle

The non-planar nature of the collision interface is more evident in the post-crash photograph of the Rover 75, Figure 20.

Figure 20 Post crash deformation (Rover 75) – Rover 75 versus small passenger vehicle. Closing velocity 112km/h. Overlap ratio 50% of the width of the smaller vehicle

For a car-to-car, head-on collision, less than maximal structural interaction can be expected to occur. **A reduction in structural interaction results in lower deformation forces (on average) and a lower degree of energy being dissipated within the front-end than in a collision with a fixed barrier.**

For a given vehicle, a front-end force-displacement characteristic can be calculated for a collision with a fixed barrier. This can be considered to represent the maximal force-displacement characteristic for this vehicle. Figure 21 shows two sketched force-displacement characteristics for a collision involving a light vehicle (vehicle A) and a heavy vehicle (vehicle B).

Due to the influence of the engine and transmission, the force at the rigid wall is higher than that calculated in the compartment. For this research, structural interaction will be calculated based on compartment forces and the influence of the engine will be neglected. See chapter 8.

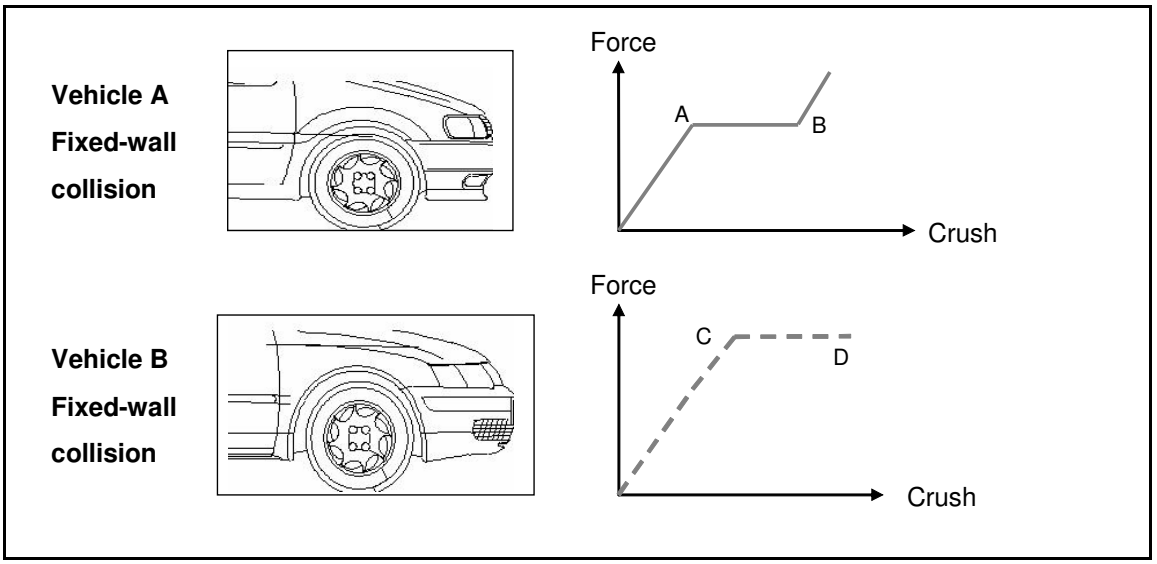

Figure 21 Sketched force-displacement characteristics for a light vehicle (vehicle A) and a heavy vehicle (vehicle B) involved in a collision with a fixed barrier

One method to predict the maximum possible degree of energy dissipation between two vehicles involved in a head-on collision is to statically combine the fixed barrier force displacement characteristics of these vehicles. The result is a force versus total displacement characteristic, where total displacement refers to the combined crush of both vehicle front-ends. This process is illustrated in Figure 22, based on the force-displacement characteristics for vehicle A and vehicle B, shown in Figure 21 above. The first step is to mirror the fixed barrier force-displacement characteristics for vehicle A and vehicle B about a theoretical collision interface, Figure 22.

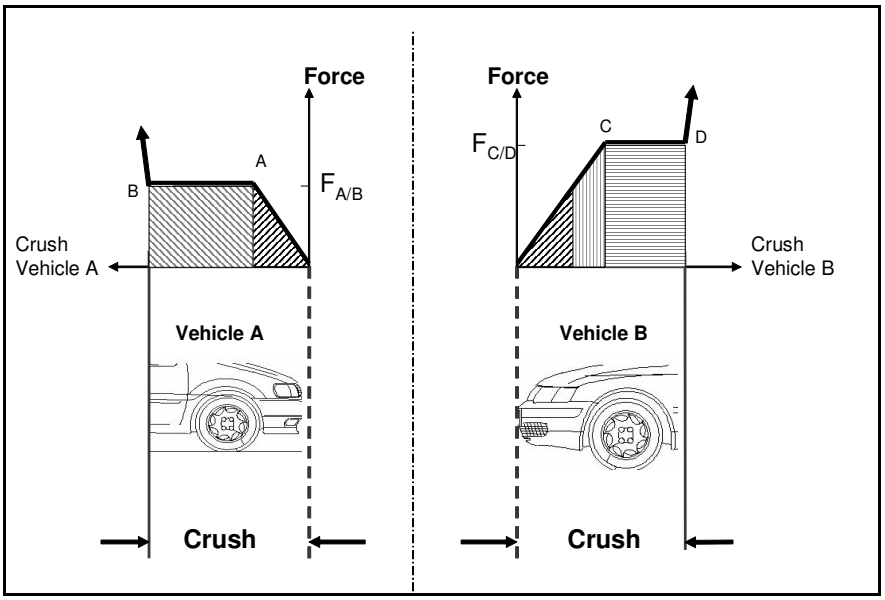

Figure 22 Mirroring force-displacement characteristics of two vehicles about a common axis to act as the basis for developing predicted maximal force versus combined front-end displacement for a car-to-car, head-on collision

The force at the crash interface is theoretically equal for both vehicles (action and reaction) and the magnitude of displacement of the front-end of each vehicle in a fixed barrier collision, corresponding to a given force level, can be added as shown in Figure 23. The shaded areas in Figure 23 correspond to the shaded areas in Figure 22.

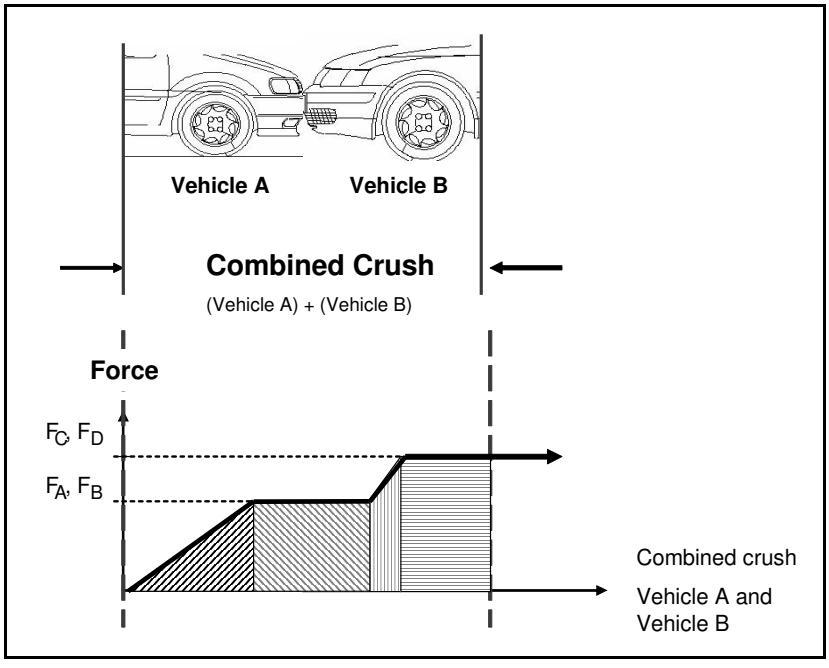

Figure 23 Predicted maximal force versus combined front-end displacement for a car-to-car, head-on collision - Statically combined fixed barrier, front-end force-displacement characteristics

The statically combined characteristics shown in Figure 23 represent the highest possible level of energy dissipation that could occur between two vehicles involved in a head-on collision. As the level of structural interaction occurring in the collision decreases, the deformation forces theoretically decrease as well. In order to dissipate the same amount of kinetic energy, a higher degree of deformation is required. This is illustrated in Figure 24, based on the statically combined force-displacement characteristic developed in Figure 23.

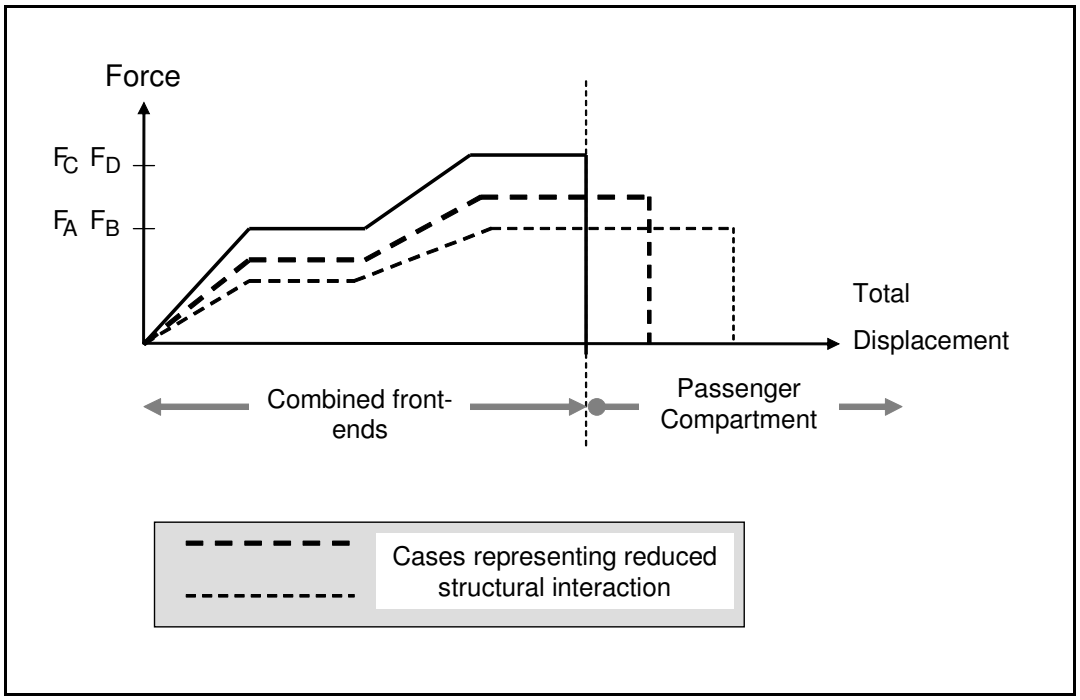

Figure 24 The theoretical influence of reduced structural interaction on the force versus total front-end crush characteristics exhibited by two vehicles in a head-on collision

Figure 24 represents a theoretical car-to-car, head-on collision of high severity in which the entire available front-end deformation travel is required for the case of maximal structural interaction. As the level of structural interaction decreases, in order to dissipate the same degree of kinetic energy through deformation, a higher degree of compartment deformation is required. **The observations made in this chapter lead to the following definition for structural interaction which forms the basis of this research:**

*The degree of structural interaction that occurs in a head-on collision can be described as the proportion of the **actual energy dissipation** through structural deformation compared to the **maximum possible energy dissipation,** for a given collision configuration. The maximum possible energy dissipation can be predicted by statically combining the force-displacement characteristics exhibited by each vehicle in a fixed barrier crash test at the given degree of barrier overlap.*

All curves previously generated in this chapter are based on the assumption that the compartment strength of the lighter vehicle exceeds the front-end force of the heavier vehicle. This was already discussed in section 2.3.2 as the Bulkhead Concept was introduced. The implications of this assumption will be discussed in more detail in the conclusion to this chapter.

4.2 The implications of structural interaction for the vehicle occupant

In a car-to-car, head-on collision, the level of structural interaction influences the magnitude of energy dissipation within the front-ends. After the entire available length of deformation travel has been deformed, any surplus kinetic energy that remains leads to overloading of the compartment and a higher risk of compartment deformation. **Maximising structural interaction increases the energy dissipation within the front-ends and therefore lowers the risk of high compartment deformation.**

The degree of structural interaction occurring in a collision influences compartment accelerations as well, as structural interaction determines the magnitude of the interaction forces. **In collisions of lower severity, in which the risk of global compartment deformation is low, a lower level of structural interaction may be beneficial to reduce compartment accelerations** and correspondingly reduce the risk of acceleration induced injury (as documented based on published literature in section 2.2).

A goal conflict exists to maximise occupant protection by minimising both compartment accelerations (demanding low structural interaction) and compartment intru-

sions (demanding high structural interaction). One solution to this goal conflict is to ensure complete deformation of the front-end of the vehicle in question at all collision severities.

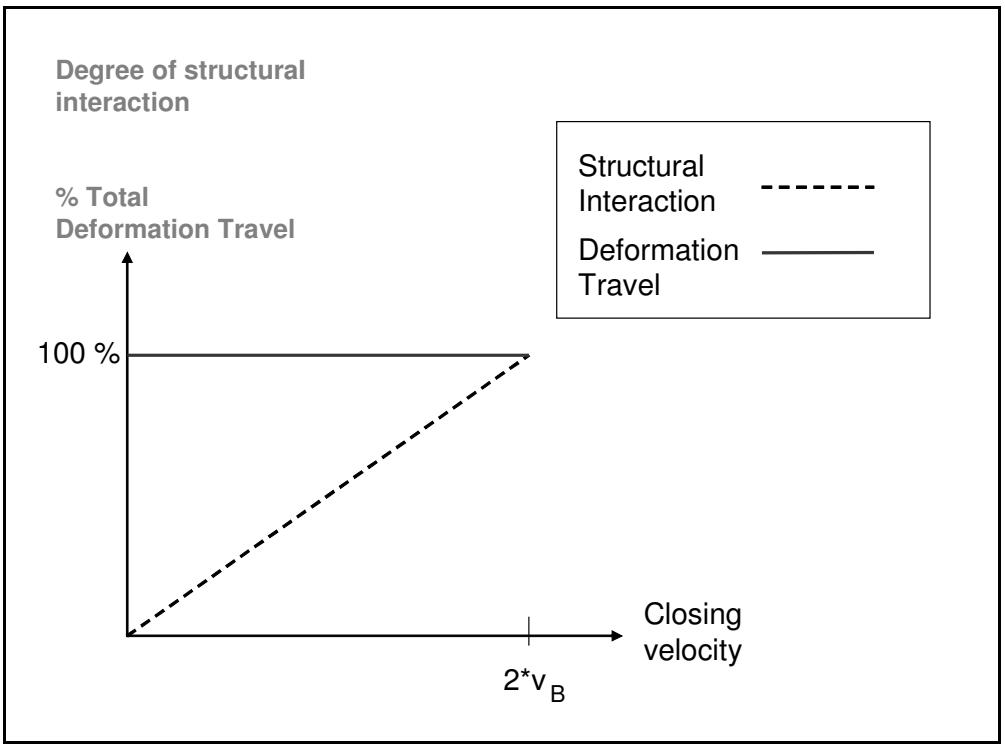

Figure 25 The theoretical relationship between the optimal degree of structural interaction and the closing velocity (up to $2v_b$ – twice the fixed barrier test velocity) to achieve complete deformation of the vehicle front-end in a car-to-car, head-on collision.

Figure 25 indicates that, to minimise compartment accelerations for all collisions, the degree of structural interaction needs to vary depending on the collision severity. However, it is not considered realistic to achieve a variable degree of structural interaction in real-world collisions. Inducing a crash severity-dependent level of structural interaction represents an enormous engineering challenge, one which may not be able to be solved without radical changes in vehicle design.

In the following chapters, the phenomenon of structural interaction is further investigated. The injury benefit achievable in collisions of low severity through a reduction in structural interaction is investigated in chapter 5. The influence of structural interaction in collisions of higher severity and its influence on energy dissipation and compartment intrusion will be investigated based on the development of new metrics to

evaluate structural interaction (section 4.4) and the analysis of experimental crash tests (chapter 8) and numerical crash test simulations (chapter 9).

4.3 Energy dissipation in head-on collisions

Theoretical characteristics are developed in this section, representing maximal structural interaction for the case of a head-on collision involving two standard passenger vehicles of different mass. Triangular force-displacement characteristics were used as a basis for the calculations, to allow the simplified generation of mathematical functions describing the interaction of vehicles for the head-on collision configuration.

The peak force (F_{peak}) for a triangular front-end force-displacement characteristic is equal to twice the mean deformation force. Based on equation (2):

$$F_{peak} = 2\left(\frac{1}{2}\frac{mv_b^{\,2}}{s_b}\right) = \frac{mv_b^{\,2}}{s_b} \tag{9}$$

the peak force for two vehicles of mass m_1 and m_2 can therefore be written as follows:

$$F_1 = \frac{m_1 v_b^{\,2}}{s_b}$$

$$F_2 = \frac{m_2 v_b^{\,2}}{s_b}$$

The front-end force-displacement characteristics for two different vehicles (vehicles 1 and 2) can be mirrored about a common crash interface and act as the basis for statically combining these characteristics.
Figure 26 shows the force-displacement characteristics for vehicles 1 and 2, assuming:

- both vehicles are tested at the same fixed barrier crash test velocity (v_b). As is the case for all frontal crash test regulations worldwide.

- both vehicles provide the same amount of available front-end deformation travel (s_b). (See section 2.3.2).

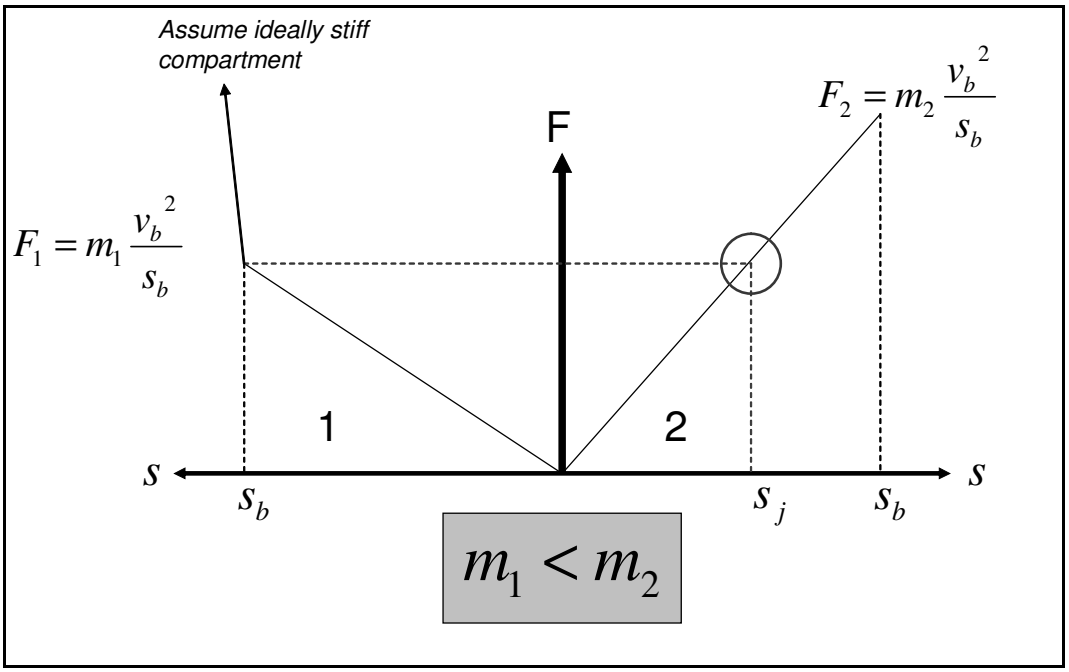

Figure 26 Front-end force-displacement characteristics for two vehicles of different mass (vehicles 1 and 2) assuming both vehicles provide the same amount of available front-end deformation travel (S_b) in a fixed barrier collision at a velocity of (v_b).

The point s_j is the point of front-end deformation of the heavier vehicle (vehicle 2) which corresponds to the peak front-end deformation force of the smaller vehicle. Based on geometry:

$$s_j = \frac{m_1}{m_2} s_b \qquad (10)$$

Statically combined force-displacement characteristics, based on the front-end force-displacement characteristics illustrated in Figure 26 and the method illustrated in Figure 23, are shown in Figure 27. These characteristics represent the maximal energy dissipation for a head-on collision involving two vehicles of different mass.

During the next pages, the strength of the compartment of the smaller vehicle is considered to be ideal (ideally stiff) for the purpose of analysis. In reality, the stiffness of the compartment may not be great enough to ensure that complete deformation of both vehicles is achieved.

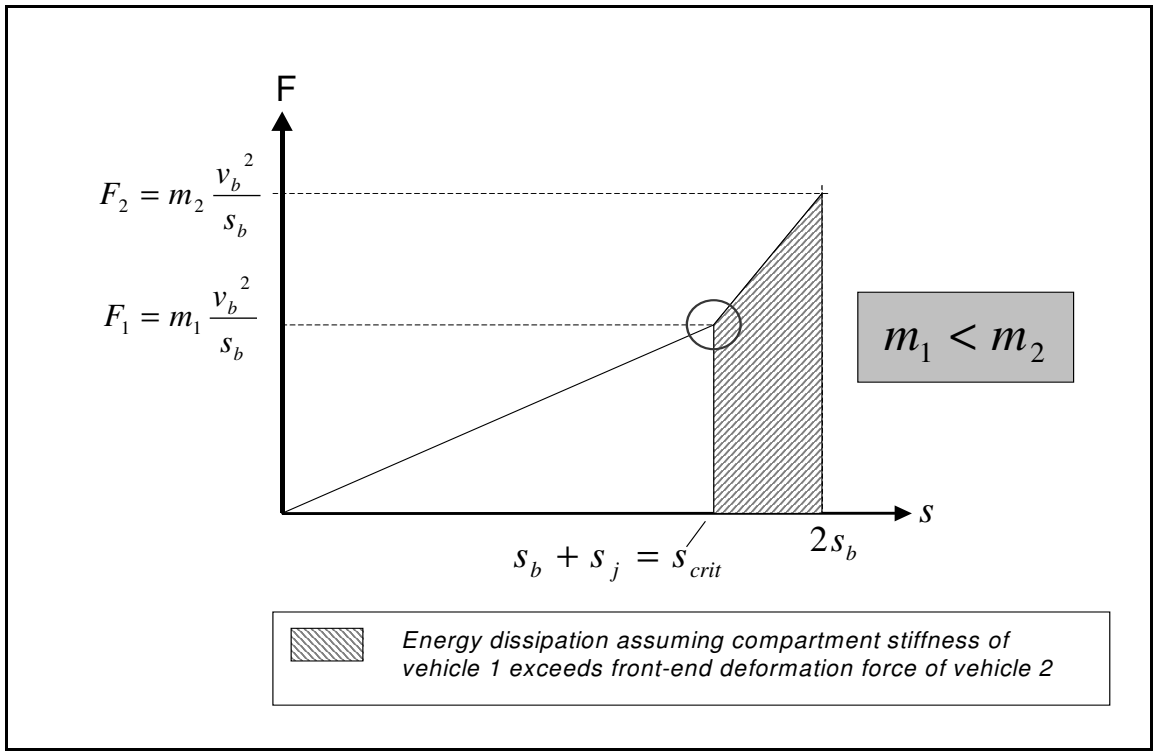

Figure 27 Force versus combined front-end deformation characteristics for two vehicles of dissimilar mass (vehicles 1 and 2) based on Figure 26

The point of deformation (s_b+s_j) can be considered to be a critical point in the combined deformation of both vehicles and will be referred to for future discussion as s_{crit}. After the point s_{crit} has been reached, the compartment resistance of the lighter car has to exceed the front-end deformation forces of the heavier car, in order to achieve the predicted force versus combined deformation characteristics shown in Figure 27 (and in order to achieve the quantity of energy dissipation in the front-ends represented by the shaded section). If this is not the case, the compartment of the lighter car will deform in preference to the front-end of the heavier car and the energy contained in the shaded section would not be dissipated. This observation is based on the Bulkhead Concept presented in section 2.3.4 and illustrated in Figure 3.

Based on equations (8) and (9), force versus combined deformation characteristics were calculated for several theoretical collisions. Figure 28 shows the combined

force-displacement characteristics for a head-on collision involving a 1000kg car and other cars of varied masses. The characteristics are based on the assumption that the EES in a fixed barrier collision is equal to 56km/h for all vehicles (i.e. the entire kinetic energy associated with the collision is dissipated through front-end deformation) and a maximum front-end deformation travel of 0.6m is provided by both cars.

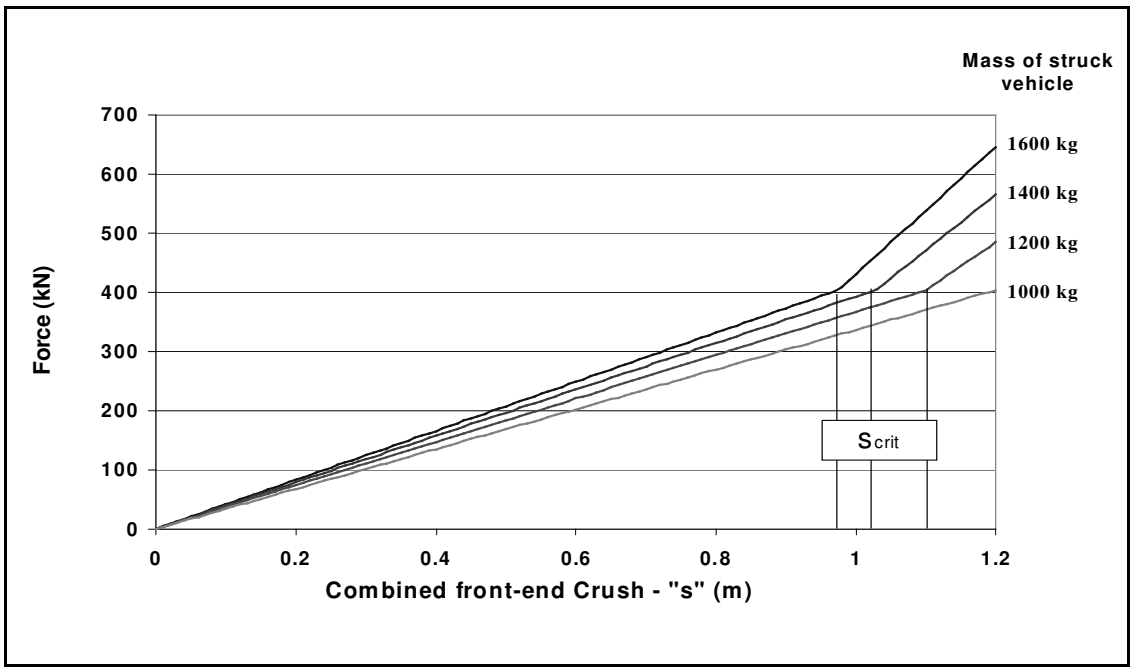

Figure 28 Theoretical force versus combined front-end crush curves for a car-to-car, head-on collision at 112km/h for a 1000kg car involved in a collision with other cars of varied masses. Each vehicle provides 0.6m of available front-end deformation travel in a fixed barrier crash test at a velocity of 56km/h

The curves developed in Figure 28 were integrated with respect to the combined displacement of both vehicle front-ends (combined vehicle crush) to yield energy dissipation with respect to the combined crush of the front-ends of both vehicles. These characteristics are shown in Figure 29 below.

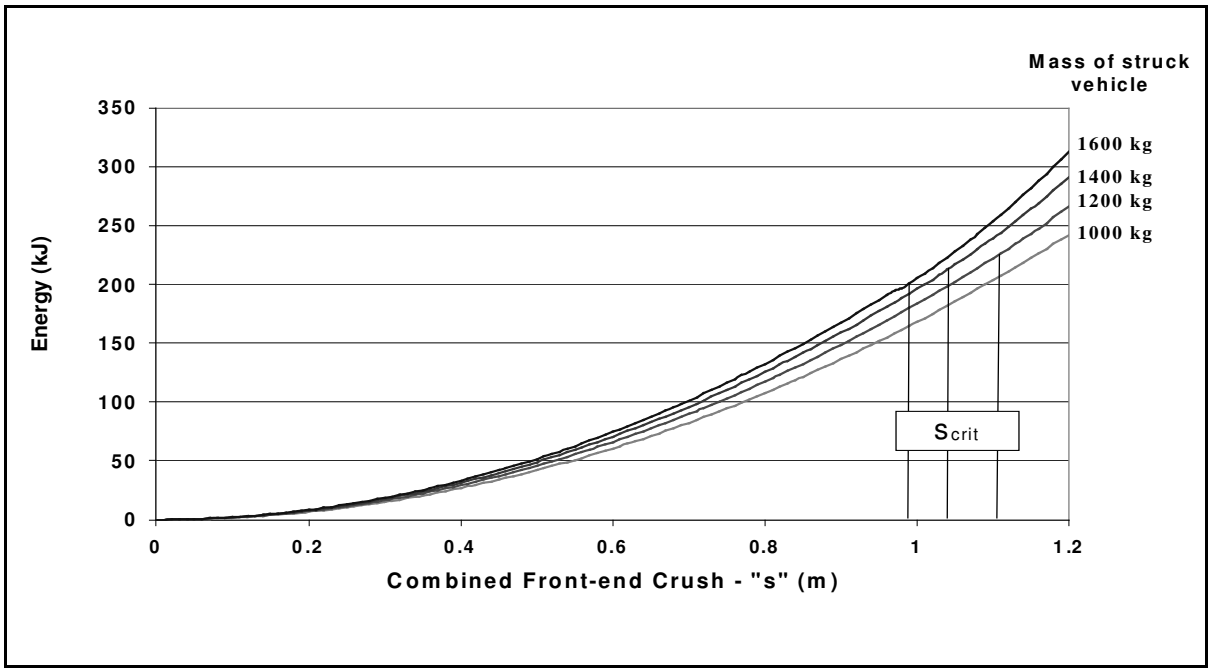

Figure 29 Theoretical cumulative energy dissipation versus combined front-end crush characteristics. Car-to-car, head-on collision at 112km/h - For a 1000kg car involved in a collision with cars of varied mass. Each vehicle provides 0.6m of available deformation travel at a fixed barrier crash test velocity of 56km/h based on triangular front-end force-displacement characteristics

The increasing nature of the energy dissipation shown in Figure 29 indicates that the late crash phase is the most critical with respect to energy dissipation. As the force-displacement characteristics shown in Figure 28 are triangular, the integral of these characteristics, reflecting energy dissipation and shown in Figure 29 , are quadratic in nature. A much higher percentage of the collision energy is dissipated through deformation in the second half of the combined deformation of the vehicle front-ends.

Figure 29 also shows the critical point of deformation (s_{crit}) of the lighter vehicle, after which compartment force (resisting deformation) of the smaller vehicle has to exceed the front-end deformation force of the heavier vehicle, in order to prevent collapse of its own compartment.

4.4 Proposed compatibility assessment metrics based on the EES

On the previous pages, the phenomenon of structural interaction was described based on the energy dissipation occurring through deformation of the structures of both vehicles involved in a head-on collision. Equations are presented in this section, considering the masses of both vehicles, to convert this energy dissipation quantity into equivalent closing velocities.

The metrics presented in this section, based on the EES metric, form the basis of the evaluation of structural interaction throughout the remainder of this thesis.

4.4.1 Considering the individual vehicle (EESV and EESF)

For a real-world collision involving a passenger vehicle, less than maximal structural interaction may occur, in which case less energy would be dissipated in the front-end than that theoretically available. The EESV metric presented in section 2.4.1 does not differentiate between the amount of energy dissipated in the front-end and the amount dissipated in the compartment. To account for this, a new EES metric is proposed which considers the degree of energy dissipated in the **front-end only** (D_F), and will be referred to as the EESF. Based on equation (8), describing the EES:

$$EESF = \sqrt{\frac{2D_F}{m}} \tag{11}$$

4.4.2 Considering both vehicles (EESVV and EESFF)

The EESV and EESF values calculated in the previous section relate to one of the vehicles involved in a collision. In a car-to-car collision, the phenomenon of structural interaction relates to energy dissipation through deformation of the structures of both vehicles. A metric is proposed which represents an **equivalent closing velocity**, considering both vehicles involved in a collision. This metric will be referred to as the EESVV.

The total change in kinetic energy (ΔE_k) of two vehicles of different masses (m_1 and m_2) involved in a head-on collision at a given closing velocity (v_c) is given as:

$$\Delta E_k = \frac{1}{2}\left(\frac{m_1 m_2}{m_1 + m_2}\right) v_c^{\,2}$$

The EESVV can be derived by substituting the energy dissipated through the structural deformation of both vehicles (D_{vv}) for the change in kinetic energy of the vehicle (ΔE_k):

$$D_{VV} = \frac{1}{2}\left(\frac{m_1 m_2}{m_1 + m_2}\right) EESVV^2$$

$$EESVV = \sqrt{2 D_{VV}\left(\frac{m_1 + m_2}{m_1 m_2}\right)} \qquad (12)$$

The EESVV for a vehicle-vehicle collision is analogous to the EESV for a single vehicle collision. Like the EESV, the EESVV does not differentiate between the energy dissipated in the compartments of each vehicle and the energy dissipated in the front-ends. A new EES metric is introduced (EESFF) considering the energy dissipation in the front-ends (D_{FF}) of both vehicles combined.

The EESFF for a vehicle-vehicle collision is analogous to the EESF for a single vehicle collision:

$$D_{FF} = \frac{1}{2}\left(\frac{m_1 m_2}{m_1 + m_2}\right) EESFF^2$$

$$EESFF = \sqrt{2 D_{FF}\left(\frac{m_1 + m_2}{m_1 m_2}\right)} \qquad (13)$$

4.4.3 Evaluating structural interaction based on the EES metrics

In this section, three new metrics have been proposed which will be used throughout the thesis to evaluate the degree of structural interaction occurring in a given collision:

EESF *An energy equivalent velocity based on the energy dissipated in the **front-end** of **one vehicle** involved in a given collision.*

EESVV *An energy equivalent velocity describing an **equivalent closing speed** for a given vehicle-vehicle collision based on the energy dissipated in the **entire structure** of **both vehicles** involved in a given collision.*

EESFF *An energy equivalent velocity describing an **equivalent closing speed** for a given vehicle-vehicle collision based on the energy dissipated in the **front-ends** of **both vehicles** involved in a given collision.*

The EESV and EESVV reflect the severity of the collision and will be used primarily to identify any changes in actual collision severity.

The EESFF metric forms the basis of the evaluation of structural interaction throughout this thesis. A key component of this evaluation is the calculation of a theoretical maximum EESFF for a given collision.

Calculating theoretical maximal EESFF values

Throughout this thesis, a collision with a fixed barrier is considered to represent maximal structural interaction. Therefore, the energy dissipation occurring in the front-end in a barrier collision ($D_{F\text{-barrier}}$) can be considered to determine an upper limit for the EESFF.

$$EESFF_{max} = \sqrt{2\left[D_{F-barrier}(\,vehicle\,1\,) + D_{F-barrier}(\,vehicle\,2\,)\right]\frac{m_1 + m_2}{m_1 m_2}} \tag{14}$$

This upper limit is only valid for the case of a collision involving identical vehicles. For collisions involving non-identical vehicles, the $EESFF_{max,}$ calculated based on the above equation, may not be able to be reached, even for the case of maximal structural interaction. If the strength of the compartments of each vehicle is not adequate to deform the front-end of the other vehicle, compartment collapse may occur at a significantly lower $EESFF_{max}$ value.

In Chapter 9 of this thesis, Structural Interaction is evaluated for several car-to-car, head-on collision simulations involving identical vehicles. Evaluating structural interaction for the case of a collision involving non- identical cars is an issue which is not covered in this thesis and is included as a recommendation for further research in the final chapter of this thesis (Chapter 10). As stated above, this would require the calculation of an additional EESFF value taking into account not only the energy dissipated in the front-ends of each vehicle in the fixed barrier collision but also the differences in front-end and compartment stiffness.

5 Structural interaction and acceleration induced injury

As discussed in chapter 3, two physical quantities need to be minimised to best protect occupants in collision situations; compartment accelerations and compartment intrusion. Structural interaction influences both of these quantities. In this chapter, the influence of structural interaction on compartment accelerations and acceleration-induced injuries is investigated based on occupant simulations.

It was discussed in the previous chapter that the risk of acceleration induced injury may be reduced in collisions of low severity, through a reduction in the degree of structural interaction. The decrease in injury risk associated with a reduction in structural interaction in low severity collisions is investigated in this chapter. High severity collisions are not considered. Any reduction in structural interaction would result in an increased risk of compartment deformation, which is considered inappropriate given the high injury risk associated with passenger compartment intrusion in real-world accidents (see chapter 3).

5.1 Description of the simulation process

The results to occupant simulations using Madymo software are presented in this chapter. A validated model of a passenger vehicle was used as the basis for the simulations, Figure 30. The vehicle driver only was considered in this investigation. The driver is modelled based on the 50^{th} percentile hybrid 3 dummy [84].

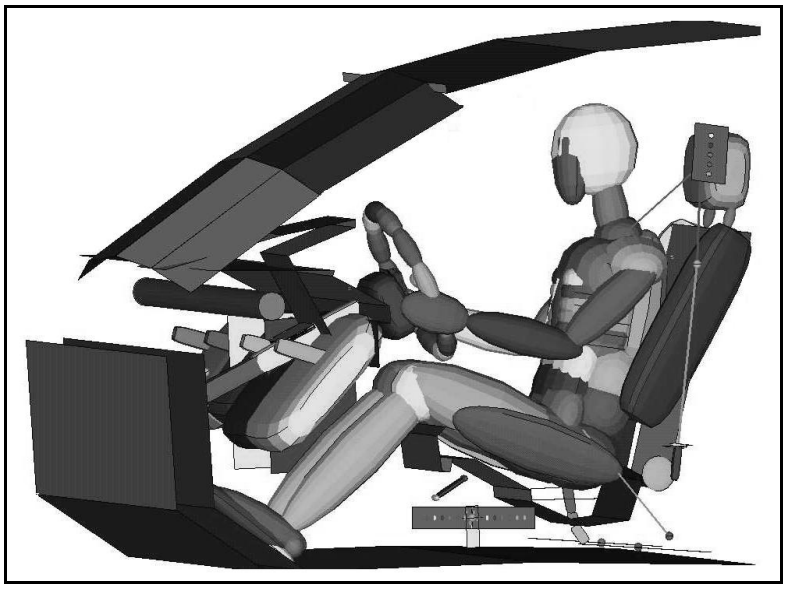

Figure 30 Madymo occupant simulation model used to investigate the influence of the occupant restraint system on occupant injury risk for collisions of different severity

To generate crash pulses reflecting those occurring in car-to-car, head-on collisions, a spring-mass model, representing two vehicles colliding head-on and their respective front-end force-displacement characteristics, was developed, Figure 31. The force-displacement characteristics of two springs, representing the vehicle front-end, could be altered to represent varying degrees of structural interaction.

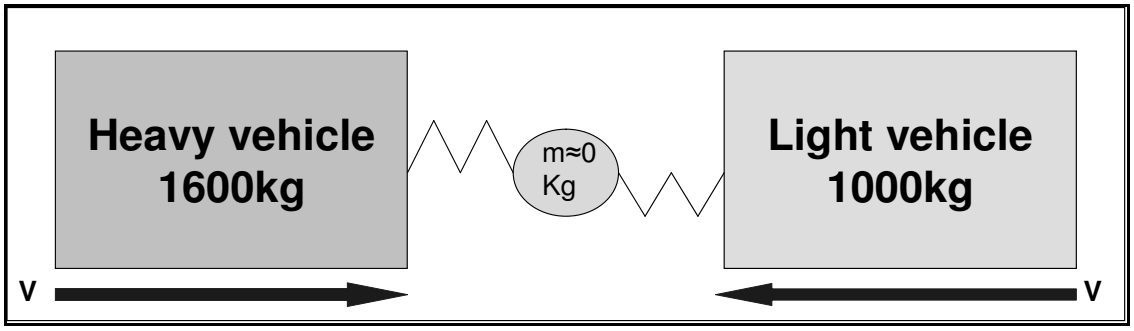

Figure 31 Spring-mass model used to generate crash pulses at varied crash velocities with different levels of structural interaction. The resulting acceleration-time characteristics of the small (1000kg) vehicle were used as a basis for the occupant simulations

Vehicle masses of 1000kg and 1600kg were chosen to yield a mass ratio of 1:1.6[23]. The interface mass weighed less than one kilogram and had no significant influence on the resulting crash pulses for each vehicle. Force-displacement characteristics for the front-end of each respective vehicle were developed. The resulting acceleration-

time characteristics of the lighter (1000kg) vehicle were used as the basis for occupant simulations, using the model illustrated in Figure 30. The initial velocity of each vehicle was varied to represent different collision severities.

5.2 Pre-simulations

To investigate the influence of structural interaction in collisions of low severity, four two-stage front-end force-deflection characteristics were developed for each vehicle, Figure 32[24]. The steepest characteristics reflect the case of maximal structural interaction. The force displacement curves were then varied (to be less steep) to represent lower levels of structural interaction, resulting in less kinetic energy being dissipated through deformation of the front-end.

Each force-displacement characteristic is described in terms of an EESF for each vehicle (see section 4.4.1 for a detailed description of the EESF), reflecting the degree of structural interaction. The resistance force of the compartments was ideally stiff, to enforce deformation of both vehicles involved in the collision and to simulate collisions in which no compartment intrusions occurred.

Note: The pre-crash simulations were one-dimensional, assuming centroidal impacts and neglecting rotational effects. The pulses generated represent collisions for vehicles having 0.6m of available crush space in a collision. This crush space is assumed to best reflect the case of an offset collision at 40% overlap-ratio.

[23] A mass ratio of 1:1.6 has been proposed as an upper limit for compatibility between two cars involved in a head-on collision at twice the fixed barrier crash test velocity, section 2.3.4.
[24] In chapter 4, triangular force-displacement characteristics were used to develop a theoretical understanding of structural interaction. For this investigation two-stage characteristics were used and are considered to better represent the force-displacement characteristics of modern passenger cars.

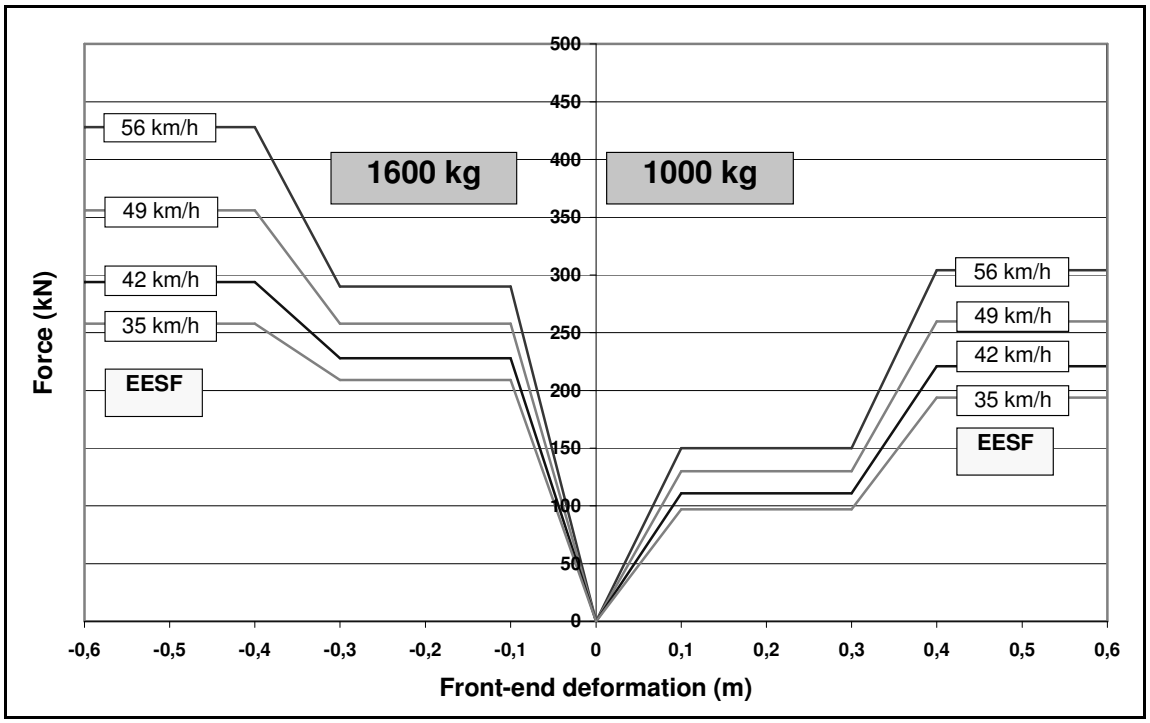

Figure 32 Front-end force-displacement characteristics used to investigate the influence of structural interaction in car-to-car, head-on collisions of low severity

A sample crash pulse for the smaller (1000kg) vehicle, generated from the collision based on the two 56km/h EESF front-end force-displacement characteristics, is shown below.

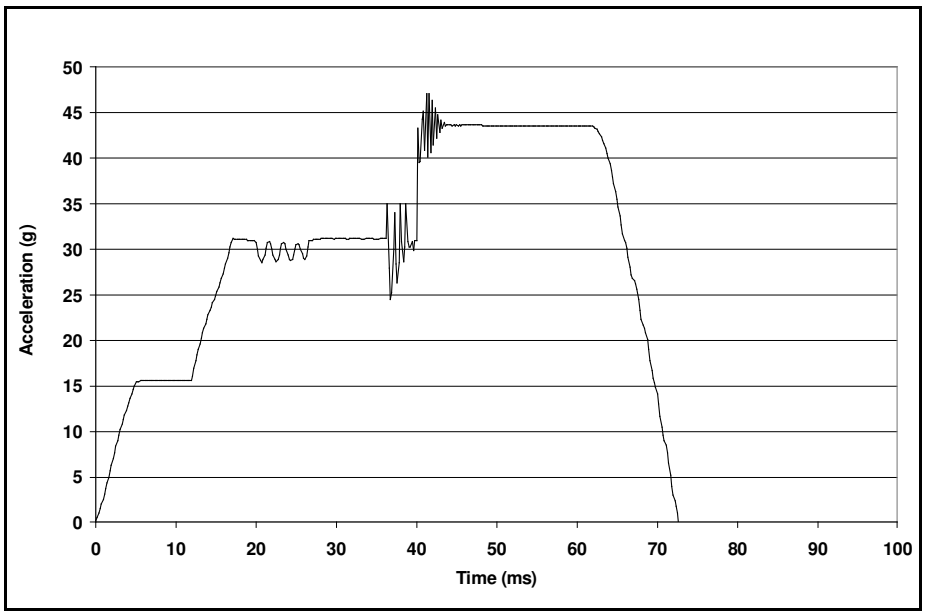

Figure 33 Sample crash pulse reflecting the acceleration-time characteristic of the compartment of the smaller vehicle – based on an EESFF of 56km/h for both vehicles (see Figure 32).

Based on the characteristics shown in Figure 32, an experimental matrix was developed to investigate the influence of structural interaction in crashes of low severity. Pre-simulations were carried out at closing velocities of 112, 100, 85 and 70km/h, respectively. For each simulation, the initial velocity of each vehicle was identical. The EESF of the front-end force-displacement characteristics of each vehicle was identical as well. To prevent over-crashing, simulations were only carried out at closing velocities equal to or less than the sum of the EESF values of both vehicles (2*EESF ≥ Closing velocity). All other collisions (shown in grey in Figure 34) were removed from the simulation matrix, as these represented an over-crash situation.

Simulation No.	EESF Each vehicle (km/h)	Closing velocity (km/h)
1	56	70
2	49	70
3	42	70
4	35	70
5	56	85
6	49	85
7	42	85
x	35	85
8	56	100
9	49	100
x	42	100
x	35	100
10	56	112
x	49	112
x	42	112
x	35	112

Figure 34 Simulation Matrix

Pre-simulations were carried out for each of the experimental combinations illustrated in Figure 34. The change in velocity of the small (1000kg) vehicle in each simulation is shown in Figure 35.

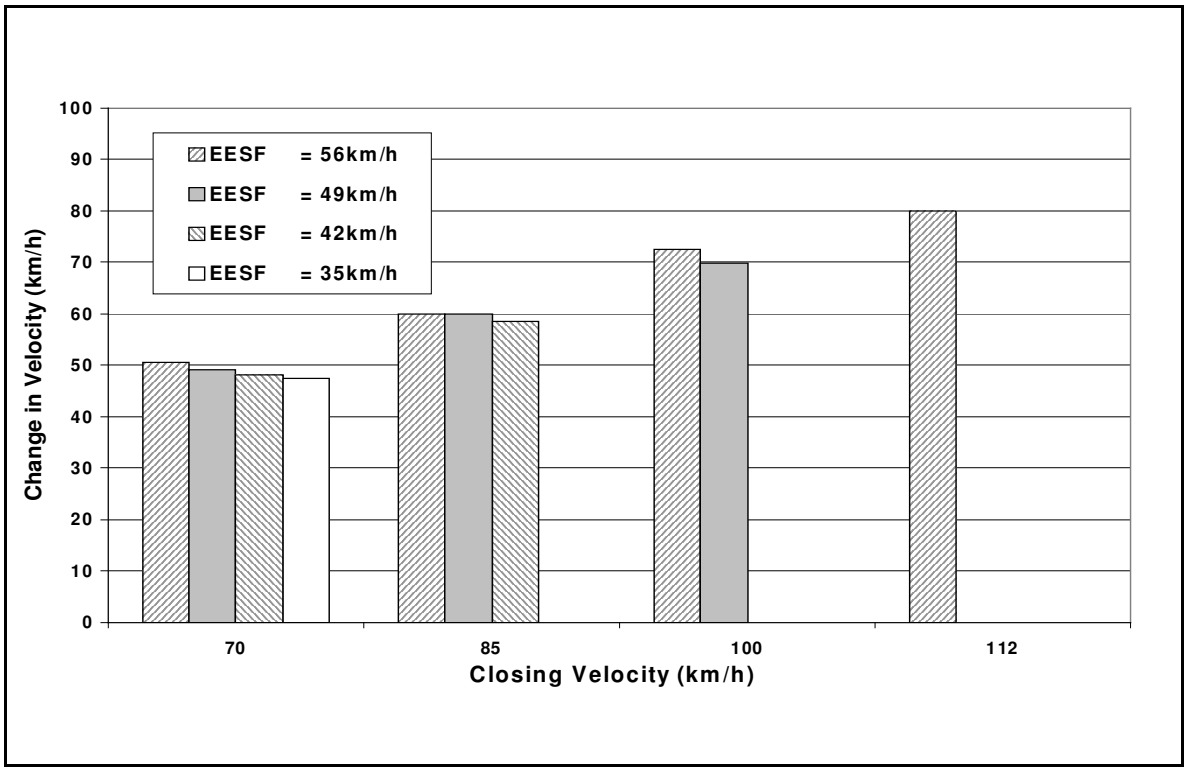

Figure 35 Change in velocity of the small (1000kg) vehicle based on the closing velocity of the collision and the degree of structural interaction (EESF) in simulated head-on collisions with a 1600kg vehicle

For each respective closing velocity, the change in velocity of the lighter vehicle is similar for each level of structural interaction reflected by the (EESF). The severity of the collisions was therefore held constant, Figure 35. The acceleration-time characteristics of the lighter body were extracted from each pre-simulation and used as the input for the occupant simulations.

5.3 Occupant simulations

The injury criteria for each simulation are shown in the following illustrations, Figure 36 to Figure 38. The maximum value of the vertical axis of each graph is equal to the prescribed EURO NCAP injury limit for each respective injury criterion [8].

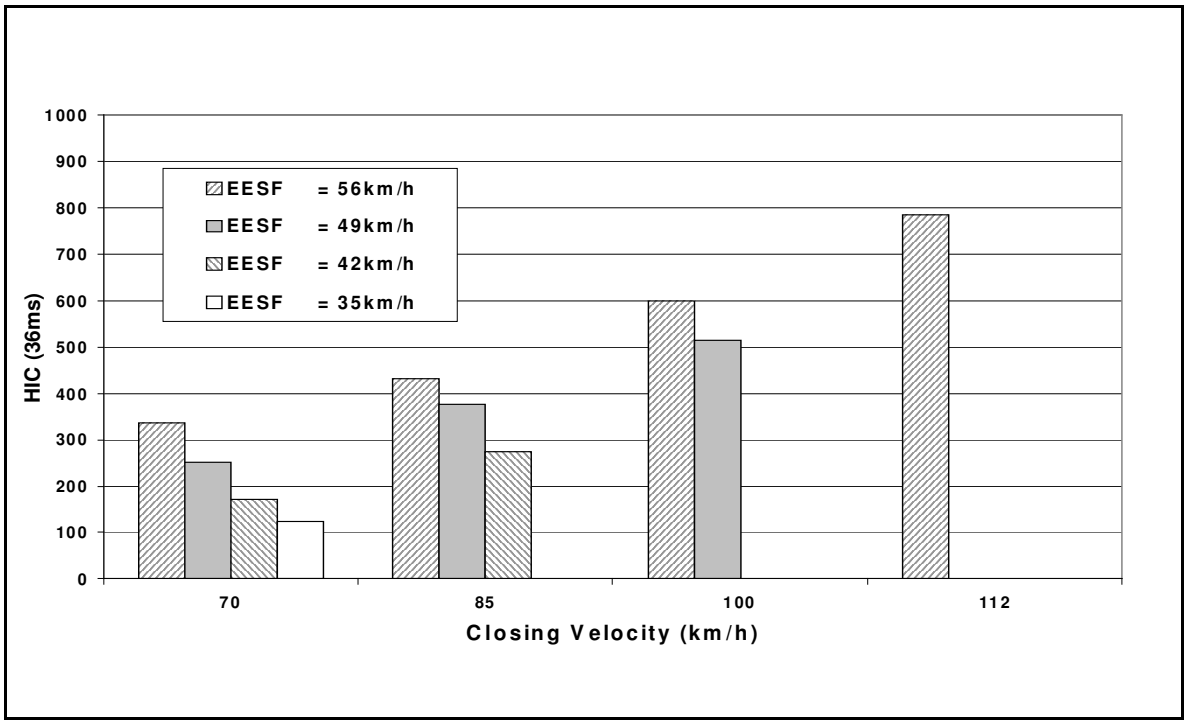

Figure 36 Head-injury-criterion (HIC) level sustained by the driver-dummy of the small (1000kg) vehicle based on the closing velocity of the collision and the degree of structural interaction (EESF) in a simulated head-on collision with a 1600kg vehicle

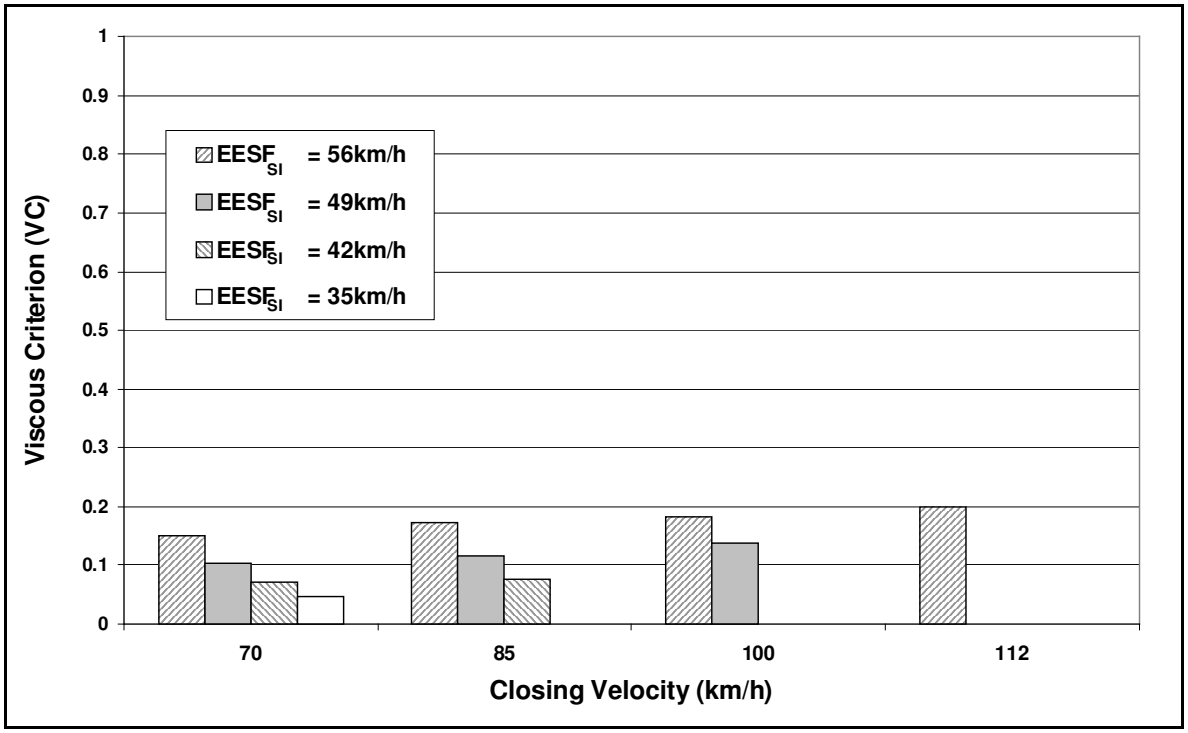

Figure 37 Viscous Criterion (VC) rating sustained by the driver-dummy of the small (1000kg) vehicle based on the closing velocity of the collision and the degree of structural interaction (EESF) in a simulated head-on collision with a 1600kg vehicle[25]

[25] The viscous criterion (VC) describes the degree of chest loading based on the velocity and degree of compression of the sternum. For more information consult [85].

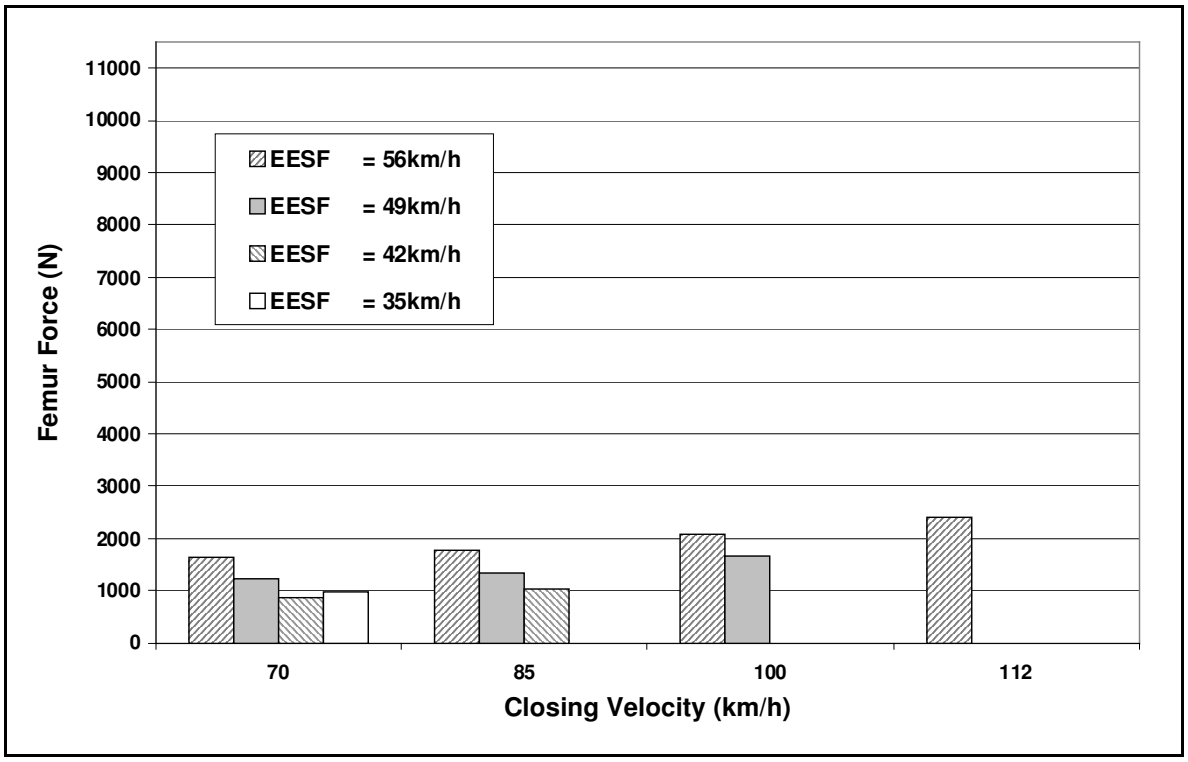

Figure 38 Peak Femur Force (average left and right) sustained by the driver-dummy of the small (1000kg) vehicle based on the closing velocity of the collision and the degree of structural interaction (EESF) in a simulated head-on collision with a 1600kg vehicle

The HIC is the most significant injury criterion in this investigation. At all closing velocities, a reduction in structural interaction (reflected by a reduction in the EESF value) resulted in a corresponding reduction in HIC values. The HIC values decreased from 336 (at an EESF of 56km/h) to 125 (at an EESF of 35km/h) for collisions at a closing velocity equal to 70km/h.

In collisions at lower closing velocities (70km/h and 85km/h) HIC levels are out of the range normally associated with significant injury risk (124.5 to 336 at 70km/h, Figure 36 and 273 to 431 at 85km/h, Figure 36). This is well below the EURO NCAP limit of 1000. Based on this, any reduction in structural interaction in collisions of lower severity would not lead to a significant reduction in occupant injury risk. At the maximum crash severity (closing speed 112km/h), the HIC loading is relatively high with respect to the EURO NCAP threshold of 1000 (785, Figure 36). This HIC value is in a range associated with significant injury risk. This is not a surprising result given the high change in velocity of the small vehicle (80km/h, Figure 35).

The injury criteria of VC and Femur Force, Figure 37 and Figure 38, are well below the respective maximum prescribed EURO NCAP limits for all crash severities and all levels of structural interaction. For each of these injury criteria, a decrease in the level of structural interaction in collisions of all severities would not result in a significant reduction in injury risk.

5.4 Summary

Whilst a decrease in structural interaction did lead to a reduction in the various injury criteria, the reduction was not highly significant. A reduction in structural interaction would also increase the risk of injury in collisions of high severity, as less energy would be dissipated in the front-end of both vehicles. The research conducted throughout the remainder of this thesis is therefore based on the assumption that increasing structural interaction is the most appropriate goal.

Limitations of the occupant simulations

The statement; that lower degrees of structural interaction would not lead to a significant decrease in occupant injury risk in collisions of lower severity, is only valid for vehicles designed for a fixed barrier crash test at an EES of 56km/h. If the fixed barrier collision-velocity was increased, vehicles would become correspondingly stiffer (see section 2.3.2). In this case, a reduction in structural interaction in collisions of lower severity may have a more significant influence on the risk of acceleration-induced injury.

The restraint system of the vehicle investigated in this section was optimised for a standard fixed barrier with an associated EES of approximately 56km/h. The change in velocity of the small vehicle, which was the focus of this investigation, was much higher than 56km/h for many of the collisions. Were the restraint system optimised for higher changes in velocity, the values of the occupant injury criterion may have been further reduced.

In addition, crash test dummies are themselves a representation of the biomechanical characteristics of human beings. All investigations were carried out with a 50^{th} percentile male, which would be more resilient to injury than older occupants and female occupants, amongst others. For more vulnerable occupants, the risk of injury in low speed collisions may be higher and a reduction in structural interaction may result in a significant reduction in injury risk.

The analysis assumes that a decrease in structural interaction led to a decrease in the EESFF value. (i.e. less energy dissipated in the front-end). However, at a given collision velocity, a reduction in structural interaction may have led to a change in the effective “shape” of the force deflection characteristic, becoming progressively more “back-loaded”. This is considered an additional potential outcome of reduced structural interaction which is not considered in this section (see further comments in “recommendations for further research”, section 10.2.

6 Topics to be addressed by a fixed barrier crash test to evaluate structural interaction

Several crash testing procedures have been proposed by different parties around the world to evaluate the crash compatibility potential of passenger cars. In this chapter, several requirements of a compatibility assessment procedure, focussed on improving the potential for good structural interaction between passenger cars, are identified. The basis for this analysis is the new theory developed in chapter 4 relating to structural interaction. This chapter acts as a basis for evaluating several proposed compatibility assessment procedures which is carried out in the following chapter.

Two considerations are relevant when discussing crash testing procedures to evaluate the potential for compatibility offered by passenger cars:

- The **configuration** of the crash test
- The nature of the safety **assessment**

At the point of vehicle design, it is not known if a vehicle will be involved in an accident and, if so, in which configuration. Due to this, crash tests are carried out in **standardised configurations**. All of the crash tests currently being considered to evaluate the compatibility potential offered by passenger cars involve a collision against a fixed barrier[26]. The configuration of the test is chosen to facilitate an evaluation of the safety characteristics of interest. Considerations related to the test configuration will be discussed in 6.1.

The **assessment method** applied within a given crash test-configuration influences vehicle development correspondingly. Manufacturers are pressured to take measures to improve the evaluation of safety performance, delivered by the safety assessment. The definitive goal of measures to mitigate injury in collision situations is to provide maximum protection to passenger vehicle occupants involved in collision

[26] Experimental crash tests to assess the compatibility potential of passenger cars have also been proposed against a Moving Deformable Barrier (MDB). To date, problems of repeatability have prevented serious consideration of this test configuration in the short-term, despite its advantage of replicating a car-to-car crash pulse in a more realistic manner [86] [72]. Many car-to-car experimental crash tests are also carried out by research institutes around the world [87] [88] [89].

situations. For this reason, the safety assessments in most test configurations are based on readings taken from instrumented crash test dummies, developed to be representative of human beings. To measure the potential for structural interaction offered by a given passenger vehicle, the characteristics of the vehicle structure itself need to be evaluated. The requirements of a compatibility assessment algorithm, focussed on improving the potential for structural interaction offered by passenger cars, will be discussed in 6.2.

6.1 Considerations relating to the test configuration

6.1.1 Deformable element

Dampening unrealistic peak forces

In crash tests against a fixed barrier without a deformable element, the inertia of rigid parts (engine and transmission) within the front-end cause unrealistic force-peaks (measured at the wall) which would not occur in a vehicle-to-vehicle collision. One function of deformable elements is to dampen these peak forces and isolate the structural forces active in real-world car-to-car collisions.

In addition to engine inertia, other small structural protrusions (such as tow hooks) which lie marginally further forward in the structure can cause force-peaks as well [70], which would not occur in car-to-car collisions. The addition of a deformable element can help to mitigate the problem of force-peaks associated with localised structural protrusions.

Activating horizontal and vertical connections

Another function of deformable elements is to activate horizontal and vertical connections between longitudinal load paths. In a collision with a fixed barrier with no deformable element, the fixed barrier acts as an ideal crash partner and longitudinal load paths in the vehicle front-end are deformed preferentially. A deformable element allows non-planar deformation of the front-end. Structural elements can move with

respect to each other in the longitudinal direction and connections between them can be engaged. These connections are highly relevant in car-to-car collisions when uneven deformation of the front-ends of both vehicles occurs (see section 4.1).

Forces transmitted to the wall

The forces transmitted to the wall by a deformable element depend on both the deformation forces of the vehicle front-end and the pressure/density characteristics of the deformable element. Deformable elements of constant pressure/density, for example, transmit a discrete force level, independent of the degree of barrier penetration and the front-end deformation forces of the car (until bottoming out occurs). All front-end deformation forces higher than those required to deform the element go undetected, assuming bottoming out doesn't occur[27]. This is a particular problem for deep layers where the crash energy could be dissipated at low force levels, dictated by the pressure/density of the deformable element, and the actual structural characteristics of the front-end would be misrepresented.

Collision Severity (EES)

When a vehicle impacts a deformable element, the kinetic energy of the vehicle can be dissipated through deformation of the vehicle structure or of the deformable element. The severity of the collision, reflected by the EES, depends on the characteristics of the deformable element, the initial velocity of the vehicle and the deformation forces of the front-end of the vehicle[28]. For deep elements of low pressure, most of the kinetic energy of the vehicle would be dissipated through barrier deformation and the front-end would be deformed to a lesser extent. In this case, the EES of the collision would be much lower than the initial velocity of the vehicle being tested (see also [65]).

[27] "Bottoming out" in a fixed barrier crash test refers to the penetration of the deformable element and the subsequent contact between structural parts and the rigid wall.
[28] This describes the severity of the collision with respect to the loading of the vehicle structure (EES). For the occupants, the collision severity is also influenced by the change in velocity of the car, which determines the change in kinetic energy of the occupants.

6.1.2 Degree of barrier overlap

The overlap ratio of a test configuration has several implications for an evaluation of the structural interaction potential of a passenger vehicle[29].

In the 100% overlap configuration, the entire front-end is activated and this usually results in higher deformation forces than in the offset configuration. The full overlap test is generally considered a more demanding test for the restraint system due to the higher associated compartment accelerations.

Conversely, the offset configuration is generally considered to be a more demanding test with respect to the vehicle structure. This is because only part of the front-end is activated and, in order to dissipate the kinetic energy of the vehicle, more deformation travel is required. In addition, the interaction forces are transmitted to one side of the compartment, so the loading of the compartment is more localised and can be considered to be more severe.

Another consideration associated with offset tests is that significant rotation of the vehicle occurs. The rotation also leads to lateral loading of the honeycomb structure of the deformable element. The stability of the honeycomb structure is much lower when loaded in the lateral direction. The final imprint left in the barrier as well as the forces recorded at the wall may not be representative of the structural characteristics of the vehicle front-end in the offset configuration.

6.1.3 Test severity

The test severity is not a critical consideration when assessing the structural interaction potential of passenger cars. However, the collision severity should be high enough to force a high degree of deformation of the front-end. Current test velocities are considered to be adequate in this respect.

[29] The overlap ratio refers to the percentage of the width of a vehicle which contacts the struck-object (either another vehicle, moving barrier or a fixed barrier).

6.1.4 Harmonisation potential

The automotive industry is becoming increasingly globalised and most vehicle manufacturers produce vehicles for sale in many different countries. For each country, the regulatory and consumer-based safety assessments can vary. In response to this, the harmonisation of vehicle safety regulations has become an agenda item for the International Harmonisation of Research Activities (IHRA) [90], which deals with harmonising research activities in the global automotive branch. The goal of harmonisation is to prevent increased investment in the vehicle development process with no associated real-world safety benefit. To achieve this, it is sensible to streamline or harmonise safety assessments around the world, whilst still considering the differences in fleet compositions. The potential for harmonisation is an important aspect of any safety assessment procedure.

6.2 Considerations relating to the assessment algorithm

6.2.1 Assessing and influencing vehicle geometry

For a given crash test configuration, the way in which vehicles are assessed influences vehicle development. To improve structural interaction, the distribution and location of front-end forces can be assessed. A convergence of structural forces, to within certain vertical limits, is expected to improve geometrical compatibility and improve structural interaction (see Figure 4).

To assess the structural interaction potential of passenger vehicles, an algorithm is required to evaluate the geometrical distribution and the location of forces exhibited by a passenger car.

6.2.2 Mass/Force dependency

As discussed in section 4.1, structural interaction is a phenomenon which relates to the collision event itself. A theoretical maximum value for energy dissipation can be calculated for a particular collision in any configuration involving any two vehicles.

The degree of structural interaction is obtained through comparing the actual level of energy dissipation with this theoretical maximum. The degree of structural interaction occurring in a collision is therefore independent of the front-end force-displacement characteristics of each vehicle. Mass and stiffness decide the maximum degree of energy dissipation possible in a collision whereas structural interaction is a value relative to this maximal value.

Therefore, any compatibility assessment focussed on evaluating the structural interaction potential of passenger cars needs to assess vehicle geometry independent of mass (i.e. independent of the deformation forces of the front-end which are influenced by vehicle mass). Otherwise the assessment would be mass-dependent and the evaluation of vehicle geometry would no longer be transparent. A compatibility assessment independent to force/mass is required before the structural interaction potential of different vehicles can be compared.

6.2.3 Repeatability/Reproducibility

Repeatability refers to the ability of a test procedure to deliver the same results for repeated crash tests carried out under identical experimental conditions and at the same facility. Reproducibility relates to the results of tests carried out at different facilities with the aim of replicated the original experimental conditions. The repeatability/reproducibility of an assessment is influenced by:

- The sensitivity of the assessment algorithm
- The sensitivity of the measurement devices
- Manufacturing tolerances of vehicles

The sensitivity of a safety assessment must be acceptable within given tolerances in manufacturing and measuring devices. A key demand of safety assessment procedures is to deliver repeatable/reproducible results.

6.3 Summary

In this chapter, a set of requirements for a compatibility assessment procedure was developed based on several **test characteristics**:

- Initial velocity
- The overlap ratio
- Characteristics of deformable elements
- Assessment algorithm

The key **requirements of a test** to measure the structural interaction potential of passenger cars can be summarised and divided into four sub-groups:

- Isolate structures present in car-to-car collisions
- Offer harmonisation potential
- Be repeatable
- Be independent of mass/force

To summarise the observations made in this chapter, a matrix linking test characteristics and test requirements is shown below, Figure 39. The relevant test **characteristics** which need to be considered to satisfy each of the respective test **requirements** are marked with an “x”. This table is the basis for the evaluation of test procedures carried out in the next chapter.

				TEST CHARACTERISTICS				
				TEST CONFIGURATION			ASSESSMENT ALGORITHM	
				Deformable Element	Overlap %	Initial Crash Velocity	Physical quantity assessed	Assessment algorithm
TEST	REQUIREMENTS	Structures present in car-to-car collisions accurately represented	* Activation of horizontal and vertical connections between longitudinal load paths	x	x*1			
			* Dampening of motor impulse	x*2				
			* Significant deformation of front-end	x*3		x		
			* Vehicle geometry accurately measured	x	x		x	
			* Entire front-end structure tested		x			
		Independent to mass/force	* Vehicles not penalised based on Mass/deformation forces				x	x
		Repeatability	* Assessment is repeatible				x	x
		Harmonisation Potential	* Other safety aspects can be evaluated	x	x	x		
			* Similar to existing passive safety assessments	x	x	x		

***1 - Offset influences horizontal shear forces**

***2 - Only if the deformable element is soft enough**

***3 - To activate the front-end, the deformable needs to be stiff enough and or shallow enough to prevent a large amount of energy being dissipated in the deformable element.**

Figure 39 Summary: Requirements of a compatibility test procedure to evaluate the structural interaction potential offered by passenger cars

7 Evaluation of compatibility test procedures

In chapter 6, the key requirements of a test procedure to measure the structural interaction potential of passenger cars were discussed. Based on this, crash tests which have been proposed to evaluate the compatibility potential offered by passenger cars are evaluated in this chapter. This evaluation is carried out based on Figure 39.

As compatibility discussions in Europe, Japan and North America (in particular) move into a decisional phase, several crash tests focussed on improving the compatibility potential of passenger cars are being considered for implementation. The goal of most of these tests is to improve the structural interaction potential offered by passenger cars. Edwards, Davies and Hobbs of the Transport Research Laboratory (TRL) in England developed a test in the full-overlap-configuration with the primary goal of evaluating the structural interaction potential of passenger cars, based on controlling the location and geometrical distribution of front-end forces [70]. Delannoy and Faure also focus on the evaluation of the structural interaction potential offered by passenger cars in another proposed compatibility test procedure in the offset configuration [23]. In the USA, an evaluation of the Average Height of Force (AHOF) of the front-end has been proposed, also with the goal of improving structural interaction through improved geometrical compatibility in the vertical direction [44].

Crash test results, simulation results and theoretical calculations are used to support the evaluation of proposed compatibility assessment procedures. To evaluate the tests proposed in Europe, a number of crash tests, financed by the ACEA (Association des Constructeurs Européens d' Automobiles) were carried out with a Rover 75[30]. In a test series involving six vehicles, modifications were made to the cross beam to vary the stiffness of four of these vehicles. For each test configuration, three different levels of cross beam stiffness were investigated (strengthened/reinforced,

[30] The ACEA is a body financed by European vehicle and truck manufacturers to represent European industry in matters of legislation and to carry out joint research [91].

standard and weakened). The standard cross beam and the two modified cross beams are shown in Figure 40[31].

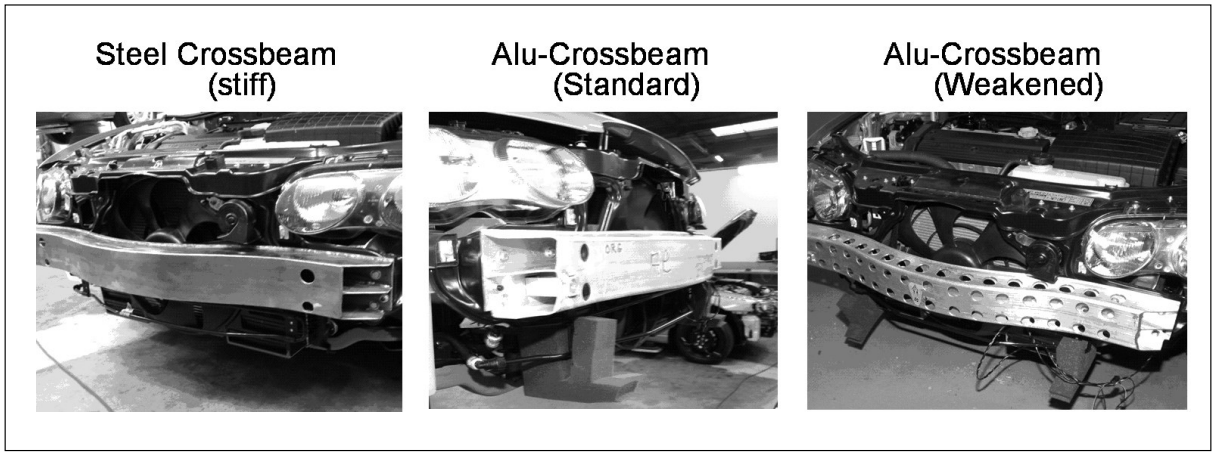

Figure 40 – Cross beam modifications, Rover 75 tests carried out by the ACEA

7.1 Full-Width Deformable Barrier (FWDB)

A compatibility test in the full-overlap configuration has been proposed by the Transport Research Laboratory (TRL) in England[32]. Wall forces are measured by 125mm by 125mm load cells, fixed to the wall. A deformable element with two 150mm deep layers of homogeneous pressure (0.34 MPa and 1.71 MPa) is located in front of the wall. The stiffer second layer of the element is also divided into 125mm by 125mm square segments, aligned with the load cells behind the element, to prevent the distribution of forces in the vertical and horizontal directions within the element (also referred to as bridging effects).The test configuration and the geometry of the load cell wall are shown in Figure 41 and Figure 42.

[31] The stiffness of the cross beams was determined based on static loading of the cross beams in a specially designed test rig. The bending stiffness of the cross beams was determined to be equal to $7.6*10^6$ N/m, $2.3*10^6$ N/m and $1.5*10^6$ N/m, for the reinforced, standard and weakened cross beams, respectively [93].

[32] The FWDB Compatibility assessment procedure is summarised in this section based on the official protocol version 1.4 [26]. See also [60] [70].

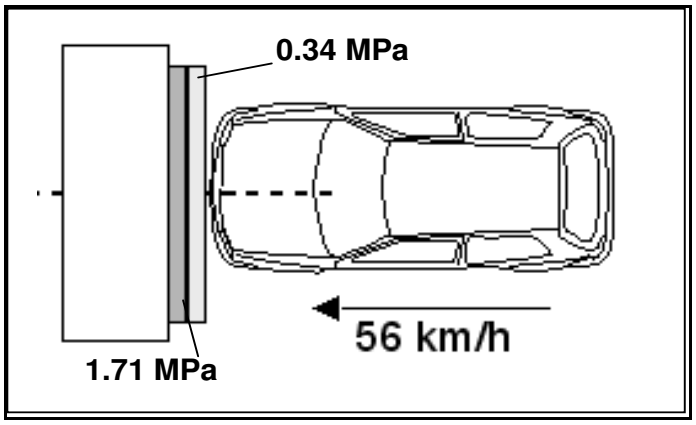

Figure 41 FWDB Test configuration

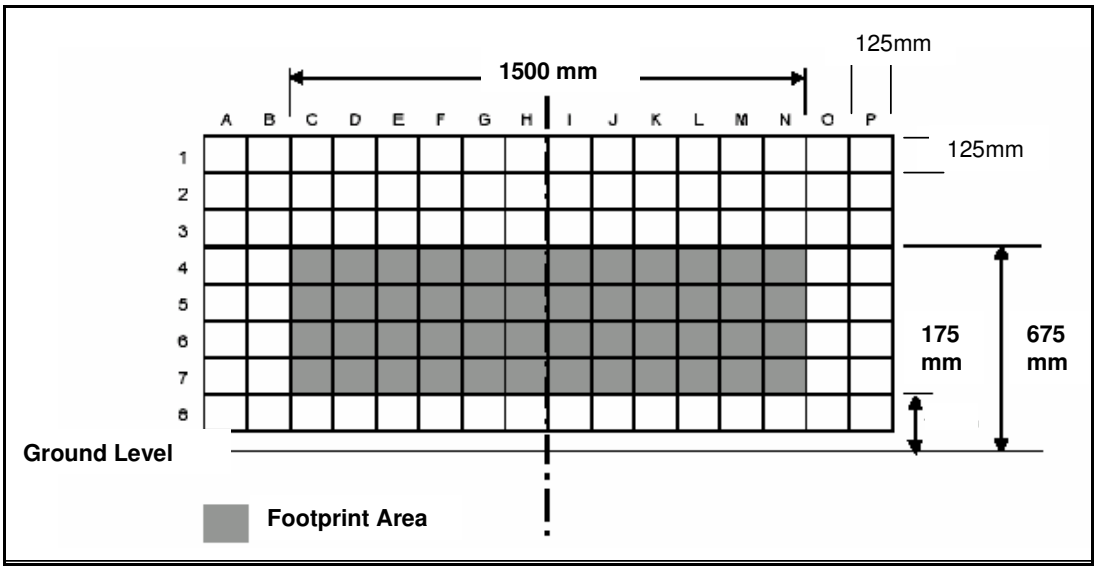

Figure 42 Geometry of the load cell wall proposed by TRL [26]

The goal of the test is to evaluate the homogeneity of the force distribution exhibited by the front-end of a passenger vehicle within a given “footprint” area, Figure 42. The force distribution is penalised according to the degree of inhomogeneity, based on a calculation of the variance of forces within the footprint area. The size and the location of the footprint area has not yet been finalised.

Smoothing

Force-time characteristics are recorded for each of the load cells shown in Figure 42. Before the homogeneity of the distribution of front-end forces is evaluated, a smoothing algorithm is applied to the force-time dataset. For each time step, the average

force value ($_sF_{ij}$) for each possible combination of four adjacent load cells is calculated, yielding a "smoothed" dataset.

$$_sF_{ij} = \frac{1}{4}\left(F_{i-1,j-1} + F_{i-1,j} + F_{i,j-1} + F_{i,j}\right) \quad (15)$$
$$where\ i\,/\,j = rows\,/\,columns$$

From the "smoothed" data set, force maxima are extracted, irrespective of the time of occurrence. These act as a simplified representation of front-end geometry and form the basis of a force homogeneity evaluation.

Homogeneity Algorithm

The homogeneity of the distribution of smoothed-peak-forces (force maxima from the smoothed dataset) is evaluated based on the variance between peak forces and a mean force value, Target Load Level (L):

$$L = \frac{\sum \text{Peak smoothed forces over entire wall}}{\text{number of load cells in the standard footprint}} \quad (16)$$

Three homogeneity values (Cell, Row and Column) are calculated:

- Cell homogeneity (H_{cl}) : Overall homogeneity
- Row homogeneity (H_r): Homogeneity between rows (vertical)
- Column homogeneity (H_c): Homogeneity between columns (horizontal)

The equations for H_{CL}, H_R and H_C are shown below [26]:

$$H_{cl} = \frac{\sum_{i=1}^{{}_sn}\left(L - {}_sf_i\right)^2}{{}_sn} \quad (17)$$
$$_sn = n_r \times n_c$$

$$H_r = \frac{\sum_{i=1}^{{}_s n_r}\left[L - \frac{1}{{}_s n_c}\sum_{j=1}^{{}_s n_c} {}_s f_{ij} \right]^2}{{}_s n_r} \tag{18}$$

$$H_c = \frac{\sum_{j=1}^{{}_s n_c}\left[L - \frac{1}{{}_s n_r}\sum_{i=1}^{{}_s n_r} {}_s f_{ij} \right]^2}{{}_s n_c} \tag{19}$$

where (n_R) and (n_C) are the number of rows and columns in the footprint area.

Load concentration factor

The homogeneity equations also evaluate the proportion of total force which is located within the footprint area, through the calculation of the target load level. Equation (17) for example, can be re-written in terms of the mathematical variance (V_{cl}) and a load concentration factor by considering the mean load cell force ($\overline{f}$):

$$\begin{aligned} H_{cl} &= \frac{\sum_{i=1}^{{}_s n}\left({}_s\overline{f} - {}_s f_i \right)^2}{{}_s n} + (L - {}_s\overline{f}^{\,2}) \\ &= V_{cl} + (L - {}_s\overline{f}^{\,2}) \end{aligned} \tag{20}$$

The second term in equation (20) reflects the proportion of loading which is located within the footprint area. To receive an H_{CL} value equal to zero, all of the force must be present within the footprint area. All structures which are located outside of the footprint area are penalised.

7.1.1 Representing vehicle structures

Barrier Deformation

Although the basis of the FWDB compatibility assessment is the forces measured by load cells, the deformable elements for the Rover75 tests were also digitised to rep-

resent the imprint of the front-end in the deformable element (weakened cross beam Figure 43, reinforced cross beam Figure 44).

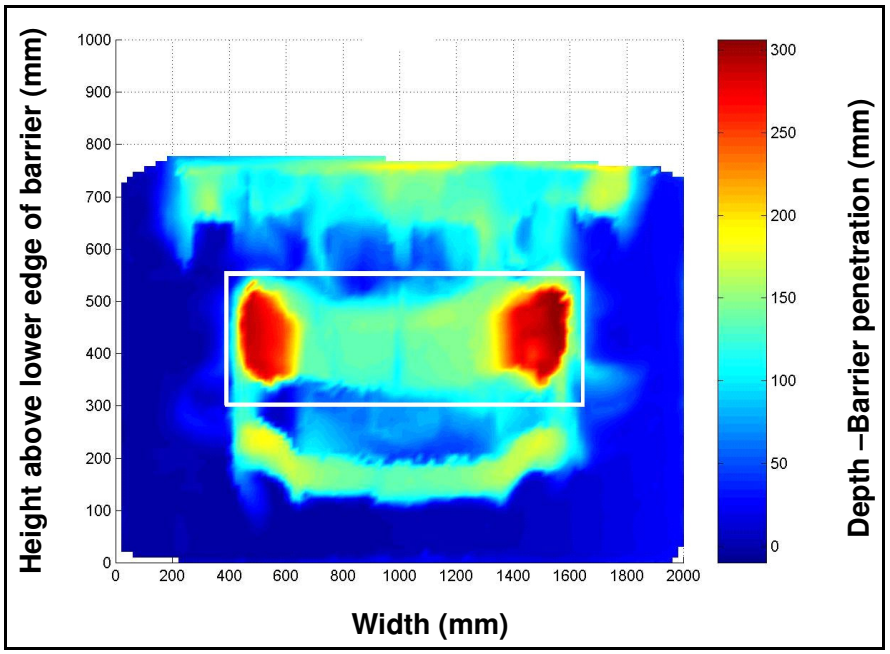

Figure 43 ACEA Rover 75 tests- Weak Cross beam. 2-Dimensional representation of the imprint of the vehicle front-end in the deformable element. FWDB test at 56km/h (see Figure 41 and Figure 42)

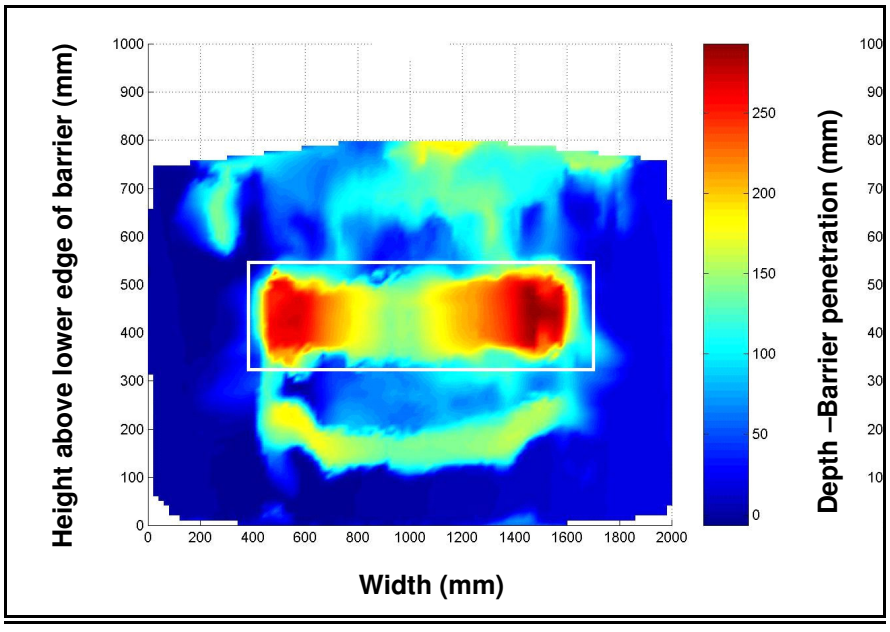

Figure 44 ACEA Rover 75 tests- Reinforced Cross beam. 2-Dimensional representation of the imprint of the vehicle front-end in the deformable element. FWDB test at 56km/h (see Figure 41 and Figure 42)

The stiffer cross beam deformed the barrier to a greater extent in the area between the imprint (red) of the two longitudinals. The representation of vehicle structures, based on barrier deformation shows plausible results.

Wall forces

Figure 45 and Figure 46 illustrate the distribution of **peak forces** (before smoothing) across the load cell wall. A clear difference in the force distribution can be observed, for each of the different cross beams of different stiffness.

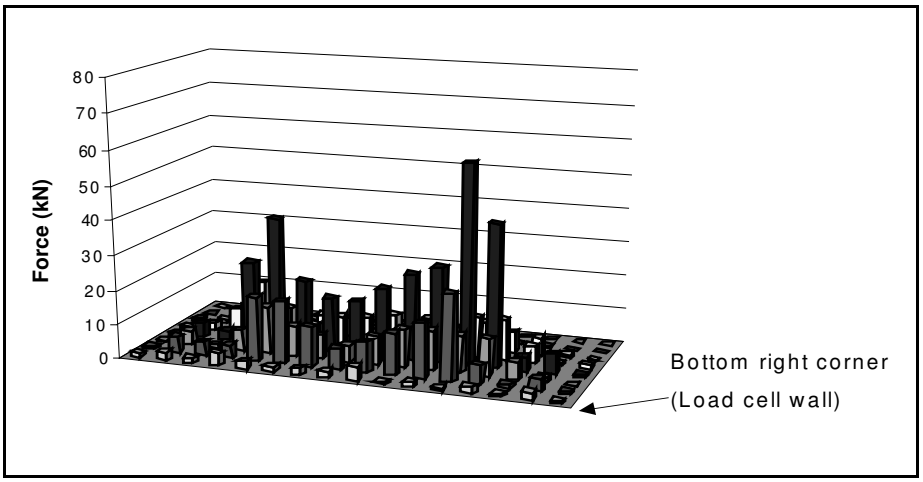

Figure 45 ACEA Rover 75 tests- Weakened cross beam. 3-Dimensional representation of load cell forces. FWDB test at 56km/h (see Figure 41 and Figure 42)

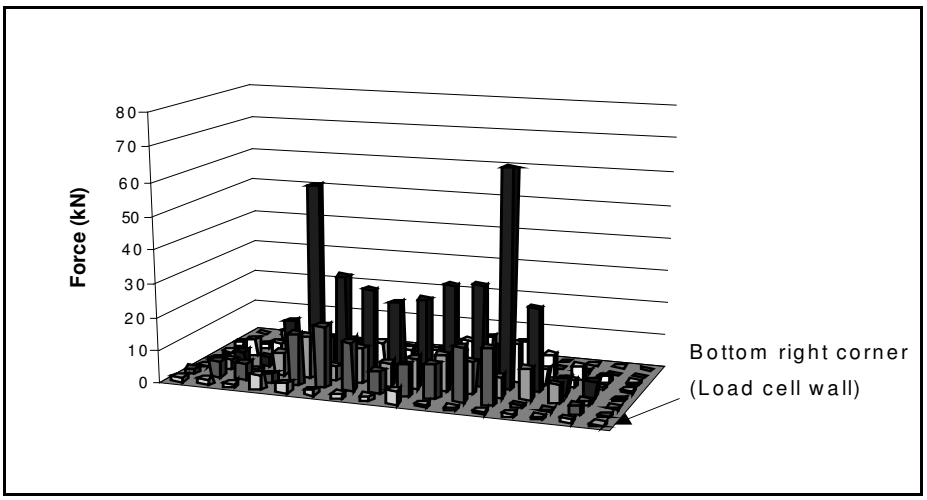

Figure 46 ACEA Rover 75 tests- Reinforced cross beam. 3-Dimensional representation of load cell forces. FWDB test at 56km/h (see Figure 41 and Figure 42)

The Rover 75 with a reinforced cross beam (Figure 46) transmitted higher forces to the wall between the peak forces caused by the longitudinals. The difference in cross beam stiffness is reflected by the force measurement as well.
Higher peak forces were registered at the wall in the area of the longitudinal members for the vehicle with the reinforced cross beam. This may have been due to the stiffer cross beam preventing bending of the longitudinals, leading to higher compression forces been transmitted to the wall.

Deformable Element Characteristics

Each of the two layers of the deformable element used in the FWDB test configuration is homogenous with respect to the density of the honeycomb structure. This can be represented using discreet pressure values of 0.34 and 1.71 MPa, respectively, Figure 41. For an object of a given cross-sectional area penetrating the element, the force transmitted to the load cells reflects the discrete pressure values associated with each layer of the deformable element (see Figure 47).

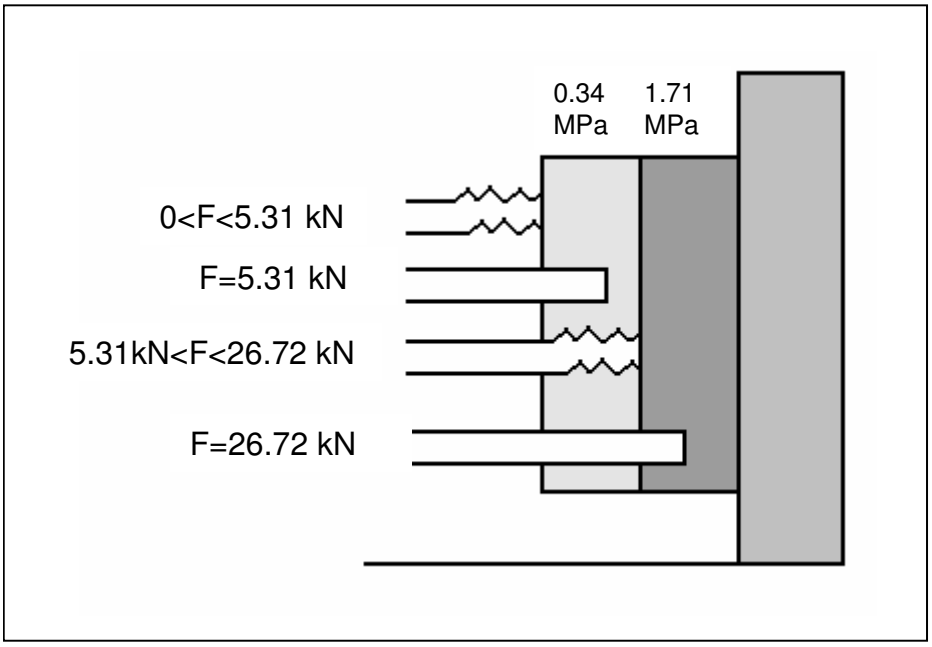

Figure 47 Forces transmitted to the wall resulting from the impact of a rigid-flat object of 125mm*125mm cross-sectional area with respect to the pressure stages of the FWDB element [61]

Ignoring dynamic influences such as inertial effects and assuming perfectly homogenous layers:

Based on the pressure stages of the deformable element, a force of 5.31kN has to be exceeded per 125mm by125mm square impact surface in order to penetrate the element[33]. After the element has been penetrated, deformation of the barrier will theoretically occur at a constant force level for 150mm, up to the interface between the two layers. To penetrate the second layer, a further increase in force is required.

The deeper the layers of constant pressure, the less information about the actual front-end force distribution can be obtained. Wall forces measured in the FWDB test are therefore a simplified representation of the geometrical distribution and location of front-end structural forces, due to the layers of constant pressure. Elements of progressively increasing stiffness are advantageous in this respect, as the force transmitted through the barrier to the wall is proportional to the degree of deformation of the barrier.

It should also be noted that the stepped nature of the deformable element illustrated in Figure 47 could lead to a mass dependency in the assessment of forces exhibited by the front-ends of different vehicles. This will be discussed in detail in 7.1.3.

Representing structures throughout the crash

The FWDB assessment is based on force maxima (after the smoothing algorithm has been applied). The peak force registered by each load cell may occur at a different instant in the crash. An artificial force-distribution is therefore created, which does not represent any specific instant in the collision.

[33] The calculation of the force transmitted to the wall is based on the common formula F=(Pressure*Area)=0.34Mpa*125mm*125mm=5.31kN.

7.1.2 Test severity

The severity of the FWDB crash test is high enough to ensure that a high degree of front-end deformation occurs. Crash test results have shown that the acceleration-time characteristic of the passenger compartment as well as the dummy loadings are very similar for crash tests involving the same vehicle in the FWDB configuration, with and without a deformable element [92]. This increases the potential for harmonisation with the existing FWRB configuration, in particular with respect to the optimisation of the restraint system[34].

7.1.3 Mass/force dependency

The proposed FWDB assessment contains a mass/force dependency. It penalises heavier vehicles which exhibit higher deformation forces[35]. The homogeneity algorithm penalises vehicles based on the absolute difference between the peak forces occurring in each cell (after smoothing) and an average force value (L). To further illustrate this point, the homogeneity ratings were calculated for two theoretical force distributions, a standard force distribution (basis) and the same force distribution multiplied by a linear factor k (basis*k):

The homogeneity of a standard force distribution is given, according to equation (17):

$$H_{cl}(basis) = \frac{\sum_{i=1}^{s n} \left(L -_{s} f_i\right)^2}{{}_{s} n}$$

For a factor k-heavier-vehicle, all peak-smoothed-forces would increase according to "k" and the target load level and measured smoothed peak forces would also increase according to "k" to give H_{cl} (basis*k):

[34] The only difference between the FWDB test configuration and the FWRB test configuration is the deformable element located in front of the wall in the FWDB configuration.
[35] The fact that heavier vehicles are stiffer is based on the assumption that all vehicles have a fixed amount of deformation travel and all vehicles are tested at the same velocity in current self protection assessment procedures (see section 2.2).

$$H_{cl}(basis*k) = \frac{\sum_{i=1}^{{}_{s}n}(kL -_{s} kf_i)^2}{{}_{s}n} = k^2 \frac{\sum_{i=1}^{{}_{s}n}(L -_{s} f_i)^2}{{}_{s}n}$$

Thus a factor k heavier vehicle will be penalised according to a factor k^2. A solution to this, proposed by the author, is to normalise the evaluation, according to the target load level (L).

$$H_{cl-normalised}(basis*k) = \frac{\sum_{i=1}^{{}_{s}n}\left(\frac{kL -_{s} kf}{kL}_{i}\right)^2}{{}_{s}n} = \frac{\sum_{i=1}^{{}_{s}n}\left(\frac{L -_{s} f}{L}_{i}\right)^2}{{}_{s}n}$$

The above equation is identical to equation (17), meaning the mass/force dependency is no longer present in the assessment. This is widely accepted today.

Note: The calculations shown above prove that the mass dependency is removed from the assessment algorithm itself. However, the representation of front-end forces is also influenced by the depth and characteristics of deformable elements. Further investigation is required to determine whether the stepped nature of the deformable element, Figure 47*, leads to a mass dependency (see also 7.1.1 – Deformable Element characteristics).*

7.1.4 Repeatability

The discreet resolution of the load cell wall has implications for the repeatability of assessment metrics based on force. A small change in vehicle geometry (e.g. the ride height) could mean that concentrated loadings would be transferred to an adjacent cell. The force distribution exhibited by the same vehicle may vary according to the point of impact. To compensate for this, the smoothing algorithm is proposed (see section 7.1).

A theoretical calculation is presented to investigate the influence of smoothing when concentrated loadings are present. A concentrated load is distributed over one, two

and four load cells respectively and the corresponding smoothed and unsmoothed variances calculated, Figure 48. In each case, the sum of all wall forces is equal.

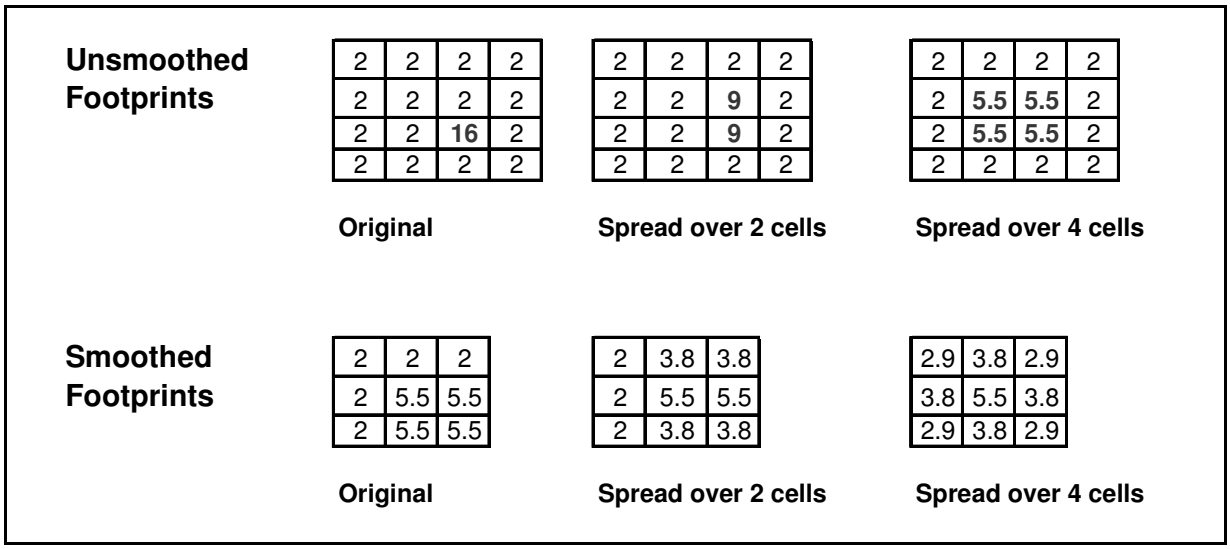

Figure 48 Standard and smoothed footprints for the case of a concentrated load distributed over 1, 2 and 4 cells (A, B and C) respectively.

For each of the three levels of load distribution (1 cell, 2 cells, 4 cells), the smoothed and unsmoothed variance is calculated as a simplified representation of the homogeneity assessments described in equations (17) (18) and (19) and illustrated in Figure 49, below.

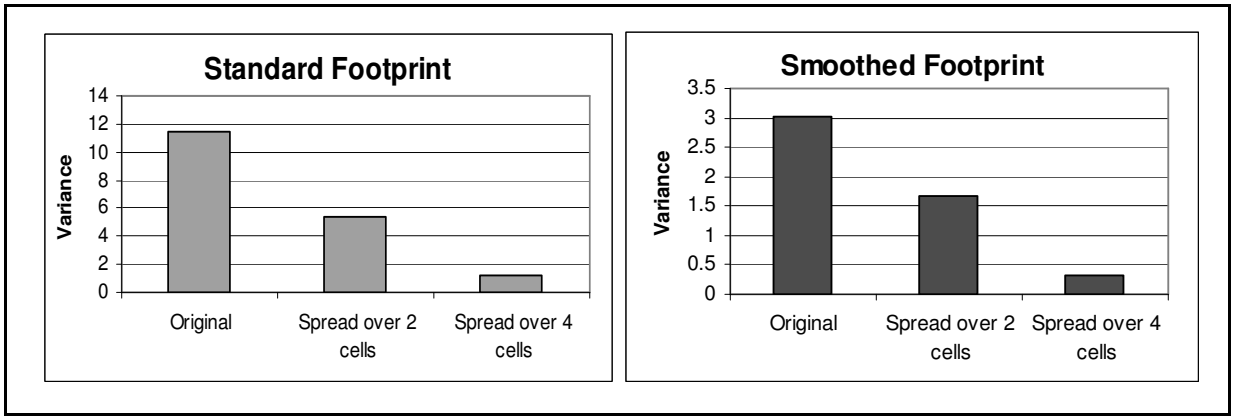

Figure 49 Smoothed and unsmoothed variances for three theoretical force distributions containing a concentrated load spread over 1, 2 and 4 load cells, respectively.

For both the smoothed and standard footprints, a similar reduction in variance occurs when the concentrated load is distributed over 1, 2 and 4 cells, respectively. This proves that the smoothing algorithm doesn't remove the sensitivity of the homogene-

ity evaluation to concentrated loadings (if no sensitivity to concentrated loadings were present, all smoothed variances would be equal). This sensitivity has implications for the repeatability of the assessment method.

To further investigate repeatability, several simulations were carried out with a Volkswagen passenger vehicle and the homogeneity of the distribution of forces calculated according to equations (17) (18) and (19). The vehicle was first crashed in the standard position then shifted; (25mm up/right 25mm down/left). This represented a relatively small translation of the vehicle with respect to the load cell length/width dimension of 125mm. The resulting variance values are shown in Figure 50, below.

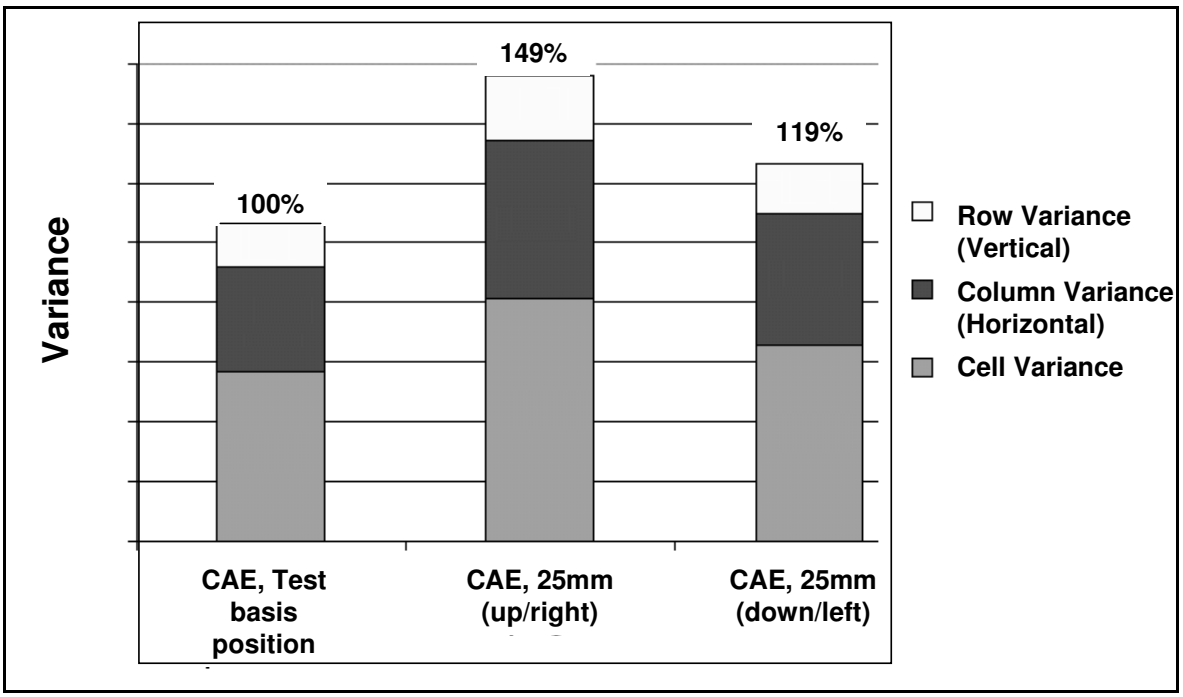

Figure 50 Variance values associated with the load-distribution for a standard passenger vehicle with respect to the point of barrier impact

Figure 50 confirms the sensitivity of the assessment for an impact tolerance of 25mm. A relatively small translation of the vehicle leads to large variations in the homogeneity of the force-distribution, calculated based on the FWDB assessment algorithm. This could result in vehicle manufacturers designing vehicles which better spread concentrated loadings across load cells to achieve a more homogenous distribution of force. Such measures would not be expected to be associated with any real-world benefit in the safety performance of motor-vehicles.

7.1.5 Influence of the assessment on vehicle geometry

The FWDB assessment, in its proposed form, places two demands on vehicle structures:

- Convergence of forces to within a footprint area (due to the load concentration factor, see 7.1)
- A more homogeneous distribution of forces within the footprint area (see equations (17) (18) and (19)

In general, both are considered appropriate goals to improve the potential for geometrical compatibility and, correspondingly, the structural interaction potential of passenger cars. The homogeneity assessment, however, is a stringent demand. It may not be necessary for vehicles to exhibit a homogeneous force distribution to the degree demanded by the resolution of the load cell wall.

Similarly, with respect to the load concentration factor, it is also a strong requirement for vehicle structures to converge completely to within the footprint area. It may be more appropriate to demand a minimum degree of support force from all vehicles within this footprint area. This would allow force matching within the assessment area. Excessively high forces in the assessment area might have negative implications for compatibility.

7.2 Progressive Deformable Barrier (PDB)

PDB Test configuration

The PDB assessment procedure is based on a fixed barrier crash test in the offset configuration at a velocity of 60km/h (Figure 51) [36]. A deformable element of progressively increasing stiffness is attached to the wall (Figure 52).

[36] The degree of offset of the PDB Assessment has yet to be finalised. It has varied between a fixed distance of 700mm and an overlap ratio of 50% of the front-end of the vehicle being tested. The description of the PDB assessment in this section is based on the official test protocol (version 2.2) [27]. See also [23] [94].

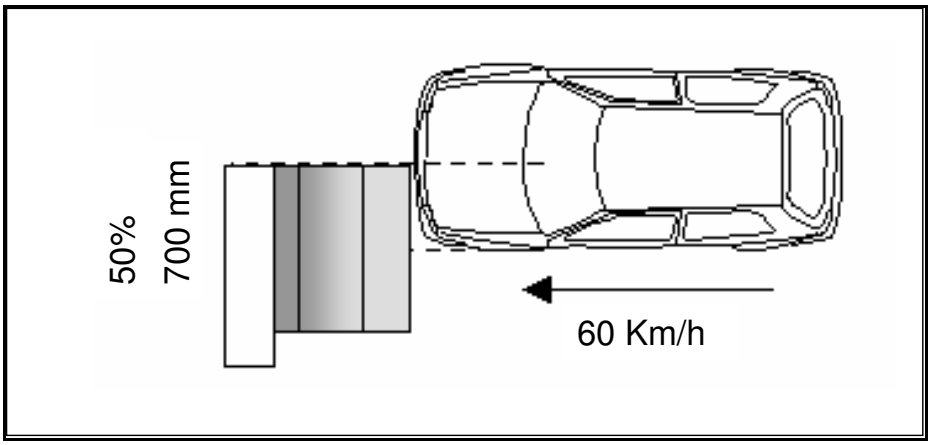

Figure 51 PDB Test Configuration

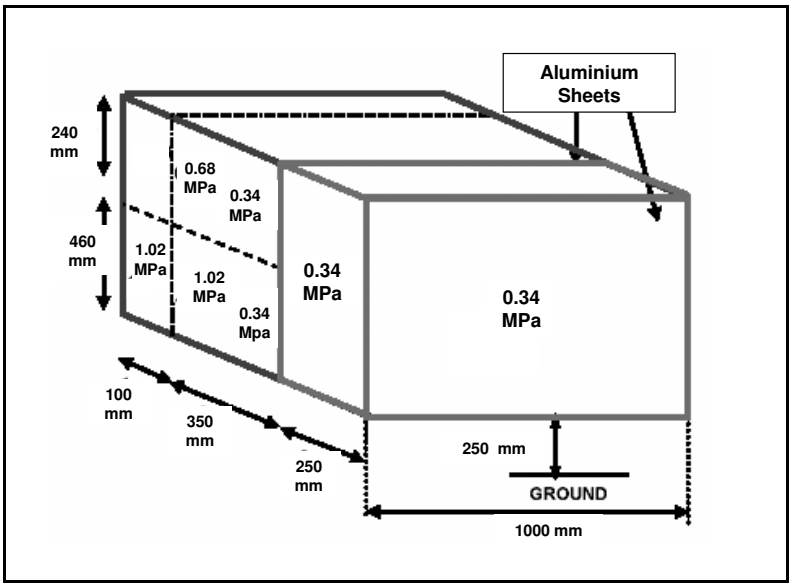

Figure 52 PDB Deformable Element

The PDB deformable element has three different levels of stiffness. The first and last layers are homogeneous (constant pressure). The middle section has a linearly increasing pressure profile. In the second and third layers, a pressure difference is also present between upper and lower sections of the element, Figure 52.

PDB Assessment

After the crash, the imprint of the vehicle front-end in the deformable element is digitised to obtain a 3-dimensional dataset representing the imprint surface. This 3-dimensional imprint surface is projected onto a 2-dimensional reference plane, lo-

cated co-planar with the front face of the undeformed barrier[37]. The imprint in the deformable element is then categorised according to depth increments (from 0 to 100mm and in 50mm increments thereafter up to the plane of the fixed barrier at a depth of 700mm), Figure 53. This 2-dimensional representation of the vehicle imprint in the deformable element forms the basis of the PDB assessment algorithm.

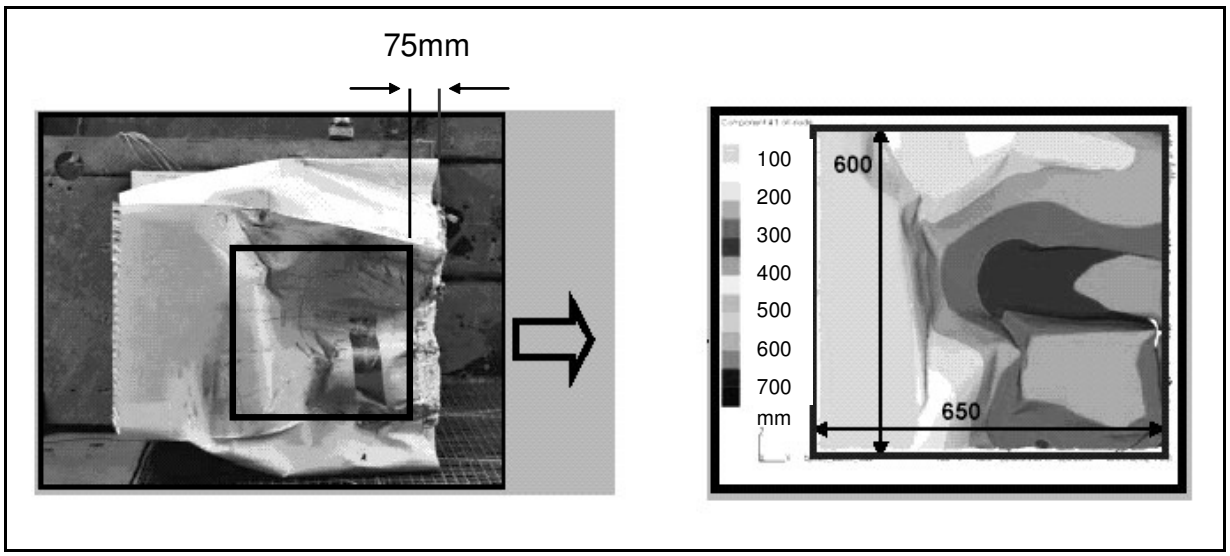

Figure 53 Digitisation of the vehicle imprint in the deformable element and conversion into a 2-dimensional representation of deformation across a range of deformation intervals

For each deformation interval (i.e. each colour in Figure 53) three values are calculated.

Zi = The average ground clearance [cm]
Xi = The average depth of deformation [cm]
Si = The equivalent 2-dimensional surface area belonging to each deformation interval (after projection onto the 2-dimensional reference plane) [cm^2]

[37] This is carried out within a given assessment window. The location of the assessment window remains open. The assessment window has been proposed to be 650mm wide and 600mm high.

These values form the basis of a calculation of a vehicle aggressivity factor [27]:

$$\text{Vehicle Aggressivity} = \frac{1}{0{,}52} R^{0{,}55}$$

where

$$R = \sum_{0}^{i} \left(\frac{Z_i}{Z_{lim}} \right)^4 \cdot \left(\frac{X_i}{X_{lim}} \right)^2 \cdot S_i \qquad (21)$$

Z_{lim} and X_{lim} are constants and i is the number of depth intervals

Vehicles which receive a higher aggressivity rating are interpreted as offering a lower level of partner protection and, correspondingly, a lower potential for compatibility and structural interaction.

7.2.1 Representing vehicle structures

The deformable element used in the PDB test has a progressively increasing pressure characteristic. The forces transmitted to the wall are thus proportional to the degree of barrier-penetration. In this respect, structures are more accurately represented than for a barrier with deep layers of constant pressure.

However, the PDB doesn't represent vehicle structures realistically due to vehicle rotation. The offset configuration induces vehicle rotation and a non-symmetrical imprint in the deformable element, Figure 54.

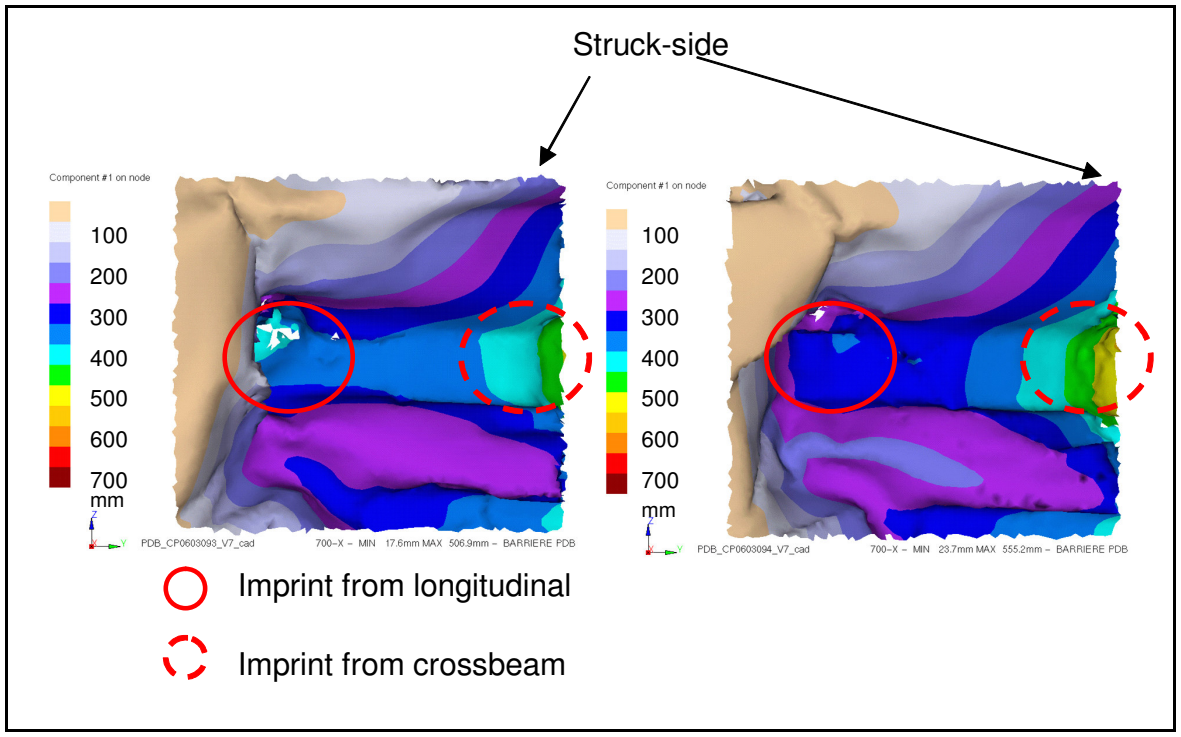

Figure 54 2 dimensional representation of the imprint left by the vehicle front-end in the PDB element within a 600mm*650mm assessment area (Rover 75 serial cross beam [left] and reinforced cross beam [right])

Figure 54 shows that the highest degree of barrier deformation occurs at the height of the cross beam on the right (struck) side of the barrier. The cross beam leaves a deeper imprint in the barrier than the longitudinal, which doesn't reflect the actual distribution of front-end forces. The longitudinal is much stiffer than the cross beam (see Figure 45 and Figure 46 depicting the force distribution in the full-width configuration).

The PDB assessment evaluates the final imprint in the deformable element left by the front-end of the vehicle. The behaviour of the structure, throughout the crash, is not considered.

7.2.2 Test Severity

In the PDB configuration, the initial velocity of the vehicle being tested is 60km/h and the depth of the deformable element is 700mm. The deformable element offers significant potential for energy dissipation through deformation of the element in preference to deformation of the front-end of the car being tested. Since the pressure of the element increases with increasing element depth, the potential for energy dissipation

through deformation of the deformable element is much higher than the current EEVC barrier test[38]. The EES of the collision could be much lower than the initial velocity of 60km/h would suggest.

7.2.3 Mass/Force Dependency

Front-end forces and initial kinetic energy are dependent on vehicle mass. Heavier vehicles possess higher front-end forces and higher initial kinetic energy, both of which lead to a greater potential for barrier penetration and a mass/force dependency in the PDB assessment.

The degree of barrier penetration is directly penalised, to the power of 2, in the PDB-Assessment according to the $(X/X_{LIM})^2$ term, where x relates to the depth of deformation, equation (21). The X_{LIM} term is constant, for all vehicles, and has no influence when comparing the aggressivity values for different vehicles. The PDB assessment contains an inherent mass dependency which is counter-productive for an assessment of the structural interaction potential of passenger cars.

7.2.4 Repeatability

The repeatability of the test procedure is unknown. No reliable repeatability tests with an identical vehicle have been carried out to date. The PDB assessment is based on the vehicle imprint in the deformable element, which is a continuous measure. The problems associated with the resolution of the load cell wall associate with compatibility metrics based on the measurement of forces is not an issue associated with this test. The potential for repeatability/reproducibility of this test are therefore higher.

7.2.5 Influence of the assessment on vehicle geometry

Height of structures

The PDB aggressivity metric (equation (21)) penalises each unit of deformation to the power of four, based on ground clearance (according to the $(Z/Z_{lim})^4$ term). This demands a general lowering of structures for all cars. This may be appropriate for larger

[38] The pressure of the EEVC deformable element is homogenous (60Psi or 0.413 MPa) [95].

and heavier vehicles, to increase geometrical compatibility with other small vehicles. For smaller vehicles, the demand for the convergence of all structures toward ground level is considered inappropriate, as this would decrease the potential for geometrical compatibility for these vehicles involved in collisions with larger vehicles. In addition, as shown in Figure 4, truck-under protection requires a ground clearance of at least 400mm (see Figure 4). Any car front structures below this could not interact with truck underrun protection. Demanding all vehicle front-end structures to converge toward the ground is not considered appropriate.

Front-end deformation forces

As mentioned in 7.2.3, vehicles are also penalised according to the degree of barrier deformation. For a given vehicle, a reduction in the aggressivity rating could be achieved by softening front structures (resulting in lower X/X_{lim} values). Front-end deformation would occur in preference to barrier deformation and a lower degree of barrier penetration would result. For heavier vehicles, this would increase partner protection yet compromise self protection. This is not considered appropriate given the high relevance of single vehicle collisions in real-world accidents. For lighter vehicles, this is inappropriate as it corresponds to a reduction in self protection for all accidents, including frontal collisions with other vehicles as well as in single vehicle collisions[39].

Assessing front-end geometry

The PDB assessment doesn't evaluate the geometrical properties of the front-end accurately due to vehicle rotation. To investigate this, the PDB assessment algorithm was applied to the left and right halves of the assessment windows for each of the three Rover 75 tests. The PDB aggressivity values are shown for the left and right halves of the assessment windows for the weakened, serial and cross beam, respectively, Figure 55.

[39] Single vehicle collisions were identified as posing the highest risk of serious and fatal injuries for passenger car occupants in the relevance study based on accident statistics carried out in Chapter 3.

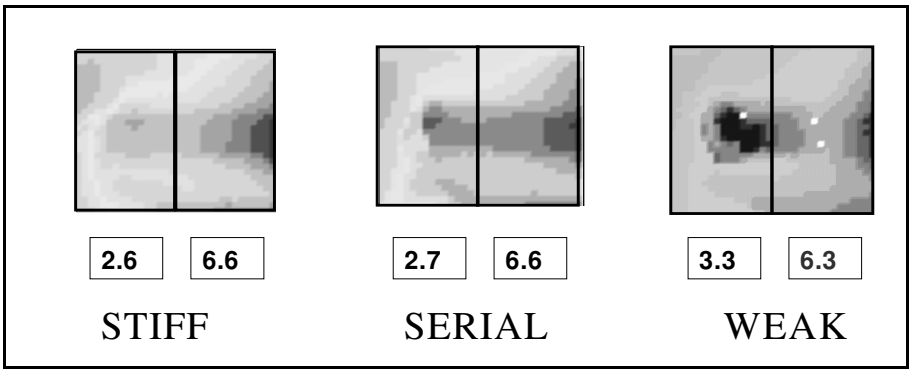

Figure 55 PDB aggressivity ratings for the left and right halves of the assessment windows for the Rover 75 tests with cross members of varied stiffness. PDB test at 60km/h and 50% barrier overlap

A stiffer cross member provides a greater area of support and represents a less aggressive front-end force distribution. The Rover 75 with the reinforced (stiff) cross beam exhibited the most homogenous imprint in the area of the longitudinal (left-half of evaluation window) and is favourably evaluated (2.6 reinforced, compared to 3.3 weak, Figure 55) which is desirable.

With respect to the struck (right) side of the elements, the stiffer cross beam is penalised (6.6 reinforced compared to 6.3 weakened), Figure 55. The stiffer member is penalised as it deforms the barrier on the struck (right) side to a greater extent, due to vehicle rotation. This is due to the asymmetry of the test configuration and is a fundamental problem associated with the PDB configuration.

7.3 Full-width rigid barrier (FWRB)

Test configuration

An evaluation of the Average Height of Forces (AHOF) takes place in the FWRB configuration at a velocity of 56km/h. The configuration is identical to the FWDB configuration, with no deformable element located in front of the barrier, Figure 56[40].

[40] The description of the Average Height of Force Assessment in the FWRB configuration is based on [24] [25] and [96].

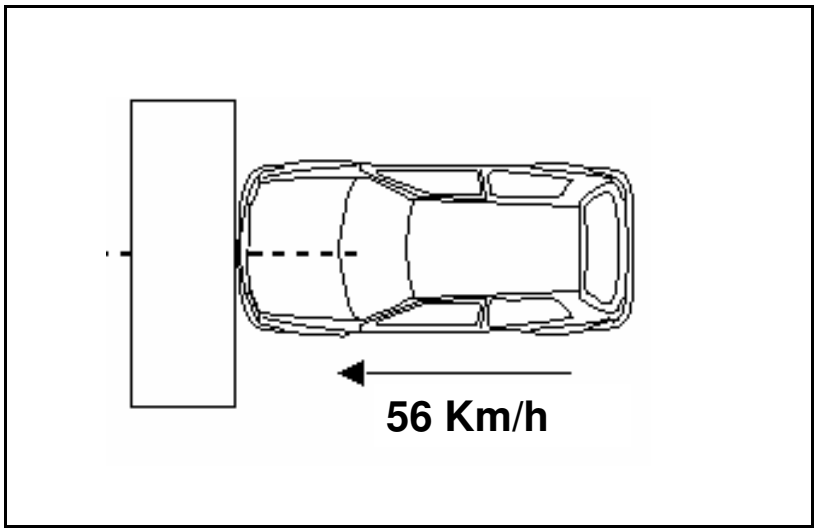

Figure 56 FWRB crash configuration. 56km/h, 100% overlap

As for the FWDB-Assessment, force-time characteristics are recorded by load cells attached to the wall and form the basis of the AHOF assessment. The load cell wall is identical to the wall illustrated in Figure 42.

Assessment algorithm

The mean height of all forces is calculated for each time step and is referred to as the Height of Force (HOF) characteristic. The height of the geometrical centre of each load cell (H_i) is multiplied by the associated force (F_i) of each load cell. The product of these two terms is summed for each load cell across the entire wall for each point in time and divided by the total force for the given time step, to yield the HOF characteristic:

$$HOF(t) = \frac{\sum_{1}^{128} F_i(t) \times H_i}{\sum_{1}^{128} F_i(t)} \tag{22}$$

where 128 refers to the number of 125mm by 125mm load cell (16*8).

The AHOF characteristic is effectively a moving average of all previous height of force values, weighted with the total force (F(t)) for each time step. Points with high total wall force are weighted more strongly than points in time where the total wall force is low.

$$AHOF(t) = \frac{\int_0^t HOF(t)F(t)dt}{\int_0^t F(t)dt} \quad (23)$$

As wall forces approach zero at the end of a collision, the AHOF characteristic approaches a constant value. Vehicles are normally categorised according to the final AHOF value, taken at the end of the collision. Upper and lower AHOF limits, corresponding to the current US-Bumper zone (16-20”, 406-508mm) have been proposed. A convergence of the AHOF value to within these vertical limits is currently being considered with the aim of improving geometrical compatibility between passenger vehicles in the vehicle fleet.

7.3.1 Representing vehicle structures

The main limitation of the FWRB configuration is that no deformable element is present. As discussed in 6.1.1, a deformable element dampens the impulse of the engine/transmission. It also activates horizontal and vertical connections between longitudinal members and prevents unrealistic peak forces from occurring. Therefore, the force distribution, recorded at the fixed barrier in the FWRB configuration, may not accurately represent the structural forces exhibited in real-world collisions. The AHOF characteristic can also be evaluated with a deformable element in front of the wall (as in the FWDB configuration) which would aid to solve these issues.

7.3.2 Test severity

As for the FWDB test, the FWRB configuration is not considered to be a demanding test with respect to the vehicle structure. The test configuration already exists, thus an increase in compartment strength or the magnitude of front-end deformation forces is not expected to result through implementation of this test. Nevertheless, for an evaluation of the structural interaction potential offered by passenger cars, the crash severity is considered adequate.

7.3.3 Mass/Force dependency

The AHOF assessment contains no mass/force dependency. Vehicles are not penalised based on mass and the higher deformation forces associated with higher mass. This can be illustrated by carrying out similar theoretical calculations as shown in 7.1.3, for a standard vehicle (basis) and the same vehicle with a factor k greater force distribution (basis*k).

Based on equations (22) and (23), the basis*k distribution can be shown to be identical to the standard HOF evaluation. Assuming all load cell forces (F_i) increase by a linear factor k:

$$HOF(basis*k) = \frac{\sum_{1}^{128} kF_i(t) \times H_i}{\sum_{1}^{128} kF_i(t)} = \frac{\sum_{1}^{128} F_i(t) \times H_i}{\sum_{1}^{128} F_i(t)} = HOF(basis)$$

The HOF value for the original force distribution (basis vehicle) is identical to the HOF value for the factor k greater force distribution. For the AHOF assessment, the total wall force corresponding to each time step (F(t)) would increase according to a linear factor of “k” as well:

$$AHOF(basis*k) = \frac{\int_{0}^{t} HOF(t)kF(t)dt}{\int_{0}^{t} kF(t)dt} = \frac{\int_{0}^{t} HOF(t)F(t)dt}{\int_{0}^{t} F(t)dt} = AHOF(basis)$$

This calculation proves that the AHOF metric is independent of the magnitude of the forces exhibited by the vehicle front-end.

7.3.4 Repeatability

As the AHOF assessment is based on load cell forces, it may also contain a level of sensitivity due to the resolution of the load cell wall (as observed for the FWDB assessment in 7.1.4). To investigate this, the AHOF was calculated for the simulations presented in the FWDB evaluation section (shown in Figure 50 for a standard pas-

senger in the basis position, then shifted 25mm up/right and 25mm down/left). The AHOF results for this vehicle are shown in Figure 57.

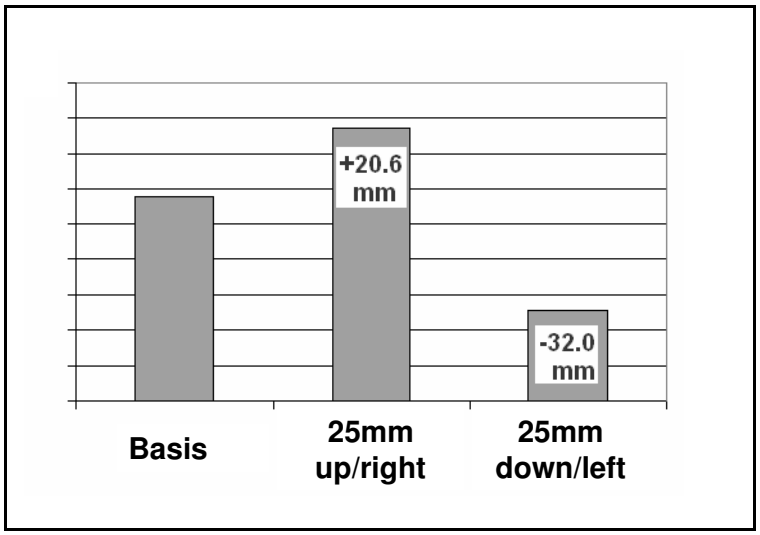

Figure 57 Reaction of the Average Height of Force to the impact point of the vehicle for a simulated collision in the FWRB configuration (56km/h, 100% overlap)

The AHOF values react with the correct tendency for each 25mm (vertical and horizontal) translation of the vehicle. The AHOF assessment varies from 5mm to 7mm from the expected change in height of 25mm. The sensitivity of the AHOF assessment to the impact point of the vehicle is quite low. The AHOF evaluation is clearly less sensitive than the FWDB homogeneity evaluation and is more likely to offer a satisfactory degree of repeatability.

7.3.5 Influence of the assessment on vehicle geometry

The AHOF assessment demands an average convergence of vehicle structures to within a “footprint” area. However, the direct influence of the AHOF assessment on vehicle geometry can not be estimated. As only an average lowering of front-end forces for heavier vehicles is demanded, several measures could be taken to lower the AHOF[41]:

[41] The AHOF metric was developed with the aim of lowering the front-end structures of larger vehicles and correspondingly increasing the chance of geometrical compatibility in car-to-car collisions. Most passenger vehicles lie within the upper and lower AHOF limits of 16-20“.

- A vertical translation of vehicle front structures to within the US-Bumper-Zone (406mm to 508mm)

- An increase in the force of lower load members and / or a decrease in the force of higher load members with little change in the heights of structural members.

The second observation indicates a potential problem related to the AHOF assessment. One measure for heavier passenger cars to lower their AHOF value is to increase the force of the lower load paths. However, the force of the lower load paths (F_S) would have to increase proportionally to the force in the upper load paths (F_L). Mathematically, for a heavier vehicle with a Secondary Energy Absorbing Structure (SEAS) at a height (H_S) and standard longitudinal members at a height of (H_L):

$$AHOF = \left(F_L H_L + F_S H_S\right) / \left(F_L + F_S\right)$$

$$rearranging:$$

$$F_S = F_L \cdot \frac{AHOF - H_L}{H_S - AHOF}$$

To reach a given AHOF limit, the force provided by the SEAS has to be proportional to the force of the longitudinals (for a fixed ground-clearance of longitudinal members and SEAS). For heavier vehicles, a large increase in force in the lower load paths would be demanded to lower the AHOF value. As SEAS generally lie farther back in the front-end structure due to approach angle requirements, an even greater increase in force may be demanded to lower the AHOF value.

7.4 Summary

The FWDB, AHOF in the FWRB configuration and PDB crash tests are summarised in Figure 58, based on the discussion presented in this chapter.

	Desirable	AHOF	FWB Homogeneity Assessment	PDB Aggresivity Metric
Structural interaction issues				
Vertical distribution of forces accurately represented	Yes	Partially*	Yes	Yes
Horizontal distribution of forces accurately represented	Yes	Partially*	Yes	No
Evaluation is independent to deformation forces/mass	Yes	Yes	No	No
Total crash duration considered	Yes	Yes	No	No
Vertical and horizontal connections are activated	Yes	No	Yes	Yes
Convergence of structures (within vertical limits) is demanded	Yes	Partially**	Yes	No ***
Evaluation offers an acceptable level of repeatibility	Yes	Yes	No	Unknown
Other passive safety characteristics				
Pulse is appropriate for restraint system optimisation	Yes	Yes	Yes	No
Increase in compartment resistance force demanded	Yes	No	No	No
Mass ratio 1:1,6 is considered	Yes	No	No	No
Demands appropriately stiff structures	Yes	Yes	Yes	No ****

* Structures may be innacurately represented as no deformable element is present
** An average convergence of vehicle structures is demanded
*** Convergence toward ground level is demanded for all vehicles
**** A softening of front-ends is favourable for the assessment

Figure 58 Summary - Evaluation of proposed compatibility assessment procedures

Based on this table, the FWDB assessment fulfils the requirement of a compatibility test to improve the structural interaction potential of passenger cars, to the greatest degree (7 positive responses). The AHOF assessment also fulfils many of the requirements of a test for structural interaction (5 positive responses). The FWDB test, however, is not considered ready for implementation, primarily due to repeatability problems associated with load cell wall resolution.

Research into compatibility assessment procedures continues in working groups and legislative bodies around the world [20] [97]. The research presented in this chapter and in the previous chapter aim to provide a framework for the further development of compatibility assessment procedures, focussed on assessing the potential for structural interaction of passenger cars.

8 Measuring energy dissipation in experimental crash tests

To evaluate structural interaction in a crash test, the amount of energy dissipated through structural deformation needs to be calculated. In this chapter, a method for measuring energy dissipation in experimental crash tests (based on accelerometers) is presented, 8.1. In 8.2, the energy dissipation associated with structural deformation is calculated for an experimental fixed barrier crash test. The method is modified and also applied to the results of experimental car-to-car, head-on collisions in 8.3. In 8.4, the degree of compatibility exhibited by vehicle pairs is evaluated and discussed for two of the car-to-car collisions analysed. The method proposed to calculate energy dissipation is discussed and the results to this chapter summarised in 8.5.

8.1 Description of the measurement procedure

8.1.1 Forces active in a passenger vehicle collision

In experimental crash tests, accelerometers can be attached to the vehicle to record the acceleration-time characteristics at the point of attachment. They are usually located in non-deforming sections of the vehicle, to prevent a disturbance of the signal due to localised deformation. By multiplying the acceleration of a given rigid section of the vehicle with the associated mass, the net force acting on the particular section of the vehicle can be calculated.

Schwarz [29] considered the vehicle to consist of two components, for the purpose of force analyses; the engine/transmission[42] and the deformable components of the vehicle structure. Multiplying the linear acceleration of the vehicle structure, parallel to the longitudinal (x) axis of the vehicle and measured at the B-pillars ($a_{x\text{-structure}}$), with the associated structural mass ($m_{structure}$) yields the structural force ($F_{x\text{-structure}}$) according to:

[42] The mass of the motor/transmission was estimated based on the motor mass and an additional factor intended to account for the mass of other rigid components located in the front-end.

$$F_{x-structure} = m_{structure}\, a_{x-structure} \tag{24}$$

where $a_{x\text{-structure}}$ is the mean acceleration of both B-pillars:

$$a_{x-structure} = \frac{1}{2}\left(a_{x-left\ \mathbf{b}\ pillar)} + a_{x-right\ b\ pillar}\right) \tag{25}$$

An analogous formula was developed for the engine/transmission as well:

$$F_{x-motor} = m_{motor}\, a_{x-motor} \tag{26}$$

In a frontal collision against a fixed barrier, the reaction force of the barrier/wall (F_{wall}) can be measured by load cells and recorded. Schwarz [29] showed that, due to inertial effects, the wall force (F_{wall}) is approximately equal to the sum of the structural force ($F_{x\text{-structure}}$) and the force exhibited by the engine/transmission ($F_{x\text{-motor}}$).

$$F_{wall} \approx F_{x-structure} + F_{x-motor} \tag{27}$$

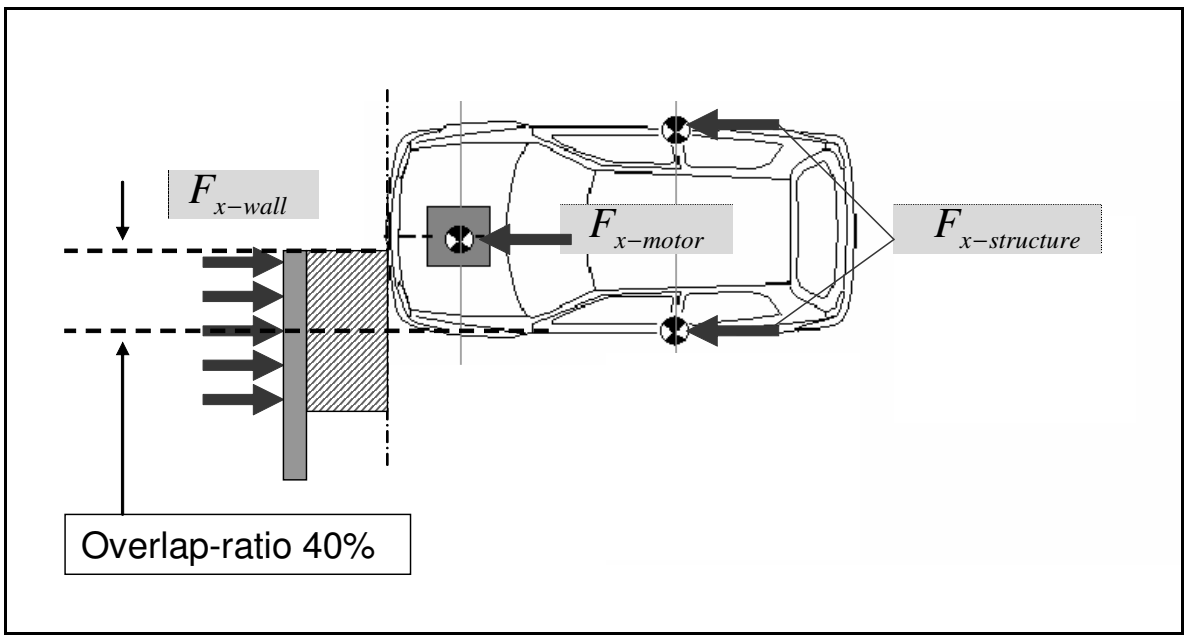

Figure 59 Schematic representation of the forces active in a fixed barrier collision based on [29]

Separating engine forces and structural forces was also proven to be valid for the car-to-car collision configuration, based on the analysis of experimental crash tests [29].

8.1.2 Measuring energy dissipation in a collision with a fixed barrier

In order to evaluate structural interaction, the amount of energy dissipated through structural deformation is required. A method is presented in this section to calculate energy dissipation based on accelerometer readings. This method is applied throughout the remainder of this thesis.

To measure energy dissipation in a collision, the inertial forces of rigid sections of the vehicle can be combined with the associated displacement of the given section to yield the net work done.

The net energy dissipated in the x-direction (D_x) can be calculated by integrating the linear force (F_x) versus linear displacement (s_x) characteristic.

$$D_x = \int F_x ds_x \tag{28}$$

where the displacement is acquired through a double integration of the acceleration-time characteristic (recorded by accelerometers) with respect to time

$$s_x = \iint a_x dt^2 \tag{29}$$

Throughout this chapter, the work done on the structure is calculated based on the structural force ($F_{x\text{-structure}}$) and the displacement of the struck side B-pillar ($s_{x\text{-structure (struck side)}}$), Figure 60.

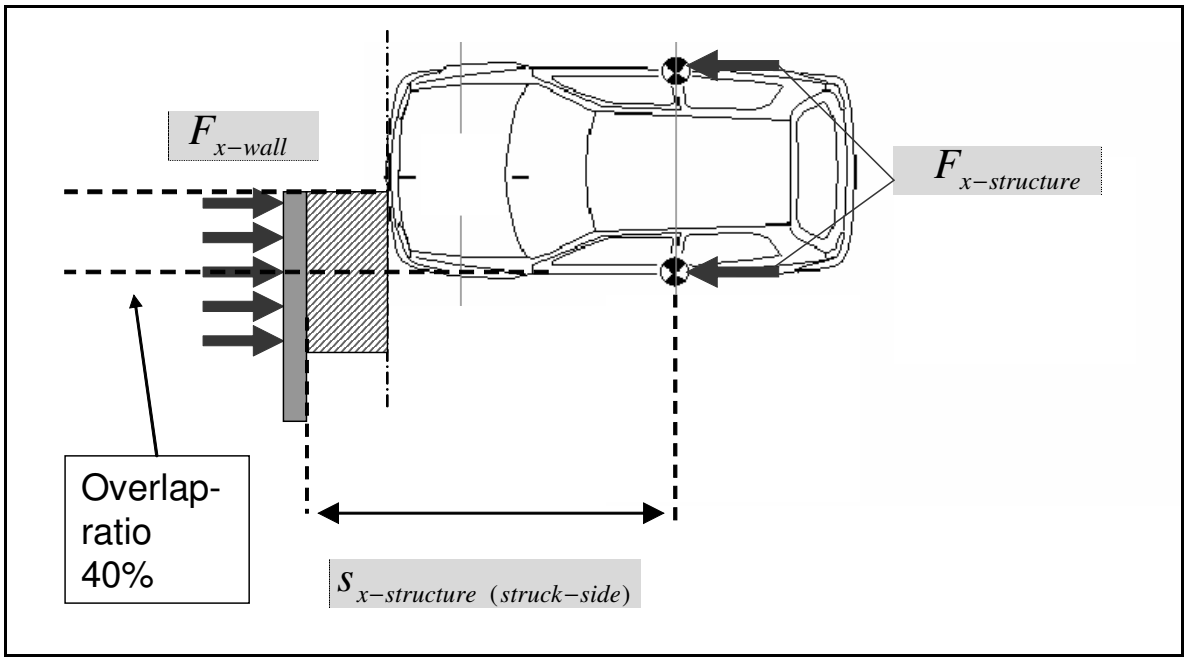

Figure 60 Calculating energy dissipation through structural deformation in a fixed barrier collision

$$D_{x-structure} = \int F_{x-structure}\ ds_{x-structure(struck-side)} \tag{30}$$

The engine/transmission was neglected in the energy calculations. The struck side accelerometers were used for the calculation of the relative displacement terms as, in many collisions, the non struck side A and B-pillars underwent a greater degree of displacement in the x-direction than the struck side A and B-pillars. This can be attributed to vehicle rotation. Both struck side and non-struck side accelerometers were used for the calculation of structural force.

8.1.3 Measuring energy dissipation in car-to-car head-on collisions

The method presented in 8.1.2 to measure the energy dissipated through structural deformation in a fixed barrier collision can be modified for the case of a car-to-car, head-on collision. Figure 61 is a schematic representation of a car-to-car, head-on collision at an overlap ratio of 50%.

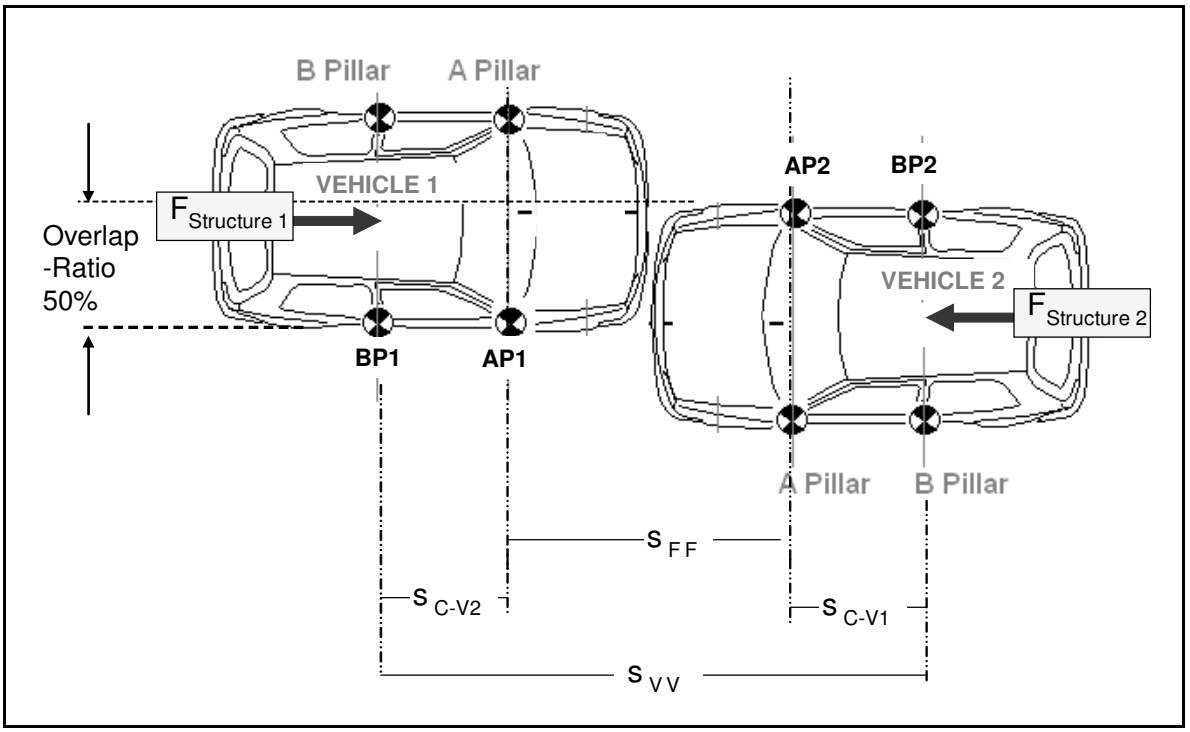

Figure 61 Car-to-car, head-on collision configuration showing the accelerometers used as the basis for energy dissipation calculations

Figure 61 indicates that the structural force ($F_{structure}$) can be calculated for each vehicle separately. Theoretically, the structural forces should be equal due to action and reaction. However, dynamic/inertial effects as well as the efficiency of the transmittance of force to the vehicle compartment, may lead to differences in the structural force calculated for each vehicle. The degree of correlation between these structural forces can be used to check the stability of the calculation of energy dissipation. **Throughout the following pages, two energy dissipation characteristics are calculated for each car-to-car collision, based on the structural force exhibited by each respective vehicle, plotted with respect to the combined crush of the vehicles.**

The deformation of the compartment of each respective vehicle ($s_{c\text{-}v1}$, $s_{c\text{-}v2}$), the deformation of the front-ends combined ($s_{x(FF)}$) and the total deformation of both structures ($s_{x(VV)}$) can be calculated based on the following equations:

$$\begin{aligned} ds_{x(C-V1)} &= ds_{x(BP1)} - ds_{x(AP1)} \\ ds_{x(FF)} &= ds_{x(AP1)} + ds_{x(AP2)} \\ ds_{x(C-V2)} &= ds_{x(BP2)} - ds_{x(AP2)} \\ &and \\ ds_{x(VV)} &= ds_{x(BP1)} + ds_{x(BP2)} = ds_{x(C-V1)} + ds_{x(FF)} + ds_{x(C-V2)} \end{aligned} \tag{31}$$

Combining the structural force with each of the respective displacement characteristics shown in equation (31) the following energy terms can be calculated, for the combined front-end (FF) and the compartments of each respective vehicle (C-V1) and (C-V2):

$$D_{x(FF)} = \int F_{x(structure)} \; ds_{x(FF)} \tag{32}$$

$$D_{x(C-V1)} = \int F_{x(structure)} \, ds_{x(C-V1)} \tag{33}$$

$$D_{x(C-V2)} = \int F_{x(structure)} \, ds_{x(C-V2)} \tag{34}$$

The sum of these three components reflects the total amount of energy dissipated through structural deformation:

$$D_{x(VV)} = D_{x(FF)} + D_{x(C-V1)} + D_{x(C-V2)} \tag{35}$$

where $D_{x(VV)}$ can also be written as:

$$D_{x(VV)} = \int F_{x(structure)} \; ds_{x(VV)} \tag{36}$$

As described in the previous pages, $D_{x(VV)}$ can be calculated based on the structural force of each respective vehicle, or by taking the average of both structural force values according to equation (36).

The degree of energy dissipation cannot be calculated for the front-end of each individual vehicle separately using this method, in the instance of a car-to-car collision. To achieve this, a discreet value would be required for the location of the collision interface, throughout the collision. This is not considered feasible as:

- The interface itself is not planar, so an average value would have to be taken. Describing the collision interface is in itself an abstract task.

- Any accelerometers located at the collision interface would probably be destroyed through contact with the structure of the other vehicle involved in the collision.

As described in section 4.1 and 4.4, structural interaction is a phenomenon which relates to the interaction of the vehicles involved in a collision. Throughout the following pages, structural interaction is calculated considering the combined deformation of both vehicles.

8.1.4 Calculating the mass of the vehicle structure

Two instrumented dummies, each weighing 75kg, were located in the front-seats of all tested vehicles. The dummies can be considered as free bodies, located in the passenger compartments, which do not significantly influence the degree of structural deformation. This is illustrated in Figure 62, below.

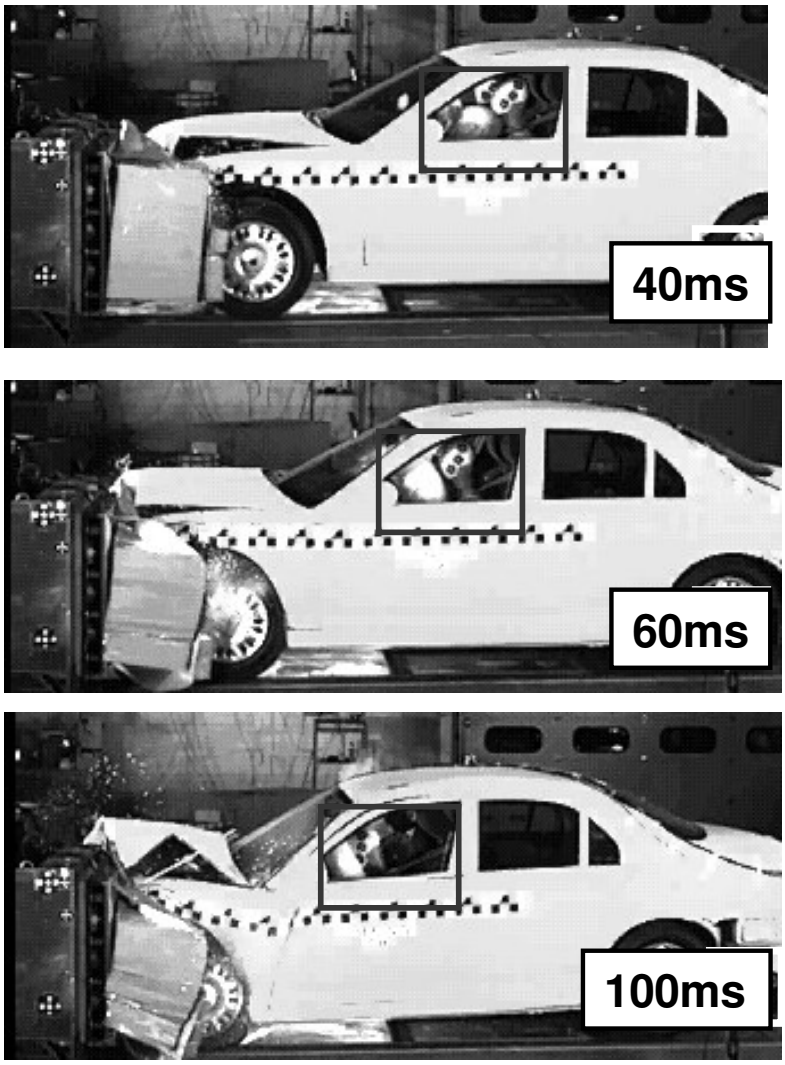

Figure 62 Interaction of the instrument dummies with the restraint system over the course of a fixed barrier collision. Rover 75 - EURO NCAP collision at 64km/h and an overlap ratio of 40% shown at 40ms, 60ms and 100ms after the point of initial impact.

The dummies interact with the structure very late in the crash. At 40ms and 60 ms after the beginning of the crash, the dummies have not begun to interact significantly with the airbag. Only at 100ms can significant interaction with the airbag be observed. At this point in the crash, the vehicle is already in rebound and the dummies have lost a large degree of their initial kinetic energy. The mass of the dummies was neglected in the energy calculations carried out in this research. Neglecting the mass of the dummies for these calculations is shown to be appropriate based on the results to numerical crash test simulations presented in chapter 9.

A further assumption was made regarding the mass of the engine/transmission. The mass of the motor and transmission (m_{motor}) was assumed to equal 20% of the total vehicle mass (after the mass of the dummies ($m_{dummies}$) was subtracted from the test

mass (m_{test}) of the vehicle). The mass of the structure was therefore calculated based on equation (37)

$$m_{structure} = 0.8\left(m_{test} - m_{dummies}\right) \tag{37}$$

The engine and transmission are not the only rigid or semi-rigid bodies located within the vehicle front-end. For this reason, the estimation of the mass of rigid parts was made based on a percentage of the total mass of the vehicle. This assumption delivers robust results throughout this thesis, although it does have certain limitations. In future research, the mass of the engine/transmission may need to be calculated based on the mass of individual rigid components located in the front-end. This topic is discussed further in the recommendations for future research, section, 10.2.

8.2 Fixed barrier crash test

The results of a fixed barrier collision are analysed in this section to confirm the hypothesis that the rigid parts in the front-end (engine/transmission) and the vehicle structure can be considered separately for calculations of energy dissipation.

This test was carried out in the standard EURO NCAP configuration (40% overlap with a deformable element fixed to the barrier). The test mass of the vehicle was 1299kg. Two instrumented dummies were located in the front of the vehicle, each weighing 75kg. The test was carried out at a high velocity (80km/h) to test the strength of the vehicle compartment. The structural force was calculated according to equation (24) based on B-pillar acceleration-time characteristics recorded by accelerometers. The structural force is plotted with respect to the relative displacement between the struck side B-pillar and the wall in Figure 63.

Assuming the engine/transmission and the vehicle structure behave independently, the structural force is approximately equal to the difference between the total wall

force and the motor force (see equation (27)). This characteristic was calculated as well and plotted with respect to the relative displacement between the struck side B-pillar and the wall, Figure 63.

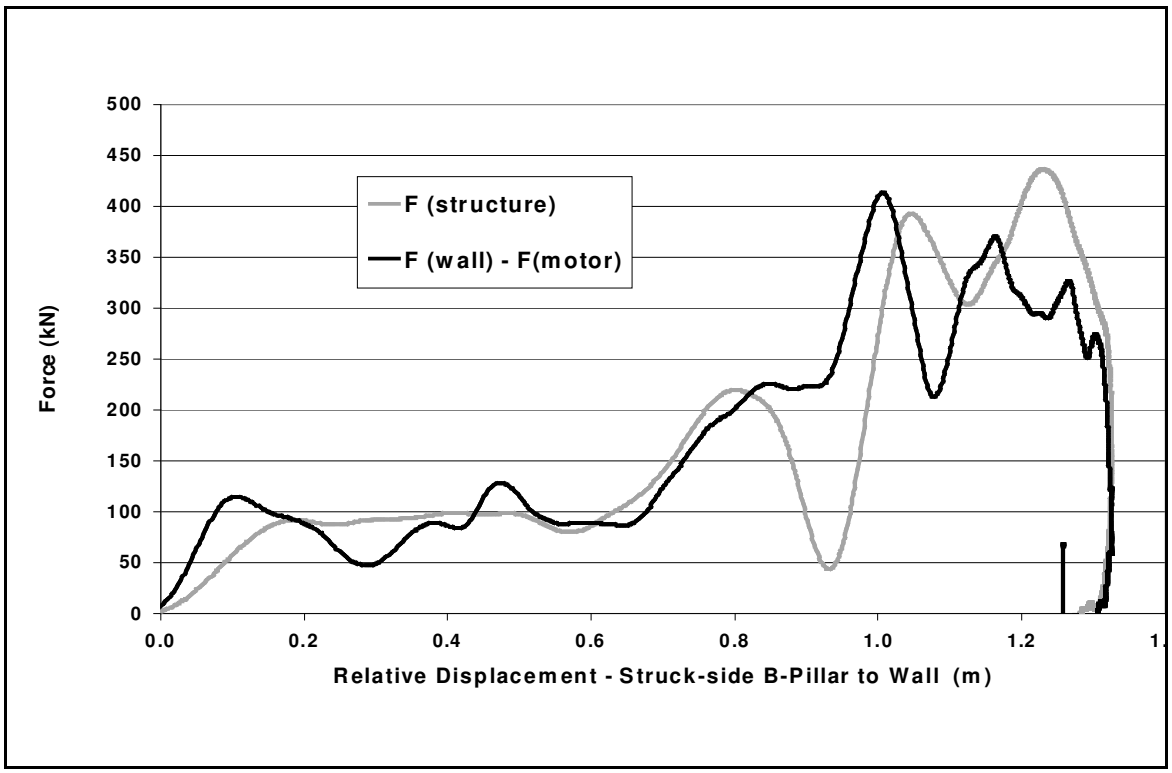

Figure 63 Structural force (calculated based on the average acceleration of the B-pillars) and the difference between the total wall force and the engine force, respectively. Both characteristics are plotted with respect to the relative displacement between the struck side B-pillar and the wall. 80km/h destruction test in the EURO NCAP configuration at 40% overlap

The force-displacement characteristics illustrated in Figure 63 exhibit a high degree of correlation throughout most of the collision. Between 0.85m and 1m of displacement, the curves diverge over a relatively small displacement interval. This is assumed to be due to the dynamic influence of the engine. This is confirmed in Figure 64, which shows the force characteristics from Figure 63 as well as the motor force plotted with respect to time. The divergence of the characteristics shown in Figure 63 corresponds to the peak force of the motor as it impacts the wall.

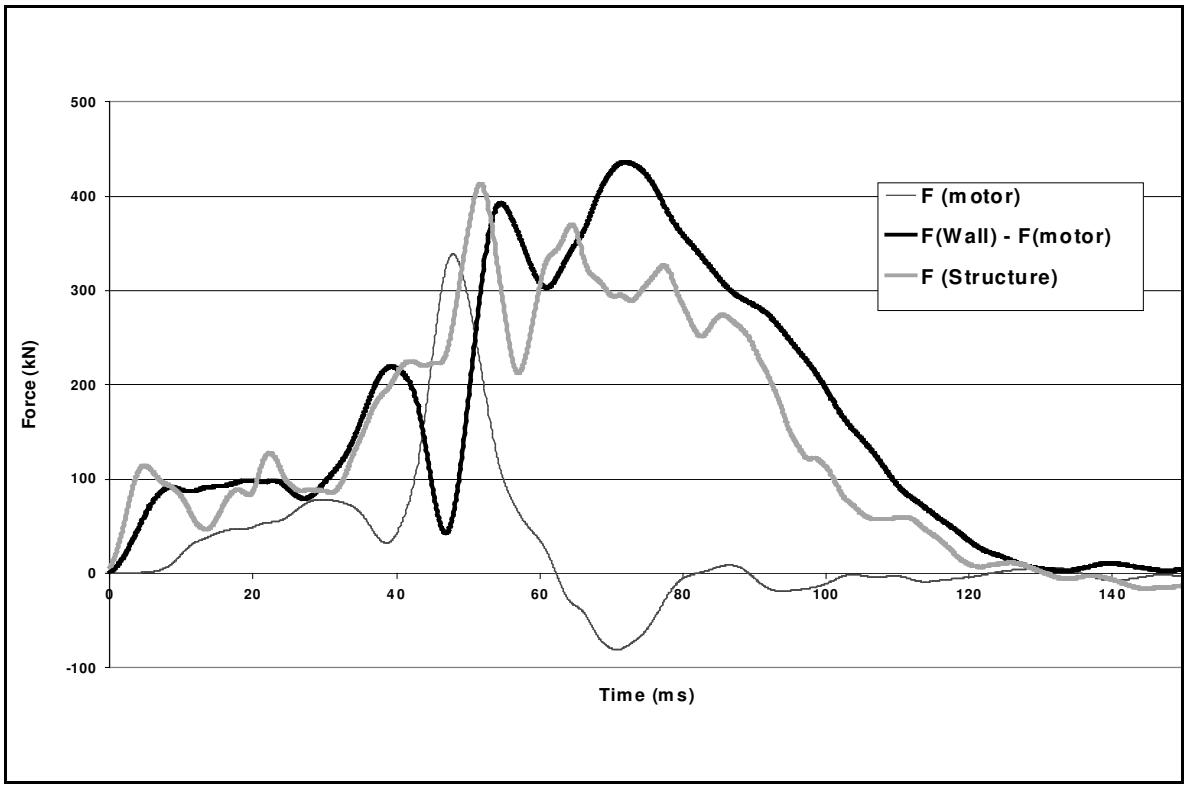

Figure 64 Structural force and motor force versus time. 80km/h destruction test in the EURO NCAP configuration at 40% overlap

Both curves shown in Figure 63 were integrated with respect to displacement to yield energy dissipation characteristics according to equation (30). The resulting energy dissipation characteristics are plotted with respect to the relative displacement between the struck side B-pillar and the wall in Figure 65.

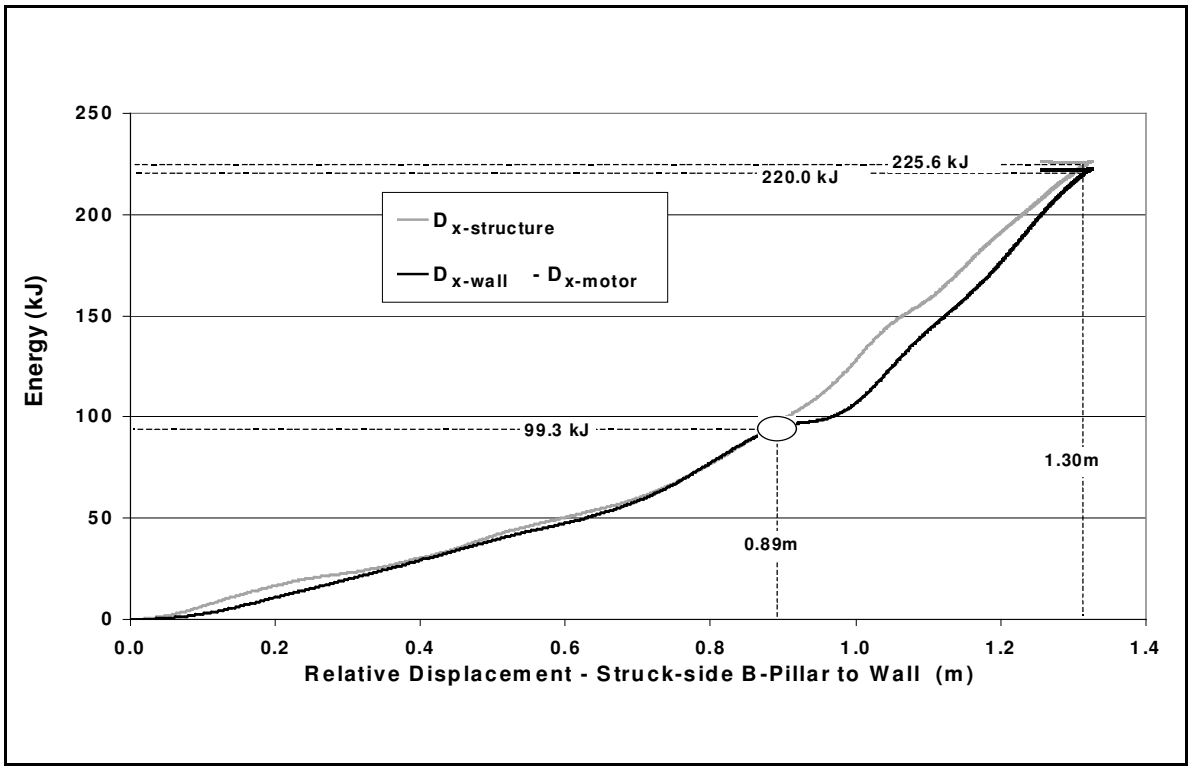

Figure 65 Cumulative energy dissipation through structural deformation based on the structural force and the difference between the total wall force and motor force, respectively. Both characteristics plotted with respect to the relative displacement between the struck side B-pillar and the wall. Destruction test in the EURO NCAP configuration at 80km/h (40% overlap).

The divergence of the force-displacement characteristics after 0.89m of relative displacement shown in Figure 63, which was caused by the engine, is reproduced in Figure 65. However, the total amount of energy dissipation through deformation is almost equal for each of the characteristics (225.6kJ compared to 220.0kJ). The dynamic influence of the engine/transmission is considered to be acceptably low to enable an accurate calculation of energy dissipation based on the structural force only and neglecting the influence of the engine/transmission.

8.3 Car-to-car, head-on crash tests

Energy dissipation characteristics are calculated for several car-to-car collisions in this section, based on the method presented in 8.1.3.

For each collision, the EESVV values are calculated, representing the severity of the collision. The EESVV values reflect the degree of loading of the vehicle structure, based on the energy dissipation through structural deformation. The EESVV values are compared to the initial closing velocity to gain an indication of the plausibility of the calculation. As a proportion of the vehicle's initial linear kinetic energy is converted into rotational energy, the EESVV values are expected to be lower than the closing velocity of the vehicles for all collisions analysed.

8.3.1 Renault Clio - Opel Astra

In this crash test, the initial velocity of each vehicle was 58.3km/h. The mass ratio of the vehicles was 1.21:1 (Opel Astra 1355kg : Renault Clio 1117kg). Two instrumented dummies, each weighing of 75kg, were located on the front-seats of both vehicles. The overlap ratio corresponded to 50% of the width of the smaller Renault Clio. The longitudinal members and sub-frame of both vehicles lay at similar heights above the ground. No under/overriding was observed, suggesting a high level of structural interaction occurred. Furthermore, no sign of a significant loss of compartment integrity or significant deformation into the passenger compartment of either vehicle was observed.

Based on equation (36) the energy dissipated through structural deformation between the struck side B-pillars was calculated. **Two energy dissipation characteristics were calculated, based on the structural force of each respective vehicle, see section 8.1.3.** The resulting characteristics are plotted with respect to the combined crush of both vehicles (relative displacement between struck side B-pillars), Figure 66.

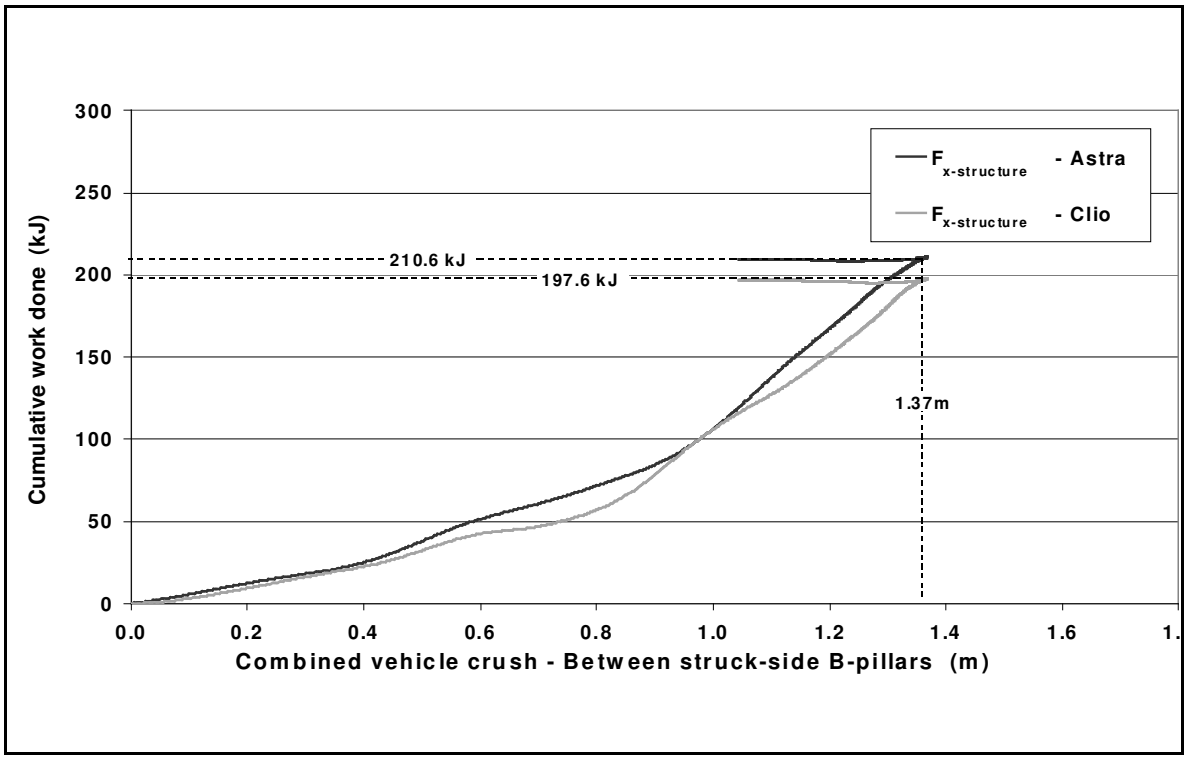

Figure 66 Energy dissipation through structural deformation – Renault Clio versus Opel Astra – Based on the structural forces of the Renault Clio and Opel Astra, respectively.

The structural interaction characteristics, calculated based on the structural force of the Renault Clio and the Opel Astra, correlate well. The energy dissipation characteristics rise throughout the crash, Figure 66. The shape of the curves reflects the theoretical quadratic curves representing maximum structural interaction which were generated in 4.3, based on triangular front-end force-deflection characteristics.

The EESVV value for this collision was calculated based on equation (12). The average of the two energy dissipation values shown for each vehicle in Figure 69 (197.6kJ, 210.6kJ), was used in the calculation.

$$EESVV = \sqrt{2D_{VV}\left(\frac{m_{structure-Clio} + m_{structure-Astra}}{m_{structure-Clio}\ m_{structure-Astra}}\right)}$$

$D_{VV} = 204.1kJ$
$m_{Clio} = 1117\,kg$
$m_{Astra} = 1355\,kg$

and calculating $m_{structure}$ based on equation (37)

$$m_{structure-Clio} = (1117 - 150) \cdot 0.8 = 773.6\,kg$$
$$m_{structure-Astra} = (1355 - 150) \cdot 0.8 = 964.0\,kg$$

resulting in an EESVV value of 111.0km/h

The actual closing velocity for this collision was 116.6km/h. The difference between the EESVV and the closing velocity is 4.8% ([116.6-111]/116.6). The difference in the EESVV and the closing velocity can be assumed to be influenced by vehicle rotation. The similarity of these two values provides a further indication that the calculation of energy dissipation through structural deformation is valid.

8.3.2 VW Polo (9N) - VW Phaeton

This crash test was carried out to determine the potential for compatibility between vehicles of significantly different mass. The mass ratio in this case was equal to 1:1.8 (Polo 9N, 1304kg: Phaeton, 2353kg) exceeding the commonly discussed upper limit of 1:1.6 (see section 2.3.4). To compensate, the intended initial velocity of each vehicle was lowered to 50km/h. The actual initial velocity of both vehicles was 50.4km/h. The longitudinal members of each vehicle were located at a similar height above the ground. No visible over- or underriding was observed. The compartment of the Polo 9N remained stable throughout the collision.

Based on the structural forces of each respective compartment, the energy dissipation characteristics (between the struck side B-pillars) were calculated according to equation (36). The resulting curves are shown in Figure 67.

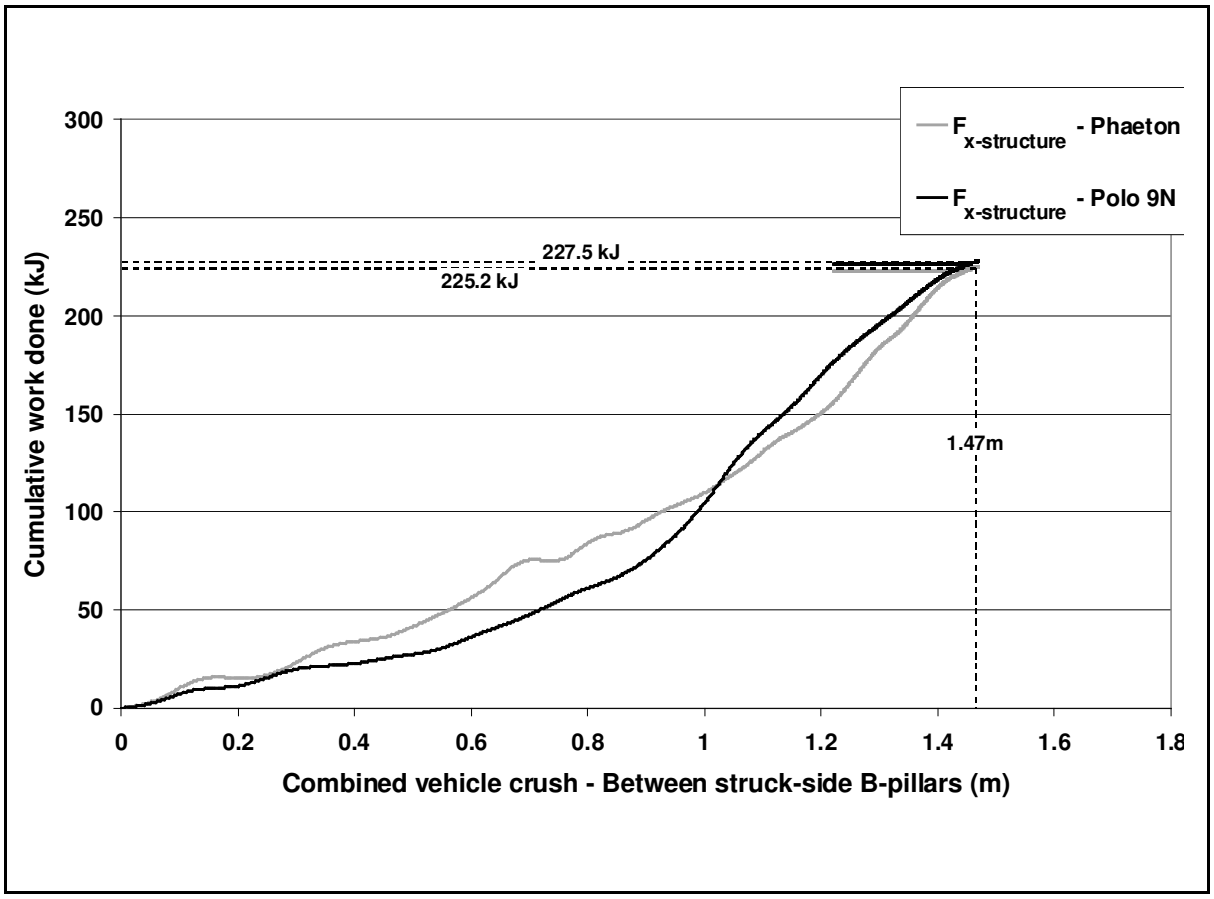

Figure 67 Energy dissipation through structural deformation – VW Polo 9N versus VW Phaeton – Based on the structural forces of the Polo and Phaeton.

The energy dissipation characteristics deviate significantly during the first 1m of combined vehicle crush, Figure 67. The force transmitted to each respective compartment varies significantly. This may have been due to dynamic effects (the influence of rigid parts such as the engine/transmission) or the efficiency of the transmittance of force through the front-end structures to the respective compartments. The mass of the Phaeton engine/transmission is much higher than that of the Polo 9N. After initial contact, both motors translated toward the compartment of the Polo 9N, which may have lead to a difference in the forces calculated based on B-pillar accelerations.

After 1m of relative displacement, the curves exhibit a better correlation. At the point of maximum deformation (1.47m), the total energy dissipation is almost equal for both curves (225.2kJ, 227.2kJ). Despite dynamic effects, the measurement of energy dissipation appears to be also feasible in head-on collisions involving two vehicles of significantly different mass.

The EESVV was calculated for this collision based on the average total energy dissipation (D_{VV}) occurring between the struck side B-pillars (226.3kJ). The structural masses were calculated according to equation (37). An EESVV value of **98.4km/h** was obtained. The closing velocity of this collision was 100.8km/h), a difference of 2.4% ([100.8 -98.4]/ 100.9) between the EESVV and the closing velocity. The difference in the EESVV and closing speed can be partly attributed to vehicle rotation. This difference of 2.4% also indicates that the measurement of energy dissipation is plausible for this collision.

8.3.3 Modified VW Polo 6N - Rover 75

In this crash test, the Polo 6N was raised by 40mm (through a suspension modification) so that the main longitudinal members of both vehicles were located at the same height. A high level of structural interaction was observed with no clear over/underriding having occurred. The mass ratio of the two vehicles was 1:1.57 (VW Polo 6N, 1105kg : Rover 75, 1732kg). The initial velocity of each vehicle was 56.7km/h. The high deformation forces exhibited by the Rover front-end exceeded the compartment strength of the VW Polo 6N. The result was a significant level of intrusion and a loss of integrity of the VW Polo 6N compartment. The A-pillar of the Polo 6N underwent a significant degree of deformation relative to the B-pillar. The striking longitudinal of the Rover 75 remained largely undeformed.

Energy dissipation curves were again calculated based on the structural forces calculated at each respective compartment, according to equation (36). The resulting curves are shown in Figure 68.

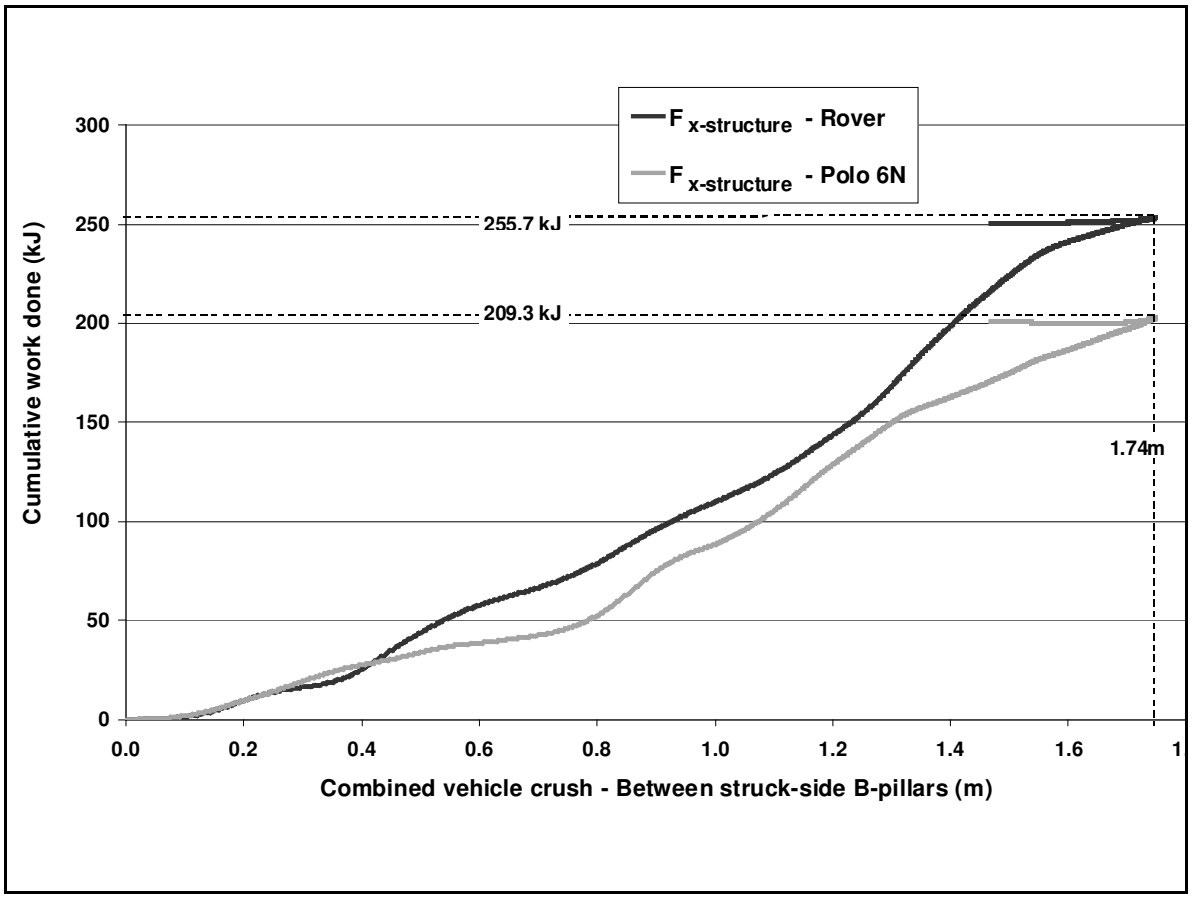

Figure 68 Energy dissipation through structural deformation – VW Polo 6N versus Rover 75 – Based on the structural forces of the Polo and Rover.

A poor correlation between the energy dissipation curves, calculated based on the structural forces of each respective vehicle, is indicated in Figure 68. Up to 1.3m of combined vehicle crush, a degree of correlation between the structural interaction characteristics can be observed. After 1.3m, the characteristics diverge. The structural forces calculated at the compartment of each respective vehicle varied significantly in this collision.

For this test, B-pillar readings were taken at both the base of the B-pillar and in the middle of the B-pillar. These were compared for both vehicles to rule out the possibility of an inaccuracy in the measurement of acceleration delivered by the accelerometers. No significant difference in the acceleration-time characteristics recorded by each accelerometer located at each respective B-pillar was observed, indicating that an error in the measurement devices was unlikely.

During the collision, the dashboard of the Polo underwent significant displacement and rotation relative to the non-deforming section of the passenger compartment. The transmittance of force through the door and sill of the Polo was most likely disturbed. The structural forces of the Polo were much lower than those recorded for the Rover 75 and a lower degree of energy dissipation, based on the Polo's structural force, resulted. Based on this observation, it is not clear if measuring energy dissipation based on accelerometers is feasible when high deformation of one of the passenger compartments occurred. Another collision, in which one of the passenger compartments underwent significant deformation, is evaluated in 8.3.4.

The EESVV was calculated for the collision. The total energy dissipated between the B-pillars was calculated as 232.5kJ (based on the average structural force of both vehicles). The structural masses were calculated according to equation (37). An EESVV value of 112.5km/h was obtained (Based the method applied in 8.3.1). This compares very well with the actual closing velocity (113.4km/h), a difference of 0.8% ([113.4km/h-112.5km/h]/113.4km/h)

8.3.4 Renault Clio - Rover 75

The initial velocity of each vehicle in this test exceeded the prescribed velocity of 56km/h by 2.7km/h (58.7km/h). This represented a significant (9%) increase in the kinetic energy of both vehicles. The mass ratio of the vehicles was 1:1.43 (Renault Clio, 1215kg : Rover 75, 1732kg) and the overlap ratio was 50% with respect to the smaller Renault Clio. Two instrumented dummies, each weighing 75kg, were located in the front-seat of each vehicle.

Although the longitudinal members of the Renault Clio and Rover 75 were located at similar heights above the ground before the collision, the Renault Clio was overridden by the Rover 75, leading to the observation that poor structural interaction occurred. Based on this and the higher than intended kinetic energy associated with the collision, significant intrusion into the compartment of the Renault Clio was observed.

Energy dissipation curves were calculated based on the structural force of the compartment of each vehicle according to equation (36). The energy dissipation curves

are plotted with respect to the combined crush of both vehicles (relative displacement between the struck side B-pillars) in Figure 69.

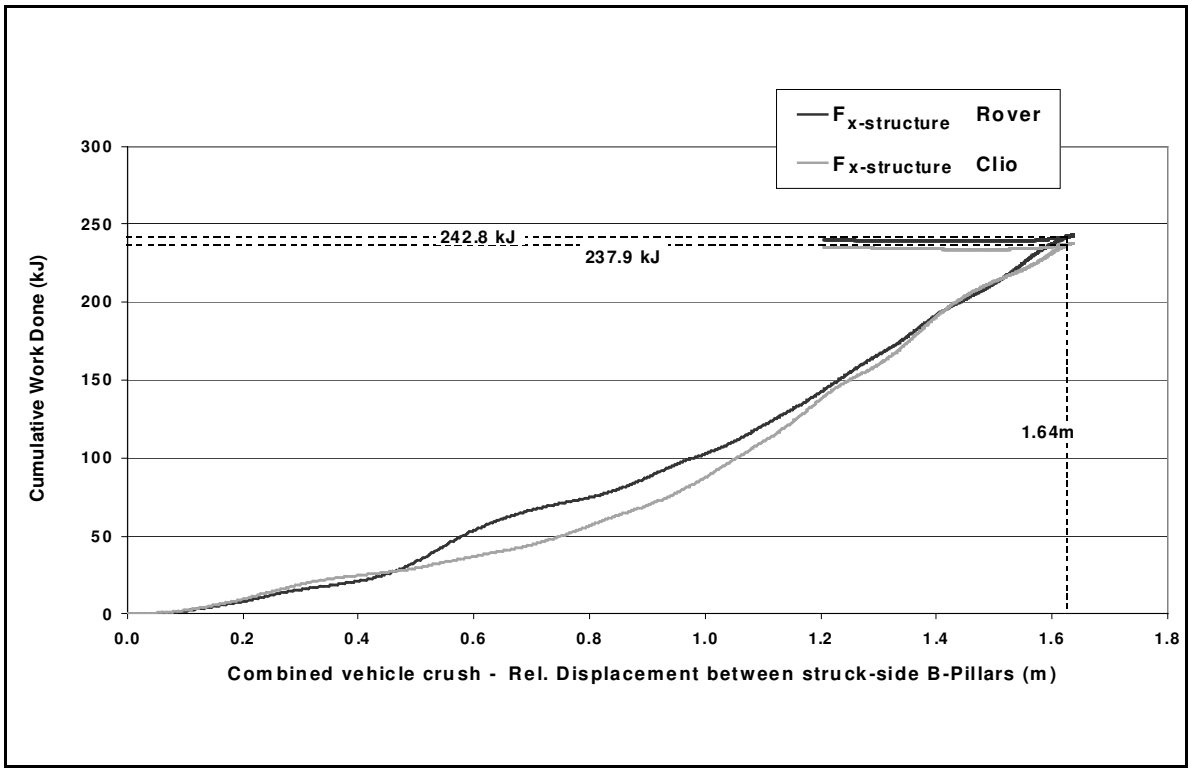

Figure 69 Energy dissipation through structural deformation – Renault Clio versus Rover 75 – Based on the structural forces of the Renault Clio and Rover 75

The level of correlation between the energy dissipation curves, based on the structural forces of the Renault Clio and Rover 75, is high throughout the entire crash. Between 0.5m and 1.2m of total vehicle crush, the energy dissipation characteristics diverge, representing either the dynamic influence of the engine/transmission or a variation in the transmittance of force to the respective passenger compartments. Values for the total energy dissipated through deformation are almost identical for both vehicles (242.8kJ, 237.9kJ). Despite the high level of intrusion into the passenger compartment of the Renault Clio, the calculation of energy dissipation appears to be reliable for this collision.

The average energy dissipated between the B-pillars was equal to 239.2kJ, resulting in an EESVV value of 110.3km/h. The EESVV of 110.3km/h also correlates well with the closing velocity of 117.4km/h. The difference between the EESVV value and the

closing velocity is 6.0% ([117.4km/h-110.3km/h]/117.4km/h). Part of this discrepancy can be attributed to vehicle rotation.

8.4 Evaluation of compatibility for the collisions analysed

The method for measuring energy dissipation based on accelerometers produced reliable results, even for collisions involving vehicles of high mass ratios and collisions in which high intrusions into the compartment occurred.

In 8.4.1, the energy dissipation characteristics for all of the collisions analysed in the previous section are subjectively compared. In 8.4.2, two crash tests are analysed in which A-pillar acceleration-time characteristics were recorded as well. This enables a breakdown of energy dissipation into the energy dissipated within the front-ends and in each respective passenger compartment. Based on this, EESFF for each collision is calculated reflecting the degree of compatibility exhibited by the two vehicles involved in the collision, 8.4.2.

8.4.1 Subjective comparison of energy dissipation characteristics

The energy dissipation curves generated in the previous section are plotted together in Figure 70. For each collision, the average energy dissipation characteristic, based on the average structural force of both vehicles, is shown.

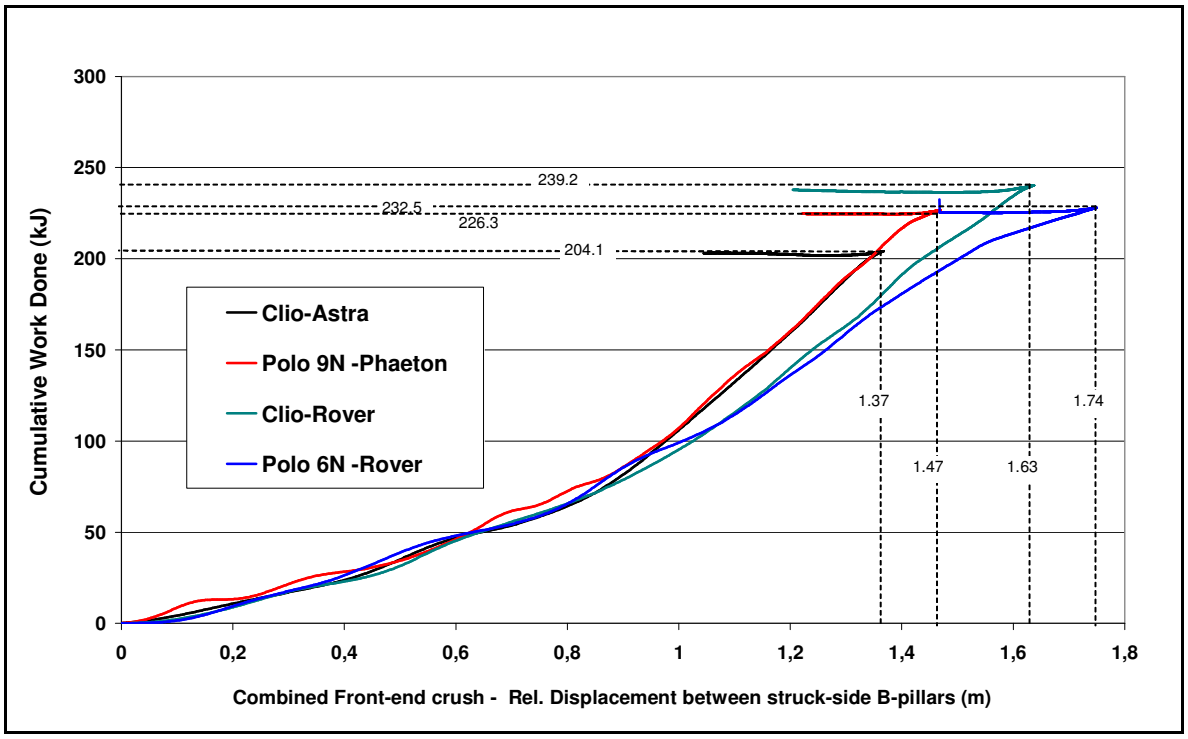

Figure 70 Comparison of the energy dissipation characteristics for all car-to-car head-on collisions analysed

Figure 70 indicates that the level of energy dissipation is similar for all crash tests up to a combined vehicle crush of approximately 0.9m. This is a surprising result given the differences in vehicle mass and front-end stiffness. Up to 0.9m, less than half of the total energy dissipation took place for all crash tests analysed. Even the effect of over/underriding, observed in the Renault Clio – Rover 75 collision, is not reflected by the energy dissipation characteristics before 0.9m of combined front-end crush.

After 0.9m of crush, the energy dissipation curves diverge significantly. For the Rover 75 – VW Polo 6N crash test, a significant degree of deformation of the compartment of the Polo 6N was observed. The deformation of the Polo 6N compartment is associated with a higher degree of total displacement between the struck B-pillars (≈1.74m, Figure 70). This was also the case for the Renault Clio – Rover 75 collision, in which a high degree of deformation of the Clio compartment also occurred.

The characteristics shown in Figure 70 clearly reflect the high compartment deformation observed in the Clio-Rover and Polo 6N – Rover crash tests.

8.4.2 Calculation of EESFF values

In two of the crash tests analysed in section 8.3, accelerometers were also located in the region of the A-pillars. This allowed a breakdown of the energy dissipation into:

- The total work done between the front-ends
  Equation (32)
- The work done through deformation of the compartment of vehicle 1
  Equation (33)
- The work done through deformation of the compartment of vehicle 2
  Equation (34)

Based on this breakdown of energy dissipation, the EESFF was calculated for these collisions and compared with the EESVV values.

8.4.2.1 Renault Clio – Rover 75

The work done through deformation of the front-ends of both vehicles combined (between the A-pillars) was calculated based on the average structural force and the relative displacement between the struck side A-pillars according to equation (32). The result is compared in Figure 71 to the total work done through deformation between the B-pillars, as calculated in section 8.3.4.

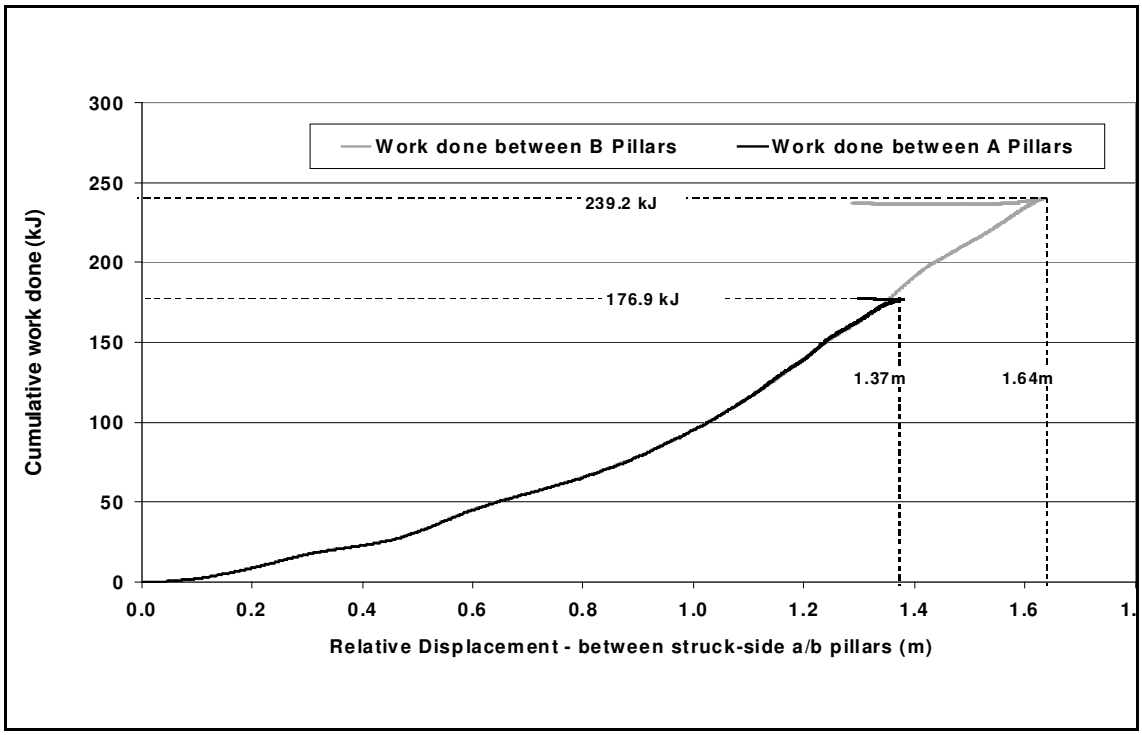

Figure 71 Energy dissipation through structural deformation – Renault Clio versus Rover 75 – Based on the average structural force of the Renault Clio and Rover 75 and the relative displacement between struck side A and B pillars, respectively.

After 1.37m of structural deformation, the relative crush of the front-ends (between the A-pillars) ceases and the remaining deformation (up to 1.64m) occurs within the passenger compartments. The high correlation exhibited by the curves up to 1.37m of combined vehicle deformation indicates that the accelerometer readings for accelerometers located at the A- and B-pillars were almost identical up to this point in the collision.

To further evaluate the degree of compatibility exhibited by the vehicles involved in this collision, the dissipation of energy was broken down into that dissipated within the front-ends and in each of the respective compartments and is shown in Figure 72.

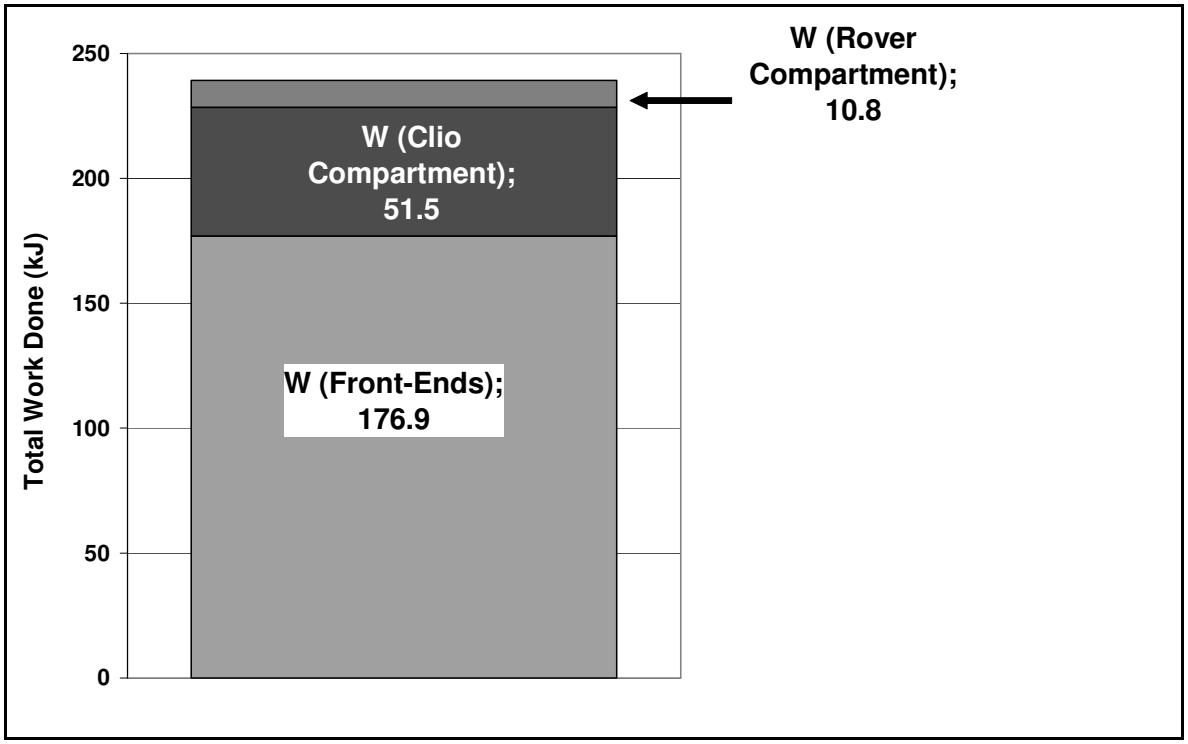

Figure 72 Total work done through deformation of both front-ends combined and each respective compartment for the Rover 75 – Renault Clio head-on crash test

Figure 72 confirms that a large amount of energy was dissipated within the compartment of the Clio (51.5kJ). Based on the values shown in Figure 72, the EESFF can be calculated for this collision:

$$m_{structure-clio} = (1215kg - 150kg) \cdot 0.8 = 852kg$$
$$m_{structure-rover} = (1732kg - 150kg) \cdot 0.8 = 1265.6kg$$
$$D_{FF} = 176.9kJ$$

$$EESFF = \sqrt{2\,(176.9kJ \cdot 1000)\,\frac{(852kg + 1265.6kg)}{(852kg \cdot 1265.6kg)}}$$
$$EESFF = 26.4\,m/s = 94.9\,km/h$$

The maximum possible EESFF for the collision can be interpreted to be approximately 112km/h, assuming each vehicle was developed for a fixed barrier collision at 56km/h (EES). The EESVV calculated for this collision was 110.3km/h, section 8.3.4. The degree of compatibility exhibited by the two vehicles involved in this collision was relatively poor based on the EESFF value of 94.9km/h.

As discussed in section 4.4.3, the EESFF value is a metric which reflects the degree of compatibility of two vehicles involved in a particular collision. The EESFF value is influenced by the degree of structural interaction, the strength of the compartments of both vehicles and the magnitude of front-end deformation forces. In order to evaluate the independent influence of structural interaction, a theoretical maximum EESFF value for the case of maximal structural interaction is required (see discussion in section 4.4.3), considering the differences in stiffness of both vehicles.

8.4.2.2 Modified VW Polo 6N - Rover 75

The work done through deformation of the front-ends (between the A-pillars) was also calculated for this crash test based on equation (32). The result is compared in Figure 72 with the total work done through deformation between the B-pillars, as calculated in 8.3.3.

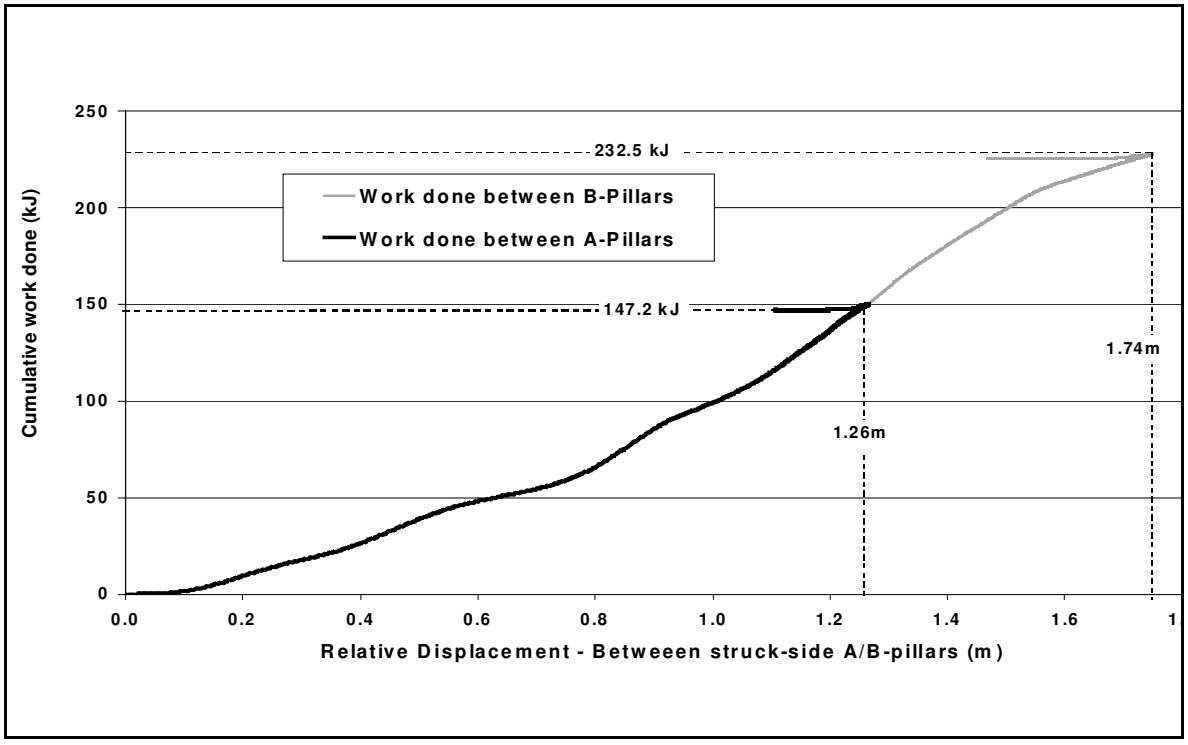

Figure 73 Energy dissipation through structural deformation – VW Polo 6N to Rover 75 – Based on average structural force of the VW Polo and Rover 75 and the relative displacement between struck side A- and B- Pillars, respectively.

Figure 73 reflects the high deformation of the compartment of the Polo 6N after a combined vehicle crush of 1.26m. After this point, the dissipation of energy and the

relative displacement between the struck side B-pillars increases whilst the dissipation of energy between the A-pillars remains constant. The two curves exhibit a very high degree of correlation up to the point of collapse of the compartment of the Polo 6N. This also reflects the accuracy of the accelerometer signals and the calculation of energy dissipation based on these experimental values. To further evaluate the degree of compatibility achieved in the collision, the dissipation of energy was broken down into that dissipated in both of the front-ends and in each of the respective compartments, Figure 73, according to equations (32) to (34).

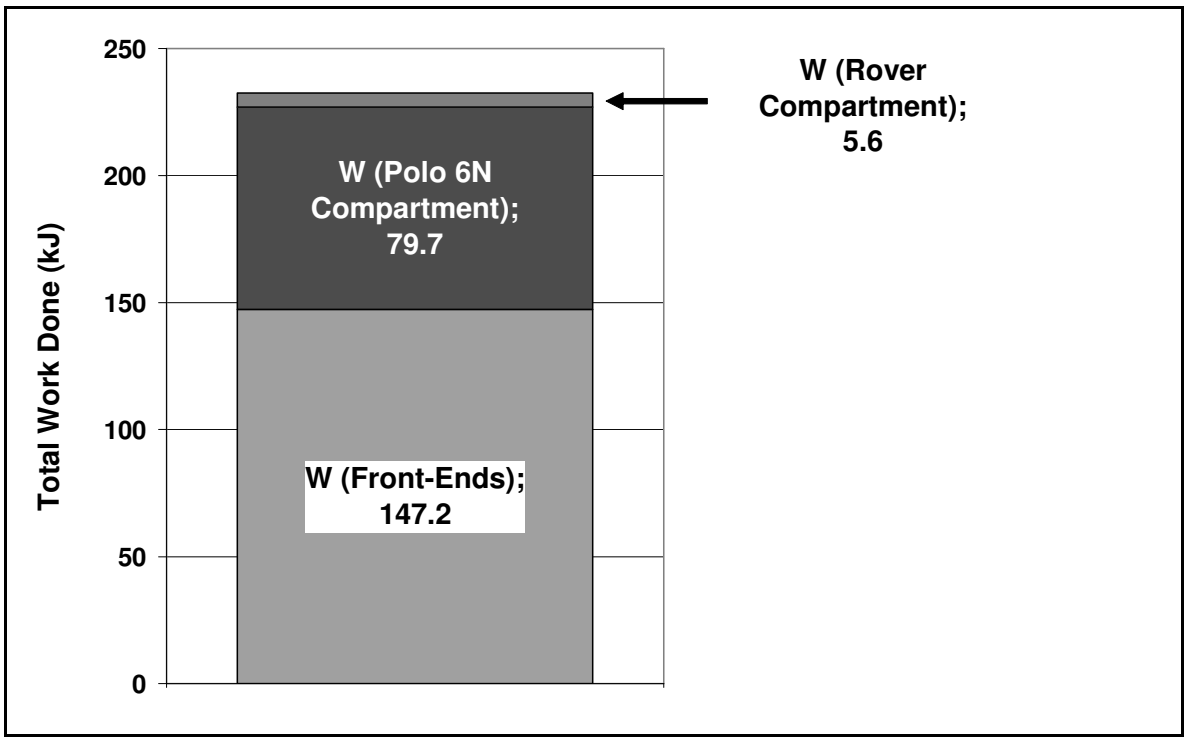

Figure 74 Total work done through deformation of both front-ends and each respective compartment for the VW Polo – Rover 75, head-on crash test

Figure 74 shows that a large amount of energy is dissipated in the compartment of the VW Polo 6N (79.7kJ). Based on the values shown in Figure 74, the EESFF can be calculated for this collision as well.

$$m_{structure-polo} = (1105kg - 150kg) \cdot 0.8 = 764kg$$
$$m_{structure-rover} = (1732kg - 150kg) \cdot 0.8 = 1265.6kg$$
$$D_{FF} = 147.2kJ$$

$$EESFF = \sqrt{2 \cdot (147.2kJ) \cdot \frac{(764kg + 1265.6kg)}{(764kg \cdot 1265.6kg)}}$$

$$EESFF = 26.9\,m/s = 89.5\,km/h$$

The EESVV value calculated for the collision was 112.5km/h. The maximum possible EESFF value can be estimated to be 112km/h, assuming both vehicles were tested at an EES of 56km/h in self protection testing. This maximum EESFF value would only be achieved for the case of perfect compatibility (i.e. perfect structural interaction and stiffness compatibility). The degree of compatibility exhibited by these two vehicles can be considered to be low for these collisions, based on the EESFF value of 89.5km/h.

8.5 Summary of the method proposed to calculate energy dissipation.

The method presented in this chapter to calculate energy dissipation through structural deformation in car-to-car collisions yielded plausible results. However, there are limitations associated with the method that are detailed and the end of this section.

The dynamic influence of the engine/transmission was acceptably low in all collisions, which allowed a robust calculation of energy dissipation through structural deformation.

The EESVV was calculated for all collisions and proved to be a useful metric to communicate the collision severity. All EESVV values were similar to the actual closing velocity of the collision (with differences between EESVV values and the closing velocity of 4.8%, 2.4%, 0.8%, 6% for each of the collisions analysed).

The energy dissipation with respect to structural deformation was compared for all collisions analysed. The characteristics were very similar in the first half of the collision (up to 0.95m of total structural deformation). This was a surprising observation considering the significant differences in the masses and structural characteristics of

the vehicles tested. After 0.95m, the characteristics diverged significantly, which was attributed to high compartment deformation in two of the four collisions analysed.

A-pillar accelerometers were fitted to the vehicle in two of the collisions analysed. This allowed the energy dissipation to be broken down into that occurring in the compartment of each respective vehicle and in the front-ends of both vehicles combined. Based on these values, the EESFF value was calculated. In both cases, the EESFF value was significantly lower than the EESVV value, suggesting only a low level of compatibility was achieved.

The EESFF is a general reflection of the degree of compatibility in a given collision. The EESFF is influenced by the degree of structural interaction, the strengths of the passenger compartments and the magnitude of front-end deformation forces. Even if maximal structural interaction were achieved in most of these collision configurations, the EESFF would be significant lower than the closing velocity if the vehicles were not compatible with respect to stiffness.

To evaluate the degree of structural interaction in such collisions, a maximum possible EESFF value is required, considering the differences in stiffness of the two vehicles. This could be predicted by statically combining the force-displacement characteristics from each vehicle from a fixed barrier collision. This will be discussed further in recommendations for further research in 10.2.

Limitations

The method presented in this chapter to measure energy dissipation in car-to-car collisions is based on some key assumptions, which are outlined below: These assumptions need to be considered should the proposed method be further applied to analyse structural behaviour in real-world collisions.

To enable the calculation of energy dissipation based on accelerometers, an assumption was made that the vehicles involved in the respective collisions consisted of two lumped-rigid-masses (engine and transmission, remaining structure) that be-

haved **independently** to each other. The key limitations associated with this assumption are listed below:

- Some level of interaction between the two rigid masses (engine/transmission, vehicle structure) is present in real-world collisions.
- The method was only applied in vehicles with front-mounted engines. The method may not be appropriate for vehicles with mid- and rear-mounted engines.
- The vehicle structures are not entirely rigid as much of the structure (mostly in the front-end) deforms during a collision to dissipate energy. The parts of the structure undergoing deformation also have an associated mass which **is** considered in the calculation of the structural force.
- The behaviour of vehicle structures was analysed based on readings taken from accelerometers located at the base of the B-pillars. These accelerometer are assumed to have provided an accurate reflection of the behaviour of the entire non-deforming (passenger compartment) areas of the vehicle structure.

9 Investigating measures to improve Structural Interaction based on FEM simulations

In chapter 8, a method was developed to measure the energy dissipated through structural deformation in car-to-car, head-on crash tests, based on accelerometer readings. In this chapter, the method is applied to evaluate structural interaction in FEM (Finite Element Modelling) numerical collision simulations.

In section 9.1, the validity of the measurement of energy dissipation in numerical simulations, based on the method developed in chapter 8, is investigated for a fixed barrier crash test. The degree of energy dissipated through structural deformation is calculated for a car-to-car, head-on collision in 9.2. This value is compared to the fixed barrier collision to determine the degree of structural interaction which occurred in the standard car-to-car collision. Two identical Volkswagen passenger vehicles were used as a basis for all car-to-car head-on crash test simulations. **This allowed structural interaction to be evaluated independently, with the influence of mass and front-end stiffness controlled. Any reduction in the EESFF value of a collision is normally attributable to a combination of structural interaction, compartment strength and front-end force. When identical vehicles are involved in a collision, compartment strength and front-end forces are identical and structural interaction has an isolated influence on the resulting EESFF values.**

In 9.3, the influence of the vertical alignment of front-end structures on the resulting degree structural interaction is investigated. Based on this, the sensitivity of structural interaction to over/underriding is determined. In 9.4, the validity of the energy calculation for the car-to-car collision simulations is discussed. In 9.5, several constructive measures are investigated with the goal of maximising structural interaction in the standard car-to-car, head-on collision configuration.

9.1 Fixed barrier collision

9.1.1 Measuring energy dissipation

A fixed barrier collision simulation was carried out with a degree of overlap equal to 40% of the width of the vehicle. This offset ratio was chosen with the aim of best replicating the structural loading occurring in a car-to-car, head-on collision at an overlap ratio of 50% (based on a Mercedes Benz study [98], comparing the structural loading in fixed barrier and car-to-car collisions). The structural loading in car-to-car collisions at 50% overlap and car-to-fixed barrier collisions at 40% overlap will be compared in detail in the following sections.

No deformable element was located in front of the fixed barrier, to ensure that the kinetic energy of the vehicle would be dissipated through deformation of the vehicle structure only. The initial velocity of the vehicle was equal to 56km/h and the vehicle test mass was equal to 1785kg. Two dummies were located in the front-seats, each with a mass of 75kg. The collision configuration is illustrated in Figure 75.

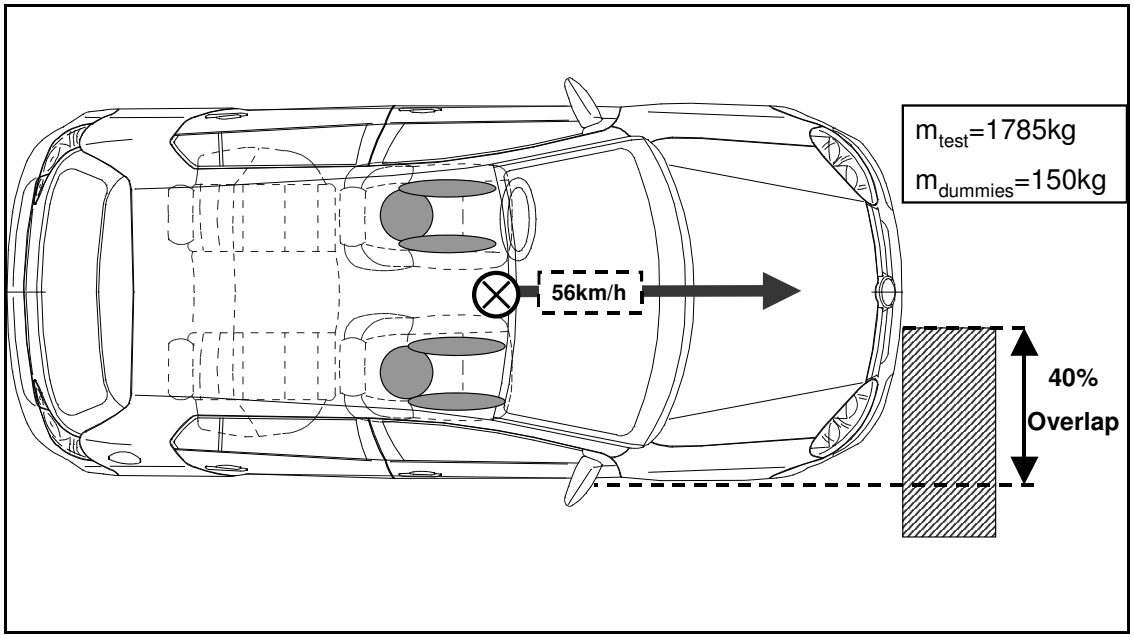

Figure 75 Fixed barrier crash test simulation configuration– 40% overlap, 56km/h

9.1.1.1 Accuracy of nodal acceleration-time characteristics

In the previous chapter, the energy dissipation associated with structural deformation was calculated based on the acceleration-time characteristics of the A and B-pillars, recorded by accelerometers. In numerical simulations, the acceleration-time characteristics of each individual node, linking the thousands of elements which make up the vehicle structure, can be used to reflect the acceleration for a given section of a vehicle. A requirement for an accurate calculation of energy dissipation based on nodal acceleration-time characteristics, is that two nodes which are located in the same non-deformed region of the vehicle structure, exhibit similar acceleration-time characteristics.

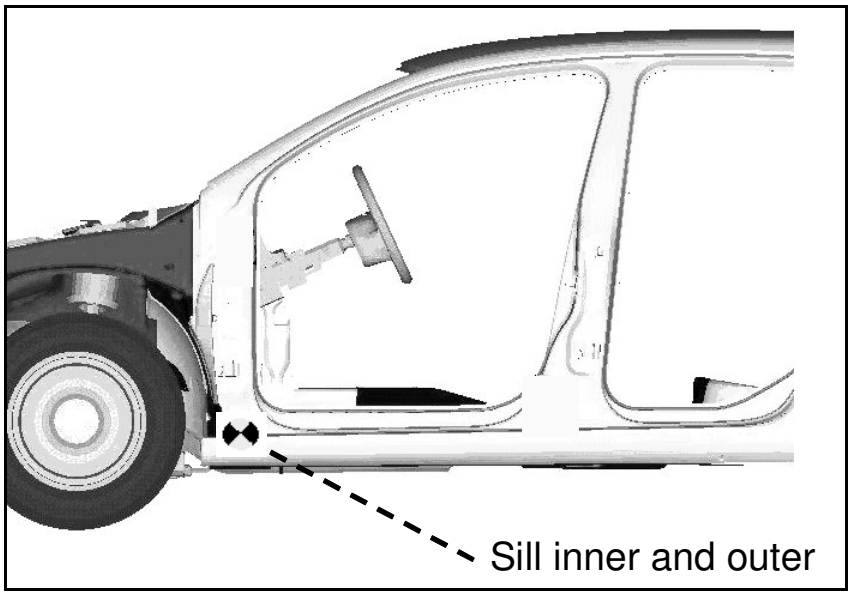

Figure 76 Location of nodes used in the comparison of nodal acceleration-time characteristics. Side-view of vehicle (left-hand drive vehicle)

To investigate this, acceleration-time characteristics for nodes located at the base of the left and right A-pillars, on the inner and outer side of the sill, were compared, Figure 76. This is a relatively rigid region of the structure, which is loaded to a very high degree in a collision as it is located at the front of the passenger compartment.

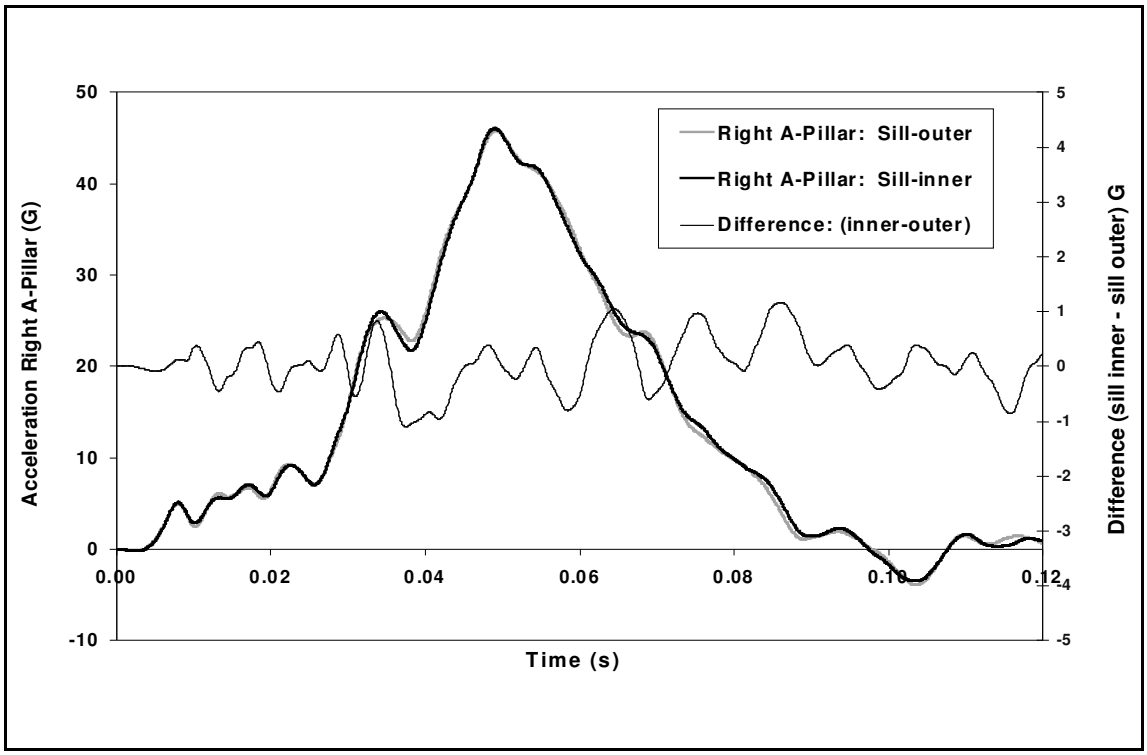

Figure 77 Acceleration-time characteristics of two nodes located at the inner and outer edge of the sill, at the base of the right A-pillar (non-struck side)

In both Figure 77 and Figure 78, a high correlation between nodal acceleration-time characteristics, for both the left and right A-pillars, can be observed. The difference in acceleration values varies between +/- 1G in Figure 77 and +/- 2G in Figure 78. Given the high correlation of the characteristics shown, the acceleration-time characteristics of individual nodes are considered to be a reliable basis for energy calculations, based on the method presented in Chapter 8.

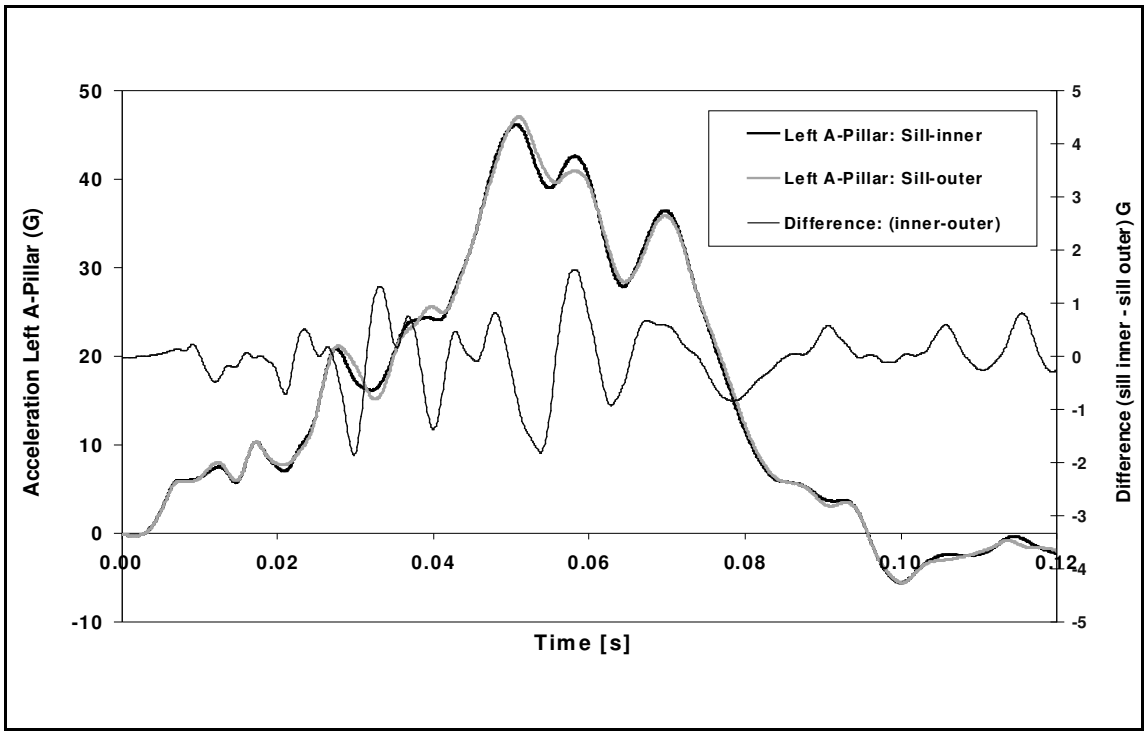

Figure 78 Acceleration-time characteristics of two nodes located on the inner and outer edge of the sill at the base of the left A-pillar (struck side)

The nodes used as a basis for the calculation of energy dissipation in the following pages are shown in Figure 79. Nodes located in the C-pillar region of the vehicle were also used in the energy analyses. This facilitates a calculation of energy dissipation between the B and C-pillars as well. The A-pillar node chosen was located higher up the A-pillar, to better reflect the actual compartment deformation, as the upper edge of the A-pillar underwent a higher amount of displacement relative to the B-pillar in all simulations.

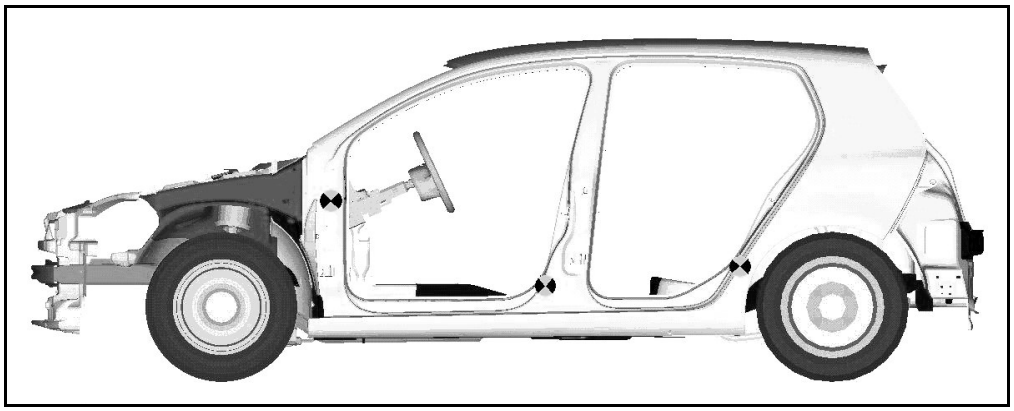

Figure 79 Location of the nodes chosen to represent the acceleration-time characteristics of the A-, B- and C-pillars for the basis of energy dissipation calculations. Side view of vehicle structure (left-hand drive vehicle)

9.1.1.2 Calculation of energy dissipation based on nodal acceleration characteristics

The structural force was calculated for the fixed barrier collision (based on equation (24) and plotted with respect to the relative displacement between the struck side A, B and C-pillars and the wall, Figure 80. C-pillar acceleration-time characteristics were used as the basis for the calculation of the structural forces.

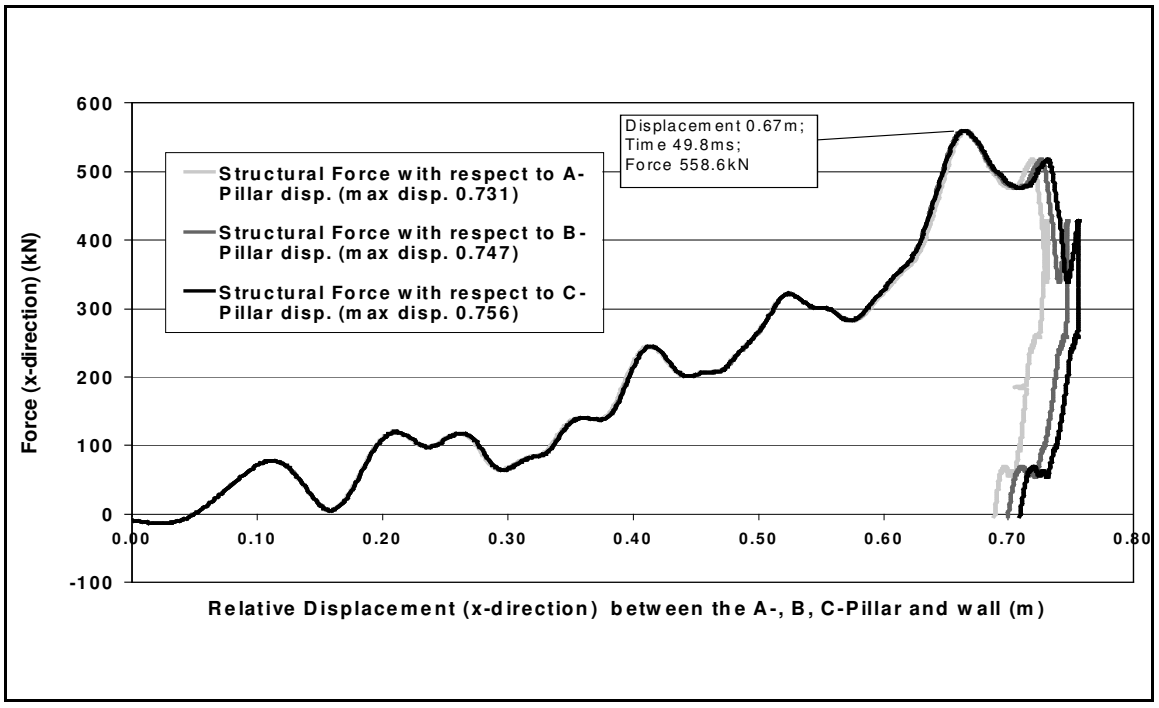

Figure 80 Structural force, calculated based on the average acceleration-time characteristics of the left and right C-pillars, plotted with respect to the relative displacement between the struck side, A-, B- and C-pillars and the wall. Fixed barrier collision, 40% overlap, 56km/h.

The relative displacement between the A, B and C-pillars and the wall reaches a maximum (0.731m, 0.747m, 0.756m) and decreases thereafter. This can be attributed to vehicle rebound. A small amount of the collision energy, absorbed by the vehicle structure, is returned to the vehicle in the form of kinetic energy. This represents the elastic component of the structural loading.

The force-displacement characteristics exhibit a very high correlation up to the point of maximum forces (558.6kN at 49.9ms/0.67m displacement). The maximum relative displacement between the B- and C-pillars and the wall are higher than the value for the A-pillar. This additional deformation represents the global deformation of the passenger compartment.

By integrating the structural force versus relative displacement characteristics, the energy dissipated between the struck side A-, B- and C-pillars and the wall, can be calculated. This was carried out based on the method presented in the previous chapter in section 8.1.2. The resulting characteristics are shown in Figure 81, below.

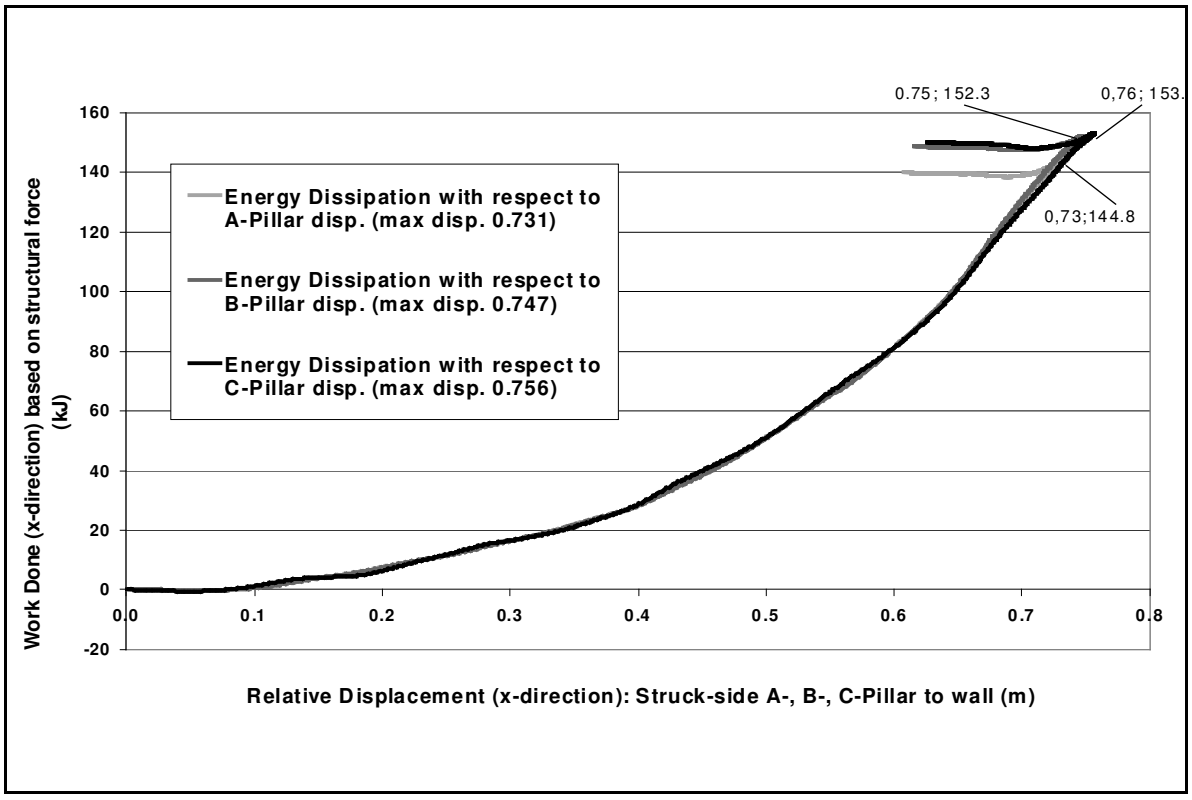

Figure 81 Energy dissipation through deformation between the struck side A-, B- and C-pillars and the wall. For a fixed barrier crash test-simulation at an overlap ratio of 40% and a velocity of 56km/h.

The majority of the energy dissipation occurs within the front-end for this collision with a fixed barrier. Of the total 153.1kJ dissipated within the structure (between the C-pillar and the wall) 144.8kJ was dissipated within the front end (between the A-pillar and the wall). The difference between these two values (8.3kJ) is the energy dissipated through compartment deformation. A negligible amount of energy is dissipated between the B- and C-pillars.

The EESV of the collision can be calculated based on the energy dissipated through deformation of the entire vehicle structure. This can be considered equal to the deformation energy dissipation between the struck side C-pillar and the wall ($D_{C\text{-}pillar}$). As the energy calculation considers the vehicle structure only, the structural mass ($m_{structure}$), was used for the calculation. Based on equation (8):

$$EESV = \sqrt{\frac{2 \cdot D_{C-pillar}}{m_{structure}}}$$

$D_{C\text{-}pillar}$ = 153.1kJ, m_{test}=1785kg

$$m_{structure} = (m_{test} - m_{dummies})\ 0.8 = (1785 - 150)\ \ 0.8 = 1308\,kg$$

$$EESV = \sqrt{\frac{2 \cdot 153.1 \cdot 1000}{1308}} = 15.3\ m/s = 55.1 km/h$$

The EESV of the collision is slightly lower than the closing velocity (55.1km/h compared to 56km/h). This small difference can be attributed to vehicle rotation.

9.1.1.3 Validity of the acceleration-based calculation of energy dissipation

The change in internal energy of each individual element can be recorded in numerical collision simulations. This value is derived based on the 3-dimensional stress-strain properties of the elements comprising the vehicle structure. The validity of the energy dissipation calculation can be determined by comparing the simulation internal energy with the energy dissipation values calculated based on accelerometers.

The method of calculating energy dissipation based on accelerometers does not consider the change in energy of the dummies or the engine/transmission (see section 8.1). These terms were removed from the total change in internal energy of all elements for the fixed barrier collision simulation. The change in internal energy was extracted for the point in time corresponding to the point of maximal vehicle deformation (49.8ms, see Figure 80).

	Energy dissipation based on nodal accelerations	**Internal Energy – Numerical Simulation**
Energy dissipation - entire vehicle	-	193.2kJ
Energy dissipation – engine/ transmission	-	-19.8kJ
Change in internal energy (dummies)	-	-18.2kJ
Energy dissipated through structural deformation	153.1kJ	155.2kJ
Error (155.2kJ–153.1kJ)/(153.1kJ)		**1.4%**

The error of 1.4% between the calculated value for energy dissipation through structural deformation (based on nodal-accelerations) and simulation internal energy is very low. The calculation of energy dissipation based on nodal accelerations is therefore valid for the fixed barrier collision.

9.1.2 Predicting maximum structural interaction

The force-versus-deformation characteristics, calculated in section 9.1.1.2 for the fixed barrier collision can be statically combined based on the approach described in section 4.1. This is achieved by mirroring the fixed barrier force-displacement characteristics for the A, B and C-pillars about the vertical axis, Figure 82.

The displacement corresponding to each discrete force value, for both the original characteristic and the mirrored characteristic, can be simply added together. The re-

sulting characteristics are a prediction of the maximal force versus displacement characteristics, for a head-on collision involving two vehicles identical to the vehicle involved in the fixed barrier collision.

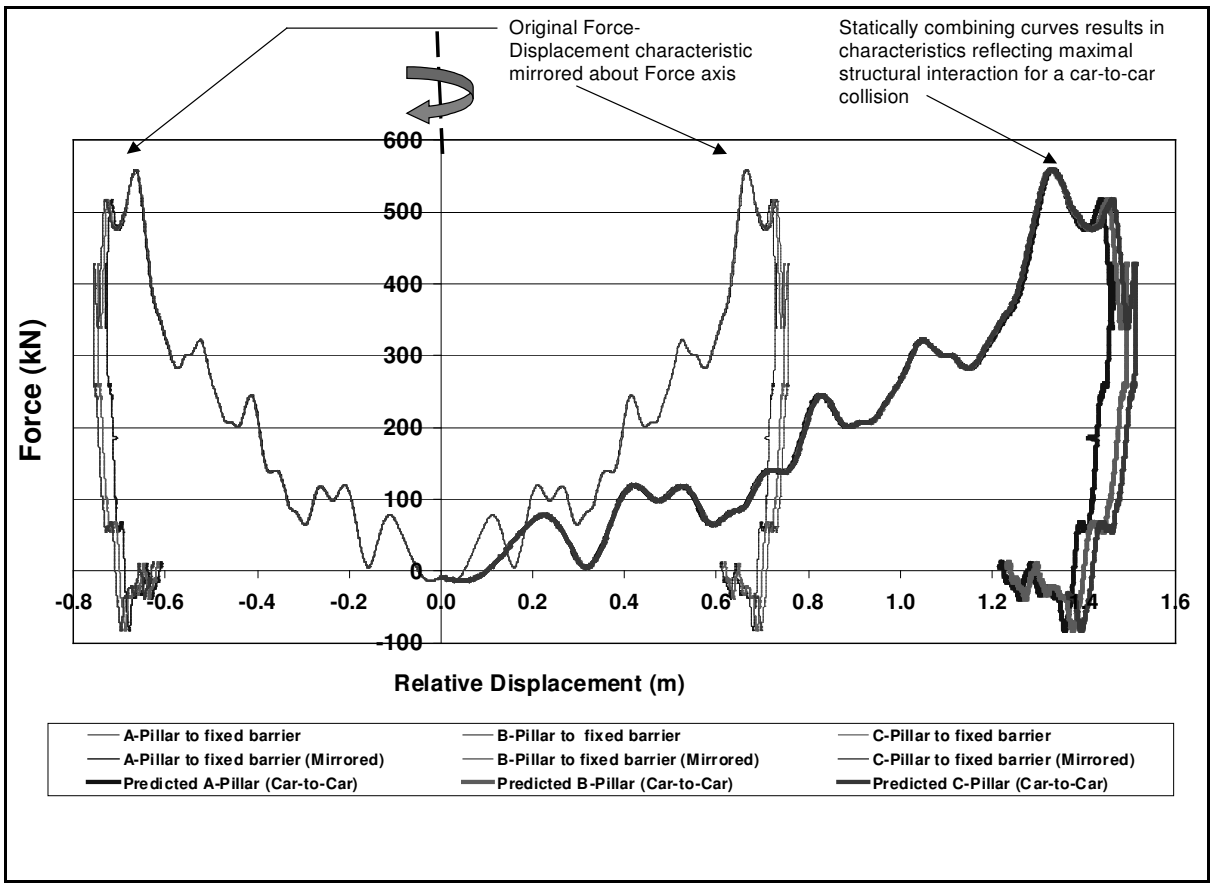

Figure 82 Statically combining the structural force-versus-displacement characteristics (relative displacement between the A, B and C-pillars and the wall) for a fixed barrier collision to yield theoretical force-versus-combined displacement characteristics for a car-to-car collision involving two identical vehicles

In this particular case, the statically combined characteristic can also be plotted by a simple elongation of the original characteristic through multiplying all displacement values in the fixed barrier collision by a factor of 2 (parallel to the horizontal axis). This is only valid for a collision involving identical vehicles.

The characteristics shown in Figure 82 can be integrated with respect to the combined displacement between the struck side A, B and C-pillars, to yield predicted maximum energy dissipation characteristics. These characteristics represent the maximum possible degree of energy dissipation that would occur in the case of maximal structural interaction, Figure 83.

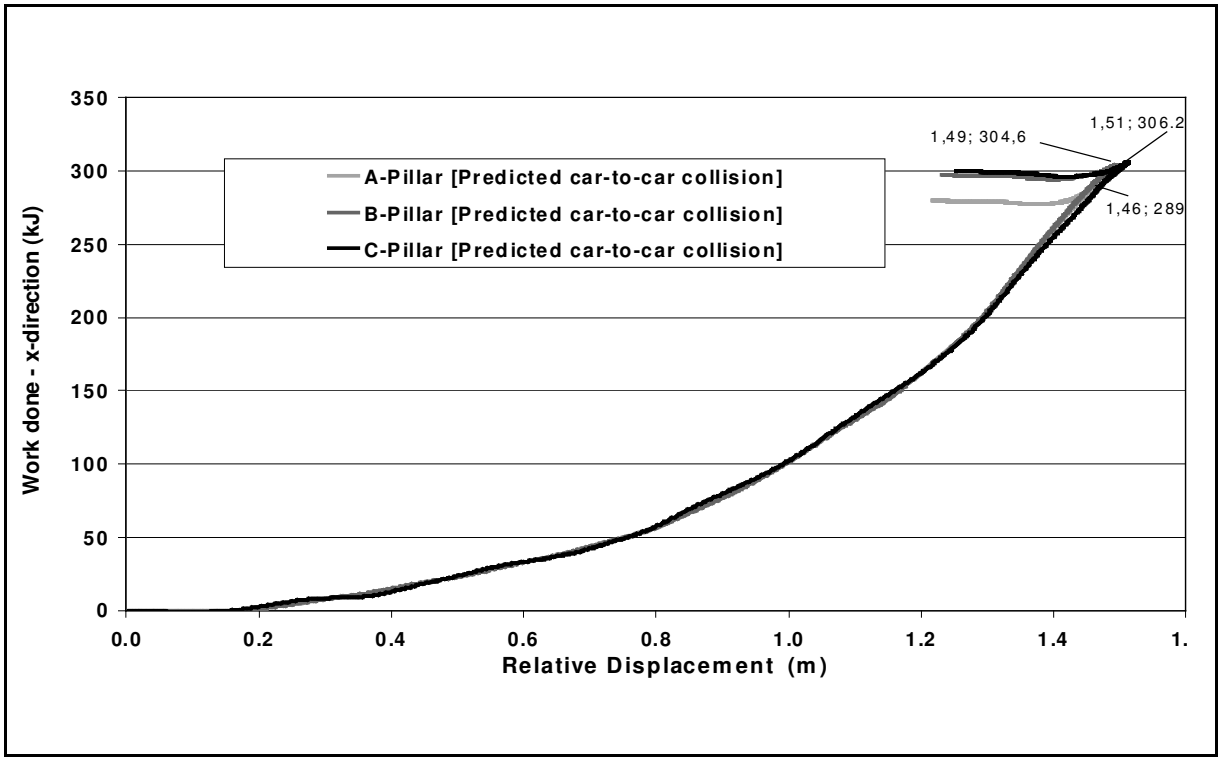

Figure 83 Work done versus combined vehicle deformation (between struck side A, B and C Pillars, respectively) calculated based on statically combined, structural force versus relative displacement characteristics for a fixed barrier collision at 56km/h and an overlap ratio of 40%

These maximum theoretical energy dissipation characteristics act as a reference for the evaluation of structural interaction for all car-to-car crash simulations presented in this chapter.

9.2 Car-to-car collision

The results of a car-to-car, head-on crash simulation involving two vehicles, identical to the car involved in the fixed barrier collision analysed in section 9.1, are presented in this section. The closing velocity was equal to double the fixed barrier crash test velocity to ensure that the collision severity for each vehicle can be considered equivalent to the fixed barrier collision severity. This enables a direct comparison of the performance of the vehicles in a fixed barrier collision with their performance in a car-to-car collision. Any difference in the structural performance of the vehicle in the car-to-car collision can be attributed directly to the degree of structural interaction.

The initial velocity of each vehicle was 56km/h (v_C=112km/h). The overlap ratio was equal to 50% of the width of each vehicle, which is comparable to a fixed barrier collision at an overlap of 40% (as discussed in section 9.1.1). The collision configuration is shown in Figure 84 below.

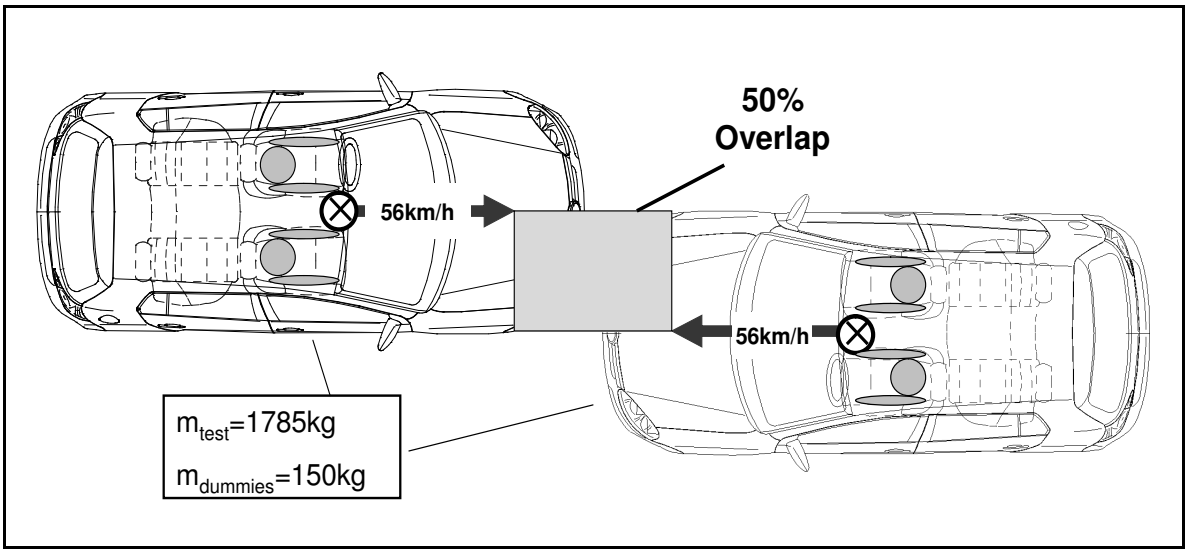

Figure 84 Collision configuration: Car-to-car, head-on crash tests carried out at an overlap ratio of 50% and a closing velocity of 112km/h

9.2.1 Energy dissipation through structural deformation

In the previous section (9.1), theoretical maximal force and energy versus combined vehicle deformation characteristics were developed representing a prediction of maximal structural interaction for a head-on collision. Based on the method defined in section 8.1.3, the energy dissipation between the struck side A, B and C pillars of each vehicle was calculated for the actual car-to-car collision. A comparison between the actual characteristics and the predicted maximal characteristics facilitates an evaluation of the degree of structural interaction which occurred. This is shown in Figure 85.

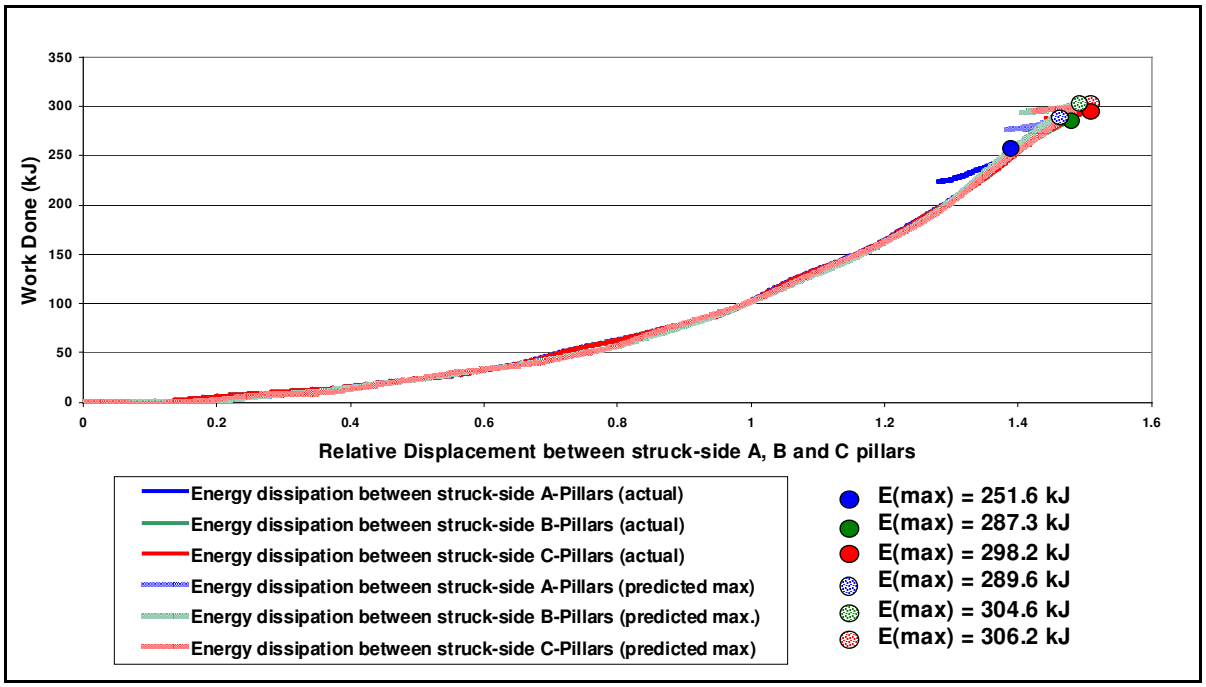

Figure 85 Comparison of the predicted maximum (based on a fixed barrier collision at 56km/h and 40% overlap) and actual level of energy dissipation between the struck side A, B and C Pillars. Car-to-car, head-on collision in the standard configuration at 112km/h and 50% overlap.

Figure 85 indicates that the energy dissipation characteristics for the statically combined car-to-fixed barrier crash test simulation are almost identical to those for the car-to-car crash test-simulations, for most of the crash duration. After approximately 1.4 metres of combined vehicle crush, the characteristics vary. Less energy was dissipated in the combined front-ends (between the struck side A-pillars) for the car-to-car collision (251.6kJ) than the predicted maximum (289.6kJ). This infers that less than optimal structural interaction occurred.

Based on Figure 85 and the subsequent discussion, two key observations relating to structural interaction can be made:

- **In a collision involving two identical vehicles, the vehicle front-end may be more aggressive than a fully planar rigid-barrier.**
- **The result of poor structural interaction is a surplus in kinetic energy after complete deformation of the front-end, which leads to increased compartment loading and compartment deformation.**

Since there is no difference in the characteristics up to 1.4 metres of combined vehicle crush, it is not sensible to evaluate the level of structural interaction based on the shape of the energy dissipation curves shown in Figure 85. The EESFF value, based on the energy dissipation in the vehicle front-ends, is therefore an appropriate quantity to evaluate structural interaction in these simulations.

EESVV and EESFF values were calculated based on equations (12) and (13) for the actual car-to-car collision and the predicted maximum energy dissipation characteristic, generated based on the fixed barrier collision.

Comparing the predicted maximum EESFF value (based on statically combined fixed barrier crash simulation) and the actual EESFF value for the car-to-car collision enables an evaluation of the degree of structural interaction. Comparing EESVV values allows a comparison of the collision severity.

	Statically combined Fixed Barrier	Car-to-Car 0mm
m1 [kg]	1785	1785
m2 [kg]	1785	1785
m(structure) [kg]	1308	1308
m(structure) [kg]	1308	1308
D (VV) [J]	306200	298130
D (FF) [J]	289600	251665
D(compartments) Rigid-wall-collision [J]	16600	16600
EESVV [km/h]	**110.2**	**108.7**
EESFF [km/h]	**107.1**	**99.9**
V (collision) [km/h]	**112.0**	**112.0**

Figure 86 Calculating the EESVV and EESFF for the statically combined and actual car-to-car collision characteristics

In the car-to-car collision, a significantly lower amount of energy was dissipated in the front-ends of both vehicles than theoretical available, leading to a reduction in the EESFF by 7.2km/h (107.1km/h – 99.9km/h, Figure 86). The actual level of structural interaction which occurred was less than maximal, even for this collision involving identical vehicles.

The difference in the EESVV metric for the predicted and actual characteristics is 1.5km/h (110.2-108.7). This indicates that more energy was dissipated in each vehicle in the fixed barrier collision than in the car-to-car collision. This can be attributed to a higher degree of vehicle rotation occurring in the car-to-car collision.

9.2.2 Validation of the measurement of energy dissipation

Based on the method applied in 9.1.1.3, the change in internal energy of all elements of the vehicle structure (neglecting the engine/transmission and the dummies) was calculated. The energy dissipated within the structure was 303.3kJ. This correlates well with the value calculated based on accelerometers (298.2kJ). The associated error is equal to

(298.2-303.3)/(303)% = -1.71%

9.3 Influence of the vertical alignment of vehicle structures in car-to-car head-on collisions

In this section, results to simulations are presented in which the vertical alignment of vehicle front-end structures was incrementally changed. The results provide a statement about the sensitivity of structural interaction, with respect to the vertical alignment of front-end structures. A vertical misalignment of structures was induced by translating one vehicle (and the road surface belonging to the vehicle) in the vertical direction. Each vehicle interacted with its own road-surface only. There was no interaction between each vehicle and the road surface belonging to the other vehicle. Simulations were carried out for collisions with an overlap ratio of 50% and 45%, in sections 9.3.1 and 9.3.2, respectively.

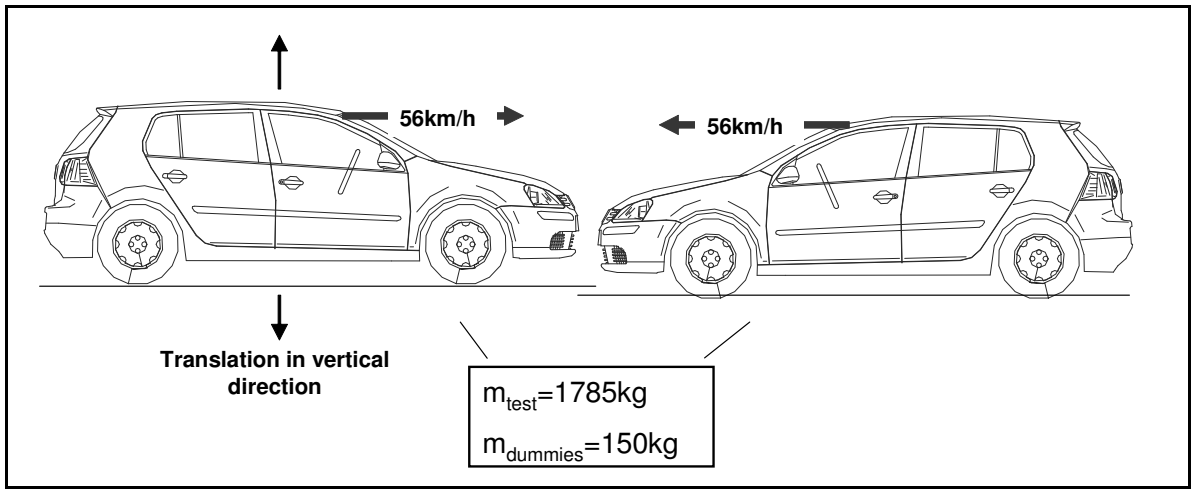

Figure 87 Varying the vertical alignment of front-end structures for a car-to-car head-on collision simulation

For collisions at overlap ratios of 45% and 50%, the vertical misalignment of structures was increased in 20mm increments (from 0-100mm) to investigate the sensitivity of the resulting structural interaction to small changes in vertical overlap. Additionally, a simulation at 200mm of vertical overlap was carried out, representing a much larger degree of vertical misalignment. This was considered to be the worst case for vertical misalignment for a collision involving two standard passenger cars.

9.3.1 50% overlap

For each degree of vertical misalignment of front-end structures, the EESVV and EESFF were calculated according to equations (12) and (13) and are shown in Figure 88.

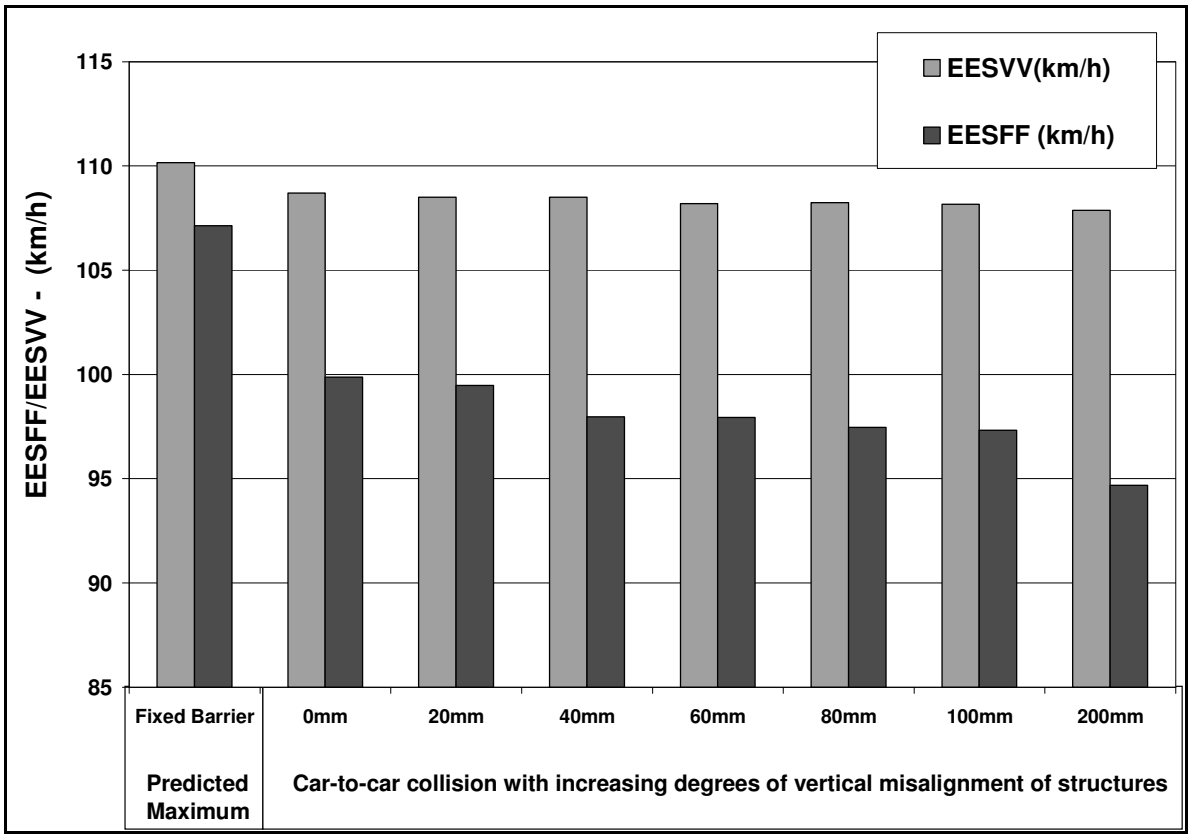

Figure 88 The influence of vertical structural misalignment on the degree of structural interaction (based on the EESFF) for a head-on collision involving two identical vehicles. 112km/h, overlap ratio 50%.

All EESFF values are significantly lower for the car-to-car collisions than the fixed barrier collision (a prediction of the EESFF value for the case of maximal structural interaction). This reflects the fact that structural interaction was well below the optimum level for all car-to-car collisions shown.

The EESVV values are similar for all car-to-car collisions and slightly lower than the EESVV values for the case of maximum predicted structural interaction (based on the fixed barrier collision). The similarity in EESVV values indicates that the collision severity was similar in all cases and allows a transparent comparison of EESFF values.

The level of structural interaction decreases (based on the EESFF values) as the degree of misalignment of front-end structures, in the vertical direction, increases. Between 0/20mm of vertical misalignment and 40mm of vertical misalignment, the degree of structural interaction falls significantly. This is due to the initial overriding of the cross beam. Between 40mm and 100mm of vertical misalignment, the degree of

structural interaction decreases to a less significant degree. This is due to the fact that the struck side longitudinal members of each vehicle come into contact with the engine/transmission of the other vehicle for all collisions up to 100mm of vertical misalignment. This ensures a homogenous transmission of force to the struck vehicle and significant deformation of the longitudinal members of both vehicles. Both of these factors did not lead to a significant reduction in energy dissipation within the front-ends, despite the increased vertical misalignment of structures.

At 200mm of vertical misalignment, the engine/transmission of the lower vehicle was overridden by the raised vehicle. The result is a further and significant reduction in the degree of structural interaction (from an EESFF value of 97.3km/h to a value of 94.7km/h).

As described in section 4.4, the EESFF reflects the degree of energy dissipated in the front-ends. As the EESFF decreases (for a constant EESVV) a higher degree of energy is dissipated in the passenger compartment and high compartment intrusions occurred. The degree of compartment intrusion is illustrated for all car-to-car collisions shown in Figure 87, scaled relative to the intrusion in the fixed barrier collision.

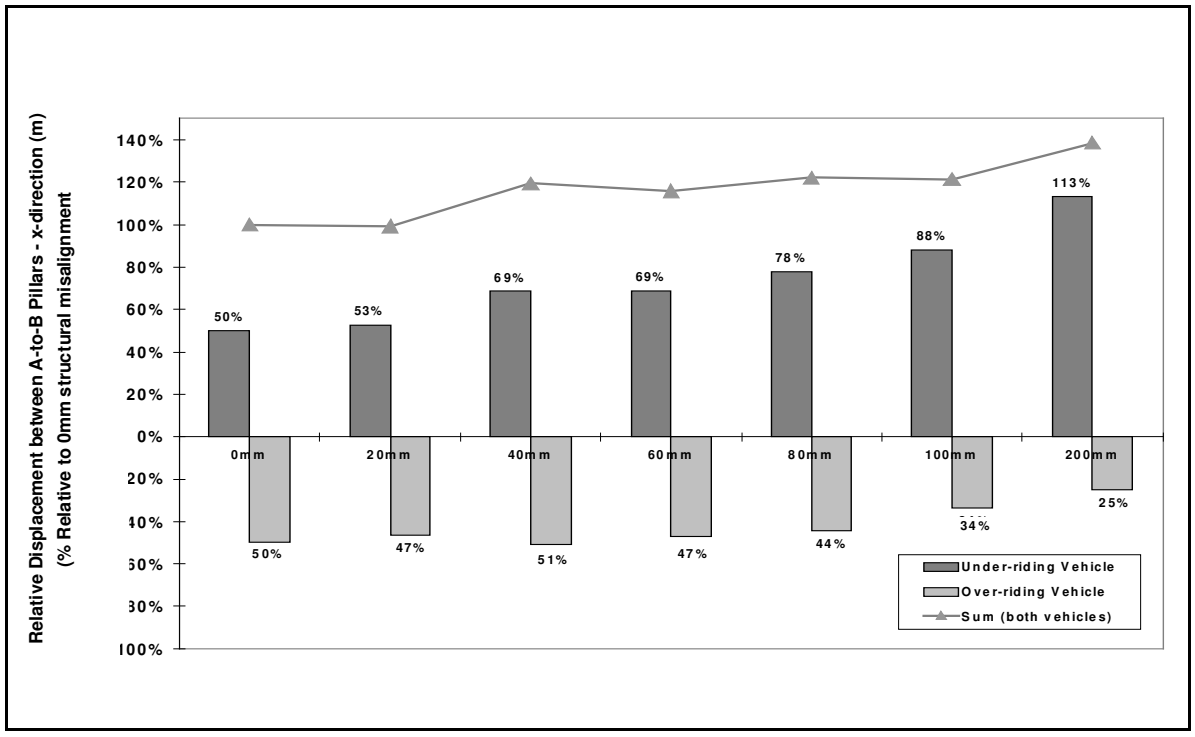

Figure 89 Relative displacement between A and B-pillars for the overriding and underriding vehicle (% with respect to the car-to-car collision with no structural misalignment) for a car-to-car head-on collision at 50% overlap and a closing velocity of 112km/h.

Figure 89 shows the relative degree of deformation of the compartment (between A and B-pillars) for the underriding vehicle (green) and the overriding vehicle (yellow) with respect to the collision with no structural misalignment. The sum of the compartment intrusions for both vehicles is represented by the grey line.

The total degree of compartment deformation (both vehicles combined) increases as the vertical misalignment of structures increases as the level of structural interaction decreases (based on the EESFF values shown in Figure 88).

As the degree of vertical misalignment of front-end structures increases, the degree of compartment deformation of the underriding vehicle increases significantly. At a vertical misalignment of structures of just 100mm, the compartment of the underriding vehicle undergoes almost twice as much deformation as that experienced in the original crash configuration (from 50% to 88%). Conversely, the degree of deformation of the compartment of the overriding vehicle remains quite static up to 60mm of vertical misalignment and decreases significantly thereafter. An increasing vertical misalignment of front-end structures is disadvantageous for the underriding vehicle yet advantageous for the overriding vehicle. The compartment of the underriding vehicle is weaker in these collisions as it is loaded, on average, at a higher point above the ground than in the case where no vertical misalignment of structures was present. This is a common observation in experimental car-to-car head-on crash tests [42]. Whilst the EESFF reflects the degree of structural interaction occurring in a car-to-car head-on collision accurately, the relative deformation of both passenger compartments can also be used as an indirect assessment of the degree of structural interaction occurring in these collisions.

9.3.2 45% Overlap

For the car-to-car collisions carried out with an overlap ratio of 50% of the width of the smaller vehicle, the longitudinal member of the striking vehicle contacted the engine/transmission of the struck vehicle. This resulted in a relatively constant degree of structural interaction, over a range of vertical structural misalignments (from 40mm to 100mm).

To further investigate this, the overlap ratio was reduced to 45%, to prevent the longitudinal members from contacting the engine/transmission block. The influence of the degree of vertical misalignment of front-end structures on the EESFF value was investigated for this collision configuration as well, Figure 90.

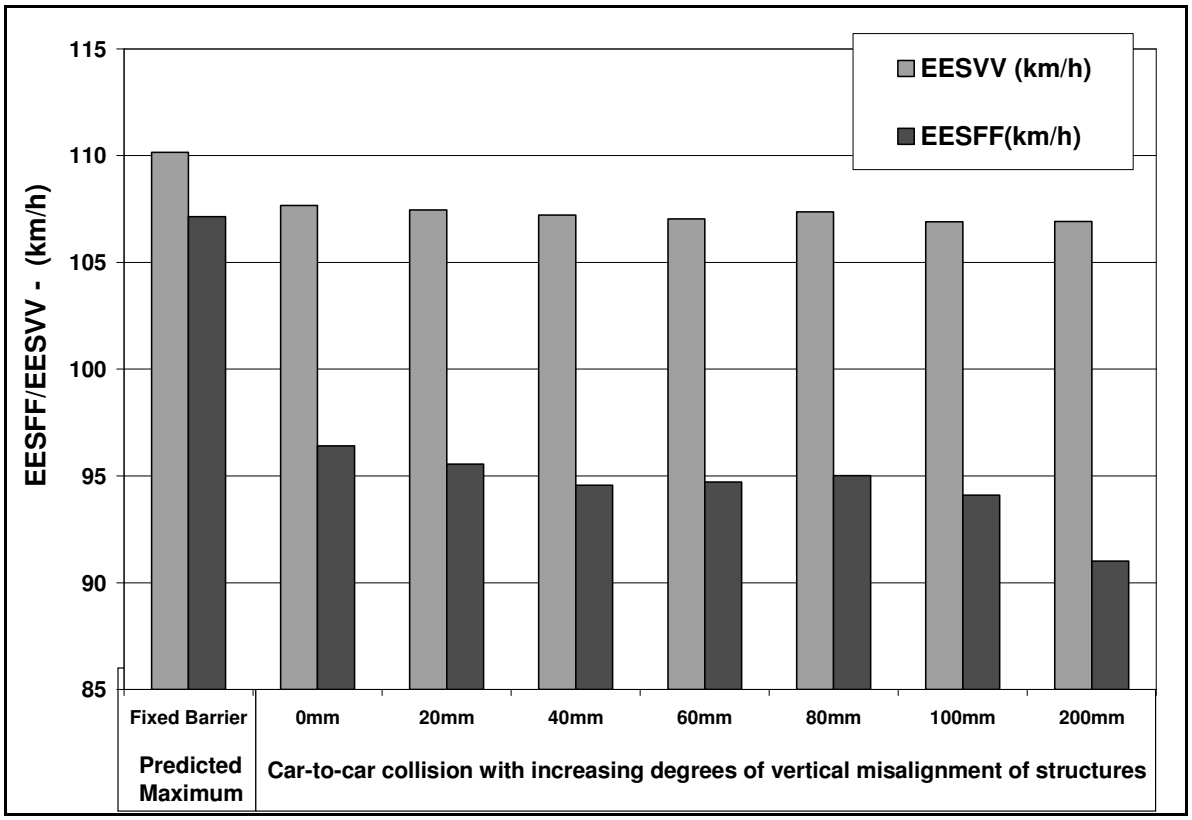

Figure 90 The influence of vertical misalignment of vehicle structures on the degree of structural interaction (based on the EESFF) for a head-on collision involving two identical vehicles. 112km/h, overlap ratio 45%.

As for the 50% offset configuration, an increase in the degree of vertical misalignment of structures leads to a general decrease in the EESFF values, whilst the EESVV values remained relatively constant. The EESFF values are again relatively constant between 40mm and 100mm of vertical misalignment. Although the engine/transmission block is not struck directly in this configuration by the longitudinals of the other vehicle, the degree of structural interaction appears relatively insensitive to the degree of vertical misalignment up to 100mm. From 100mm to 200mm of vertical misalignment, the EESFF decreases significantly (from 94.1km/h to 91.0km/h). To further investigate the reason for the static nature of the EESFF metric between 40mm and 100mm of structural misalignment, the relative intrusion between the struck side A and B-pillars is shown in Figure 91.

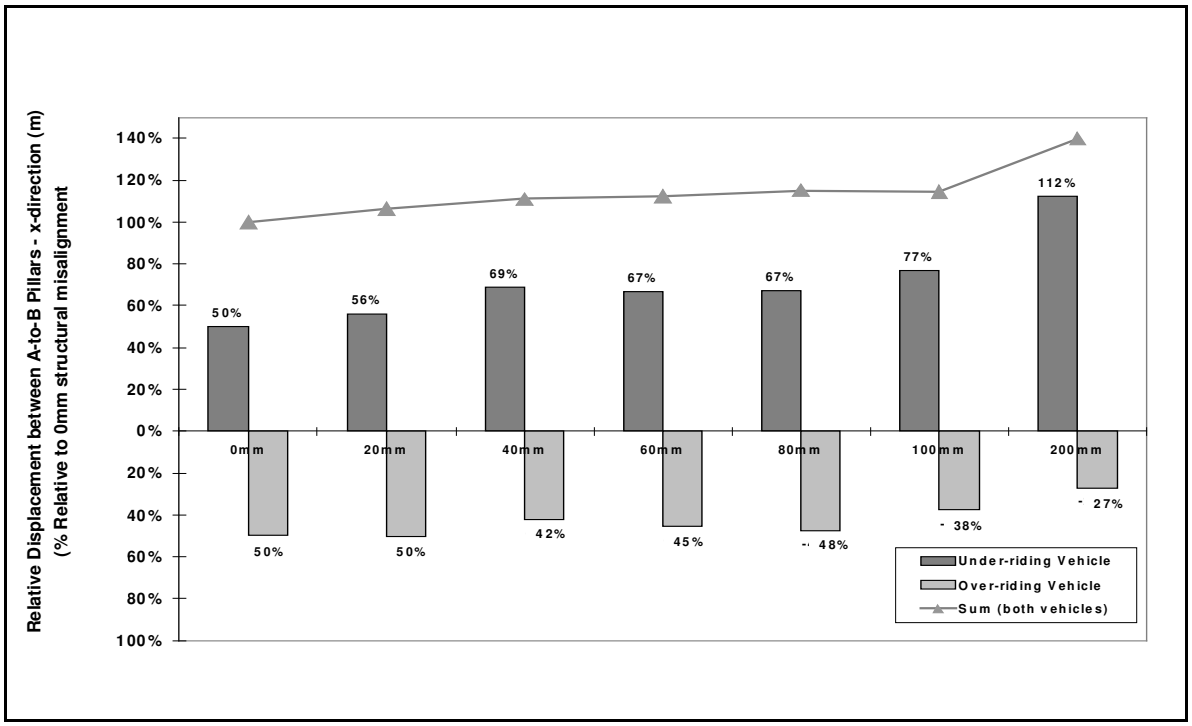

Figure 91 Relative displacement between A and B-pillars for the overriding and underriding vehicle (% with respect to the car-to-car collision with no structural misalignment) for a car-to-car head-on collision at 45% overlap at a closing velocity of 112km/h.

The total amount of deformation occurring within the compartments of both vehicles increases with increasing structural misalignment. As for the 50% overlap configuration, the deformation of the compartment of the underriding vehicle increases greatly (from 50% to 113%) as the degree of vertical structural misalignment increases. At the same time, the degree of compartment deformation of the underriding vehicle decreases (from 50% to 27%). This is the same trend which was observed for the 50% overlap configuration.

Whilst the EESFF accurately reflects the trend of structural interaction, the deformation of the compartment of each respective vehicle is much more sensitive to the degree of vertical misalignment. To further investigate this, the force-displacement characteristics of the compartment of the underriding vehicle were analysed for these collisions at an overlap ratio of 45%.

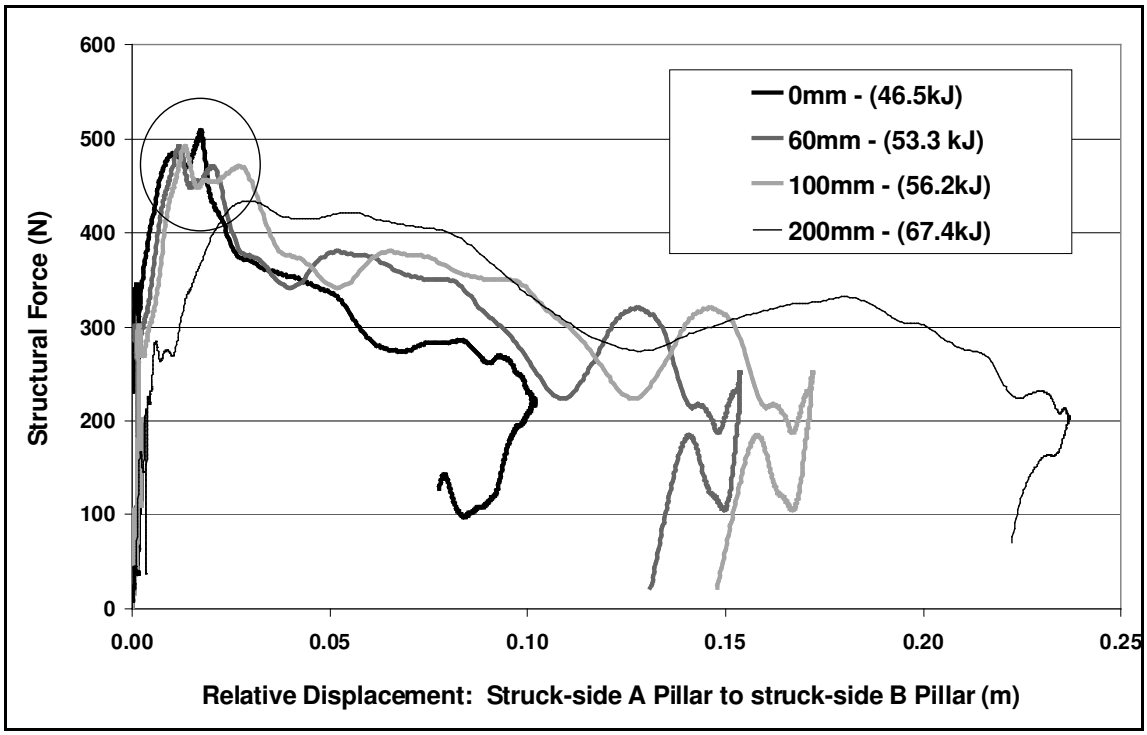

Figure 92 Comparing deformation of the compartment of the underriding vehicle: Structural force of the underriding vehicle with respect to the displacement between the struck side A and B Pillars of the underriding vehicle for car-to-car, head-on crash simulations at varying degrees of vertical misalignment at an overlap ratio of 45%.

Figure 92 shows the structural force with respect to the relative displacement between the struck side A and B-pillars of the underriding vehicle, for 0mm, 60mm, 100mm and 200mm of vertical structural misalignment. The energy dissipated through compartment deformation is shown for each characteristic (in brackets).

At 0mm, 60mm and 100mm of vertical structural misalignment, the peak force is very similar (see circled region of Figure 92). This suggests the compartment strength is similar in each case. At 200mm of vertical structural misalignment, the peak force is lower.

The degree of energy dissipated in the compartment of the underriding vehicle increases greatly (from 46.5 to 67.4kJ) from 0mm to 200mm of vertical structural misalignment. **The characteristics in Figure 92 confirm that, although compartment strength appears to be similar in each case, an increasing misalignment of structures leads to an energy surplus (through less than optimal interaction of the front-ends) which is dissipated through compartment deformation. Struc-**

tural interaction appears to be a key requirement to minimise compartment deformation in car-to-car, head-on collisions.

9.4 Validity of results to simulations involving vertical structural misalignment

The change in internal energy of all elements comprising the vehicle structure was extracted (after subtracting the change in energy of the engine/transmission and the dummies) and compared with the energy dissipation values calculated based on accelerometers, Figure 93.

	Fixed Barrier	Car-to-car: 50% Overlap						
	40% Overlap	0mm	20mm	40mm	60mm	80mm	100mm	200mm
Internal Energy(kJ)	310.46	303.32	300.84	303.33	302.28	299.20	298.98	298.50
Accelerometer (kJ)	306.2	298.13	297.09	297.1	295.39	295.61	295.21	293.6
Error	-1.37	-1.71	-1.25	-2.05	-2.28	-1.20	-1.26	-1.64
		Car-to-car: 45% Overlap						
		0mm	20mm	40mm	60mm	80mm	100mm	200mm
Internal Energy(kJ)		295.48	296.45	296.77	293.55	293.55	294.66	300.35
Accelerometer (kJ)		292.46	291.4	290.06	289.08	290.87	288.39	288.43
Error		-1.03	-1.70	-2.26	-1.52	-0.91	-2.13	-3.97

Figure 93 Comparison between actual change in internal energy of the vehicle structure and the value calculated based on accelerometers. Car-to-car head on collision at a closing velocity of112km/h and a overlap ratio of 45% and 50% respectively for 0mm, 20mm, 40mm, 80mm, 100mm and 200mm of vertical structural misalignment.

The difference between the calculated energy dissipation values and those delivered by the simulations is very low with an associated error ranging from 1% to 4%. This further validates the method of measuring energy dissipation based on accelerometers.

9.5 Investigating constructive measures to improve structural interaction

In section 9.2, it was shown that the level of structural interaction for the car-to-car collision was significantly lower than the predicted maximal degree of structural interaction. In this section, constructive measures to improve structural interaction are investigated.

In section 9.3 it was shown that, when poor structural interaction occurs, a kinetic energy surplus results which is dissipated through compartment deformation. Two measures could therefore be taken to improve structural interaction:

- increase energy dissipation within the front-ends from the beginning of the collision (section 9.5.1).
- ensure the passenger compartment is adequately stiff to prevent compartment deformation and force deformation of the opponent front-end (section 9.5.2).

The following analysis responds to these two points.

9.5.1 Constructive measures in the front-end

Several constructive measures are investigated in this section, involving structural changes to the front-end and their influence on the degree of structural interaction that results. To ensure the mass of the vehicles and therefore the collision energy remained constant, the material properties only were altered. The following structural changes were investigated:

Reinforced cross beam	Stiffness * 2
Weakened cross beam	Stiffness * 0.5
Reinforced wheel house	Stiffness * 2

All collisions were carried out in the standard car-to-car collision configuration at 112km/h at an overlap ratio of 50%. For each collision, EESVV and EESFF values were calculated. The results are shown in Figure 94, below, with the predicted maxi-

mum EESVV and EESFF (fixed barrier) and the results for the car-to-car collision with no vertical misalignment of structures shown for comparison.

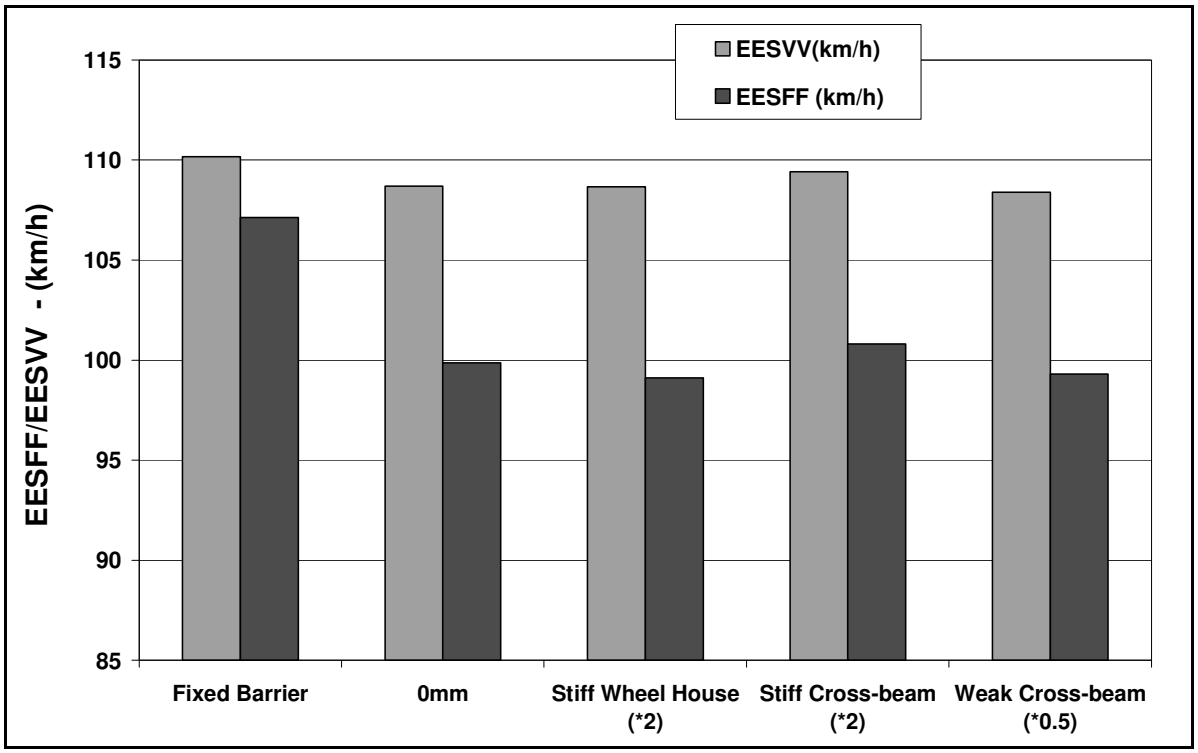

Figure 94 The influence of structural changes within the front-end on the degree of structural interaction (based on EESFF values) for collisions in the standard car-to-car crash configuration at a closing velocity of 112km/h and 50% overlap.

An increase in stiffness of the wheel house led to a decrease in the total amount of energy dissipation within the vehicle front-ends. This observation suggests that changing the stiffness of individual components within the front-end may not necessary lead to an improvement in structural interaction and may even be detrimental. The stiffness characteristic of the front-end unit as a whole should be considered. Future investigations should focus on investigating structural changes in combination to determine which combinations of parameters lead to more favourable global stiffness characteristics of the front-end (further discussed in Recommendations for Further Research, section 10.2).

Reinforcing the cross beam led to an increase in the EESFF values although a corresponding change in the EESVV can be observed as well.

The constructive measures investigated in this section have only a minor influence on the degree of structural interaction occurring. For all simulations, the EESFF was significantly lower than the maximum predicted value based on the fixed barrier collision.

9.5.2 Compartment stiffness

To further investigate the possibility to improve the degree of energy dissipation within the combined vehicle front-ends, the compartment strength of the underriding vehicle was increased. Figure 95 shows the areas of the compartment which were stiffened (shown in red). The strength of the compartment was increased by a factor of 10, again based on the stress-strain properties of the material comprising the compartment.

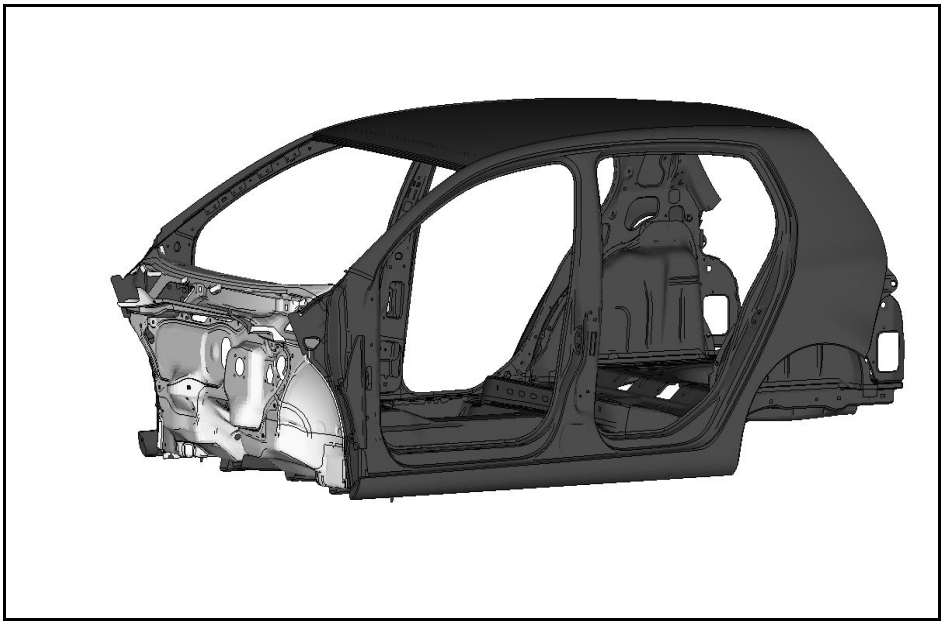

Figure 95 Region of the compartment of the underriding vehicle strengthened by a factor of 10 to represent an ideally stiff passenger compartment (shown in red)

The firewall of the vehicle (shown in white) was not strengthened. The aim of this was to allow a similar amount of dissipation of energy within the firewall for the vehicle with a strengthened compartment and the standard vehicle. The degree of vertical misalignment of structures was equal to 100mm. The force-displacement characteristics for the compartment of the underriding vehicle for collisions with a 100mm vertical misalignment of structures are shown in Figure 96, below.

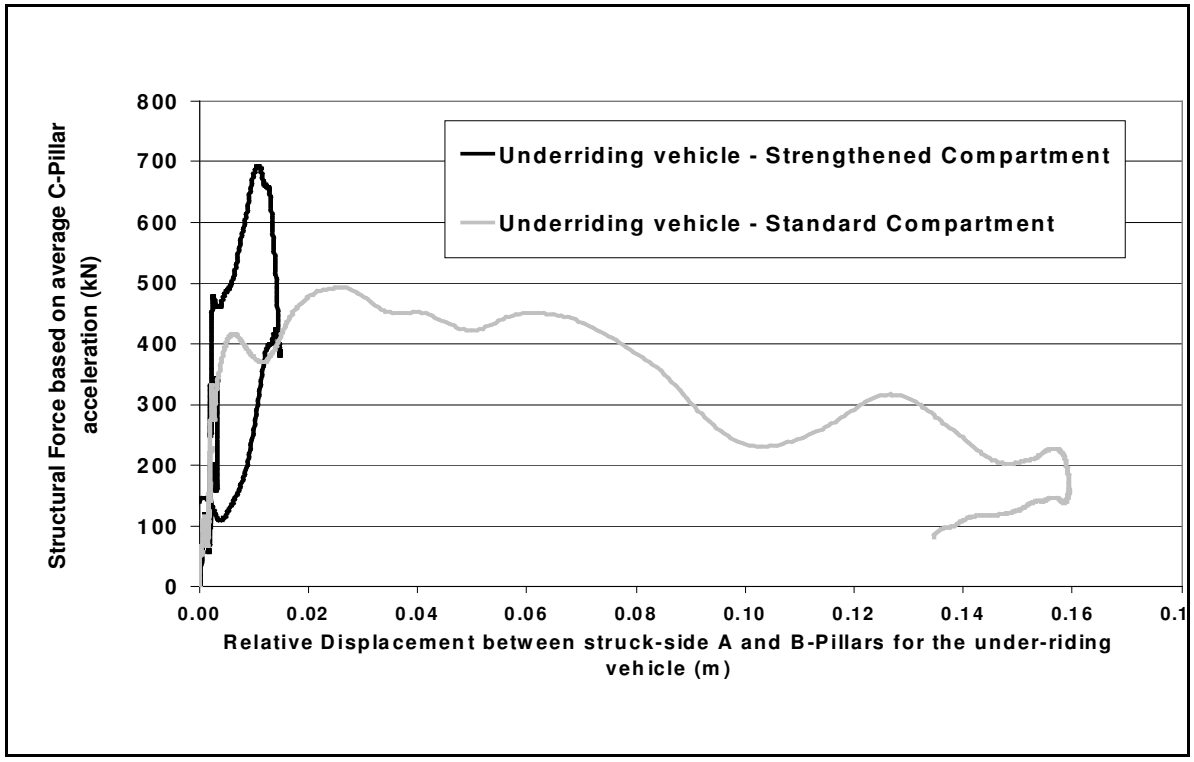

Figure 96 Force versus compartment deformation characteristics (based on the relative displacement between struck side A and B-pillars) for the underriding vehicle with a standard and strengthened passenger compartment, respectively. Car-to-car collision at 50% overlap and a closing velocity of 112km/h.

The “factor-10” increase in the compartment strength leads to a great reduction in the total deformation of the compartment of the underriding vehicle. The peak force exhibited by the compartment also increased from approximately 500kN (standard compartment) to approximately 700kN (strengthened compartment). The EESFF values were calculated for the case of the standard and strengthened compartment, respectively, and are shown in Figure 97. The maximum theoretical EESFF value (based on the fixed barrier collision) and the EESFF value for the standard car-to-car, head-on collision with no vertical misalignment of front-end structures (0mm) are shown for comparison.

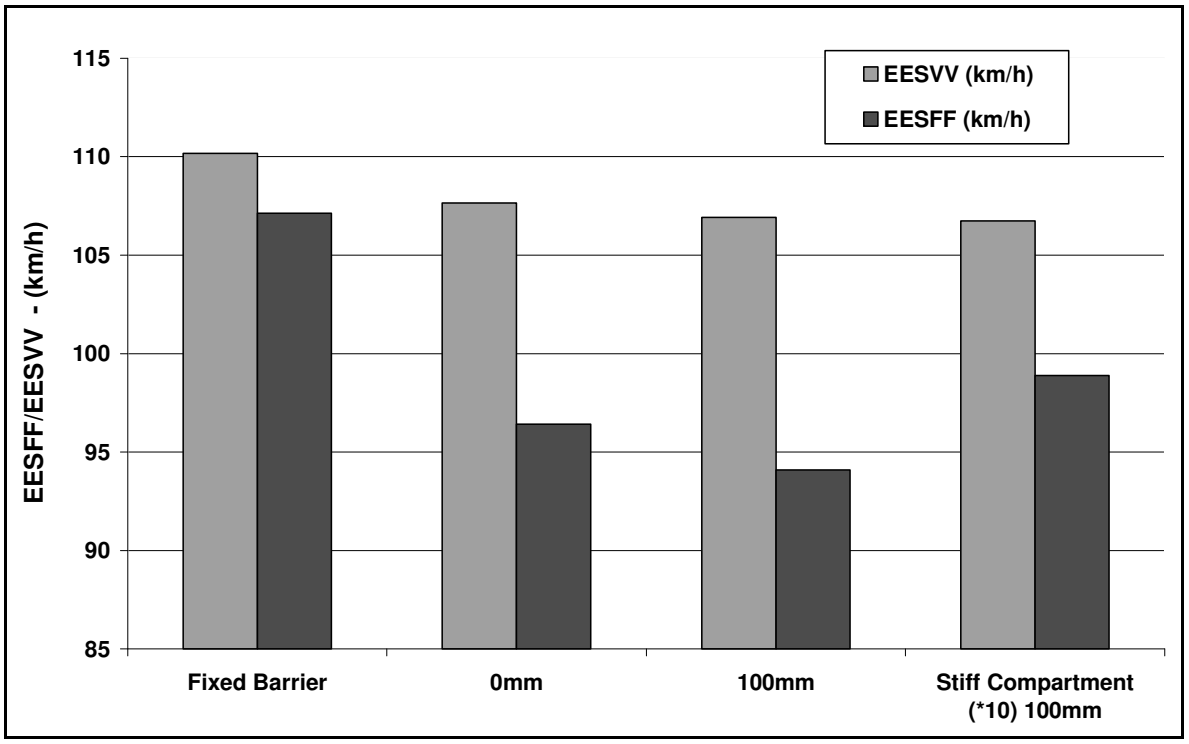

Figure 97 Influence of increasing the strength of the compartment of the underriding vehicle on the EESFF values for a car-to-car collision with a vertical misalignment of front structures equal to 100mm at 50% overlap and a closing velocity of 112km/h.

Figure 97 shows that the strengthened compartment increases the degree of energy dissipation through deformation of the combined front-ends significantly (reflected by an increase in the EESFF from 94km/h to 99km/h).

However, the EESFF value achieved is much lower than the theoretical maximum (fixed barrier) of 110km/h. **Whilst increasing the strength of the compartment of the underriding vehicle increases the energy dissipation within the front-ends, it does not result in maximal energy dissipation through structural deformation.**

9.5.3 Ideal interaction-panel located in the front-end

To further investigate the maximum possible degree of structural interaction achievable for a car-to-car, head-on collision, several simulations were carried out with rigid panels of no-mass located in the front-end of one of the vehicles.

The panels were ideally stiff and oriented vertically and perpendicular to the initial velocity vector of both vehicles. The panels were free to translate parallel to the initial velocity vector of both vehicles and were constrained in all other degrees of freedom (rotational and translational). The purpose of the introduction of the shields into the front-end of the vehicle was to simulate a vehicle front-end with ideal (infinite) shear connections between all potential load paths. This was considered to reflect the case of ideal structural interaction. The purpose of the simulations was to determine whether the predicted maximum EESFF value correlated with the calculated EESFF in a collision in which maximal structural interaction occurred. No attempt was made to evaluate the feasibility of incorporating such shear connections into the front-end.

Three panels were investigated of varied vertical width, 1000mm, 250mm and 100mm. The 1000mm panel covered the entire front-end of the vehicle. The 250mm and 100mm panels were located to correspond to the centre of the longitudinals. The panels were located deep in the front-ends of one of the vehicles so as not disturb the initial interaction of the structures. The width of the panel corresponded exactly to the overlap ratio of 50%. No vertical misalignment of structures was introduced in the simulations. Figure 98 shows the interaction of the vehicle structures with the 1000mm interaction panel (width in vertical direction) at the point in time corresponding to maximum deformation (65ms).

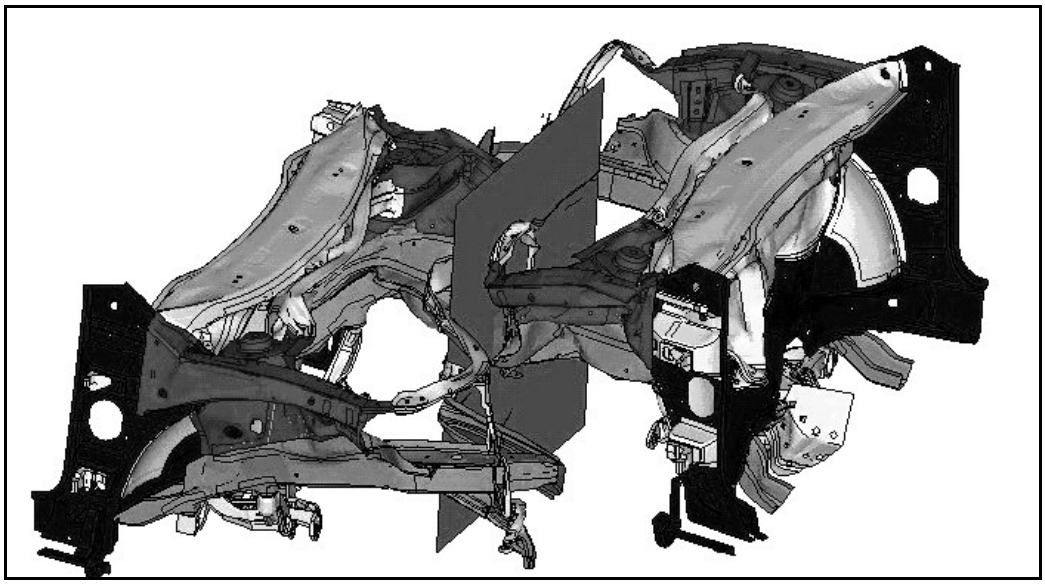

Figure 98 Interaction of the front-end structures with the rigid panel with a vertical width of 1000mm. Car-to-car, head-on collision at 112km/h and 50% overlap with no vertical misalignment of front-end structures. Motor, transmission, alternator and other front-end components removed from picture for visualization purposes. Time point corresponds to point of maximal structural deformation (65ms).

For each of the three panels investigated (100mm, 250mm and 1000mm vertical width) the energy dissipation was calculated. The resulting EESVV and EESFF are shown in Figure 99.

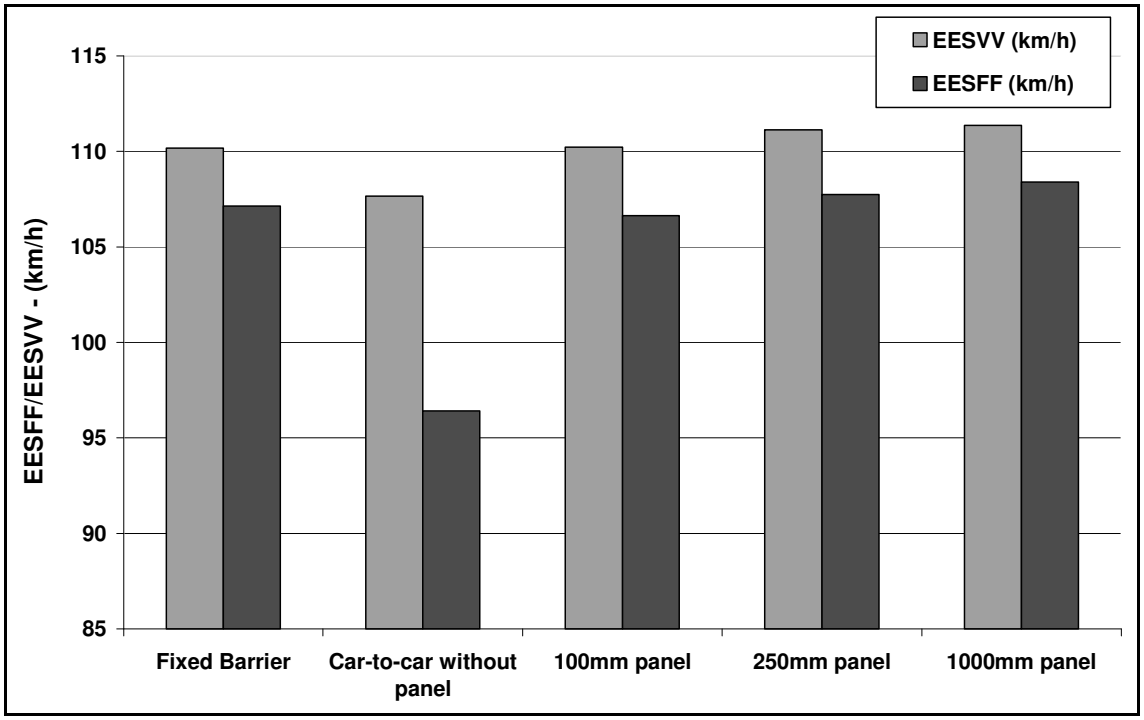

Figure 99 Influence of the introduction of a rigid panel of no mass into the front-end structure on the resulting structural interaction, based on the EESVV and EESFF values. Car-to-car head-on collision at 50% overlap and 112km/h with no vertical misalignment of front-end structures.

The inclusion of a rigid panel into the front-end of one of the vehicles leads to a great increase in the degree of structural interaction. The EESFF increases by between10 and12km/h, depending on the size of the panel. The most interesting observation is that the degree of structural interaction is not highly sensitive to the vertical width of the panel. Even with a panel of vertical width as low as 100mm, a very significant increase in the degree of structural interaction was observed.

The EESVV values increase with the introduction of rigid panels to be approximately equal to the predicted maximum EESVV value (based on the rigid barrier collision carried out at 40% overlap). This proves that the assumption made that the a fixed barrier collision at 40% overlap is analogous to a car-to-car collision at 50% overlap (see 9.1.1).

To further investigate the nature of the increase in energy dissipation within the combined front-ends after the introduction of a rigid panel into the front-end, the force-displacement characteristics for the combined front-ends (between the A-pillars) are shown for a collision with and without a rigid panel, Figure 100.

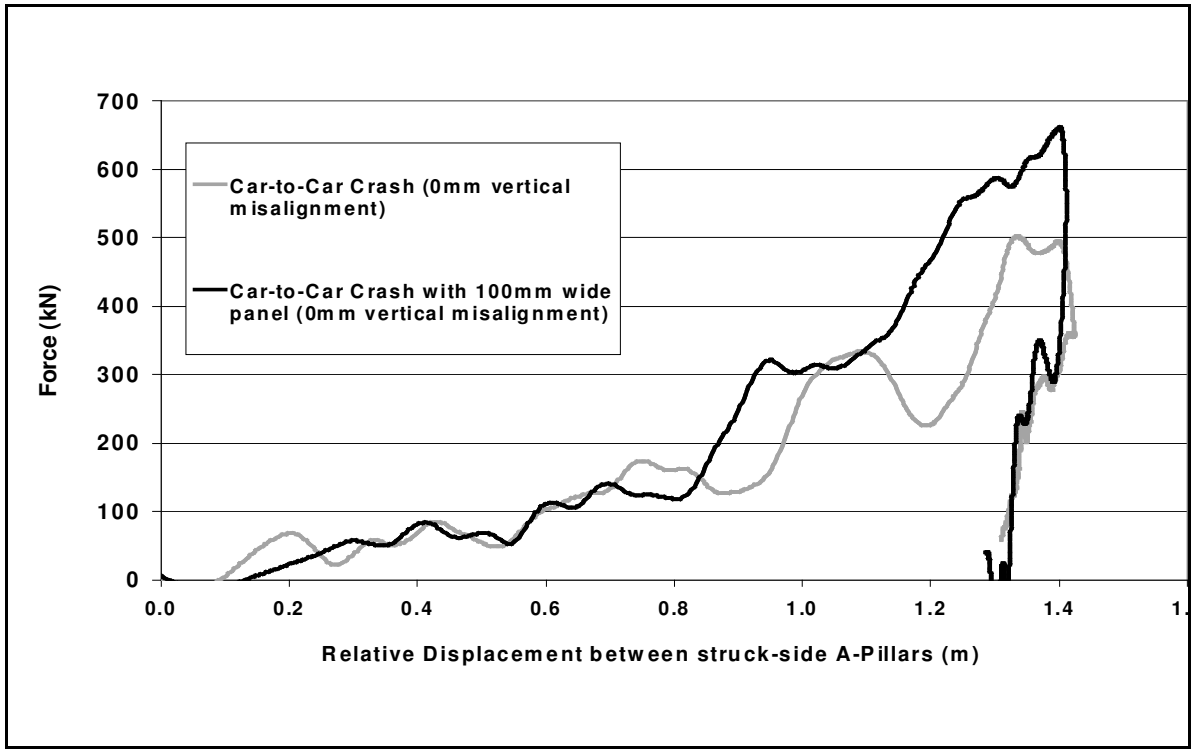

Figure 100 Force-displacement characteristics exhibited by the combined vehicle front-ends with and without a rigid panel located in the front-end of one vehicle. Car-to-car, head-on collision at 50% overlap and a closing velocity of 112km/h.

Figure 100 shows that the same degree of total front-end deformation occurred for the car-to-car collision without the rigid panel and the car-to-car collision with the rigid panel located in the front-end of one of the vehicles (approx 1.4m). The total amount of available deformation travel in both front-end does not seem to have been influenced by the level of structural interaction. The reason for the increased energy dissipation in the front-ends with the rigid panel was a clear increase in the deformation force after 0.8m of combined front-end crush. This indicates that, for the standard car-to-car collision, the load paths within the front-end were not activated to a maximal degree after 0.8m of combined vehicle crush.

To ensure that this wasn't due to an increase in the energy dissipated through deformation of the firewall of the vehicles, which may not have been detected by accelerometers located at the A, B and C-pillars, the deformation in this region is compared in Figure 101.

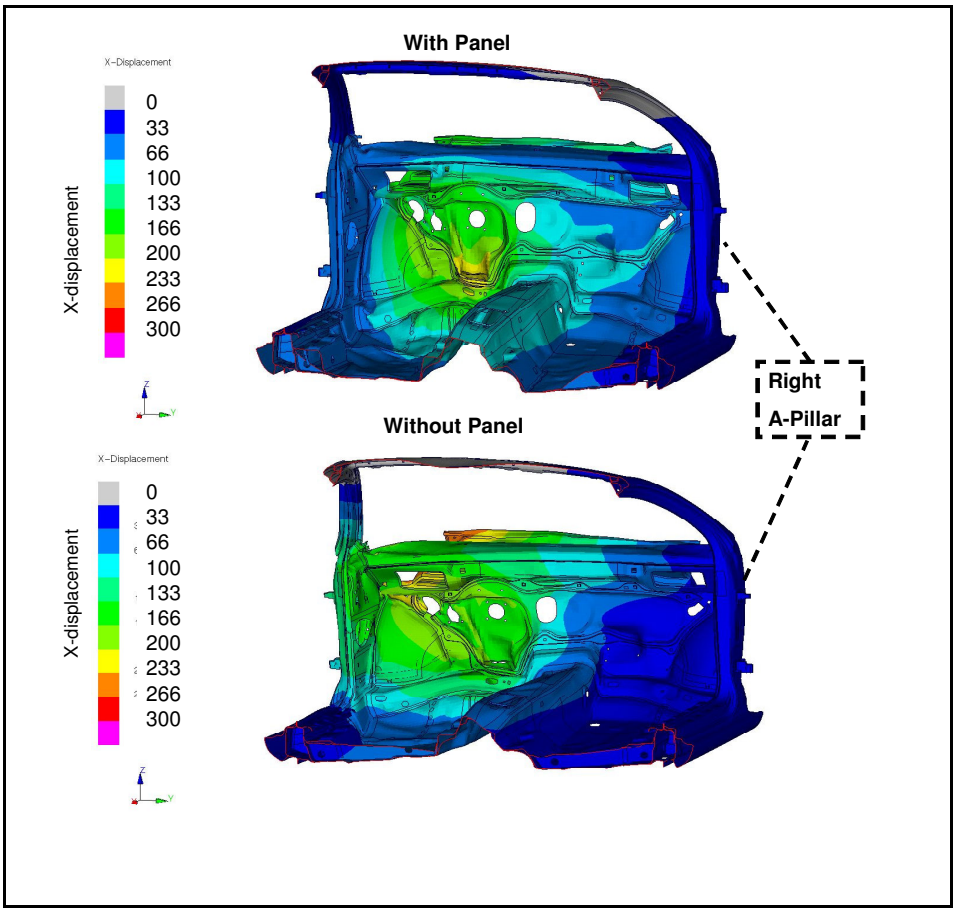

Figure 101 Comparison of the degree of intrusion in the firewall for the standard car-to-car collision and the car-to-car collision with a rigid panel of a vertical width of 1000mm. Car-to-car head-on collisions at 50% overlap and a closing velocity of112km/h.

The maximum degree of deformation is similar for both collisions. For the collision with the rigid panel, the vehicle was deformed more in the middle of the vehicle with almost no deformation occurring in the region of the struck side A-pillar. The total degree of energy dissipated in the firewall can be interpreted to be similar for both collisions.

9.6 Summary

To facilitate an evaluation of structural interaction, predicted maximal energy dissipation characteristics were developed by statically combining the force-displacement characteristics of a passenger vehicle in a fixed rigid barrier collision. A predicted maximal EESFF value was calculated based on this predicted energy displacement characteristic.
Car-to-car head-on collisions were then carried out involving two vehicles, identical to the vehicle involved in the fixed barrier collision. The actual degree of structural interaction was evaluated for these collisions, by comparing the actual and the predicted maximum EESFF values.

At the beginning of the chapter, it was observed that the degree of structural interaction was significantly lower than the predicted maximum (103.3km/h compared to 110.2km/h) for a car-to-car head-on collision involving identical vehicles. The result of the decreased level of structural interaction was a kinetic energy surplus, which led to higher loading and deformation of the passenger compartment of the underriding vehicle.

An increasing vertical misalignment of structures caused a trend of a reduction in structural interaction. The reduction, however, was not highly significant when compared to the difference between the actual and predicted maximal degree of structural interaction for the car-to-car, head-on collision. Between 0mm and 100mm of vertical structural misalignment, the reduction in EESFF values was relatively low. At 200mm of vertical structural misalignment, the EESFF values decreased significantly as the motor block of the underriding vehicle was over-ridden by the front-end of the overriding vehicle. This observation was similar for collisions at an overlap ratio of

45% and 50%. This suggested that the vertical alignment of structures was not the most critical factor influencing structural interaction in these collisions.

Several constructive measures were investigated with the aim of improving the degree of structural interaction in the standard car-to-car collision. Increasing the compartment strength of one of the vehicles increased the degree of structural interaction greatly but did not fully compensate for lost energy dissipation in the front-end. Incorporating a rigid panel into the front-end lead to the most significant increase in structural interaction (based on the EESFF value) suggesting that, with idealised constructive changes to the front-end, the degree of structural interaction could be improved to the maximum predicted level. It also confirmed that the predicted maximum EESFF value, calculated based on the fixed barrier crash test at 40% overlap, was accurate. These observations lead to a key statement relating to structural interaction:

Poor structural interaction results in lower interaction forces and less energy dissipation in the front-ends. This leads to an energy surplus which increases the risk of compartment deformation. Reinforcing the compartment can partially but not fully compensate for this by increasing interaction forces in the front-ends. To maximise energy dissipation in the front-ends, structural interaction needs to be maximised as well.

In addition, this chapter acts as a validation for the measurement of energy dissipation based on accelerometers developed in chapter 8. The error between calculated values for energy dissipation (based on accelerometers) and energy values extracted from simulation varied between approximately 1% and 4%. This further validated the method of measuring energy dissipation based on accelerometers developed in chapter 8.

This chapter also confirms that the EESVV is an appropriate metric to convey collision severity. Based on EESVV values, the 50% overlap ratio for a car-to-car collision was shown to be analogous to the 40% overlap ratio for a fixed barrier collision with respect to collision severity.

The EESFF also proved to be an effective metric to convey the degree of structural interaction in these car-to-car collisions. For collisions involving non-identical vehicles, the maximum EESFF value is influenced by both compartment strength and front-end deformation forces as well. Therefore, to evaluate structural interaction in collisions involving non-identical vehicles, an extra theoretical maximal EESFF value would have to be calculated taking into account the different compartment strengths and front-end forces of each vehicle. This is discussed in recommendations for future research in section 10.2.

10 Conclusions, findings and recommendations for further research

The first section in this chapter (10.1) summarizes the key findings and conclusions of the research, broken down according to the stated research aims as outlined in section 1.2. The findings made and the conclusions drawn are by no means an exhaustive response to the research aims. Section 10.2 outlines the areas where further research is required to add to the understanding of the phenomenon of structural interaction. The ultimate and defining goal of all research into vehicle safety is the mitigation of injury risk faced by vehicle occupants (and other participants) in traffic. The discussion of further research requirements focuses on the steps required to bring about an improvement in structural interaction in the real -world.

10.1 Conclusions and key research findings

The main stated aims of the research were to **define**, **measure** and **evaluate** structural interaction for the car-to-car, head-on collision mode (see section 1.2). Additional aims were outlined in section 1.2 relating to assessment (crash-testing) procedures and the analysis of accident data. The key conclusions of the research are outlined below:

10.1.1 Relevance of structural interaction in the real-world accident environment

The relevance of structural interaction in the real-world accident environment was evaluated based on German accident data. The following conclusions were drawn:

- Measures to improve structural interaction should focus primarily on frontal impacts *(frontal impacts were of higher statistical significance than side impacts, side impacts were dominated by more aggressive collision objects such as trees/poles)*
- Self-protection should not be compromised to improve compatibility *(single vehicle accidents remain of high statistical significance in the accident environment)*

- Other collision objects (particularly trucks) should be considering when determining the appropriate height of vehicle front structures

Refer to chapter 3 for more details.

10.1.2 Defining structural interaction

Structural interaction can be defined as: "the proportion of **actual energy dissipation** through structural deformation compared to the **maximum possible energy dissipation**, for a given collision configuration".

A further contribution of the research, responding to the definition above, was the proposal of two metrics to convey the collision severity (EESVV) and the degree of compatibility (EESFF) in the head-on collision mode. The definition above and the EESFF and EESVV metrics are considered key contributions of the research presented in this thesis and led to the development of methods to measure and evaluate structural interaction in head-on collisions.

Refer to chapter 4 for more details.

10.1.3 Identifying topics to be addressed by crash-testing procedures

Several issues were identified as fundamental requirements of crash-testing procedures to evaluate the structural interaction potential of passenger cars (Chapter 6):

- Force/mass dependency should be removed from the assessment *(structural interaction is not determined by the magnitude of front-end force levels which are inherently linked to vehicle mass)*
- Able to isolate structures which interact in car-to-car collisions
- Offer harmonization potential
- Offer adequate repeatability and reproducibility

Several proposed crash-testing procedures were evaluated according to the four points above.
Refer to chapters 6 and 7 for more details.

10.1.4 Measuring and evaluating structural interaction

The degree of energy dissipated through structural deformation in a given collision needs to be **measured** before structural interaction can be evaluated

- The degree of energy dissipated in a collision can be calculated based on accelerometer readings and an estimate of vehicle structural mass *(assuming a lumped-rigid-mass model of the vehicle)*
- The method developed in this thesis to measure energy dissipation yielded reliable results, particularly in numerical simulation *(error in energy calculations in numerical simulations lay between 1 and 4%)*

Evaluating structural interaction requires the prediction of the maximum possible energy dissipation in a given collision configuration

- The maximum possible energy dissipation in a given collision configuration can predicted based on the energy dissipated in an analogous (considering severity, offset, barrier height, etc) collision with a rigid-wall
- For a car-to-car, head-on collision, predicting maximal structural interaction requires that the front-end force-displacement characteristics of each vehicle in an analogous collision with a rigid-wall are **statically combined**

Refer to chapters 4, 8 and 9 for more details.

10.1.5 Improving structural interaction in the head-on collision mode

The following conclusions relate to the simulation-based investigation carried out in chapter 9 for the head-on collision mode involving identical vehicles.

- The degree of structural interaction for two identical vehicles involved in a head-on collision is reflected by the EESFF value as both vehicles have identical mass and front-end stiffness characteristics *(see 10.2 for comments regarding non-identical vehicles)*
- The prediction of maximal structural interaction, based on rigid-wall front-end force-displacement characteristics was effective
- Structural interaction is relatively insensitive to the degree of vertical misalignment of structures *(up to 100mm of structural misalignment)*

- Changes to isolated components in the front-end of the vehicles do not necessarily improve the degree of structural interaction for a given collision mode (the front-end needs to be considered as a complete unit)

Refer to chapter 9 for more details.

10.2 Recommendations for further research

Several key areas were identified where further research is required to improve the understanding of the phenomenon of structural and, ultimately, improve structural interaction and safety in the real world:

Monitoring and further investigating the appropriateness of improving structural interaction

The findings presented in this thesis assume that maximising structural interaction for all collision modes is the best design target. However, this assumption is based on occupant simulations involving vehicles with simplified front-end stiffness profiles (chapter 5), designed for the 64km/h offset collision mode. Increasing structural interaction, whilst mitigating the risk of compartment intrusion, can lead to increased compartment accelerations. This a fundamental trade-off in vehicle design when considering structural interaction. The appropriateness of maximising structural interaction needs to be continually monitored, especially should vehicle become stiffer. As structural interaction in real collisions is better understood, other factors (such as the influence of structural interaction on the effective shape of the front-end force-displacement characteristics including the degree to which pulses are back-loaded) will require investigation.

Measuring structural interaction in varied collision modes

The conclusions drawn in this thesis relate specifically to the car-to-car, head-on collision mode involving identical vehicles. There is a clear requirement to further investigate structural interaction in collisions involving non-identical vehicles (including car-to-car, car-to-truck and car-to-fixed objects such as guardrails, trees) in varied collision configurations. Structural interaction may also be considered in non-automotive applications. Several technical considerations need to be addressed to achieve this.

- Further development of the EESFF metric to accommodate a range of collision partners and collision modes

- Further development of methods to statically combine force-displacement characteristics of collision partners to effectively predict maximal structural interaction based on the ESSFF or an analogous metric.
- Further development of the methods presented to measure energy dissipation based on accelerometer readings including revision of the calculation of structural mass.

Further steps required to bring about an improvement in structural interaction in the real-world

In order to improve structural interaction in the real-world, further development of crash-testing procedures is required. This involves addressing the issues identified in chapters 6 and 7 to facilitate the development of a standardized crash-testing procedure which fairly evaluates vehicle structures and drives vehicle development in such a way to improve structural interaction. None of the currently proposed procedures is considered ready for implementation. Before any test can be implemented, two objectives need to be fulfilled:

- Design measures which improve structural interaction need to be identified through either analysis of accident statistics or experimental and simulation-based collision investigations
- A crash-testing procedure needs to be developed which can detect these characteristics of vehicle design and objectively evaluate them.

Finally, retrospective analyses of accident data are required after the introduction of any compatibility assessment procedure to quantify the improvement brought about through the introduction of an assessment procedure.

Consideration of developing markets

Developing markets are becoming increasingly motorized. Given the diversity of participants in traffic in these markets and the high number of traffic accidents, it is highly recommended that structural interaction and compatibility be considered when conducting research into traffic safety in developing markets.

Bibliography

[1] Klanner, W. *Status Report and Future Development of the EURO NCAP Programme,* 18th International Technical Conference on the Enhanced Safety of Vehicles, Nagoya, Japan, 2003. Paper 485

[2] Seiffert, U. Wech, L. 2003. *Automotive Safety Handbook*, SAE International Professional Engineering Publishing, Suffolk, U.K. pp 7-10, 18, 27-69. 241-254.

[3] http://www.destatis.de/basis/d/verk/verktab6.php, Statisisches Bundesamt Germany, 20.06.2004.

[4] Baumann, K. Schöneburg, R. Justen, R. *THE VISION OF A COMPREHENSIVE SAFETY CONCEPT.* 18th International Technical Conference on the Enhanced Safety of Vehicles, Nagoya, Japan, 2003. Paper 493.

[5] Seiffert, U. 2005. The future of automotive safety. 19th International Technical Conference on the Enhanced Safety of Vehicles, Washington.

[6] *AGREEMENT Concerning the adoption of uniform conditions of approval and reciprocal recognition of approval for motor vehicle equipment and parts*, Geneva 1958. Data of Entry into Force 1 October 1995. United Nations March 20th, 1995.

[7] http://www.crashtest.com/explanations/nhtsa/usncap.htm

[8] http://www.euroncap.com *European New Car Assessment Program – Frontal Impact Testing Protokoll - version 4.1 March 2004*

[9] *Lie, A. Tingvall, C. HOW DOES EURO NCAP RESULTS CORRELATE TO REAL LIFE INJURY RISKS – A PAIRED COMPARISON STUDY OF CAR-TO-CAR CRASHES?* IRCOBI Conference, Montpellier, September 2000.

[10] Becker, H. Donner, E. Graab, B. Zobel, R. 2003. *Großzahlenmaterial, "In-Depth" Erhebung und Einzelfallanalyse, Werkzeuge zur Verbesserung der Fahrzeugsicherheit im Volkswagenkonzern.* Tagung - Verkehrssicherheit Interdisziplinär, Dresden, Germany, June 2003.

[11] Tingvall, C. Krafft, M. Kullgren, A. Lie, A. *THE EFFECTIVENESS OF ESP (ELECTRONIC STABILITY PROGRAMME) IN REDUCING REAL-LIFE ACCIDENTS*, 18th International Technical Conference on the Enhanced Safety of Vehicles, Nagoya, Japan, 2003. Paper number 261.

[12] Rieger, G. Scheef, J. Becker, H. Stanzel, M. Zobel, R. *ACTIVE SAFETY SYSTEMS CHANGE ACCIDENT ENVIRONMENT OF VEHICLES SIGNIFICANTLY - A CHALLENGE FOR VEHICLE DESIGN*. The 18th International Technical Conference on the Enhanced Safety of Vehicles, Washington; USA, 2005. Paper No. 05-0074

[13] http://www-nrd.nhtsa.dot.gov/departments/nrd-51/THORAdv/THORAdv.htm

[14] Rattingen, M van. Bermond, F. Masson, C. Vezin, P. Hynd, D. Owen, C. Martinez, L. Knack, S. Schaefer, R. *Biofidelity impact response requirements for an advanced mid-sized male crash test dummy.* The 18th International Technical Conference on the Enhanced Safety of Vehicles, Nagoya; Japan, 2003. Paper No. 76

[15] Seiffert, U. *Höhere Aufprallgeschwindigkeit versus Kompatibilität*, Tagung Crash Tech Special, TÜV Akadamie GmbH, München, 1998

[16] Faerber, E. 2003. *EEVC RESEARCH IN THE FIELD OF IMPROVEMENT OF CRASH COMPATIBILITY BETWEEN PASSENGER CARS.*. 18th International Technical Conference on the Enhanced Safety of Vehicles, Nagoya, Japan, 2003. Paper number 346.

[17] Faerber, E. Cesari, D. Hobbs, A. Huibers, J. Von Kampen, B. Paez, J. Wy kes, N. 1998. *IMPROVEMENT OF CRASH COMPATIBILITY BETWEEN CARS*. 17th International Technical Conference on the Enhanced Safety of Vehicles, Windsor, Ontario, Canada, 1998. Paper number 98-s3-0-02

[18] Zeidler, F. Knöchelmann, F. Scheunert, D. *Possibilities and Limits in the Design of Compatible Cars for Real World Accidents.* SAE Conference 1999, Detroit, Paper No. 99B-216.

[19] Zobel, R. *Accident Analysis and Measures to Improve Compatibility*, SAE Conference 1999. Paper No. 1999-01-0065.

[20] O'Reilly, P. 2005. *STATUS REPORT OF IHRA COMPATIBILITY AND FRONTAL IMPACT WORKING GROUP.* 19th International Technical Conference on the Enhanced Safety of Vehicles, Washington, USA, 2005. Paper 05-0365

[21] Zobel, R. *Barrier impact tests and demands for compatibility of passenger vehicles*. VDI Tagung, 1997.

[22] Zobel, R. *Testverfahren zur Ermittelung der Kompatibilität Anforderungen und Realisierungsmöglichkeiten.* Haus der Technik, Essen, February -March 2000.

[23] Delannoy, P. Faure, J. *COMPATIBILITY ASSESSMENT CLOSE TO REAL LIFE ACCIDENTS,* 18th International Technical Conference on the Enhanced Safety of Vehicles, Nagoya, Japan, 2003. Paper 94.

[24] Jerinsky, M. Hollowell, W. 2003. *NHTSA's REVIEW OF A VEHICLE COMPATIBILITY PERFORMANCE METRIC THROUGH COMPUTER SIMULATION.* International Mechanical Engineering Congress and Exposition, Washington DC, November 2003.

[25] Summers, S. Hollowell, W. Prasad, A. 2002. *Design Considerations for a Compatibility Test Procedure,* Society of Automotive Engineers (SAE) Congress, Detroit, 2002. 02B-169

[26] TRL. 2003. *Full-Width-Deformable-Barrier Assessment and Protocol.* Version 1.4. 16th July 2003. (Transport Research Laboratories). England.

[27] UTAC, *SELF AND PARTNER PROTECTION TEST AND ASSESSMENT PROTOCOL BASED ON CURRENT REGULATION R94 AND PDB BARRIER*; Version 2.2, 28 April, 2004.

[28] Bloch, J. *INTRODUCTION OF COMPATIBILITY IN THE DEVELOPMENT OF A FRONTAL IMPACT TEST PROCEDURE.* 14th International Technical Conference on the Enhanced Safety of Vehicles, Munich, Germany. 1994.

[29] Schwarz, T.. *Selbst und Partnerschutz bei frontalen Pkw-Pkw-Kollisionen* (Kompatibilität). VDI Fortschrittbericht, Düsseldorf, Germany, 2002.

[30] Schwarz, T. Busch, S. Zobel, R. 2002. *Influence of deceleration pulse on driver injury levels in vehicle-to-vehicle collisions.* Institute of Mechanical Engineers (United Kingdom) – Vehicle Safety Conference – London, 2002.

[31] Eppinger, R. Sun, E. Kuppa, S. Saul. R. *Supplement: Development of Improved Injury Criteria for the Assessment of Advanced Automotive Restrain Systems – II, NHTSA, March 2002.*

[32] Mark, S. 2003. *Effect of Frontal Crash Pulse Variations on Occupant Injuries*, 18th International Technical Conference on the Enhanced Safety of Vehicles, Nagoya, Japan, 2003. Paper 400

[33] Zobel, R. *Principles for the development of passenger car safety information system for consumers, based on real-life accident evaluation.* Crash Tech 1998. Munich.

[34] *NHTSATRAFFIC SAFETY PLAN FOR OLDER PERSONS*, NHTSA, March 1993

[35] Laituri, T. Sullivan, D. Sullivan, K. Prasad, P. *A theoretical math model for projecting AIS3+ Thoracic Injury for Belted Occupants in Frontal Impacts.* Stapp Car Crash Journal Vol 48 (November 2004), pp455-477.

[36] Shimamura, M. Ohhashi, H. Yamazaki, M. *The Effects of Occupant Age on Patterns of Rib Fractures to Belt-Restrained Drivers and Front Passengers in Frontal Crash in Japan.* Stapp Car Crash Journal, Vol 47 (Ocotber 2003) pp 349-365.

[37] Hobbs, C. A. 1993. *THE RESPONSE OF CAR STRUCTURES TO FRONTAL IMPACT AND THEIR INFLUENCE ON OCCUPANT PROTECTION.* Conference Proceedings, ISATA – ROAD AND VEHICLE SAFETY CONFERENCE September 1993, Aachen, Germany.

[38] Faerber, E. *Kompatibilität bei Kollisionen zwischen Pkw*. Haus der Technik e.v. Tagung Kollisionschutz im Straßenverkehr, Essen, Germany, 2000

[39] Zeidler, F. Knöchelmann, F . *The influence of Frontal Crash Test Speeds on the Compatbility of Passenger Cars in Real World Accidents (GERMAN)* VDI conference "Innovativer Insassenschutz in PKW Kollisionen" Düsseldorf, Germany 1997.

[40] Zobel, R.. *EVALUATION OF THE SAFETY PERFORMANCE OF PASSENGER VEHICLES.* The 11th International Conference on the Enhanced Safety of Vehicles, Washington DC. 1987.

[41] Digges, K. Bahouth, G. *Stiffness and Geometric Incompatibility in Collisions Between Cars and Light Trucks.* SAE Conference 2003. Paper 2003-01-0907

[42] Eucar Project Final Technical Report. *Development of Criteria and Standards for Vehicle Compatibility.* Volkswagen AG. October 24th 2000.

[43] Lund, A. Chapline, J. 1999. *Potential Strategies for Improving Crash Compatibility in the U.S. Vehicle Fleet.* SAE Conference 1999, Detroit. Paper No. 1999-01-0066.

[44] Summers, S. Hollowell, W. Prasad, A. *NHTSA'S RESEARCH PROGRAM FOR VEHICLE COMPATIBILITY.* 18th International Technical Conference on the Enhanced Safety of Vehicles, Nagoya, Japan, 2003. Paper number 307.

[45] *Verma, M.* Lavelle, J. Lange, R. *PERSPECTIVES ON VEHICLE CRASH COMPATIBILITY AND RELATIONSHIP TO OTHER SAFETY CRITIERIA.* 19th International Technical Conference on the Enhanced Safety of Vehicles, Nagoya, Japan, 2003. Paper number 412.

[46] Appel, H. 1975. *Sind kleine Wagen unsicherer als große?* VDI Nachrichten No. 7. 14. February 1975, pp 14-16.

[47] Seiffert, U. *Möglichkeiten und Grenzen der neuen Frontal- und Seitenaufprall-Gesetzgebung*, Automobiltechnische Zeitschrift (ATZ) 99, 1997, pp 494-504

[48] Appel, H. 1999. *Crash Compatibility for Passenger Cars, how to achieve*? VDI Bericht Nr 1471.

[49] Zobel, R. Überlegungen zur strukturellen Abstimmung von Fahrzeugen unterscheidlicher Masse bei unterscheidlichen Kollisionstypen, Fachtagung Fahrzeugsicherheit/Kleinwagen, Haus der Technik Essen, July 1996.

[50] Beuse, N. Summers, L. Summers, S. Park, B. *EVALUATION OF STIFFNESS MEASURES FROM THE U.S. NEW CAR ASSESSMENT PROGRAM.* 18th International Technical Conference on the Enhanced Safety of Vehicles, Nagoya, Japan, 2003. Paper 527.

[51] Thomas, G. Schwarz, T. Zobel, R. 2005. *Required measures to improve the structural interaction potential of passenger-cars. SAE Conference. Washington, USA. April 2005. Paper No. 2005-01-1351.*

[52] Appel, H. 1973. *Aggresivität als Teilproblem der passiven Sicherheit*. Annual Conference Fahrzeugtechnik, Stuttgart, Germany, 1973.

[53] Barbat, S. Xiaowei, L. Prasad, P. *EVALUATION OF VEHICLE COMPATIBILITY IN VARIOUS FRONTAL IMPACT CONFIGURATIONS*. 17th International Technical Conference on the Enhanced Safety of Vehicles, Amsterdam, 2001. Paper 97.

[54] Barbat, S. Xiaowei, L. Prasad, P. A COMPARITIVE ANALYSIS OF VEHICLE-TO-VEHICLE AND VEHICLE-TO-RIGID FIXED BARRIER FRONTAL IMPACTS. 17th International Technical Conference on the Enhanced Safety of Vehicles, Amsterdam, 2001. Paper 31.

[55] Barbat, S. Xiaowei, L. Phillip, Przybylo. Prasad, P. VEHICLE-TO-VEHICLE FULL FRONTAL CRASH OPTIMIZATION USING A CAE-BASED METHODOLOGY, 18th International Technical Conference on the Enhanced Safety of Vehicles, Nagoya, Japan, 2003. Paper 413.

[56] Fujii, S. Fukushima, M. Abe, A. Ogawa, S. Fujita, H. Sunakawa, T. Tanaka, Y. *VEHICLE FRONT STRUCTURE IN CONSIDERATION OF COMPATIBILITY.* 18th International Technical Conference on the Enhanced Safety of Vehicles, Nagoya, Japan, 2003. Paper No. 518.

[57] Meyerson, S. Nolan, J. *Effects of geometry and stiffness on the frontal compatibility of utility vehicles.* 17th International Technical Conference on the Enhanced Safety of Vehicles, Windsor, Ontario, Canada, 1998. Paper number 91.

[58] Zuby, D. Geometry and Stiffness in Frontal Crash Compatibility. IHRA Meeting France, June 2001, Unpublished.

[59] Röllecke, M. Köhler, A. Smart Sensors for Passenger Safety Systems, AIRBAG 200+ 5th International Symposium and Exhibition on Sophisticated Car Occupant Safety Systems, Karlsruhe, Germany, 2000, December 4-6.V10

[60] Edwards; M. Davies, H. Hobbs, A. 2003. *THE ESSENTIAL REQUIREMENTS FOR COMPATIBLE CARS IN FRONTAL COLLISIONS* 17th International Technical Conference on the Enhanced Safety of Vehicles, Amsterdam, 2001. Paper number 158.

[61] Haenchen, D. Schwarz, T. Thomas, G. Zobel, R. 2003. *Feasible Steps Towards Improved Crash Compatibility.* SAE Conference 2004, Detroit. Paper No. 2004-01-1167.

[62] Volkswagen Accident Research Database, Accident number 013421

[63] Alliance of Automobile Manufacturers, *Automakers Enhance Occupant Safety With New Voluntary Commitment*, Press Release*, December 4th, 2003.*

[64] Seiffert, U. Hamilton, J and Boersch, F. 1974. *Compatibility of traffic participants.* Third International Congress on Automotive Safety. Volume 1 24-1. San Francisco, California. July 1974.

[65] Zobel, R. Thomas, G. Schwarz, T. *TOWARDS A BENEFICIAL, SCIENTIFICALLY MEANINGFUL, AND APPLICABLE COMPATIBILITY-TESTING.* The 19th International Conference on the Enhanced Safety of Vehicles, Washington, DC. 2005. Paper 05-0052.

[66] Frei, P. Kaeser, R. Hafner, R. Schmid, M. Dragan, A. Wingeier, L. Muser, M. Niederer, P. Walz, F. *Crashworthiness and Compatibility of Low Mass Vehicles in Collisions*, SAE Conference 1997, Paper number 970122.

[67] Association for the Advancement of Automotive Medicine, 1998. *THE ABBREVIATED INJURY SCALE 1990 REVISION, UPDATE (98).*

[68] Zobel, R. Analyse des realen Unfallgeschehens – Methoden und Prinzipien der VW-Unfallforschung, Technical Congress, “Kollisionschutz im Straßenvekehr”, Haus der Technik Essen, 1995.

[69] Thomson, R. Edwards, M. 2005. *PASSENGER VEHICLE CRASH TEST PROCEDURE DEVELOPMENTS IN THE VC-COMPAT PROJECT.* 19th International Technical Conference on the Enhanced Safety of Vehicles, Washington, USA, 2005. Paper 05-0008:

[70] Edwards; M. Davies, H. Hobbs, A. 2003. *DEVELOPMENT OF TEST PROCEDURES AND PERFORMANCE CRITERIA TO IMPROVE COMPATIBILITY IN CAR FRONTAL COLLISIONS.* 18th International Technical Conference on the Enhanced Safety of Vehicles, Nagoya, Japan, 2003. Paper 86.

[71] Schwarz, T. Zobel, R. 2003 *Improvement of Compatibility of Passenger Vehicles – Next feasible steps.* The 18th International Technical Conference on the Enhanced Safety of Vehicles, Nagoya; Japan, 2003. Paper No. 287.

[72] Seyer, K. Newland, C. Terrel, M 2004. *AUSTRALIAN RESEARCH TO SUPPORT THE IHRA VEHICLE COMPATIBILITY WORKING GROUP*. 18th International Technical Conference on the Enhanced Safety of Vehicles, Nagoya, Japan, 2003. Paper number 274.

[73] Monnet, S. PSA'S VIEWS ON COMPATIBILITY - A POTENTIAL TWO-STEP APPROACH TO IMPROVE COMPATIBILITY AMONG THE VEHICLE FLEET. 17th International Technical Conference on the Enhanced Safety of Vehicles, Windsor, Ontario, Canada, 1998. Paper number 343

[74] Zeidler F, *Deformationsverhalten von Kraftfahrzeugen bei Aufprallversuchen unter praxisgerechten Versuchsbedingungen. Vekehrsunfall 1979.*

[75] European Commission Regulation for motor vehicles and their trailers. (ECE Regulation) ECE-R 94, Kirschbaum Verlag Bonn, 1998.

[76] Federal motor vehicle standard (USA) 49CFR Part 571

[77] Workshop, ACEA Sub-group compatibility / Working Group Truck Safety, Official Minutes, UTAC Paris, 01.12.2003.

[78] Appel, H. Deter, T. Meißner, T. Rasenack, W. 1994. *Grenzen des Down-Sizing von Pkw unter Package- und Sicherheitsaspekten*, Motor und Umwelt, AVL List Gmbh June 1994.

[79] Jewkes, D. Lövsund, P. Viano, D. 1999. *Safety of a Downsized Vehicle Fleet: Effects of Mass Distribution, Impact Speed and Inherent Protection in Car-to-Car Crashes*, SAE Conference 1999, Detroit. Paper No. 1999-01-0074.

[80] Weber, M. *Die Aufklärung des Kfz-Versicherungsbetruges Grundlagen der Kompatibilitätsanalyse und Plausibilitätsprüfung.* 1. Auflage, Schriftenreihe Unfallrekonstruktion, Münster 1995.

[81] Wu, W. *Geometric Compatibility Between Cars and Roadside Safety Equipment,* European Vehicle Passive Safety Network 2, Workshop October 16th-17th Rhode, Germany 2003.

[82] www.irtad.bast.de, *International roads and traffic database*.

[83] Kersten, R.: *Methodik zur Entwicklung von crashkompatiblen Gesamtfahrzeugkonzepten*, Dissertation, TU Braunschweig, Verlag Mainz, 2004.

[84] Madymo User Manuals, Version 4.3, TNO Automotive, 1999.

[85] Lau, I.V., and Viano, D.C., *The Viscous Criterion: Bases and Applications of an Injury Severity Index for Soft Tissues*, Proceedings of 30th Stapp Car Crash Conference (P-189), pp. 123-142, SAE Technical Paper No. 861882, Society of Automotive Engineers, 1986.

[86] Hackenberg, U. Rabe, M. Friedewald, K. 1999. *Konstruktive Aspekte der Kompatibilität – Influence of Compatibility on Car Design.* VDI Report 1471, Innovativer KFZ Insassen- und Partnerschutz, Tagung Berlin, 1999.

[87] Bangemann, C. Auto motor und sport Zeitschrift: 19/1999

[88] Franken, M. 1999. *Autoreisen müssen sanfter werden*. VDI Nachrichten, Berlin, October 1999.

[89] *Kleine Autos – Grosse Risiken ?* www.winterthur-insurance.ch/ pdf/crash tests/CrashTest_d.pdf

[90] http://www-nrd.nhtsa.dot.gov/ihra/

[91] http://www.acea.be/ASB/ASBv1_1.nsf

[92] Davies, H. Edwards, M. *Full-width load cell wall – Test Development*, Meeting – International Harmonisation of Research Activities (IHRA), June 11th, 2001. Paris.

[93] Martin T. *Static tests on Rover 75 Cross beam*. Presentation, UTAC, France, 18.03.2004

[94] Delannoy, P. Diboine, A. *STRUCTURAL FRONT UNIT GLOBAL APPROACH.* 18th International Technical Conference on the Enhanced Safety of Vehicles, Nagoya, Japan, 2003. Paper No. 199.

[95] Department of transport and regional services, Australia, http://www.dotars.gov.au/transreg/str_offset.htm#Why

[96] Summers, S. Hollowell, W. Prasad, A. *2000 NHTSA'S COMPATIBILITY RESEARCH PROGRAM UPDATE ,* Society of Automotive Engineers Congress, Detroit, 2000. PAPER 01B-257

[97] Faerber, E. 2005. EEVC Approach to the Improvement of Crash Compatibility between Passenger Cars 19th International Technical Conference on the Enhanced Safety of Vehicles, Washington, USA, 2005. Paper 05-0155

[98] Decker, J. Grösch, L. Justen, R. Schwede, W. 1990. *Realitätsnahe Frontale Crash Versuche und daraus abgeleitete Schutzmaßnahmen in Merecedes Benz Fahrzeuge. Automobiletechnische Zeitschrift (*AZT), 92 (1990). pp616-733.

[99] Reaffirmation of J224 – Collision Deformation Classification, Society of Automotive Engineers (SAE) J224, 2001

Additional uncited references

Delannoy, P. Martin, T. Castaing, P. 2005. *COMPARTIVE EVALUATION OF FRONTAL OFFSET TESTS TO CONTROL SELF AND PARTNER PROTECTION.* 19th International Technical Conference on the Enhanced Safety of Vehicles, Washington, USA, 2005. Paper 05-0010

Hirayama, S. Obayashi, K. Okabe, T. 2003. *COMPATIBILITY FOR FRONTAL IMPACT COLLISIONS BETWEEN HEAVY AND LIGHT CARS*: 19th International Technical Conference on the Enhanced Safety of Vehicles, Nagoya, Japan, 2003 - Paper 454

Mizuno, K. Teteishi, K. Arai, Y. Nishimoto, T. *RESEARCH ON VEHICLE COMPATIBILITY IN JAPAN,* 18th International Technical Conference on the Enhanced Safety of Vehicles, Nagoya, Japan, 2003. Paper number 113.

Nolan, J. Powell, M. Preuss, C. Lund, A. *Factors Contributing to Front-Side Compatibility: A comparison of Crash Test Results. 43rd Stapp Car Crash Conference Proceedings*. 1999.

O'Reilly, P. 2003. *STATUS REPORT OF IHRA COMPATIBILITY AND FRONTAL IMPACT WORKING GROUP.* 18th International Technical Conference on the Enhanced Safety of Vehicles, Nagoya, Japan, 2003. Paper 402

Paine, M. *OBSERVATIONS ABOUT VEHICLE DESIGN AND STRUCTURAL PERFORMANCE*, Sixteenth International Technical Conference of the Enhanced Safety of Ve-hicles (ESV) Windsor, Canada, June 1998 Paper Number 98-S1-W-21

Park, B. Hackney, J. Morgan, R. Chan, H. Lowrie, J. Devlin, H. *The New Car Assessment Program: Has it Led to Stiffer Light Trucks and Vans over the Years.* SAE Conference 1999, Detroit. Paper No. 1999-01-0064.

Schwarz, T. Takla, M. Thomas, G. Zobel, R. *Improving Structural Interaction In passenger vehicle Collisions*. Institute of Mechanical Engineers, England (IMechE) Vehicle safety conference, London, December 2004.

Schwarz, T. 1999. *Vergleich der Crashtestbedingungen für Personenkraftwagen mit dem realen Unfallgeschehen*, Diplomarbeit 6/99 (FG 7), Technische Universität Berlin, ISS – Fahrzeugtechnik, März, 1999.

Takizawa, S. Sugimoto, T. Suzuki, H. *A STUDY OPF COMPATIBILITY TEST PROCEDURE IN FRONTAL IMPACT.* 18th International Technical Conference on the Enhanced Safety of Vehicles, Nagoya, Japan, 2003. Paper number 437

Takla, M. Tomas, J. *SAFETY OF OCCUPANTS OF PASSENGER CARS IN COLLISIONS WITH TRUCKS.* ISATA – ROAD AND VEHICLE SAFETY CONFERENCE September 1993, Aachen, Germany.

Werkmeister, K. Borchers, N. A BALANCED ACTIVE AND PASSIVE SAFETY CONCEPT FOR NEW VEHICLE GENERATIONS, The 18th International Technical Conference on the Enhanced Safety of Vehicles, Nagoya; Japan, 2003. Paper No. 352

Zobel, R. Schwarz, T. *Ermittlung der Zellensteifgkeit zur kompatiblen Auslegung von Pkw-Frontstrukturen.* Crash Tech 2002. Munich.

Appendix

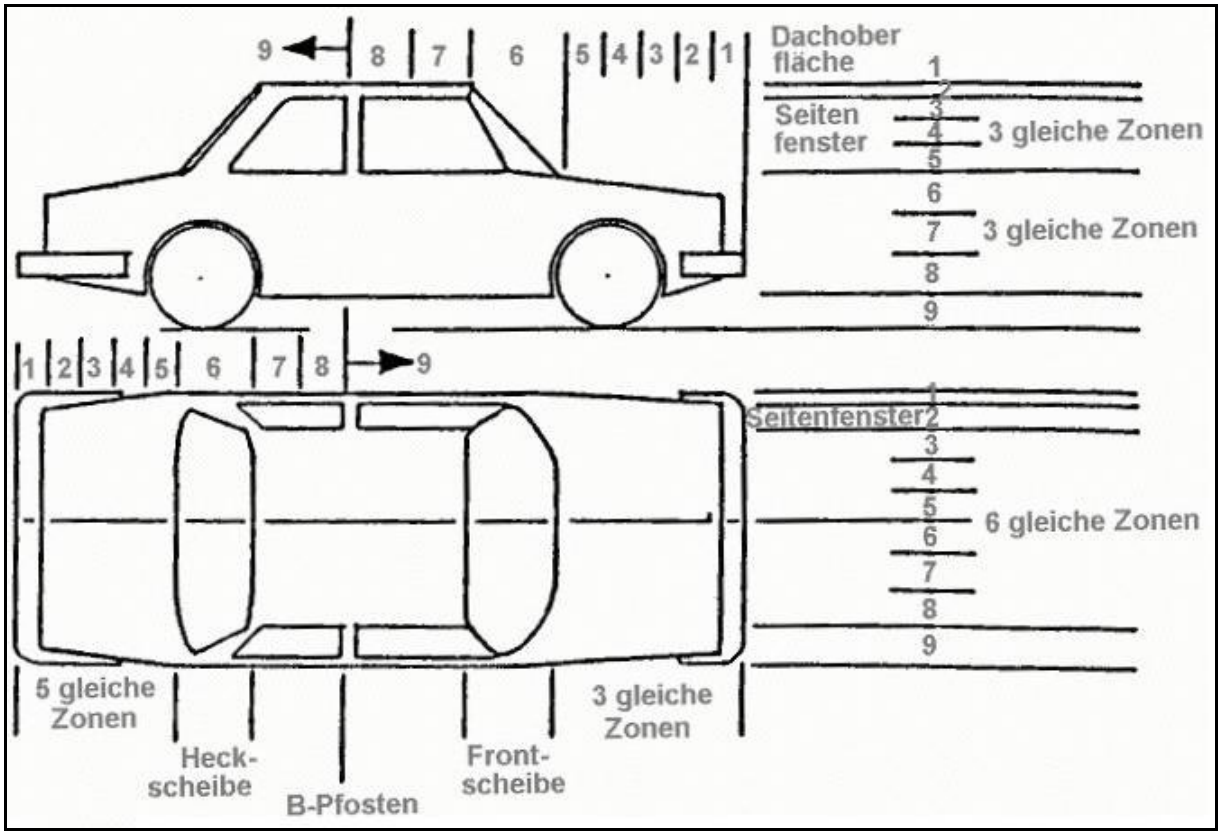

Figure 102 VDI6 – „Vehicle Deformation Index“ [99]